



Conference on Application of Polar Dielectrics 2014

July 7-11, 2014 | Vilnius, Lithuania



Final Program and Abstract Book

Sponsors of European Conference on Application of Polar Dielectrics 2014

— MAIN SPONSOR —



— SPONSORS —



RADIANT TECHNOLOGIES, INC. 
TECHNOLOGIES, INC.
radiant@ferrodevices.com

World Leader in
**Ferroelectric IC
Technology and Testers**



Device Test Systems for:

- Ferroelectric Materials
- MEMS, Sensors, and Actuators
- Multiferroics
- Magnetolectrics/Magnetoelectrics
- Electro Ceramics

PLEASE VISIT RADIANT TECHNOLOGIES BOOTH FOR A DEMONSTRATION WWW.FERRODEVICES.COM

Table of Contents

Final Program	4-14
Poster Session I	15-17
Poster Session II	18-20
Welcome	21
Conference Committees	22
General Information	23-26
Abstracts (oral)	28-124
Abstracts (posters)	125-209
Useful information	210

Final Program

Monday, July 7th, 2014

14:00 – 21:00 Registration

18:00 – 21:00 **Welcome Reception**

Tuesday, July 8th, 2014

08:00 – 19:00 Registration

08:50 – 09:00 **Opening**

09:00 – 09:50 **Plenary Session I (The Theatre hall)** | Chaired by: N. Setter

S. Wada

Preparation of New Barium Titanate-based Nano-complex Ceramics with High-density Heteroepitaxial Interfaces by Solvothermal Solidification Method and Their Dielectric and Piezoelectric Enhancement

Material Science and Technology, Interdisciplinary Graduate School of Medical and Engineering, University of Yamanashi, 4-4-37 Takeda, Kofu, Yamanashi 400-8510, Japan

09:50 – 10:20 **Coffee**

10:20 – 12:40 Chaired by:
M. Alexe

The Theatre hall
Perovskites I

10:20 – 11:00 **M. Guennou** (invited) Structure and phase transitions in Bi-based perovskites
Public Research Centre Gabriel Lippmann, Materials Science Department, 41 Rue du Brill, L-4422 Belvaux Luxembourg

11:00 – 11:40 **H. Fuess** (invited) *In situ* structure investigation of piezoceramics by neutron, X-ray and electron diffraction
Institute of Geo- and Materials Science, Alarich-Weiss-Str. 2, Technische Universität Darmstadt, Germany

11:40 – 12:00 R.V. Yusupov Manganese-related dynamic polar centres in SrTiO₃
Kazan Federal University, Kremlevskaya 18, 420008 Kazan, Russia

12:00 – 12:20 C. Briegel Influence of time and heat treatment on properties of lead-free KNN ceramics
Applied Material Mechanics, Fraunhofer Institute for Ceramic Technologies and Systems IKTS, 01277 Dresden, Germany

10:20 – 12:40 Chaired by:
A. Tagantsev

Aula Parva
Thin films & Interfaces I

10:20 – 11:00 **P. Zubko** (invited) Functional Properties of Artificially Layered Ferroelectrics
University College London, London Centre for Nanotechnology, 17-19 Gordon Street, London, WC1H 0AH, UK

11:00 – 11:20 W. Sakamoto Electrical Properties Improvement of Chemically Synthesized Lead-Free Piezoelectric (Bi_{1/2}Na_{1/2})TiO₃ Thin Films by Mn doping
EcoTopia Science Institute, Nagoya University, Furo-cho, Chikusa-ku, Nagoya 464-8603 Japan

11:20 – 11:40	D. A. Mota	Polar behavior of oxygen deficient KTaO_3 thin films prepared by rf sputtering <i>IFIMUP and IN-Institute of Nanoscience and Nanotechnology, Department of Physics and Astronomy, Faculty of Science of University of Porto, Rua do Campo Alegre, 687, 4169-007 Porto, Portugal</i>
11:40 – 12:00	R. Bachelet	Ferroelectric BaTiO_3 thin films grown on $\text{Si}(001)$ by molecular beam epitaxy <i>Institut des Nanotechnologies de Lyon, CNRS UMR 5270, ECL, 36 avenue Guy de Collongue, 69134 Ecully cedex, France</i>
12:00 – 12:20	V. Železný	Infrared Spectroscopy of Strained $\text{BaTiO}_3/\text{SrTiO}_3$ Superlattices on Scandate Substrates <i>Institute of Physics, ASCR, Na Slovance 2, 182 21 Praha 8, Czech Republic</i>
12:20 – 12:40	M. Bousquet	Pt-less silicon integration of PZT sol-gel thin films <i>CEA, LETI, MINATEC, 17 Rue des Martyrs, F38054 Grenoble, France</i>
10:20 – 12:40	Chaired by: J. Roedel	Seminar Room Multiferroics & Composites I
10:20 – 11:00	A. Kumar (invited)	Flexomagnetic effect in multiferroic composites and E-beam Irradiated Nano-electro-mechanical-ferroelectric-systems <i>CSIR-National Physical Laboratory, New Delhi-110012</i>
11:00 – 11:40	F. D. Morrison (invited)	Structure-property relations in La- and Nd-doped BiFeO_3 : competition between geometry optimisation and magnetism <i>School of Chemistry and EaStCHEM, University of St Andrews, St Andrews, KY16 9ST, United Kingdom</i>
11:40 – 12:00	J. A. Moreira	Dynamic and structural properties of orthorhombic rare-earth manganites under high pressure <i>IFIMUP and IN-Institute of Nanoscience and Nanotechnology, Departamento de Física e Astronomia da Faculdade de Ciências, Universidade do Porto, Rua do Campo Alegre, 687, 4169-007 Porto, Portugal</i>
12:00 – 12:20	L.P. Curecheriu	Nonlinear dependence of dielectric constant in polymer-based composite <i>Faculty of Physics, Al.I. Cuza University, Iasi 700506, Romania</i>
12:40 – 14:20	Lunch	
14:20 – 15:40	Chaired by: J. Hlinka	The Theatre hall Perovskites II
14:20 – 15:00	S. Vakhrushev (invited)	X-ray scattering study of $\text{PbZr}_{1-x}\text{Ti}_x\text{O}_3$ single crystals at small x and at MPB <i>Ioffe Institute, 26 Politekhnicheskaya, St.-Petersburg, 194021 Russia St.Petersburg State Polytechnical University, St.-Petersburg, Russia</i>
15:00 – 15:20	M. H. Lente	Sintering and physical properties of $(\text{Na}, \text{K})\text{NbO}_3$ -based piezoceramics <i>Universidade Federal de São Paulo - Instituto de Ciência e Tecnologia Rua Talim, 330 - Vila Nair -São Jose dos Campos - SP - Brazil – CEP: 12231-280</i>
15:20 – 15:40	M. Blömker	(Co-)doping of lead-free $\text{Bi}_{1/2}\text{Na}_{1/2}\text{TiO}_3$ - $\text{Bi}_{1/2}\text{K}_{1/2}\text{TiO}_3$ -based piezoceramics <i>Institute of Materials Science, TU Darmstadt, Alarich-Weiss-Straße 2, 64287 Darmstadt, Germany</i>

14:20 – 15:40		Chaired by: M. Guennou	Aula Parva Thin films & Interfaces II
14:20 – 15:00	A. Sigov (invited)	I-V characteristics of thin-film ferroelectric structures with negative conductivity <i>Moscow State Technical University of Radioengineering, Electronics and Automation, Moscow, Russia</i>	
15:00 – 15:20	M. Cuniot-Ponsard	Electro-optic and converse piezoelectric coefficients of highly polar epitaxial films: GaN grown on Si, and (Sr,Ba)Nb ₂ O ₆ (SBN) grown on Pt coated MgO <i>Laboratoire Charles Fabry (LCF), IOGS, CNRS, Univ Paris-Sud, 2 Avenue Augustin Fresnel, 91127 Palaiseau cedex, France</i>	
15:20 – 15:40	M. Bousquet	PZT film thickness dependence on the structural, microstructural and electrical properties <i>CEA, LETI, MINATEC, 17 Rue des Martyrs, F38054 Grenoble, France</i>	
14:20 – 15:40		Chaired by: V. E. Gevorkyan	Seminar Room Multiferroics & Composites II
14:20 – 15:00	Marin Alexe (invited)	Coupling between Polarization and Spin Transport in Multiferroic Tunnel Junctions <i>Max Planck Institute of Microstructure Physics, Halle (Germany) / University of Warwick (UK)</i>	
15:00 – 15:20	J. Pokorný	Lattice dynamics of bismuth ferrite revisited <i>Institute of Physics, Academy of Sciences of the Czech Republic, Prague, Czech Republic</i>	
15:20 – 15:40	G. Herranz	Magnetoelectric Imaging at Buried Interfaces <i>Institute of Materials Science of Barcelona ICMAB-CSIC, Campus de la UAB, 08193 Bellaterra, Catalonia, Spain</i>	
15:40 – 16:00 Coffee			
16:00 – 17:20		Chaired by: S. Wada	The Theatre hall Perovskites III
16:00 – 16:20	Ph. Colomban	Stress-induced phase transition in a poled KNbO ₃ crystal: Microthermal expansion and micro-Raman study <i>Sorbonne Universités, UPMC Univ Paris 06, UMR 8233, MONARIS, F-75005, Paris, France</i> <i>CNRS, UMR 8233, MONARIS, F-75005, Paris, France</i>	
16:20 – 16:40	E.D. Politova	Ferroelectric Properties of the Potassium Sodium Niobate-Based Ceramics <i>L.Ya. Karpov Institute of Physical Chemistry, Obukha s.-st. 3-1/12, b. 6, Moscow, 105064, Russia</i>	
16:40 – 17:00	J. Macutkevicius	Phase Transitions Dynamics in Ag _{1-x} Li _x NbO ₃ <i>Faculty of Physics, Vilnius University, Saulėtekio av. 9/3, LT-10222 Vilnius, Lithuania</i>	
17:00 – 17:20	M. S. Kim	Effects of Na excess on dielectric and electrical properties of (Na _{0.53+x} K _{0.47})(Nb _{0.55} Ta _{0.45})O ₃ ceramics <i>School of Advanced Materials Engineering, Changwon National University, Gyeongnam 641-773, Republic of Korea</i>	

16:00 – 17:20		Chaired by: Z.-G. Ye	Aula Parva Thin films & Interfaces III
16:00 – 16:20	M. El Marssi	High strain effect on the soft mode, ferroelectricity and phase transition in lead-free $[\text{BaTiO}_3]_{(1-x)\lambda}/[\text{BaZrO}_3]_{x\lambda}$ <i>Université de Picardie Jules Verne, LPMC, 33 rue Saint-Leu, F-80039 Amiens, France</i>	
16:20 – 16:40	A. Bartasyte	Thickness dependent stress relaxation, twinning and thermal expansion of epitaxial LiNbO_3 and LiTaO_3 thin films on C-sapphire <i>Femto-ST Institute, University of Franche-Comté and CNRS (UMR 6174), 32 avenue de l'Observatoire, Besançon, France, 25044 Jean Lamour Institute, Lorraine University and CNRS (UMR 7198), Parc du Saurupt, Nancy, France, 54011</i>	
16:40 – 17:00	A. Klein	Electrochemical instability at PZT/electrode interfaces during polarisation reversal <i>Technische Universität Darmstadt, Institute of Material Sciences, Surface Science, Jovanka-Bontschits-Str. 2, 64287 Darmstadt, Germany</i>	
17:00 – 17:20	S. Li	Electrode and interface influences on ferroelectric properties of BaTiO_3 single crystals <i>Technische Universität Darmstadt, Institute of Material Sciences, Jovanka-Bontschits-Straße 2, 64287 Darmstadt, Germany</i>	
16:00 – 17:20		Chaired by: M. Josse	Seminar Room Multiferroics & Composites III
16:00 – 16:20	A.N. Salak	Multiferroic Antipolar and Polar Phases in Metastable Perovskite $\text{BiFe}_{0.5}\text{Sc}_{0.5}\text{O}_3$ <i>Department of Materials and Ceramic Engineering/CICECO, University of Aveiro, 3810-193 Aveiro, Portugal</i>	
16:20 – 16:40	R. Vilarinho	Polar properties and phase diagram of the magnetoelectric $\text{Gd}_{1-x}\text{Y}_x\text{MnO}_3$ system <i>IFIMUP-IN, Faculty of Sciences, University of Porto</i>	
16:40 – 17:00	C. E. Ciomaga	Dielectric and non-linear properties of $\text{SrTiO}_3@/\text{BaTiO}_3$ core-shell ceramic <i>Dept. of Physics, Alexandru Ioan Cuza University, Blv. Carol I, nr.11, 700506, Iasi, Romania</i>	
17:40 – 19:00		Poster Session I	

Wednesday, July 9th, 2014

08:00 – 19:00 Registration

09:00 – 09:50 **Plenary Session II (The Theatre hall)** | Chaired by: H. Fuess

J. F. Scott

Real-time Dynamics of Nano-domains: Effect of Cylindrical “hoop” Stresses

Cavendish Laboratory, Department of Physics, Cambridge University

09:50 – 10:20 **Coffee**

10:20 – 12:40 Chaired by:
A. Sigov

The Theatre hall
Perovskites IV

10:20 – 11:00 **J. Hlinka**
(invited)

Lattice modes of antiferroelectric PbZrO_3
Institute of Physics, Academy of Sciences of the Czech Republic, Prague 8, Czech Republics

11:00 – 11:40 **I. M. Reaney**
(invited)

The Role of Pseudosymmetry in the Functional Properties of Perovskite Structured Ceramics
Materials Science and Engineering, Mappin St., University of Sheffield, Sheffield, S13JD

11:40 – 12:00 B. Mihailova

Further insights into the mesoscopic-scale atomic arrangements in perovskite-type relaxor ferroelectrics from x-ray absorption spectroscopy
Fachbereich Geowissenschaften, Universität Hamburg, Grindelallee 48, 20146 Hamburg, Germany

12:00 – 12:20 A. Kania

Relationship between Structural Characteristics and Polar Properties of Nonstoichiometric Silver Niobate $\text{Ag}_x\text{NbO}_{2.5+x/2}$
A. Chelkowski Institute of Physics, University of Silesia, Uniwersytecka 4, Katowice, Poland

10:20 – 12:40 Chaired by:
S. Lang

Aula Parva
Ferroelectric & Piezoelectric properties I

10:20 – 11:00 **J. Roedel**
(invited)

Lead-free bismuth-based relaxor ferroelectric composites
Institute of Materials Science, TU Darmstadt, Alarich-Weiss-Straße 2, 64287 Darmstadt, Germany

11:00 – 11:20 D. Zabeck

Performance of thin film polyvinylidene fluoride for pyroelectric energy harvesting
Department of Mechanical Engineering, University of Bath, Bath, BA2 2ET, UK

11:20 – 11:40 H.W. Gundel

High frequency dielectric characterization of high-k functional thin films
IETR UMR CNRS 6164, Lunam Université, Université de Nantes, 2 rue de la Houssinière, 44322 Nantes Cedex 3, France

11:40 – 12:00 J. Sestoke

Simultaneous Monitoring of the Electromechanical Coupling Coefficients and Domain Structural Changes of the PMN-32%PT Crystals during Poling Process
Prof. Kazimieras Barsauskas Ultrasound Research Institute, Kaunas University of Technology Studentų St. 50, Kaunas, Lithuania, LT-51368

12:00 – 12:20	A. Moure	Study of the Domain Structure of $\text{Bi}_4\text{Ti}_3\text{O}_{12}$ Ceramics by Raman Confocal Spectroscopy and its Influence on the Electrical Polarization <i>Ceramics for Smart Systems Group, Electroceramic Department, Instituto de Cerámica y Vidrio, CSIC, Kelsen 5, 28049 Madrid, Spain</i>
12:20 – 12:40	P. Vaněk	Electrical Activity of Ferroelectric Biomaterials <i>Institute of Physics ASCR, Na Slovance 2, CZ-18221 Prague, Czech Republic</i>
10:20 – 12:40	Chaired by: P. Vilarinho	Seminar Room Non Perovskites
10:20 – 11:00	M. Josse (invited)	About the relaxor behaviour in TTBs: a crystal-chemical viewpoint <i>Université de Bordeaux, CNRS, ICMCB, 87 av. dr. A. Schweitzer, 33600 Pessac, France</i>
11:00 – 11:20	V. I. Voronkova	Polymorphism Peculiarities of Bi_2WO_6 and Bi_2MoO_6 Aurivillius Phases <i>M.V. Lomonosov Moscow State University, Faculty of Physics, Leninskie gory, 119991, Moscow, Russia</i>
11:20 – 11:40	E. Smirnova	Incipient ferroelectric-like behavior of langasites <i>Saint-Petersburg, Russia, Ioffe Physical-Technical Institute</i>
11:40 – 12:00	Y. Zheng	Growth of Large Diameter YCOB and LGS Crystals for Nonlinear Optical and Piezoelectric Applications <i>Shanghai Institute of Ceramics, Chinese Academy of Sciences, Jiading, Shanghai/P. R. China</i>
12:00 – 12:20	A. Bartasyte	Resonant Raman scattering in LiNbO_3 and LiTaO_3 <i>Femto-ST Institute, University of Franche-Comté and CNRS (UMR 6174), 32 avenue de l'Observatoire, Besançon, France, 25044 Jean Lamour Institute, Lorraine University and CNRS (UMR 7198), Parc du Saurupt, Nancy, France, 54011</i>
12:20 – 12:40	M. D. Fontana	Photorefractive properties probed by Raman spectroscopy in ferroelectric materials <i>Université de Lorraine, Laboratoire Matériaux Optiques, Photonique et Systèmes, 2 Rue E. Belin 57070 Metz (France) Supélec, Laboratoire Matériaux Optiques, Photonique et Systèmes, 2 Rue E. Belin 57070 Metz (France)</i>
12:40 – 14:20	Lunch	
14:20 – 15:40	Chaired by: A.N. Salak	The Theatre hall Perovskites V
14:20 – 15:00	Z.-G. Ye (invited)	Synthesis, Structure and Properties of $\text{Pb}(\text{Zr}_{1-x}\text{Ti}_x)\text{O}_3$ Single Crystals <i>Department of Chemistry and 4D LABS, Simon Fraser University, Burnaby, British Columbia, V5A 1S6, Canada Electronic Mater. Res. Lab. & Intl. Center for Dielectric Research, Xi'an Jiaotong University, Xi'an, 710049, China</i>
15:00 – 15:20	M. Ivanov	Grain Size Effect on Dielectric Permittivity of $0.36\text{BiScO}_3 - 0.64\text{PbTiO}_3$ Perovskite Ceramics <i>Faculty of Physics, Vilnius University, Saulėtekio av. 9/3, LT-10222 Vilnius, Lithuania</i>
15:20 – 15:40	S. Sadykov	Electroluminescence studies of the polarization switching in PLZT relaxor ceramics <i>Daghestan State University, 367000 Makhachkala, Daghestan, Russia</i>

14:20 – 15:40	Chaired by: V. Fridkin	Aula Parva Ferroelectric & Piezoelectric properties II
14:20 – 15:00	A. Bell (invited)	Variation of Piezoelectric Properties and Mechanisms Across the Relaxor-Ferroelectric Continuum in $\text{BiFeO}_3\text{-(K}_{1/2}\text{Bi}_{1/2})\text{TiO}_3\text{-PbTiO}_3$ Ceramics <i>Institute for Materials Research, University of Leeds, Leeds, UK</i>
15:00 – 15:20	T. Schenk	Insights into Analyzing the Electric Field Cycling Behavior of Ferroelectric Doped Hafnium Oxide <i>NaMLab gGmbH, Noethnitzer Str. 64, D-01187 Dresden, Germany</i>
15:20 – 15:40	O. Malyshkina	Evolution of dielectric hysteresis loops in alternating field of constant amplitude <i>Tver State University, Tver, Russia</i>
14:20 – 15:40	Chaired by: S. Vakhrushev	Seminar Room Theory & Modeling I
14:20 – 15:00	A. Tagantsev (invited)	Antiferroelectricity: competing instabilities and domain walls <i>Ceramics Laboratory, Swiss Federal Institute of Technology (EPFL), CH-1015 Lausanne, Switzerland</i> <i>Ioffe Physical Technical Institute, 26 Politekhnicheskaya, 194021 St. Petersburg, Russia</i>
15:00 – 15:20	A. Leschhorn	Microscopic model of polarization switching <i>Institute of Electrical Engineering Physics, Saarland University, 66041 Saarbruecken, Germany</i>
15:20 – 15:40	P. Aguado-Puente	First principles investigation of 2-dimensional electron gases in ferroelectric thin films <i>CIC NanoGUNE and DIPIC, Tolosa Hiribidea 76, 20018 San Sebastián, Spain</i>
15:40 – 16:00	Coffee	
16:00 – 17:20	Chaired by: V. Ya. Shur	The Theatre hall Perovskites VI
16:00 – 16:20	S.Y. Lim	Piezoelectric and dielectric properties of doping and A-site non-stoichiometric effect on $(\text{Na}_{0.5}\text{K}_{0.5})\text{NbO}_3$ ceramics <i>School of Advanced Materials Engineering, Changwon National University Gyeongnam 641-773, Korea</i>
16:20 – 16:40	J. Ćirković	Processing-Dependent Dielectric and Ferroelectric Properties of BST Ceramics <i>Institute for multidisciplinary research, University of Belgrade, Kneza Višeslava 1, 11030 Belgrade, Serbia</i>

		Aula Parva
16:00 – 17:20	Chaired by: A. Schönecker	Ferroelectric & Piezoelectric properties III
16:00 – 16:20	E. D. Politova	Phase Transitions, Ferroelectric and Piezoelectric Properties of Bismuth-Based Perovskite Ceramics <i>L.Ya.Karpov Institute of Physical Chemistry, Obukha s.-st., 3-1/12, b.6, 105064, Moscow, Russia</i>
16:20 – 16:40	X.-K. Wei	Atomic-scale determination of spontaneous polarization in the antiphase boundary of antiferroelectric PbZrO ₃ <i>Ceramics Laboratory, Swiss Federal Institute of Technology Lausanne (EPFL), Lausanne CH-1015, Switzerland Peter Grünberg Institute and Ernst Ruska Center for Microscopy and Spectroscopy with Electrons, Research Center Jülich, 52425 Jülich, Germany</i>
16:40 – 17:00	R. Renoud	Response of a ferroelectric to an electric field: the Rayleigh law and its extensions <i>Institut d'Electronique et de Télécommunication de Rennes, University of Nantes, Nantes, France</i>
17:00 – 17:20	C. Borderon	Dielectric losses due to domain walls in ferroelectric materials <i>Institut d'Électronique et de Télécommunications de Rennes, University of Nantes, Nantes, France</i>
		Seminar Room
16:00 – 17:20	Chaired by: K. Roleder	Theory & Modeling II
16:00 – 16:20	E. Bousquet	Geometric Ferroelectricity in Fluoro-Perovskites <i>Physique Théorique des Matériaux, Université de Liège, B-4000 Sart Tilman, Belgium</i>
16:20 – 16:40	L. Padurariu	Local field engineering for designing tunable composite materials <i>Faculty of Physics, Alexandru Ioan Cuza University, 11 Bv. Carol I, 700506 Iasi, Romania</i>
16:40 – 17:00	E. E. Tornau	Phase transition properties of Bell-Lavis model <i>Semiconductor Physics Institute, Center for Physical Sciences and Technology, Goštauto 11, LT-01108 Vilnius, Lithuania</i>
17:00 – 17:20	A. Starkov	Application of the matrix homogenization method for calculation of effective properties of laminated composites <i>Institute of Refrigeration and Biotechnology, National Research University of Information Technologies, Mechanics and Optics, Kronverksky pr. 49, 197101 St. Petersburg, Russia</i>
17:20 – 17:40	V. E. Gevorkyan	Polarization Switching Phenomena in the Polymer Ferroelectrics at the nanoscale <i>Southern Federal University, Russia</i>
17:40 – 19:00	Poster Session II	

Thursday, July 10th, 2014

09:00 – 09:50 **Plenary Session III (The Theatre hall)** | Chaired by: I. Reaney

V.Ya. Shur

Domain Nanotechnology in Uniaxial Ferroelectrics of Lithium Niobate and Lithium Tantalate Family

Ferroelectrics Laboratory, Institute of Natural Sciences, Ural Federal University, 51 Lenin Ave., 620000 Ekaterinburg, Russia

09:50 – 10:20 **Coffee**

10:20 – 12:40 Chaired by: **The Theatre hall**
M. D. Fontana **Ferroelectric & Piezoelectric properties IV**

10:20 – 11:00 **P. M. Vilarinho** Single crystals versus polycrystals of $K_{0.5}Na_{0.5}NbO_3$ towards
(invited) optimized electromechanical performance

Department of Materials and Ceramics Engineering, CICECO, University of Aveiro, 3810-193 Aveiro, Portugal

11:00 – 11:20 D.B. Deutz Design driven development of piezoelectric touch-sensitive
luminous flexible plastics

Novel Aerospace Materials, Faculty of Aerospace Engineering, Delft University of Technology, Kluyverweg 1, 2629 HS Delft, The Netherlands

11:20 – 11:40 G. Clarke Phase pure, monocrystalline bismuth ferrite nanoparticles for
biomedical applications

Nanomedicine, Department of Clinical Medicine, Trinity College Dublin, Ireland

11:40 – 12:00 K. V. Lalitha Stress induced structural transformation at the MPB of
 $BiScO_3$ - $PbTiO_3$ solid solution

Department of Materials Engineering, Indian Institute of Science, Bangalore, India

12:00 – 12:20 J.-H. Jeon Templated Grain Growth of Textured $(K,Na,Li)(Nb,Ta)O_3$
Piezoelectric Ceramics

Korea Institute of Materials Science, 797 Changwondaero, Changwon, Korea

12:20 – 12:40 Y. Tajitsu Sensing complicated motion of human body using piezoelectric
chiral polymer fiber

Kansai University, Electrical Engineering Department, 3-3-35 Yamate Suita, Osaka 564-8680, Japan

10:20 – 12:40 Chaired by: **Aula Parva**
F. Morrison **Devices & Applications**

10:20 – 11:00 **A. Schönecker** Smart Microsystems based on Piezoceramic Thick Films –
(invited) Application Overview

Fraunhofer IKTS, 01277 Dresden, Winterbergstraße. 28, Germany

11:00 – 11:20 R. Sliteris Air-coupled Ultrasonic Transducers based on an Application of
the PMN - 32% PT Single Crystals

Prof. K. Barsauskas Ultrasound Research Institute of Kaunas University of Technology, Studentu St. 50, Kaunas, Lithuania, LT-51368

11:20 – 11:40 M. Zirkl PyzoFlex[®] - a novel, ferroelectric Human Machine Interface for
flexible Electronics

Institute of Surface Technologies and Photonics, JOANNEUM RESEARCH Forschungsgesellschaft mbH, Weiz, Austria

11:40 – 12:00	C. R. Bowen	Manufacture and characterisation of piezoelectric broadband energy harvesters based on asymmetric bistable laminates <i>Department of Mechanical Engineering, University of Bath, Bath, BA2 7AY, UK</i>
10:20 – 12:40	Chaired by: P. Zubko	Seminar Room Domain engineering I
10:20 – 10:40	L.S. Kokhanchik	E-beam recording of regular domain structures on the nonpolar surface of LiNbO ₃ crystals and their investigations by PFM and SHG microscopy <i>Institute of Microelectronics Technology and High Purity Materials, Chernogolovka, Moscow region, 142432, Russia</i>
10:40 – 11:00	T. Sluka	Towards Devices Based on Charged Domain Walls in Ferroelectrics <i>Ceramics Laboratory, EPFL Swiss Federal Institute of Technology, Lausanne, CH-1015 Switzerland</i> <i>DPMC-MaNEP, University of Geneva, 24 Quai Ernest-Ansermet, 1211 Geneva 4, Switzerland</i>
11:00 – 11:20	A. Akhmatkhanov	Investigation of Domain Kinetics in MgO Doped Stoichiometric Lithium Tantalate <i>Ferroelectrics Laboratory, Institute of Natural Sciences, Ural Federal University, 51 Lenin Ave., 620000 Ekaterinburg, Russia</i>
11:20 – 11:40	P. Mokřý	Optical properties near neutral and charged ferroelectric domain walls <i>Regional Centre for Special Optics and Optoelectronic Systems (TOPTEC), Institute of Plasma Physics, Academy of Sciences of the Czech Republic, Soboteká 1660, CZ-51101 Turnov, Czech Republic</i>
11:40 – 12:00	V.Ya. Shur	Charged Domain Walls in Lithium Niobate with Inhomogeneous Modification of Bulk Conductivity <i>Ferroelectrics Laboratory, Institute of Natural Sciences, Ural Federal University, 51 Lenin Ave., 620000, Ekaterinburg, Russia</i>
12:40 – 14:20	Lunch	
14:20 – 18:00	Excursion	
19:00 – 22:00	Conference Dinner	

Friday, July 11th, 2014

09:00 – 09:50 **Plenary Session IV (The Theatre hall)** | Chaired by: A. Bell

V. Fridkin

Ferroelectric properties and the Bulk Photovoltaic Effect at the Nanoscale

Shubnikov Institute of Crystallography of the Academy of Sciences, Russia

09:50 – 10:20 **Coffee**

Chaired by:		The Theatre hall
10:20 – 11:40	T. Sluka	Domain engineering II
10:20 – 10:40	A. Crassous	Fine tuning of the ferroelectric domain structure in La-doped BiFeO ₃ towards domain wall based electronics <i>Ceramics Laboratory, Ecole Polytechnique Fédérale de Lausanne, CH1015-Lausanne, Switzerland</i>
10:40 – 11:00	L. J. McGilly	Controlling ferroelectric domain wall motion <i>Ceramics Laboratory, Swiss Federal Institute of Technology (EPFL), CH-1015 Lausanne, Switzerland</i>
11:00 – 11:20	V. Yu. Topolov	Orientation Effects in the Formation of Hydrostatic Piezoelectric and Energy-harvesting Parameters of Novel Composites Based on Relaxor-ferroelectric Single Crystals <i>Department of Physics, Southern Federal University, 5 Zorge Street, 344090 Rostov-on-Don, Russia</i> <i>Scientific Design & Technology Institute “Piezopribor”, Southern Federal University, 10 Milchakov Street, 344090 Rostov-on-Don, Russia</i>
11:20 – 11:40	J. R. Whyte	Controlling domain dynamics in topographically engineered ferroelectric capacitors <i>School of Mathematics and Physics, Queen's University Belfast, Belfast, U.K.</i>
Chaired by:		Aula Parva
10:20 – 11:40	J. Banyas	Conductivity
10:20 – 10:40	A.V. Shlyakhtina	Oxygen ion and mixed conductivity in the Pr ₂ O ₃ -ZrO ₂ system <i>Semenov Institute of Chemical Physics, Russian Academy of Sciences, Moscow, 119991, Russia</i>
10:40 – 11:00	Y. Cho	Conduction in nanodomain inversion dots in congruent lithium tantalate single crystal <i>Research Institute of Electrical Communication, Tohoku University, Katahira, Aoba-ku, Sendai 980-8577, Japan</i>
11:00 – 11:20	V. Venckute	Preparation and characterization of solid electrolytes based on TiP ₂ O ₇ pyrophosphate <i>Faculty of Physics, Vilnius University, Saulėtekio av. 9/3, LT-10222 Vilnius, Lithuania</i>
11:20 – 11:40	A. Dziaugys	Dielectric, XRD and ultrasonic investigations of Cu _{0.15} Fe _{1.7} PS ₃ mixed crystal <i>Faculty of Physics, Vilnius University, Saulėtekio av. 9/3, LT-10222 Vilnius, Lithuania</i>
11:40 – 12:20	Closing ceremony (The Theatre hall)	

POSTER SESSION I

Tuesday, July 8th, 2014

17:40 – 19:00

- P1-1** **D. Gabrielaitis, M. Kinka, M. Albino, M. Josse, V. Samulionis, R. Grigalaitis, M. Maglione, J. Banys**
Rare-Earth and Niobium ion substitution effects on the dielectric response of $\text{Ba}_2\text{REFeNb}_{4x}\text{Ta}_x\text{O}_{15}$ (RE = Nd, Eu) ceramics
- P1-2** **A. Olšauskaitė, Š. Svirskas, M. Ivanov, T. Šalkus, A. Kežionis, J. Banys, M. Dunce, E. Birks, M. Antonova, A. Sternberg**
Broadband dielectric spectroscopy of $x\text{Na}_{0.5}\text{Bi}_{0.5}\text{TiO}_3-(1-x)\text{Sr}_{0.7}\text{Bi}_{0.2}\text{TiO}_3$ solid solutions
- P1-3** **J. Belovickis, J. Macutkevicius, Š. Svirskas, V. Samulionis, J. Banys, O. Shenderova**
Dielectric spectroscopy of polymer based PDMS nanocomposites with ZnO nanoparticles
- P1-4** **A. Sakanas, R. Grigalaitis, J. Banys, L. Mitoseriu, V. Buscaglia, P. Nanni**
The Alternative Expression of Lichtenecker's Mixing Formula and Its Application to the Broadband Dielectric Spectroscopy of $\text{BaTiO}_3 - \text{Ni}_{0.5}\text{Zn}_{0.5}\text{Fe}_2\text{O}_4$ Composites
- P1-5** **A. Sakanas, R. Grigalaitis, J. Banys, L. Mitoseriu, V. Buscaglia, P. Nanni**
Dielectric spectroscopy characterization of $0.7\text{BaTiO}_3 - 0.3\text{Ni}_{1/2}\text{Zn}_{1/2}\text{Fe}_2\text{O}_4$ composite ceramics
- P1-6** **R. Mackeviciute, J. Banys, P. Szklarz**
Dielectric properties of diammoniumhypodiphosphate $(\text{NH}_4)_2\text{H}_2\text{P}_2\text{O}_6$ (ADhP)
- P1-7** **R. Mackeviciute, R. Grigalaitis, M. Ivanov, R. Sliteris, J. Banys**
Dielectric and pyroelectric properties of PMN-29PT single crystal near MPB
- P1-8** **E. Palaimiene, J. Macutkevicius, A. Kania, J. Banys**
Dielectric properties of $0.9\text{PbMg}_{1/3}\text{Ta}_{2/3}\text{O}_3 - 0.1\text{PbTiO}_3$ single crystals
- P1-9** **J. Macutkevicius, A. Molak and J. Banys**
Broadband dielectric spectroscopy of NaNbO_3 ceramics
- P1-10** **J. Macutkevicius, A. Paddubskaya, J. Banys, P. Kuzhir, S. Maksimenko, M. Letellier, V. Fierro, A. Celzard**
Broadband dielectric properties of carbon foams
- P1-11** **I. Kranauskaitė, J. Macutkevicius, J. Banys, D. Krasnikov, S. Moseenkov, V. Kuznetsov**
Influence of carbon nanotube length on composite dielectric properties
- P1-12** **V. Samulionis, Š. Svirskas, J. Banys, A. Sánchez-Ferrer, R. Mezzenga**
Ultrasonic and Dielectric Studies of Polyurea Elastomer Composites with Inorganic Nanoparticles
- P1-13** **V. Samulionis, Š. Svirskas, J. Banys, A. Sánchez-Ferrer, R. Mezzenga, N. Gimeno, M.B. Ros**
Phase Transitions in Polymers with Highly Ordered Liquid-Crystalline Phases
- P1-14** **A. Molnar, R. Bilanych, R. Yevych, A. Kohutych, V. Samulionis, J. Banys, K. Rushchanskii, Yu. Vysochanskii**
Nonequilibrium effects near the Lifshitz point in $\text{Sn}_2\text{P}_2(\text{Se}_x\text{S}_{1-x})_6$ uniaxial ferroelectrics
- P1-15** **Ryszard Skulski, Dariusz Bochenek, Artur Chrobak, Ewa Nogas-Ćwikiel, Przemysław Niemieć**
Dielectric and magnetic properties of $(1-x)\text{PZT}-(x)\text{PFW}$ ceramics with $0.25 < x < 0.55$
- P1-16** **I. Gruszka, A. Kania, S. Miga, E. Talik**
Multiferroic properties of lead iron niobate $\text{PbFe}_{1/2}\text{Nb}_{1/2}\text{O}_3$ ceramics and single crystals

-
- P1-17** **J.Suchanicz, G.Klimkowski, D.Sitko, M.Antonova, A.Sternberg**
SrTiO₃ and Pr effects on structural, dielectric and ferroelectric properties of Na_{0.5}Bi_{0.5}TiO₃ ceramic
-
- P1-18** **J.Suchanicz, K.Konieczny, I.Faszczowy, M.Karpierz, U.Lewczuk, B.Urban, G.Klimkowski, M.Antonova, A.Sternberg**
Sb effect on structural, dielectric and ferroelectric properties of Na_{0.5}K_{0.5}NbO₃ ceramics
-
- P1-19** **R. Boschilia, A.L. Boaventura, A.C. Hernandes, E. Antonelli**
Effect of sintering temperature and time on dielectric properties of Ba(Ti_{0.75}Zr_{0.15})O₃-(Ba_{0.77}Ca_{0.23})TiO₃ 50/50 ceramics
-
- P1-20** **Yu.A. Draginda, S.P. Palto, S. G. Yudin, V. V. Lazarev**
Organic one-dimensional photonic crystals with ferroelectric properties
-
- P1-21** **Cristina E. Ciomaga, Mirela Airimioaei, George Stoian, Marco Deluca, Carmen Galassi and Liliana Mitoseriu**
Effect of reoxidation annealing on electrical properties in ceramic composites
-
- P1-22** **A. Sotnikov, H. Schmidt, M. Weihnacht, R. Möckel, C. Reuther, J. Götze**
Elastic constants of GdCa₄O(BO₃)₃ single crystal in a wide temperature range
-
- P1-23** **Oleg Ivanov, Elena Danshina**
Elastic and anelastic properties of the relaxor ferroelectric 0.55SrTiO₃-0.45BiScO₃
-
- P1-24** **Elena Danshina, Oleg Ivanov**
Relaxor properties of the KBiScNbO₆ double perovskite
-
- P1-25** **P. Konsin, B. Sorkin**
The vibronic-proton mechanism of the ferroelectric phase transition in the KH₂PO₄-type systems
-
- P1-26** **N. Horchidan, A. Ianculescu, H. Ursic, B. Malic, M. Deluca, L. Curecheriu, L. Padurariu, L. Mitoseriu**
The influence of microstructure on functional properties of Ba(Sn_xTi_{1-x})O₃ ceramics
-
- P1-27** **L.P. Curecheriu, M.T. Buscaglia, V. Buscaglia, C. Padurariu, Mitoseriu**
Combining antiferroelectric-ferroelectric in composite in searching new functional properties
-
- P1-28** **O. Kvyatkovskii**
Local structural and electronic properties of chemically disordered ferroelectric relaxor PbMg_{5/3}Nb_{2/3}O₃
-
- P1-29** **E.V. Barabanova, O.V. Malyshkina, S.I. Pugachev**
Effect of metallization method on the dielectric properties of PZT ceramics
-
- P1-30** **E.P. Kharitonova, V.I. Voronkova**
Conductivity and Dielectric Properties of Nd₅Mo₃O₁₆-Based Solid Solutions
-
- P1-31** **E.I. Orlova, I.A. Verin, N.I. Sorokina, V.I. Voronkova**
Growth and properties of KTiOPO₄ single crystals doped with barium and chromium
-
- P1-32** **L. Xu, J. Xiao, B. F. Costa, J. A. Paixão**
Calorimetric study of ferroelectric BiInO₃-PbTiO₃ crystals
-
- P1-33** **F. Le Goupil, J. Dec, A-K. Axelsson, L. J. Dunne, M. Valant, G. Manos, T. Lukaszewicz, A. Berenov, and N. McN Alford**
Relaxor Strontium-Barium Niobate: A Lead-Free Anisotropic Electrocaloric Material
-
- P1-34** **Mehmet Sanli alp, Vladimir V. Shvartsman, and Doru C. Lupascu**
Direct measurements of the electrocaloric effect in relaxor ceramics
-
- P1-35** **V. Stepkova, P. Marton, N. Setter and J. Hlinka**
Close-circuit domain quadruplets in BaTiO₃ nanorods embedded in SrTiO₃ film
-
- P1-36** **B.Kh. Khannanov, E.I. Golovenchits, and V.A. Sanina**
Rare-earth polar order and polarization due to multiferroic domain formation in YCrO₃
-

-
- P1-37** **D.S. Chezganov, M.M. Smirnov, D.O. Alikin, M.M. Neradovskiy, D.V. Zorikhin, D.K. Kuznetsov, V.Ya. Shur**
Domain Switching by Electron Beam Irradiation of Z+ Polar Surface in Mg-doped Lithium Niobate
-
- P1-38** **M. Mtebwa, L. Feigl, N. Setter**
PLD Growth and Domain Patterns of Highly Tetragonal Epitaxial PZT (110) Thin Films
-
- P1-39** **M. P. Campbell, J. R. Whyte, A. Kumar, J. M. Gregg**
Domain wall conduction in Ytterbium Manganite
-
- P1-40** **A. Irzhak, D. Irzhak, L. Kokhanchik**
Study of planar domain structures in LiNbO₃ crystals using Raman spectroscopy and X-ray diffractometry
-
- P1-41** **M. Dunce, E. Birks, A. Kuzmin, R. Ignatans, A. Plaude, M. Antonova, A. Sternberg**
X-ray diffraction and Raman spectroscopy studies in Na_{1/2}Bi_{1/2}TiO₃-SrTiO₃-PbTiO₃ solid solutions
-
- P1-42** **L.A Saska, A.A Felix, A.Z. Simões, M.A Ramirez**
Solid state reaction of multifunctional strontium modified CaCu₃Ti₄O₁₂ powders
-
- P1-43** **H.H. Kim, D.C. Oh, and G.I. Jang**
Properties and Deposition of TiNOx Thin films using Reactive Magnetron Sputtering
-

POSTER SESSION II

Tuesday, July 9th, 2014

17:40 – 19:00

- P2-1** **D.A. Kiselev, R.N. Zhukov, A.S. Bykov, S.V. Ksenich, M.D. Malinkovich, Yu.N. Parkhomenk**
Electric field distribution on grain boundaries in LiNbO₃ thin films
- P2-2** **A. Sigov, Yu. Podgorny, A. Vishnevskiy, and K. Vorotilov**
Charge transport phenomenon in PLZT thin films
- P2-3** **A. Kozyrev, A. Mikhailov, S. Ptashnik, N. Alford, P. Petrov**
Strontium Titanate Thin Film Multilayer Structures for Switchable FBAR Applications
- P2-4** **Š. Bagdzevičius, J. Banys, N. Setter**
Pulsed laser deposition and characterization of compressively-strained SrTiO₃ thin films
- P2-5** **T. Samoylova, M. Gaidukov, A. Gagarin, A. Tumarkin, A. Kozyrev**
Injected charge as a cause of slow dielectric relaxation in thin film Pt/BSTO/Cu structures
- P2-6** **K. Vorotilov, D. Seregin, A. Sigov**
PZT films prepared by sol-gel with low lead content seeding layer
- P2-7** **S. Hillmann, S. Li, K. Rachut, T.J.M. Bayer, A. Klein**
Control of carrier injection into dielectric BST thin films
- P2-8** **G.A. Komandin, O.E. Porodinkov, I.E. Spector, A.A. Volkov, K.A. Vorotilov, D.S. Seregin, A.S. Sigov**
Dielectric response of Pb(Zr,Ti)O₃ thin films on platinized silicon substrate in THz-IR frequency range
- P2-9** **A.V. Tumarkin, S.V. Razumov, A.G. Gagarin, M.M. Gaidukov, A.B. Kozyrev**
Composition control of multicomponent ferroelectric films
- P2-10** **A.V. Solnyshkin, A.A. Bogomolov, I.L. Kislova, V.A. Belyakov**
Dynamic pyroelectric response of ferroelectric films on various substrates
- P2-11** **H. Odagawa, T. Yanagitani, Y. Cho**
Measurement of Polarization Structure in Layered Piezoelectric Thin Films Using Scanning Nonlinear Dielectric Microscopy
- P2-12** **K. Bormanis, A.I. Burkhanov, Luu Thi Nhan, M. Antonova, and S.V. Mednikov**
Low Frequency Relaxation of Barium-Strontium Niobate Ceramics Under Light Irradiation
- P2-13** **M.N. Palatnikov, K. Bormanis, N.V. Sidorov and O.V. Makarova**
Resistance to Radiation of Lithium Niobate Crystals
- P2-14** **Yadвига Bodnarchuk, prof dr Tatyana Volk, dr Radmir Gainutdinov, Feng Chen, Hongliang Liu**
Fabrication of regular microdomains patterns by the AFM method in helium-implanted optical waveguides on strontium-barium niobate crystals
- P2-15** **V. Yu. Topolov, A. E. Panich, S. E. Filippov, AND E. A. Panich**
Highly Anisotropic Piezo-active 1–3–0 composites: Microgeometry – Volume-fraction Relations
- P2-16** **S.N. Kallaev, Z.M. Omarov, K.G. Abdulvakhidov, S.A. Sadykov**
Heat capacity of nanocrystalline BaTiO₃ ferroelectric ceramics
- P2-17** **A. Nesterov, O. Petrov, M. Trubitsyn, M. Vogel, M. Volnianskii**
NMR study of ⁷Li spin-lattice relaxation in Li₂O-7GeO₂ compounds
- P2-18** **V.N. Osadchy, D.M. Kosmin, A.V. Tumarkin, A.G. Altyinnikov, A.D. Kanareykin, I.V. Kotelnikov, R.A. Platonov, A.B. Kozyrev, E.A. Nenasheva**
Suppression of slow capacitance relaxation phenomenon in M/Ba_xSr_{1-x}TiO₃/M ceramic ferroelectric structures by annealing in oxygen atmosphere

-
- P2-19** **R.A. Platonov, V.A. Volpyas, O.I. Soldatenkov, A.B. Kozyrev**
The dynamics of thermal processes in capacitance thermal-to-electric energy converter
-
- P2-20** **I.V. Kubasov, M.D. Malinkovich, A.S. Bykov, R.N. Zhukov, D.A. Kiselev, S.V. Ksenich**
Actuator for precision positioning based on single crystalline lithium niobate
-
- P2-21** **V. Dyu, E. Khudyakova, S. Shandarov, M. Kisteneva, A. Akrestina, Yu. Kargin**
Light-induced absorption in $\text{Bi}_{12}\text{TiO}_{20}:\text{Al}$ crystal
-
- P2-22** **S. Navickaitė, R. Bansevicius, V. Jūrėnas, V. Bakanauskas**
Piezoelectric Laser Scanning/Deflecting Manipulator for Organizing the Swarm of the Nanosatellites
-
- P2-23** **J. Miao, J. Xiao, M. R. Silva, M. Kumaresavanji, J. P. Araújo, B. F. Costa, J. A. Paixão**
Fabrication for Magnetic Nanoparticle System of $\text{M}_{0.9}\text{Fe}_{0.1}\text{O}$ (M=Ni, Cu) by Co-precipitation
-
- P2-24** **Jae-Hyeon Ko, Min-Seok Jeong, Byoung Wan Lee, Krystian Roleder, Annette Bussmann-Holder, Andrzej Majchrowski, Young Ho Ko, Kwang Joo Kim**
Enhanced Polarization Fluctuations in $\text{PbZr}_{0.72}\text{Sn}_{0.28}\text{O}_3$ Compared to PbZrO_3 Single Crystals Studied by Brillouin Light Scattering
-
- P2-25** **A. S. Perin, V. M. Shandarov, V. G. Kruglov**
Spatial modulation instability in undoped Lithium niobate Fabry-Perot interferometer
-
- P2-26** **Yu. Vasyukiv, M. Smyk, I. Skab, R. Vlokh**
Topological defects of the optical anisotropy parameters as a tool for stress tensor field reconstructions in glasses
-
- P2-27** **O. Mys, A. Grabar, I. Martynyuk-Lototska, B. Zapeka, M. Kostyrko, R. Vlokh**
The $\text{Pb}_2\text{P}_2\text{Se}_6$ crystals – new efficient acoustooptic materials
-
- P2-28** **A. Kanshu, V. Kruglov, A. Perin, D. Petnev, V. Shandarov, F. Chen**
Optical Modulation of Femtosecond Laser-Written 1D Photonic Lattice in Lithium Niobate
-
- P2-29** **L.P. Lyashenko, L.G. Shcherbakova, D.A. Belov**
Oxygen-Ion Conductivity of Nanostructured R_2MO_5 (R = Sm, Gd, Dy, Er, Y, Sc; M = Ti, Zr, Hf)
-
- P2-30** **I.V.Ciuchi, F. Craciun, C. Galassi, L. Mitoseriu**
Piezoelectric Properties of La^{3+} doped PZT Ceramics across the antiferroelectric/ferroelectric phase boundary
-
- P2-31** **E.D.Yakushkin**
Uniaxial Ferroelectric in External Magnetic Field
-
- P2-32** **Jakub Havlíček, Jaroslav Hamrle, Jaromír Pištora, Yoichiro Hashizume, Soichiro Okamura**
Optical and electro-optical properties of PZT crystal determined by Mueller matrix ellipsometry
-
- P2-33** **A. Starkov, I. Starkov**
The temperature change in the piezoelectrocaloric element under the periodic electric field
-
- P2-34** **H. L. Saadon, Basil Ali, Adil A. Al-Fregi**
Nonlinear Optical Limiting Effect of New Organotellurium Compounds Containing Azomethine and Azo Groups Under CW Laser Illumination
-
- P2-35** **D.A. Belov, A.V. Shlyakhtina, K.S. Pigalskiy, A.N. Shchegolikhin, I.V. Kolbanev, O.K. Karyagina**
First-order phase transformation in the new oxide ion conductors with pyrochlore structure containing B-site cations in different valence state
-
- P2-36** **M. G. Ranieri, B. Z. Simões, M. A. Ramirez, A.Z. Simões**
Piezo Force Response of $\text{BiFeO}_3/\text{LaFeO}_3$ heterostructures
-

-
- P2-37** **M. Starykevich, A.N. Salak, A.D. Lisenkov, M.L. Zheludkevich, M.G.S. Ferreira**
Zn-Al₂O₃ metal-insulator layer on aluminium via combined electrochemical route
-
- P2-38** **M. V. Silibin, A. V. Solnyshkin, D. A. Kiselev, A. N. Morozovska, E. A. Eliseev, S. A. Gavrilov, D. C. Lupascu, V. V. Shvartsman**
Interface effect on the boundary of ferroelectric polymer and ceramic inclusion in nanocomposite PVDF/BPZT
-
- P2-39** **G.M. Vizdrik**
Interfacial effects in Al/PVDFTrFE/SiO/nSi heterostructures.
-
- P2-40** **Xiaojing Zhu, Emiliano Bilotti, Xiangjian Meng, and Mike Reece**
Characterization of extruded ferroelectric film P(VDF-TrFE)
-
- P2-41** **A.V. Solnyshkin, M. V. Silibin, A. N. Morozovska, E. A. Eliseev, S. A. Gavrilov, V. V. Shvartsman, D. C. Lupascu**
Macro- and microscopic ferroelectric properties of P(VDF-TrFE) copolymer films
-
- P2-42** **I. Bykov, Yu. Zagorodniy, L. Yurchenko, V. Trachevsky, V. Dimza, L. Jastrabik, A. Dejneka**
The peculiarities of influence of copper and lanthanum dopants on ferroelectric and relaxor properties of PLZT ceramics: The investigations by dielectric and radiospectroscopy (EPR, NMR) methods
-

Welcome

Dear Colleagues,

On behalf of the International Advisory Committee we are pleased to welcome you at the European Conference on Applications of Polar Dielectrics (ECAPD-2014) in Vilnius.

ECAPD is a principal European and International forum where the latest research and technological advances in the field of polar dielectric materials are being presented and discussed. The aim of the ECAPD series of conferences is to allow exchange of knowledge and cooperation between specialists in the field and across different related topics, and to realize new trends and problems.

The conference is the 12th in a series that started in Zürich (Switzerland) in 1988 and was followed by the editions in London (UK) in 1992, Bled (Slovenia) in 1996, Montreux (Switzerland) in 1998, Jurmala (Latvia) in 2000, Aveiro (Portugal) in 2002, Liberec (Czech Republic) in 2004, Metz (France) in 2006, Rome (Italy) in 2008, Edinburgh (UK) in 2010 and Aveiro (Portugal) in 2012.

The conference is held in the central campus of Vilnius University, which is one of the oldest universities in Europe, situated in the heart of the historical centre of Vilnius, the capital of Lithuania. The Old Town of Vilnius is distinguished by numerous churches and baroque architecture and is on the list of Unesco World Heritage List. Major attractions and places of interest are a few minutes away, allowing a fulfilling free time.

We are pleased to have you here in Vilnius,

Conference Chair
prof. Jūras Banys

Conference Committees

International Advisory Board

N. Setter - Chairwoman

M. Alexe
J. Banys
S. Bauer
A. Bell
G. Catalan
J. Hlinka
A. Krumins
A. Kholkin
S. Lang
M. Maglione
F. Michelotti
L. Pardo
I. Reaney
E. Ringgaard
J. Roedel
K. Roleder
J. F. Scott
A. S. Sigov
A. K. Tagantsev
S. Trolier-McKinstry
S. Vakhrushev
S. Wada
R. W. Whatmore

Local Organizing Committee

J. Banys - Chairman

R. Grigalaitis
V. Samulionis
M. Ivanov
R. Mackevičiūtė
E. Palaimienė
Š. Svirskas
D. Jablonskas
I. Kranauskaitė
A. Sakanas
S. Balčiūnas
A. Džiaugys
S. Rudys
M. Kinka

ECAPD 2014 CONFERENCE SECRETARIAT Sigita Mušketaitė



Meeting, Destination and Association
Management Company (MMC, DMC, AMC)

ViaConventus UAB / JSC
Kestucio str. 47, LT-08124 Vilnius, Lithuania
Phone: +370 611 62286
Fax: +370 5 2000 782
E-mail: info-ecapd2014@ff.vu.lt
Website: www.ecapd2014.ff.vu.lt

General Information

CONFERENCE VENUE

ECAPD 2014 Conference takes place in Vilnius University (VU) – the oldest and largest Lithuanian higher educational institution. It was founded at a time when the reformation movement was active in Lithuania and Jesuit monks were invited to help fight the mood of reformation. Jesuit monks were quick to take over education. In 1569, they established a college and in 1579 the University of Vilnius was born.

Address: Universiteto str. 3, Vilnius

OFFICIAL LANGUAGE

The official Conference language is English. No translation will be provided.

PROGRAM CHANGES

The organisers cannot assume liability for any changes in the Conference program due to external or unforeseen circumstances.

REGISTRATION AND HOSPITALITY DESK

Please follow indicative signs to reach registration desk and our staff.

June 7	14:00 – 21:00
June 8	08:00 – 19:00
June 9	08:00 – 19:00
June 10	09:00 – 12:40
June 11	09:00 – 12:20

All Conference materials and documentation will be available at the Conference registration counter. ECAPD 2014 Conference staff will be pleased to help you with all the enquiries regarding registration, Conferences material and program. Please do not hesitate to contact the staff members if there is anything they can do to make your stay more enjoyable.

NAME BADGES

All registrants have been issued name tags, which must be worn to gain admission to the Conference facilities and social program. Please note that admission to scientific sessions is strictly restricted to participants wearing their badges. All participants are kindly requested

to wear your name badge during Welcome reception.
Name tags are colour-coded as follows:

Delegate – GREEN

Accompanying person – RED

ECAPD 2014 Secretariat – PURPLE

Sponsor - YELLOW

ONSITE REGISTRATION FEE

Conference fees in Euro including VAT:

Professional	400 €
Student	200 €
Accompanying person	100 €

Registration fee includes:

- Admission to all Scientific Sessions
- Admission to the Welcome Reception
- Handouts of the Conference
- Coffee breaks and Lunches
- Tour to Trakai
- Conference Dinner

Accompanying person fee includes:

- Admission to the Welcome Reception
- Conference Dinner
- Tour to Trakai

COFFEE BREAKS

July 8, 2014 | 09:50 – 10:20

July 8, 2014 | 15:40 – 16:00

July 9, 2014 | 09:50 – 10:20

July 9, 2014 | 15:40 – 16:00

July 10, 2014 | 09:50 – 10:20

July 11, 2014 | 09:50 – 10:20

Coffee, tea and other refreshments will be served in the Cafeteria in Vilnius University.
Please follow the signs to reach coffee stations.

LUNCH

July 8, 2014 | 12:40 – 14:20

July 9, 2014 | 12:40 – 14:20

July 10, 2014 | 12:40 – 14:20

INTERNET AREA

Wireless internet access is available throughout the Conference venue.

Log in: ECAPD 2014

Password: conventus

CURRENCY

The official currency in Lithuania is Litas. You can exchange your foreign currency at Lithuanian banks, exchange bureaux. Credit cards are accepted in most shops, hotels and restaurants. You will find a cash dispenser on nearly every corner and they are accessible 24 hours. Credit cards like Visa, MasterCard are fitly accepted.

All official prices such as Conference fees, social events, etc. set by ECAPD are quoted in Euro. Payments in other currencies is accepted on-site, where Litas will also be accepted. For your information please note that the exchange rate is 1Euro = 3.4528 LT.

LOST AND FOUND

A lost and found service is available at the registration area of the Conference venue.

Technical Instructions for Presenters

ORAL PRESENTATIONS

All meeting halls will be equipped with PC, LCD projector and microphones. The date/hour/room of your presentation(s) is available in the Conference Program. If you are using a slide presentation (Power Point) make sure that you bring it on the USB Flash (stick) or a CD.

Note! If you are planning to use your own computer for presentation inform secretariat about that in advance. Some technical changes must be made before your presentation.

Social events

OPENING RECEPTION

July 7 | 18:00 – 21:00

Restaurant in Vilnius University | Address: Universiteto str. 3

Opening reception is free of charge for Conference participants.

CONFERENCE DINNER

July 10 | 19:00 – 22:00

Vilnius City Hall | Address: Didzioji str. 31

Conference dinner is free of charge for Conference participants.

Note! You have received a Conference dinner ticket in your Conference bag, please bring it to the dinner to guarantee your entrance.



Excursion to Trakai

July 10 | 14:20 – 18:00

Excursion is free of charge for Conference participants.

About Trakai Town

Trakai - the former capital of the Grand Duchy of Lithuania - is a small town located about 28 km from Vilnius. Situated in a picturesque lakeside area it is one of the most popular tourist attractions of the country. The historical part of the town conserved the ruins of Peninsula Castle, the authentic heritage of small ethnic group Karaites and of course the top must see site – the famous insular Castle on the lake, the original gothic style architectural monument from the end of the XIV century, a historical Museum of Trakai nowadays.

ABSTRACT BOOK

Dielectric and Piezoelectric Enhancement of Barium Titanate-based Nano-complex Ceramics based on High-density Heteroepitaxial Interfaces

Satoshi Wada

University of Yamanashi, Japan

swada@yamanashi.ac.jp

For next-generation material science, interface engineering is very key issue, and it can be expected that new phenomena and enhanced properties are originated from interface with structure gradient region. Recently, a new technique was proposed to prepare nano-structured ceramics with heteroepitaxial interfaces between barium titanate (BaTiO_3 , BT) and potassium niobate (KNbO_3 , KN) prepared at low temperatures below 300 °C, and their dielectric and piezoelectric properties were enhanced because of their heteroepitaxial interfaces. To explain the above results, we proposed the following hypothesis, i.e., KN had larger cell volume by 0.5 % than that of BT, and BT unit cell was expanded by epitaxial junction with KN. The origin of high dielectric property of BT is considered of the large converse displacement between the Ti^{4+} ion and the O^{2-} ion octahedron. This is because in the BT unit cell, there is very space in the surrounding Ti^{4+} ion. Thus, anisotropic expansion of BT unit cell can lead to enhancement dielectric properties. On the other hand, bismuth ferrite (BiFeO_3 , BF) had smaller unit cell volume by 1 % than that of BT. Therefore, we expected that the BT unit cell can be compressed and their dielectric properties for the BT-BF nano-structured ceramics were quiet smaller than those for the BT-KN nano-structured ceramics. To confirm the above idea, we prepared BT-KN and BT-BF nano-structured ceramics were prepared by solvothermal method in this study, and their dielectric properties were compared on the view of unit cell volume change of BT. After the reaction, the compacts were washed by ethanol, and dried at 200 °C. The density of the compacts was again measured by the Archimedes method, and the crystal structure of the compact was investigated by XRD. The microstructure was observed using scanning electron microscopy (SEM) and transmittance electron microscope (TEM). For electric measurements, the ceramics were polished and cut into a size of $2 \times 2 \times 0.5 \text{ mm}^3$. Gold electrodes were sputtered on the top and bottom surfaces with an area of $2 \times 2 \text{ mm}^2$. The dielectric properties were measured at various frequencies from 40 Hz to 10 MHz from 20 to 480 °C using an impedance analyzer (Agilent, HP4294A). The strain vs. electric-field (S - E) curves were measured at room temperature and 0.1 Hz using a ferroelectric character evaluation system, and a slope of the S - E curve was regarded as an apparent piezoelectric constant (d_{33}^*). These nano-complex ceramics prepared in this study were porous with a porosity of around 25 ~ 35 %. The dielectric measurements showed that for the BT-KN nano-structured ceramics with KN/BT ratio of 1, the dielectric constant was 300 at 20 °C and 1 MHz, while for the BT-BF nano-complex ceramics with BF/BT ratio of 1, the dielectric constant was 70 at 20 °C and 1 MHz. The strain vs. electric-field curves were also measured for these ceramics, and it was found that the apparent d_{33}^* estimated from its slope of the strain vs. electric-field curves was almost 100 pm/V for the BT-KN nano-complex ceramics, while the apparent d_{33}^* for the BT-BF nano-complex ceramics was less than 20 pm/V. To explain the results, we proposed structure-gradient region (SGR) model dependent of lattice mismatch and material hardness.

Structure and phase transitions in Bi-based perovskites

M. Guennou¹

1- Public Research Centre Gabriel Lippmann, Materials Science Department, 41 Rue du Brill, L-4422 Belvaux Luxembourg

Perovskites display a large variety of structural and physical properties, which can be tuned by chemical composition, or external parameters such as temperature, pressure, strain, electric or magnetic fields. Much of the current interest in perovskites focuses on so-called multiferroics, which possess several ferroic properties such as ferromagnetism, ferroelectricity, and/or ferroelasticity. The interaction of coexisting structural instabilities in multiferroic materials gives rise to intriguing coupling phenomena and extraordinarily rich phase diagrams, both in bulk materials and strained thin films.

After a short reminder of instabilities in perovskites, we will focus on the family of bismuth-based BiMO_3 perovskites which display a remarkable diversity of structures namely related to their $6s^2$ 'lone pair' electrons. We will then discuss in more detail our recent results on the model multiferroics BiFeO_3 and BiMnO_3 which stand out for their multiple and intriguing interacting mechanisms: electric polarity, octahedra rotations, magnetism and cooperative Jahn-Teller distortion.

For the investigation and tuning of the different instabilities, we have chosen the external parameter pressure, which allows modifying the interatomic distances and, thus the interactions, to a much larger extent than any other parameter. Our complementary use of Raman scattering and synchrotron X-ray diffraction (XRD) has led to four main observations: (i) a succession of multiple phase transitions/instabilities with intriguingly large unit cells, (ii) the reduction of the Jahn-Teller distortion through a different process than the model system LaMnO_3 , (iii) a high-pressure phase with an unprecedented giant distortion and polarity for a perovskite under high-pressure and (iv) an insulator-to-metal (IM) phase transition at very high-pressure.

- [1] A. A. Belik, *Journal of Solid State Chemistry* **2012**, *195*, 32.
- [2] D. S. Keeble, E. R. Barney, D. A. Keen, M. G. Tucker, J. Kreisel, P. A. Thomas, *Adv. Funct. Mat.* **2013**, *23*, 184.
- [3] R. Haumont, P. Bouvier, A. Pashkin, K. Rabia, S. Frank, B. Dkhil, W. A. Crichton, J. Kreisel, *Phys. Rev. B* **2009**, *79*, 184110.
- [4] M. Guennou, P. Bouvier, G. S. Chen, R. Haumont, G. Garbarino, J. Kreisel, *Phys. Rev. B* **2011**, *84*, 174107.
- [5] S. Gomez-Salces, F. Aguado, F. Rodriguez, R. Valiente, J. Gonzales, R. Haumont, J. Kreisel, *Phys. Rev. B* **2012**, *85*, 144109.
- [6] M. Guennou, P. Bouvier, P. Toulemonde, C. Darie, C. Goujon, P. Bordet, M. Hanfland, J. Kreisel, *Phys. Rev. Lett.* **2014**, *112*, 075501.

***In situ* structure investigation of piezoceramics by neutron, X-ray and electron diffraction**

H. Fuess¹

Institute of Geo- and Materials Science, Alarich-Weiss-Str. 2, Technische Universität Darmstadt, Germany

hfuess@tu-darmstadt.de

The microscopic structural details of piezoceramics were extensively studied by diffraction techniques, namely neutron and synchrotron radiation, and by transmission electron microscopy. In this studies $\text{Pb}[\text{Zr}_{1-x}\text{Ti}_x]\text{O}_3$ (PZT) piezoceramics and lead-free $\text{Bi}_{1/2}\text{Na}_{1/2}\text{TiO}_3$ -based compounds, which were prepared in the group of Prof. Rödel, were investigated.

Performed studies on PZT were focused on the morphotropic phase boundary (MPB) with $x = 0.52$ - 0.54 . The change in scattered intensities has been followed as a function of an external electric field by synchrotron experiments. The appearance of nandomains has been correlated with the results from X-ray diffraction. Changes in the domain structure under an applied electric field were monitored by *in situ* transmission electron microscopy [1]. The presence of a monoclinic phase was verified by convergent beam electron diffraction (CBED) [2].

Neutron diffraction scattering demonstrated the deviation from cubic symmetry in the lead-free materials. *In situ* TEM revealed the reversible formation of domains under an applied electric field [3]. Stroboscopic *in situ* measurements in the femto-second region elucidated the structural behavior as a function of an external electric field. Structural findings were correlated with macroscopic piezoelectric properties.

[1] R. Theissmann, L. A. Schmitt, J. Kling, R. Schierholz, K. A. Schönau, H. Fuess, M. Knapp, H. Kungl, M. J. Hoffmann, Nanodomains in morphotropic lead zirconate titanate ceramics: On the origin of the strong piezoelectric effect, *J. Appl. Phys.*, 102, 024111, (2007).

[2] R. Schierholz and H. Fuess, Symmetry of domains in morphotropic $\text{PbZr}_{1-x}\text{Ti}_x\text{O}_3$ ceramics, *Phys. Rev. B*, 84, 064122, (2011).

[3] L. A. Schmitt, J. Kling, M. Hinterstein, M. Hoelzel, Wook Jo, H.-J. Kleebe, H. Fuess, Structural investigations on lead-free $\text{Bi}_{1/2}\text{Na}_{1/2}\text{TiO}_3$ -based piezoceramics, *J. Mater. Sci.*, 46, 4368-4376, (2011).

Manganese-related dynamic polar centres in SrTiO₃

R.V. Yusupov¹, D.G. Zverev¹, A.A. Rodionov¹, O.E. Kvyatkovskii², A. Dejneka³, V.A. Trepakov^{2,3}

1- Kazan Federal University, Kremlevskaya 18, 420008 Kazan, Russia

2- Ioffe Physical-Technical Institute RAS, 194021 St-Petersburg, Russia

3- Institute of Physics AV CR, Na Slovance 2, 18221, Prague 8, Czech Republic

Email address: Roman.Yusupov@kpfu.ru

Pure strontium titanate SrTiO₃ (STO) is a so-called quantum paraelectric, which means that the transition to a ferroelectric state in the low temperature range is prohibited by the quantum mechanical effects. On the other hand, there are few ways to induce such transition, e.g., by application of the electric field, uniaxial pressure, illumination with the UV-light or doping with the appropriate off-centre impurities. One of the interesting examples of the impurity-induced effects in STO is the case of its doping with manganese.

Manganese-doped STO (STO:Mn) is among the materials that are studied for decades, in which new intriguing although sample-dependent dielectric and magnetic anomalies are found. Electron paramagnetic resonance (EPR) studies of this material at the temperatures above 100 K reveal the spectra of cubic Mn⁴⁺ and Mn²⁺ centers, several axial Mn³⁺ centers associated with oxygen vacancies, Mn⁴⁺-Mn⁴⁺ pairs. An on-going intense discussion is related to the substitutional position of the Mn²⁺ ions: whether these species replace the octahedral Ti⁴⁺ or 12-fold-coordinated Sr²⁺ and whether this impurity is centrally-symmetric or not.

We report on the new results of the X-band (9.6 GHz) EPR studies of the high-quality Verneuil-grown STO:Mn single crystals from Furuuchi Chemical Corporation. In the EPR spectra the peculiar transformation of the $S = 5/2$ Mn-related signal is observed. While at room temperature and above it reveals an ideal cubic symmetry, on cooling down the spectrum broadens significantly and can hardly be identified below 100 K. At $T \sim 10$ K the spectra of the two low-symmetry $S = 5/2$ Mn-related centres appear and grow steeply in intensity on temperature decrease.

One centre is almost axial, with the principal axis tilted by ~ 12 degrees from the quasi-cubic [001] direction in the (100) or (010) plane. Angular variation of the spectrum is well described by the spin-Hamiltonian with the parameter values of $g_{zz} = 2.0155$, $g_{xx} = g_{yy} = 2.0059$, $D = 645$ MHz and $E = \frac{1}{2}(D_{xx} - D_{yy}) = 31$ MHz. This centre symmetry is monoclinic C_s .

Another centre is of the rhombic C_{2v} symmetry and its principal direction is along the quasi-cubic [011] crystal axis. Angular variation of the spectrum is also described by an $S = 5/2$ spin-Hamiltonian with the following parameters: $g = 2.0032$, $D = 1445$ MHz, $E = -140$ MHz.

Spectra of both centres reveal almost identical temperature dependences and very close hyperfine splitting due to the interaction with $I = 5/2$ manganese nuclear spin ($A = 243$ MHz). The ratio of the two spectra intensities varies strongly from sample to sample.

Ab initio calculations [1] indicate several possibilities of the axial $S = 5/2$ Mn-related centre formation. Among the proposed models there are off-centre Mn²⁺ ion in the Sr (A) site with the C_{4v} symmetry and complex centres that involve the Mn³⁺ ion in the Ti (B) site and an electron either localized at one of the nearest Ti-ions (C_{4v}) or delocalized within two of them (C_{2v}). All the proposed structures imply a nonzero electric dipole moment that may be a source for the observed low-temperature dielectric phenomena in STO:Mn. Reliability of different microscopic models will be discussed within the scope of the described EPR observations.

This work was supported in part by RFBR research projects No. 14-02-31166, 12-02-00879, Program of Presidium RAS "Quantum mesoscopic and disordered systems", and Project CZ.1.5/2.100//03.0058 of the MSM CR.

[1] O.E. Kvyatkovskii, Ab initio calculations of neutral and charged impurity centers of manganese and chromium in strontium titanate, Physics of the Solid State, vol. 54, pp. 1397-1407, (2012).

Influence of time and heat treatment on properties of lead-free KNN ceramics

C. Briegel¹, P. Neumeister¹, A. Schönecker¹

1- Applied Material Mechanics, Fraunhofer Institute for Ceramic Technologies and Systems IKTS, 01277 Dresden, Germany

Email: christoph.briegel@ikts.fraunhofer.de

In the field of piezoelectric ceramics, lead zirconium titanate (PZT) plays a unique role. However, based on the high amount of lead, which is toxic and environmentally harmful, there has been an intensive research on lead-free alternatives in recent years. Modified potassium sodium niobate ceramics (KNN) showed here the most promising results [1-2]. The KNN derivative $(\text{Li}_{0.04}\text{Na}_{0.52}\text{K}_{0.44})_{0.998}(\text{Nb}_{0.84}\text{Ta}_{0.10}\text{Sb}_{0.06})\text{O}_3$ exhibits piezoelectric properties, which are comparable to these of PZT [3]. Besides the good properties, KNN also possesses several disadvantages. Through evaporation of alkali metals during sintering or hygroscopic behavior of the starting

Table 1 Capacitance, loss angle, permittivity of impedance spectroscopy measurements of KNN samples $(\text{Li}_{0.04}\text{Na}_{0.52}\text{K}_{0.44})_{0.998}(\text{Nb}_{0.84}\text{Ta}_{0.10}\text{Sb}_{0.06})\text{O}_3$ analysed over time; sample 1-5 gold coating, 6-10 silver coating.

1 st Measurement		1 day after synthesis		
sample	treatment	C(1.000kHz)[nF]	tanδ [1e-4]	ε (rel)
1-5	gold sputtering	0.841	3101	2049
6-10	silver firing process	0.555	733	1351
	difference	0.286	2368	698
2 nd Measurement		10 days after synthesis; poled		
sample	treatment	C(1.000kHz)[nF]	tanδ [1e-4]	ε (rel)
1-5	gold sputtering	0.4560	580	1122
6-10	silver firing process	0.4475	321	1089
	difference	0.009	259	33
3 rd Measurement		7 weeks after synthesis		
sample	treatment	C(1.000kHz)[nF]	tanδ [1e-4]	ε (rel)
1-5	gold sputtering	0.4295	269	1056
6-10	silver firing process	0.4385	250	1067
	difference	0.009	19	12

materials (carbonates) it is non-trivial to find a low-cost processing-route, which delivers piezoceramics with good as well as reproducible properties. The characteristics of ceramics are not only dependent on impurities, weighing errors or evaporation of dopants, but also strongly on heat treatments, which occur during calcination, sintering or other possible tempering steps. Within our research, we systematically review the synthesis route aiming for a stable production process.

In the present contribution we report on the influence of time and heat treatment after sintering on the properties of KNN lead-free ferroelectric ceramics. We could observe that impedance spectroscopy measurements provide significantly changing results. On the first view, it appeared that samples show different properties due to their electrode coating. Here, KNN samples with a silver coating exhibit lower tan δ and permittivity values compared to samples with gold electrodes. However, with progressing time, the values equalize continually. Eventually, after a sufficiently long period of about seven weeks, both silver and gold coated samples showed similar measurement data. This led us to conclude, that an additional heat treatment, the silver firing step, has accelerated the changing process. It should be noted that poling also has had an essential effect, which can be seen in the “2nd measurement”. This time-dependent behavior is related to domain-wall-processes (e.g. clamping effects), which are strongly accelerated at high temperatures. These studies show that KNN ceramics require a sufficient conditioning time (“aging”) to reach their equilibrium state. By using the Arrhenius equation, a relationship between temperature treatment of KNN ceramics and associated time-depending changes of their properties are gained. Furthermore, this knowledge may help to improve the piezoelectric and dielectric properties of KNN by additional heat treatments in term of better preconditions for poling.

[1] Ke Wang and Jing-Feng Li, (K,Na)NbO₃-based lead-free Piezoceramics: Phase transition, sintering and property enhancement, J. Adv. Ceram., vol 1, p. 24-37, (2012)

[2] Jürgen Rödel and Torsten Granzow, Perspective on the Development of Lead-free piezoceramics, J. Am. Ceram. Soc., vol. 92, p. 1153-1177, (2009)

[3] Juan Du and Thomas R. Shrout, $(\text{Li}_{0.04}\text{Na}_{0.52}\text{K}_{0.44})_{0.998}(\text{Nb}_{0.9-x}\text{Ta}_{0.10}\text{Sb}_x)\text{O}_3$ Lead-Free Piezoelectric Ceramics with High Performance and High Curie Temperature, Chin. Phys. Lett., vol. 25, p. 1446, (2008).

Functional Properties of Artificially Layered Ferroelectrics

P. Zubko¹, S. Fernandez², C. Lichtensteiger², J.-M. Triscone²

1- University College London, London Centre for Nanotechnology, 17-19 Gordon Street, London, WC1H 0AH, UK

2- DPMC, University of Geneva, 24 Quai Ernest Ansermet, CH1211, Geneva 4, Switzerland

p.zubko@ucl.ac.uk

Artificially layered heterostructures of transition metal oxides offer tremendous opportunities for fundamental studies of the complex interactions between these fascinating materials as well as for engineering of wholly new functionalities not present in their bulk phases. High-quality epitaxial superlattices composed of ultrathin ferroelectric and dielectric layers are emerging as a model system for investigating nanoscale ferroelectricity, providing a simple method for controlling the internal depolarisation field and allowing ultrathin ferroelectric layers to be probed using macroscopic electrical characterisation techniques. The functional properties of these artificially layered materials are dominated by the structure and dynamics of regular nanoscale domains which form periodic stripe structures that minimise the depolarisation-field energy. By performing X-ray diffraction studies with in-situ applied electric fields, the domain-wall displacements can be directly probed and related to the large enhancement of the dielectric susceptibility [1]. A detailed characterisation of the dielectric and ferroelectric properties of a range of superlattices with different periodicities reveals a number of interesting features that distinguish the nanodomain structures in ultrathin ferroelectrics from those of their bulk or thick-film counterparts. We will discuss the static and dynamic properties of such nanodomains, their interactions between neighbouring ferroelectric layers and the effect they have on the ferroelectric, dielectric and piezoelectric properties of the superlattices [2,3].

[1] P. Zubko, N. Stucki, C. Lichtensteiger and J.-M. Triscone, X-ray Diffraction Studies of 180° Ferroelectric Domains in PbTiO₃/SrTiO₃ Superlattices under an Applied Electric Field, *Physical Review Letters* 104, 187601 (2010).

[2] P. Zubko et al., Electrostatic Coupling and Local Structural Distortions at Interfaces in Ferroelectric/Paraelectric Superlattices, *Nano Letters* 12, 2846 (2012).

[3] P. Zubko, N. Jecklin, N. Stucki, C. Lichtensteiger and J.-M. Triscone, Ferroelectric Domains in PbTiO₃/SrTiO₃ Superlattices, *Ferroelectrics* 433, 127 (2012).

Electrical Properties Improvement of Chemically Synthesized Lead-Free Piezoelectric $(\text{Bi}_{1/2}\text{Na}_{1/2})\text{TiO}_3$ Thin Films by Mn doping

Wataru Sakamoto¹, Narimichi Makino¹, Makoto Moriya¹, Takashi Iijima², Toshinobu Yogo¹

¹EcoTopia Science Institute, Nagoya University, Furo-cho, Chikusa-ku, Nagoya 464-8603 Japan

²National Institute of Advanced Industrial Science and Technology (AIST), Tsukuba West, Tsukuba, Ibaraki, 305-8569 Japan

sakamoto@esi.nagoya-u.ac.jp

Now, $\text{Pb}(\text{Zr,Ti})\text{O}_3$ (PZT)-based materials are most widely used as piezoelectric materials because of their excellent piezoelectric properties. However, from the aspect of environmental issues, lead-free piezoelectric materials have widely attracted attention as candidate materials in place of PZT-based ceramics recently. Among several lead-free piezoelectric materials, $\text{Bi}_{0.5}\text{Na}_{0.5}\text{TiO}_3$ (BNT) is expected as one of the most promising candidates, because it has a rhombohedrally distorted perovskite structure, a large ferroelectric polarization and a high Curie temperature (T_c) of 320°C as shown in the work by Takenaka and Sakata (1989) [1]. On the other hand, the demand for thin-film processing has increased for the piezoelectric micro-electromechanical system (MEMS) device development. In this study, synthesis of piezoelectric BNT thin films is performed by chemical solution deposition. As for preparation of perovskite BNT thin films, several defects are easily generated because of volatility of constituent Bi and Na during a process for the crystallization. So, BNT thin films usually encounter the problem of low insulating properties. It makes several electrical measurements difficult. To improve the insulating resistance of BNT films, Bi and Na excess compositions and Mn doping effects on electrical properties were examined. All the BNT thin films prepared in this study crystallized in a perovskite single phase without formation of second phases on Pt/TiO₂/SiO₂/Si substrates. However, thin films prepared from BNT precursor solutions with stoichiometric and A site ion excess (3 mol% of Bi and 10 mol% of Na) compositions showed low electrical resistivity and couldn't be applied by sufficient electric fields for ferroelectric measurement. Insulating resistance of resultant BNT films was remarkably improved by Mn doping into Ti site of BNT. Leakage current density reduced from 10⁻⁵ A/cm² to 10⁻⁷ A/cm² (at 200 kV/cm) by Mn doping. This improvement of insulating properties makes it possible to apply sufficient electric field on the films. Improved P - E hysteresis loops were obtained as shown in Figure 1. Therefore, an appropriate amount of Mn doped into BNT effectively suppresses the influence of the defects formed in the BNT thin films. At 1 mol% Mn-doped BNT thin film, remanent polarization (P_r) and coercive field (E_c) were 20 $\mu\text{C}/\text{cm}^2$ and 160 kV/cm, respectively. Furthermore, field-induced strain behavior of the Mn-doped BNT thin films was evaluated (the result is shown in Fig. 1). The effective- d_{33} of the $\text{Bi}_{0.5}\text{Na}_{0.5}\text{Ti}_{0.99}\text{Mn}_{0.01}\text{O}_3$ thin film calculated from the slope of the field-induced butterfly curve was approximately 60 pm/V.

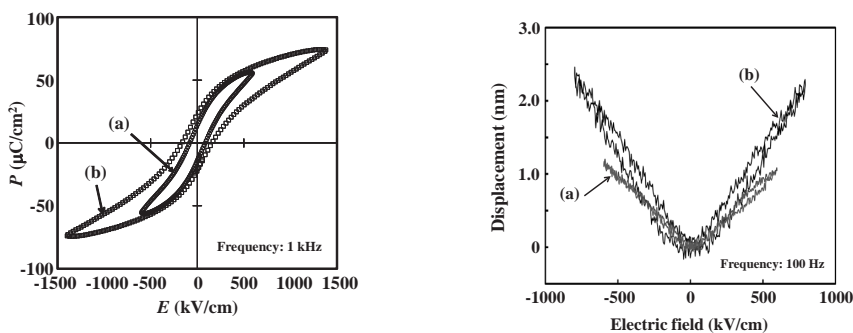


Figure 1 Polarization (P)-electric field (E) hysteresis loops (left) and field-induced displacement curves (right) of $\text{Bi}_{0.5}\text{Na}_{0.5}\text{Ti}_{1-x}\text{Mn}_x\text{O}_3$ thin films crystallized at 700°C on Pt/TiO₂/SiO₂/Si substrates: (a) $x = 0$ and (b) $x = 0.01$.

[1] T. Takenaka, K. Sakata, Dielectric, Piezoelectric and Pyroelectric Properties of $(\text{BiNa})_{1/2}\text{TiO}_3$ -Based Ceramics, *Ferroelectrics*, vol. 95, pp. 153-156 (1989).

Polar behavior of oxygen deficient KTaO_3 thin films prepared by rf sputtering

D. A. Mota¹, Y. Romaguera-Barcelay¹, A. Tkach¹, J. Pérez de la Cruz¹, P. M. Vilarinho², J. Agostinho Moreira¹ and A. Almeida¹

1- IFIMUP and IN-Institute of Nanoscience and Nanotechnology, Department of Physics and Astronomy, Faculty of Science of University of Porto, Rua do Campo Alegre, 687, 4169-007 Porto, Portugal

2- Department of Ceramics and Glass Engineering, CICECO, University of Aveiro, 3810-193 Aveiro, Portugal

Main author email address: dmota@fc.up.pt

Among materials with high dielectric constant, perovskite compounds such as SrTiO_3 , CaTiO_3 or KTaO_3 that do not exhibit any ferroelectric phase transition but continuous increase of the dielectric constant with temperature decreasing down to 0 K [1] can be found. These materials are classified as incipient ferroelectrics and possess a highly polarizable lattice. Consequently, their properties are very sensitive to impurities, strain, applied electric fields and defects.

Defect physics is probably one of the most challenging issues to be addressed. The presence of defects can change the macroscopic properties of a material, which can either cause performance degradation or improve it. For example a very interesting type of defect [2] and at the same time able to induce a polarized state in KTaO_3 could be the introduction of oxygen vacancies which can yield distortions as reported by infrared studies [3].

In this work, oxygen deficient potassium tantalate ($\text{KTaO}_{3-\delta}$) thin films, grown by RF magnetron sputtering on platinum substrates, are structurally characterized and their polar properties studied in detail by carrying out leakage currents, dielectric measurements, polarization reversal and depolarization current. X-ray diffraction patterns show that $\text{KTaO}_{3-\delta}$ thin films are under compressive strain of 2.3%, relative to KTaO_3 crystals, due to lattice distortions associated with oxygen vacancies. Leakage current studies reveal that carriers follow the Poole-Frenkel formalism showing the presence of trapped charge defects in the film. Moreover, a Cole-Cole process evidences the existence of a dipolar relaxation, apparently arising from frozen-in cation vacancy dipoles, bearing the major contribution to a polarized state [4] which vanishes above ~ 367 °C. Beyond this temperature, an equilibrium state is stabilized, wherein the compressive strain is reduced to 1.7%, stemming from oxygen diffusion into vacancies sites.

[1] V. V. Lemanov, A. V. Sotnikov, E. P. Smirnova, M. Weihnacht, R. Kunze, Perovskite CaTiO_3 as an incipient ferroelectric, *Solid State Communications*, 110., 611-614, (1999).

[2] J. N. Eckstein, Oxide interfaces: Watch out for the lack of oxygen, *Nature Materials*, 6., 473-474, (2007).

[3] S. Jandl, M. Banville, P. Dufour, S. Coulombe, Infrared study of oxygen vacancies in KTaO_3 , *Physical Review B*, 43., 7555-7560, (1991).

[4] J. Vanderschueren, and J. Gasiot, *Thermally Stimulated Relaxation in Solids* (Springer), Field-induced thermally stimulated currents, (1979).

Ferroelectric BaTiO₃ thin films grown on Si(001) by molecular beam epitaxy

L. Mazet¹, R. Bachelet^{1*}, L. Louahadj¹, R. Moalla¹, D. Albertini², B. Gautier², G. Saint-Girons¹, C. Dubourdieu¹

1- Institut des Nanotechnologies de Lyon, CNRS UMR 5270, ECL, 36 avenue Guy de Collongue, 69134 Ecully cedex, France

2- Institut des Nanotechnologies de Lyon, CNRS UMR 5270, INSA de Lyon, 20, avenue Albert Einstein, 69621 Villeurbanne, France

*romain.bachelet@ec-lyon.fr

Ferroelectric oxides are of particular interest for many applications especially in the fields of nanoelectronics (memory and logic applications) and energy (energy harvesting, low voltage operations). Integration of ferroelectric films on silicon can boost their potential applications and can open doors towards logic devices of reduced power consumption for instance [1]. Among the ferroelectric materials, BaTiO₃ is an attractive candidate with a well-known perovskite structure largely studied for its dielectric, piezoelectric and ferroelectric properties. However, direct integration of BaTiO₃ on silicon is challenging due to the oxidation of the silicon surface, the chemical interactions between them and due to the large lattice mismatch (~ 4.0 %) and thermal expansion mismatch between them [2, 3, 4]. Moreover, the control of the ferroelectric polarization is a crucial point for the targeted applications. In many applications, it is desirable that the polarization be pointing perpendicular to the Si surface.

In the present work, epitaxial BaTiO₃ was grown on Si (001) by molecular beam epitaxy (MBE) using a 4 nm-thick SrTiO₃ epitaxial buffer layer. Different growth conditions such as temperature and oxygen pressure were varied to optimize the BaTiO₃ film quality. Also, the effect of thickness from 2 to 40 nm was investigated. The surface quality was monitored *in-situ* by reflection high-energy electron diffraction (RHEED) and *ex-situ* by X-ray reflectometry (XRR) and atomic force microscopy (AFM). X-ray diffraction (XRD) was performed to determine the lattice parameters. The ferroelectric properties were studied by piezoresponse force microscopy (PFM) that enables both the detection and the switching of the ferroelectric state with a resolution down to 10 nm [5]. Flat epitaxial ferroelectric films were obtained in optimized conditions that will be discussed (*cf.* Figure 1).

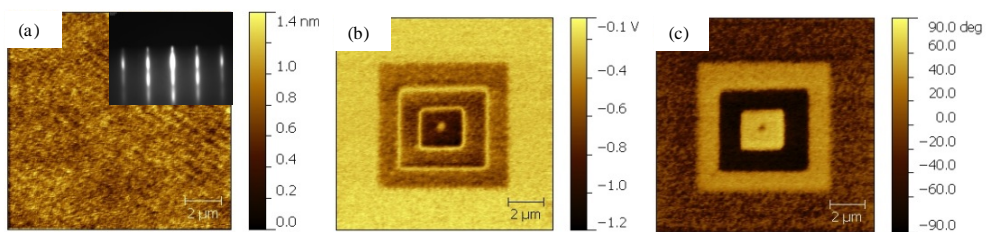


Figure 1. PFM images of a 20 nm-thick BaTiO₃ film (a) Topography (b) amplitude and (c) Phase. Inset in (a) is a RHEED pattern taken along the <110> direction of BaTiO₃.

- [1] S. Salahuddin *et al.*, Nano Lett. 8(2), 405 (2008).
- [2] V. Vaithynathan *et al.*, J. Appl. Phys. 100, 024108 (2006)
- [3] G. Niu *et al.*, Microelectronic Engineering 88, 1232 (2011)
- [4] C. Dubourdieu *et al.*, Nature Nanotechnology 8, 748 (2013)
- [5] A. Gruverman, S. Kalinin, J. Mat. Science 41, 107 (2006)

Infrared Spectroscopy of Strained BaTiO₃/SrTiO₃ Superlattices on Scandate Substrates

V. Železný¹, A. Soukiassian², X.X. Xi³, D.G. Schlom²

1 - Institute of Physics, ASCR, Na Slovance 2, 182 21 Praha 8, Czech Republic

2 - Department of Materials Science and Engineering, Cornell University, Ithaca, New York, 14853-1501, USA

3 - Department of Physics, Temple University, Philadelphia, Pennsylvania 19122, USA

Main author email address: zelezny@fzu.cz

Ferroelectric superlattices of (BaTiO₃)₈/(SrTiO₃)₄]₅₀ and (BaTiO₃)₈/(SrTiO₃)₄]₄₀ were grown on DyScO₃, SmScO₃, EuScO₃ and TbScO₃ substrates by reactive molecular epitaxy. The (110) substrate cut using the *Pbnm* space group setting is suitable for their epitaxial growth. The superlattice quality was characterized by several techniques. The reflectance measurements were done independently for a bare substrate and substrate covered with superlattice. Far-infrared spectra (30 – 650 cm⁻¹) were measured in two polarizations: along the *c* (long) axis and perpendicular to it on the (110) cut of the substrates in the temperature ranges 10 – 300 K in cryostat and 300 – 650 K in furnace. Room-temperature spectra were taken in a broader spectral range up to 3000 cm⁻¹ which enabled us to determine the high-frequency contribution from electronic transitions included in ϵ_{∞} . The spectra were quite complicated because of the large number of infrared-active phonons coming from both the substrate and superlattice.

In order to evaluate the superlattice spectra it is necessary to separate them from those from substrate. Until recently, however, the infrared technique could not be effectively used for studies of superlattices because it was difficult to separate the signals coming from the superlattice and the substrate it was grown upon. This problem was partly overcome only a few years ago, when scandate single crystals, whose infrared spectra are quite distinct to the ones of the ferroelectric superlattices, were introduced as substrates. The substrate single crystal has the *Pbnm* space group with four chemical formulas in the unit cell. 25 infrared active phonons distributed among $7B_{1u} + 9B_{2u} + 9B_{3u}$ irreducible representations polarized along the crystal axes *c*, *b* and *a* respectively had to be considered for substrate. The dielectric function of our superlattice cannot be modeled by the sum of all its modes, because the number of infrared active phonons in superlattice with 12-unit cell period is even large. In the tetragonal phase the following decomposition holds ($47A_1 + 12B_1 + 59E$) and for orthorhombic phase ($59A_1 + 59B_1 + 59B_2$) must be used. Instead of it an effective medium model taking into account a hypothetical perovskite with three infrared active modes is used.

The phonon parameters and dielectric function of the superlattice could be extracted using a fitting procedure. The complex dielectric function of the superlattice can be modeled by three polar perovskite TO modes. The parameters of the lowest mode, TO1, which corresponds to both components SrTiO₃ and BaTiO₃, vary depending on the particular substrate. The temperature dependence of the DyScO₃ lowest mode shows slight softening and sharpening with decreasing temperature, in the case of SmScO₃ it remains the same in the whole temperature interval, therefore, it is not clear if any phase transition occurs.

It can be said generally that the strain induced in the superlattice suppresses the transitions between different ferroelectric phases (tetragonal-orthorhombic-rhombohedral) characteristic for bulk BaTiO₃ and stabilizes a single ferroelectric phase (orthorhombic). Relatively large permittivity of order 10³ and low-frequency permittivity dispersion indicate that relaxor ferroelectric behavior can be expected.

This behavior can explain difference of the mode behavior in comparison to other superlattices is due to large Ba/Sr ratio, which prefers the polarization perpendicular to the plane, to its large thickness, which results in its relaxation, and partly to pinning of the superlattice to the substrate.

This work was partially supported by Grant Agency of the Czech Republic under Contract No. P204/11/1011.

Pt-less silicon integration of PZT sol-gel thin films

M. Bousquet¹, B. Viala¹, H. Achard¹, J. Georges¹, A. Reinhardt¹, G. Le Rhun¹

1- CEA, LETI, MINATEC, 17 Rue des Martyrs, F38054 Grenoble, France

Main author email address: marie.bousquet@cea.fr

Ferroelectric lead zirconate titanate $\text{Pb}(\text{Zr}_{1-x}\text{Ti}_x)\text{O}_3$ (PZT) thin films are part of the most popular functional materials for microelectronics (FeRAMs, capacitors, pyroelectric sensors, actuators, etc.) due to their superior ferroelectric, dielectric, pyroelectric and piezoelectric properties. All these applications (excepted FeRAMs) are based on a standardized fabrication process based on platinized silicon wafer (Si/SiO₂/TiO₂/Pt). Indeed TiO₂/Pt is considered as the best seed layer for polycrystalline PZT film growth and anti-diffusion layer with silicon. However, TiO₂/Pt undergoes remarkably large stress (larger than GPa) even at low thickness, what makes it detrimental or restrictive when applied to released PZT membranes processes for example. Additionally, the use of platinized wafers drastically restricts the design of capacitors and actuators to the single Metal/Insulator/Metal (MIM) scheme (i.e. continuous bottom electrode). Therefore, the assessment of Pt-less alternative templates for PZT will open capacitors or actuators design towards innovative devices based on interdigital electrodes (IDE) scheme (i.e. patterned bottom electrode possible). IDE makes breakdown voltage independent of thickness (i.e. optimizable by design) and allow d_{33} actuation (or g_{33} for charges generation) which is twice larger than d_{31} (or g_{31}) for PZT [1 - 3]. Thus, Pt-less silicon integration also have major advantages for membrane-based devices: (i) low-stress structures, (ii) reduced film thickness, (iii) in-plane polarization (i.e. IDE spacing and film thickness are independent), and (iv) reduced actuation voltage in the d_{33} mode.

The aim of this work is to take a decisive step towards Pt-less silicon integration of PZT sol-gel thin films for microelectronics (as an example, producing d_{33} -mode membrane actuators on silicon substrates). For this purpose, sol-gel PZT films are deposited and crystallized on insulating buffer layers instead of the conventional TiO₂/Pt buffer layer. Among different buffer layers, zirconium oxide (ZrO₂) and titanium oxide (TiO₂) appear as good candidates favouring perovskite growth and acting as anti-diffusion barrier limiting the critical interdiffusion between Pb and the Si substrate.

In this work, we report experimental results on growth, structural, microstructural, mechanical and dielectric properties of 385 nm thick PZT films deposited by sol-gel on 8 inch-diameter Si wafer. In particular, we highlight the crucial role played by the thickness of the seed layers and the annealing temperature on the quality of the PZT films.

As a result, PZT thin films grown on ZrO₂ buffer layers (from 20 to 100 nm) are well-crystallized into the perovskite phase and are randomly oriented at 700°C (i.e. standard temperature). On the contrary, the crystallization of PZT on TiO₂ buffer layers requires a higher critical thickness of 40 nm and a reduced annealing temperature of 650°C. If the thickness of TiO₂ buffer layer is lower and/or the crystallization temperature different, pyrochlore phases dominate. Residual stress is also reported and correlated with structural and microstructural properties. Finally, the influence of the various templates on the “in-plane” dielectric properties of PZT (i.e. of interest for IDE capacitors and d_{33} actuation) is discussed.

[1] B. Xu, Y. Ye, L. E. Cross, J. J. Bernstein, and R. Miller, Appl. Phys. Lett. **74**, 3549 (1999).

[2] N. Chidambaram, A. Mazzalai, D. Balma, and P. Muralt, IEEE Trans. Ultrason., Ferroelectrics, and Frequency Control **60**, 1564 (2013).

[3] Q.Q. Zhang, S.J. Gross, S. Tadigadapa, T.N. Jackson, F.T. Djuth, and S. Trolier-McKinstry, Sens. Actuators A **105**, 91 (2003).

Flexomagnetic effect in multiferroic composites and E-beam Irradiated Nano-electro-mechanical-ferroelectric-systems

Ashok Kumar

CSIR-National Physical Laboratory, New Delhi-110012

Email: ashok553@gmail.com

Among the ferroics, magnetic materials are the oldest discovery by humankind. Last decade is well known for the rebirth of single phase multiferroic bismuth ferrite (BiFeO_3) which simultaneously possesses all the three ferroic order parameters. There is an enormous rush among the scientific communities to search a novel room temperature multiferroics for nonvolatile memory and magnetic field sensors applications. In this regard, we have successfully discovered some lead based novel room temperature multiferroics. A lot of attention has been paid on flexoelectric, flexomagnetic, and flexoelectromagnetic phenomenon. Study of these effects and their cross-coupling are important in design and development of next generation micro-electro-mechanical system (MEMS) and nano-electro-mechanical system (NEMS) devices. These effects become more prominent at nanoscale. A systematic study is required on the effect of inhomogeneous strains on the ordered parameters responsible for their functionalities. Piezoelectric materials require crystalline phase with no inversion symmetry, however, no such conditions needed for flexoelectricity or flexomagnetism. Flexomagnetic effect represents the magnetic phases developed under inhomogeneous strain gradient. Generally, bulk systems necessitate external stress to develop strain gradients whereas nanoscale systems naturally develop either homogeneous or in-homogeneous strains during the growth process. The magnitude of strain gradient in nanoscale systems depends on the growth conditions such as substrates, temperatures, pressures and surrounding medium. The cross coupling of strain with ferroics order parameters are also important to understand the underlying physics and technology. I will discuss on the flexomagnetism in $0.8\text{Pb}(\text{Zr}_{0.52}\text{Ti}_{0.48})\text{O}_3$ (PZT)/ $0.2\text{Pb}(\text{Fe}_{0.67}\text{W}_{0.33})\text{O}_3$ (PZTFW) and CoFe_2O_4 (CFO) composites. Suitable composite of multiferroic PZTFW and high magnetostrictive ferro/ferri-magnetic CFO crystals were prepared to study the flexomagnetism. In this report, *in-situ* external stress has been applied to the composite to generate magnetization. Magnetic force microscopy (MFM) was used to investigate the magnetic domains and phases with and without application of external stress. MFM images suggest that the magnetic phase of the PZTFW (multiferroics) in the composite matrix at nanoscale possess superparamagnetic phase or almost no magnetic phase contrast in absence of strain gradient. However, application of *in-situ* external flexoelectric strain significantly develops the magnetic phase in the PZTFW. Apart from this novel phenomenon, new vortex kind of magnetic ferroelectric domains were observed near the interface of two separate ferroic phases under strain gradient. Zero Field Cooled (ZFC) and Field Cooled (FC) magnetization studies on these systems at low magnetic field ~ 50 Oe provide the clear microscopic picture of magnetic moment under strain gradient. Flexomagnetism will be discussed in context of magnetostriction and electrostriction which play an important role in the controlling and cross coupling of order parameters, may be useful in design of flexoelectric (magnetic) based magneto-electric sensors. Electro-magneto-mechanical effects are ubiquitous in multiferroic materials.

E-beam with suitable energy is a nondestructive versatile tool which can probe the mechanical deviation under the irradiation of e-beam in any free-standing nanostructure. Ferroelectric composites PZT/PVDF nanorods with 1-5 microns length and 50-200 nm diameters were irradiated with 300 kV e-beams with extremely low current. Interestingly, it was found that nanorods move away almost 5 to 50 nm from the original position depending on the position and time of irradiation and probing/imaging area. This mechanical deviation is reversible and robust in nature which indicates that it may be useful for future NEMS devices.

Structure-property relations in La- and Nd-doped BiFeO₃: competition between geometry optimisation and magnetism

Christopher M. Kavanagh,¹ Richard J. Goff,¹ Aziz Daoud-Aladine,² Philip Lightfoot,¹ and
Finlay D. Morrison^{1*}

1. School of Chemistry and EaStCHEM, University of St Andrews, St Andrews, KY16 9ST, United Kingdom
2. ISIS Facility, Rutherford Appleton Laboratory-STFC, Chilton, Didcot, Oxfordshire OX11 0QX, United Kingdom

finlay.morrison@st-andrews.ac.uk

Rare earth doping has been demonstrated as an effective way of mitigating both the thermodynamic metastability and leakage current in the widely studied multiferroic perovskite BiFeO₃. We have investigated the structure-property relations in La- and Nd-doped BiFeO₃ using a combination of temperature dependent powder neutron diffraction and impedance spectroscopy. Specifically, structural variations were studied using a combination of both conventional “bond angle/bond length” and symmetry-mode analyses. The latter is particularly useful as it allowed the effects of A-site displacements and octahedral tilts/distortions to be considered separately. The structural variations in these materials occur due to a changing balance between magnetic properties and other bonding contributions. This results in changes in the magnitude of the octahedral tilts and A-site displacements giving rise to phenomena such as negative thermal expansion and invariant lattice parameters i.e., the Invar effect. Both Bi_{0.5}La_{0.5}FeO₃ and Bi_{0.7}Nd_{0.3}FeO₃ adopt an orthorhombic GdFeO₃-type structure (space group: *Pnma*, the same as the paraelectric high temperature phases of BiFeO₃ [1,2]) with *G_z*-type antiferromagnetism, figure 1a. For Bi_{0.5}La_{0.5}FeO₃, the temperature dependent dielectric permittivity is controlled by changes in the FeO₆ octahedral tilt magnitudes, accompanied by a structural distortion of the octahedra with corresponding A-site displacements along the *c*-axis; this behaviour is unusual due to an increasing in-phase tilt mode with increasing temperature. The anomalous orthorhombic distortion is driven by magnetostriction, figure 1b, at the onset of antiferromagnetic ordering resulting in an Invar effect along the magnetic *c*-axis and anisotropic displacement of the A-site Bi³⁺ and La³⁺ along the *a*-axis [3]. In Bi_{0.7}Nd_{0.3}FeO₃ the dielectric properties are again dependent in a subtle change in distortion mode driven by a change in the axis of A-site displacements, but, in contrast to the La-doped sample, superexchange couples with these A-site displacements driving a decreasing anti-phase tilt on cooling resulting in a dielectric anomaly and negative thermal expansion, figure 1c.

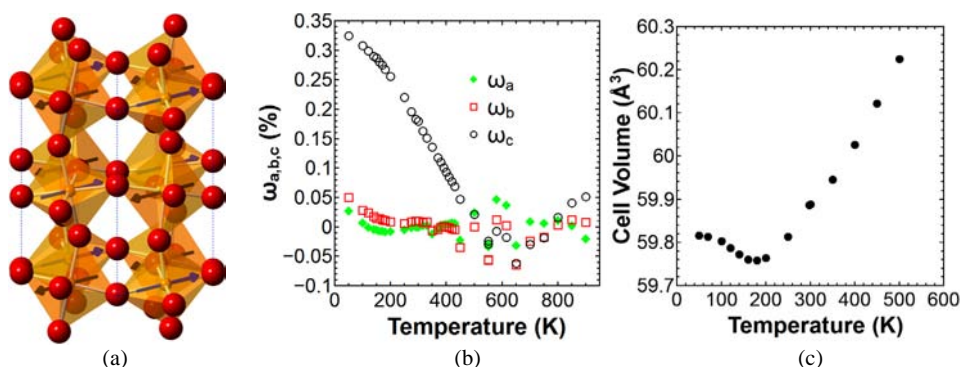


Figure 1 Nuclear and magnetic *Pnma'* crystal structure (a); magnetostrictive strain, ω , in Bi_{0.5}La_{0.5}FeO₃ (b); and negative thermal expansion in Bi_{0.7}Nd_{0.3}FeO₃ (c).

- [1] D.C. Arnold, K.S. Knight, F.D. Morrison and P. Lightfoot, “Ferroelectric-Paraelectric Transition in BiFeO₃: Crystal Structure of the Orthorhombic Phase”, *Phys. Rev. Lett.*, **102**, 027602, (2009).
[2] D.C. Arnold, K.S. Knight, G. Catalan, S.A.T. Redfern, J.F. Scott, P. Lightfoot and F.D. Morrison, “The Beta-to-Gamma Transition in BiFeO₃: A Powder Neutron Diffraction Study”, *Adv. Funct. Mater.*, **20**, 2116-2123, (2010).
[3] C.M. Kavanagh, R.J. Goff, A. Daoud-Aladine, P. Lightfoot and F.D. Morrison, “Magnetically Driven Dielectric and Structural Behavior in Bi_{0.5}La_{0.5}FeO₃”, *Chem. Mater.*, **24** (23), 4563-4571, 2012.

Dynamic and structural properties of orthorhombic rare-earth manganites under high pressure

D. A. Mota¹, A. Almeida¹, V. H. Rodrigues², M. M. R. Costa², P. Tavares³, P. Bouvier⁴, M. Gennou⁵,

J. Kreisel⁵, J. Agostinho Moreira¹

1-IFIMUP and IN-Institute of Nanoscience and Nanotechnology, Departamento de Física e Astronomia da Faculdade de Ciências, Universidade do Porto, Rua do Campo Alegre, 687, 4169-007 Porto, Portugal.

2-CEMDRX, Departamento de Física, Faculdade de Ciências e Tecnologia, Universidade de Coimbra, 3004-516 Coimbra, Portugal.

3-Centro de Química - Vila Real, Departamento de Química, Universidade de Trás-os-Montes e Alto Douro, 5000-801 Vila Real, Portugal.

4-Laboratoire des Matériaux et du Génie Physique, CNRS, Grenoble Institute of Technology, MINATEC, 3 parvis Louis Néel, 38016 Grenoble, France.

5-Département Science et Analyse des Matériaux, CRP Gabriel Lippmann, 41 rue du Brill, L-4422 Luxembourg.

E-mail address: jamoreir@fc.up.pt

In this contribution, we report a high pressure Raman scattering study in orthorhombic rare-earth manganites $RMnO_3$, with $R = Pr, Nd, Sm, Eu, Gd, Tb$ and Dy , and synchrotron X-ray diffraction in $R = Pr, Sm, Eu$, and Dy . The analysis of the pressure evolution of the Raman bands associated with out-of-phase MnO_6 rotations and in-phase O_2 stretching modes shows that pressure is accommodated in different ways according the A-cation size. For larger A-cations, the Raman results reveal that RO_{12} dodecahedra behave more rigidly than the MnO_6 octahedra, and the MnO_6 octahedra distort more than the MnO_6 chains bend as pressure increases. Nevertheless, as the A-cation size decreases, the MnO_6 octahedra behaves more rigidly than the RO_{12} dodecahedra, and, although the octahedron continues to distort, the chains bend more pronouncedly. This result is corroborated by the A-cation size dependence of the compressibility of the unit cell, which clearly shows that the pressure has a strong effect on the ac -plane, its effect being more pronounced for the larger A-cation size compounds. Since the symmetric stretching mode is the most sensitive to pressure, the Mn-O2 bonds are more sensitive to pressure than the bending of the MnO_6 network, namely for the larger rare-earth ions. Taking this into consideration, for larger rare-earth ion manganites, the effect of pressure is to reduce the Mn-O2 bonds, which implies the reduction of the a and c parameters. Moreover, as the compressibility of the a -axis is the larger one, we can conclude that, for the same pressure, the long Mn-O2 bond length reduces more than the short Mn-O2 bond length. This result evidences a reduction of the Jahn-Teller effect as pressure increases.

An insulator-to-metal phase transition was evidenced for all compounds, with an increase of the critical pressure with decreasing the A-cation size. The pressure hysteresis and the coexistence of x-ray peaks from phases with different symmetries in the neighbourhood of the critical pressure reveals the first order nature of the phase transition. Moreover, the symmetry of the high pressure phase depends on the A-cation.

The anomalous pressure behavior of shear strain e_4 clear evidences the structural rearrangement on the ac -plane of $RMnO_3$, with $R = La$ to Gd , associated with the reduction of both Jahn-Teller and octahedra tilting. However, for the case of $DyMnO_3$, the increase of the e_4 shear strain with increasing pressure points to an increase of structural deformations. This issue requires further experimental studies. In all compounds, no hint of complete suppression of Jahn-Teller distortion was found on the pressure dependence of Raman spectra and shear strain.

Finally, our results reveal that hydrostatic pressure and chemical pressure have different effects for manganites with large A-cations, and that chemical pressure is reasonably comparable to hydrostatic pressure for smaller cations.

Nonlinear dependence of dielectric constant in polymer-based composite

L.P. Curecheriu, L. Padurariu, Mitoseriu

1- Faculty of Physics, A.I. Cuza University, Iasi 700506, Romania

lavinia.curecheriu@uaic.ro

Nowadays there is a high demand for the development of new types of inexpensive, flexible, environmentally friendly and light-weight electronic components for radiofrequency sensing platforms, actuators, biosensors, wearable healthcare devices, and flexible antennas for wireless applications (microwave MWs devices). The combination of nanoparticles (ferroelectric, magnetic or metallic) in a polymer matrix with good dielectric performances is an approach expected to result in new electrical properties with potential use in supercapacitor structures, sensing applications, flexible non-volatile memory applications and optoelectronics.

In the present paper, the field dependence permittivity in case of composite materials formed by nanoparticles (metallic and ferroelectric) embedded in a flexible polymer matrix (dielectric or ferroelectric) were investigated.

The polymer membranes (chitosan and PVDF) with different filler materials (gold and barium titanate) and concentrations were prepared by dry phase inversion method. The nonlinear dielectric properties for both types of materials (polymer-ferroelectric and polymer-conductive nanoparticles) were investigated at room temperature. The results show that by increasing filler materials an increased tunability together with an increase of dielectric constant were obtained. The obtained results can be explained through the highly inhomogeneous local field in composites containing components with contrasting permittivities and conductivities. The local field distribution for a composite material can be determined using finite element method (Fig.1a).

The experimental trend is in a good agreement with the model calculations for different chitosan-based nanocomposite materials.

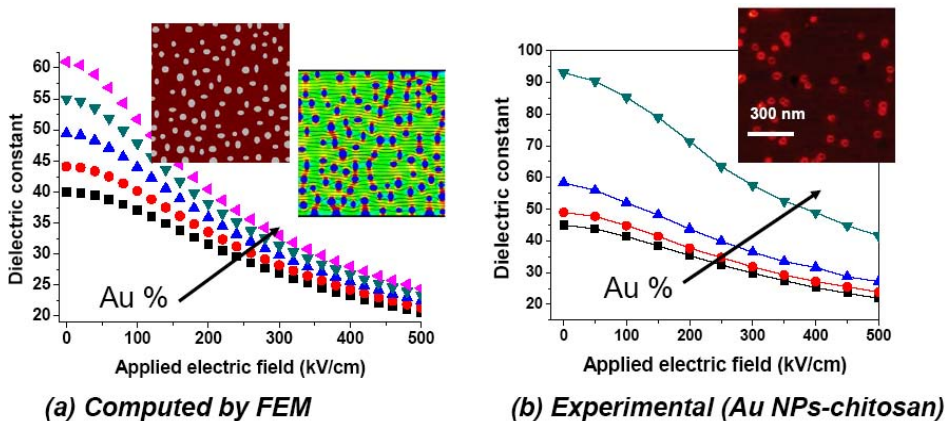


Figure 1: (a) Computed and (b) experimental permittivity vs. field dependence (tunability) obtained for metallic NPs embedded in dielectric matrix

Acknowledgements: The financial support of the PNII-RU-TE-2012-3-0150 grant is acknowledged.

X-ray scattering study of $\text{PbZr}_{1-x}\text{Ti}_x\text{O}_3$ single crystals at small x and at MPB

S.Vakhrushev^{1,2}, D.Andronikova², A. Bosak³, Yu. Bronwald², R. Burkovsky², D. Chernyshov⁴,
I.N. Leontyev⁵, Z.-G. Ye⁶

1- Ioffe Institute, 26 Politekhnicheskaya, St.-Petersburg, 194021 Russia

2- St.Petersburg State Polytechnical University, St.-Petersburg, Russia

3- European Synchrotron Radiation Facility, Grenoble, France

4- Swiss-Norwegian Beamlines at ESRF, Grenoble, France

5- LE STUDIUM[®], Loire Valley Institute for Advanced Studies Orleans&Tours, France

6 - Simon Fraser University, V5A 1S6, Burnaby, Canada.

s.vakhrushev@mail.ioffe.ru

In recent years the revival of the interest to the physics of $(\text{PbZrO}_3)_{1-x}(\text{PbTiO}_3)_x$ (PZT) solid solution is observed. To large extent this revival is related to development in the single crystal growth and to the new experimental possibilities in studying the extremely small single crystals using high-flux synchrotron radiation sources. In this report we are going to present the results of the study of PZT single crystals with lead titanate concentrations corresponding to the different regions of the phase diagram ($x=0.7\%$, 1.5% , 3.3% , 20% 40% and 48%). To explore the structural changes and critical phenomena in the mentioned single crystals we have used a combination of the X-ray diffraction and X-ray diffuse scattering techniques.

We would like to formulate here following most important conclusions:

In the paraelectric phases of the PZT single crystals with $x \leq 40\%$ we clearly observed "butterfly-like" diffuse scattering, identical to that earlier observed in relaxors and in pure PbZrO_3 . In the low- x compositions (up to 3.3%) this scattering was strongly weakened in the intermediate rhombohedral phase, but still survived down to the low-temperature antiferroelectric phase where it practically disappeared.

At the 40% concentration temperature dependence of the diffuse scattering demonstrate well pronounced critical behaviour demonstrating that the phase transition is nearly of the second order.

In the MPB region (48%) diffuse scattering was weak and had different symmetry [2] as it will be discussed in the report.

For the low- x compositions ($x \leq 3.3\%$) we carefully analyzed the M-type $\tau_{ss}=(h+\frac{1}{2} k+\frac{1}{2} l)$ superstructural peaks. Earlier these superstructure was observed in the electron diffraction experiments [3] but not with X-ray or neutrons. From the absence of the extinction rules conclusion can be made that these reflections are unrelated to the oxygen octahedra tilts. In addition to the main superstructural peaks we have observed 8 satellites at the positions $\tau_{ss}+\{\delta\delta\delta\}$, forming a cube around the superstructure peaks. Using the model of the antiphase domains similar to that proposed in [3] we succeeded to describe these satellites

[1] A. K. Tagantsev et al., The origin of antiferroelectricity in PbZrO_3 , Nature communications, vol.4, p2229, (2013).

[2] R. G. Burkovsky et al., Structural Heterogeneity and Diffuse Scattering in Morphotropic Lead Zirconate-Titanate Single Crystals, Phys. Rev. Lett., vol.117, p. 97603, (2012).

[3] G. Ricote et al., A TEM and neutron diffraction study of the local structure in the rhombohedral phase of lead zirconate titanate, J. Phys.: Condens. Matter, vol. 10, pp. 1767 - 1786, (1998).

Sintering and physical properties of (Na, K)NbO₃-based piezoceramics

M. G. D. Pedreca, M. H. Lente

Universidade Federal de São Paulo - Instituto de Ciência e Tecnologia

Rua Talim, 330 - Vila Nair - São Jose dos Campos - SP - Brazil – CEP: 12231-280

e-mail address: mlente@unifesp.br

Over the last decades piezoelectric ceramics derived from materials with perovskite structure have been used in electro-electronic industry for piezoelectric ultrasonic transducers. In particular, the most commercially explored compositions are those based on lead zirconate titanate (PZT) system [1]. However, because of the high toxicity of lead and the current concern about the discard of electronic materials that contains it, many researches have been developed in order to produce piezoelectric materials that adequately replace those with lead. Among the new compositions that may replace lead-based piezoelectric ceramics, one of the most promising family of ceramics is based on solid solutions in the KNbO₃-NaNbO₃ pseudo-binary system [2, 3]. However, the major problems concerning this material is reported to be the difficulty of obtaining high density by conventional solid-state preparation and sintering in air and free from secondary phases. Therefore, due to scientific and technological motivations, in this work we have focused on the production and characterization of "pure" and doped (Na_{1-x}, K_x)NbO₃ dense ceramics free from spurious phases. By using the conventional route of mixing the oxide powders, in this work we have investigated the phase and microstructure development of (Na_{0.52}, K_{0.48})NbO₃ ceramics as a function of calcination and sintering conditions. In parallel, we have also used diferent additives to improve the densification process and the piezoelectric properties as well. The present study revealed that good densities and dielectric and piezoelectric properties can be obtained in the pure and doped (Na_{0.52}, K_{0.48})NbO₃ ceramics even by normal sintering.

[1] K. Uchino - *Ferroelectric Devices* - Marcel Dekker, Inc., (2000).

[2] J. Rodel, W. Jo, K. T. P. Seifert, Eva-Maria Anton, and T. Granzow, *J. Am. Ceram. Soc.*, **92**, 1153 (2009).

[3] E. Cross, *Nature*, **432**, 24 (2004).

(Co-)doping of lead-free $\text{Bi}_{1/2}\text{Na}_{1/2}\text{TiO}_3\text{-Bi}_{1/2}\text{K}_{1/2}\text{TiO}_3$ -based piezoceramics

M. Blömker¹, E. Erdem², S. Wollstadt¹, J. Rödel¹

¹ - Institute of Materials Science, TU Darmstadt, Alarich-Weiss-Straße 2, 64287 Darmstadt, Germany

² - Institut für Physikalische Chemie I, Albertstr. 21, Universität Freiburg, Germany

bloemker@ceramics.tu-darmstadt.de

As of today, the overwhelming majority of the production of piezoelectric sensors and actuators is lead-containing. Lead is a known neurotoxin, hence according to latest EU-regulations lead-based materials are to be replaced by viable alternatives [1]. To address this urgent need, the system $\text{Bi}_{1/2}\text{Na}_{1/2}\text{TiO}_3\text{-Bi}_{1/2}\text{K}_{1/2}\text{TiO}_3$ (BNT-BKT) is a promising candidate for certain piezoelectric applications [2, 3]. For various piezoelectric systems, (co-)doping is used to tailor the defect chemistry in order to influence for instance Schottky barriers, defect dipoles or domain walls [4, 5].

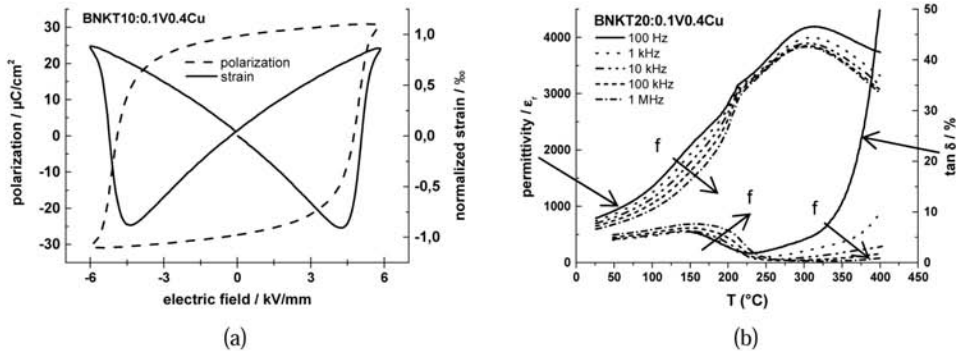


Figure 1. (a) Large signal polarization and strain measurement of co-doped $\text{Bi}_{0.5}(\text{Na}_{0.9}\text{K}_{0.1})_{0.5}\text{Ti}_{0.995}\text{V}_{0.001}\text{Cu}_{0.004}\text{O}_3$ (BNKT10:0.1V0.4Cu) ceramics as function of the electric field, $f = 1\text{ Hz}$. (b) Small signal permittivity and $\tan \delta$ measurements of BNKT10:0.1V0.4Cu as function of the temperature.

In this study, aliovalent (co-)doping of BNT-BKT on the B-site of the perovskite lattice was performed with Mn, Al, Cu, V, Mo and combinations of the respective elements. MPB doping of BNT-BKT, aimed at actuator applications and doping on the rhombohedral side of the MPB, focusing on high power applications was carried out. XRD characterizations were undertaken to investigate phase purity. Small signal measurements as function of temperature (for instance as in Figure 1.) allow for conclusions on the transition from ferroelectric to relaxor behavior, while large signal polarization and strain measurements of doped MPB BNT-BKT consistently revealed polarization loop pinching and a strain increase compared to undoped samples. The piezoelectric constant d_{33} was additionally determined as a function of temperature. For rhombohedral ceramics, P_r and P_{\max} could be improved. Furthermore impedance spectroscopy was employed to elucidate the resonance behavior (k_p and Q_m) of the ceramics and in order to study defects and their associations, electron paramagnetic resonance spectroscopy of dopant elements was used to assess their oxidation states.

[1] EU-Directive 2011/65/EU: RoHS. Off. J. Europ. Un. 2011:L 174:88

[2] J. Rödel, W. Jo, K.T.P. Seifert, E.-M. Anton, T. Granzow, D. Damjanovic, Perspective on the Development of Lead-free Piezoceramics, *J. Am. Ceram. Soc.* 92, pp. 1153-1177, (2009).

[3] T. Shrout and S. Zhang, Lead-free piezoelectric ceramics: Alternatives for PZT?, *J Electroceram.* 19, pp. 113-126, (2007).

[4] M. Dawber, J. F. Scott, A. J. Hartmann, Effect of donor and acceptor dopants on Schottky barrier heights and vacancy concentrations in barium strontium titanate, *J. Eur. Ceram. Soc.* 21, pp. 1633-1636, (2001).

[5] R. A. Eichel, H. Kungl, P. Jakes, Defect structure of non-stoichiometric and aliovalently doped perovskite oxides, *Materials Technology* 28, pp. 241-246, (2013).

***I-V* characteristics of thin-film ferroelectric structures with negative conductivity**

A. Sigov, Yu. Podgorny, P. Lavrov, and K. Vorotilov

Moscow State Technical University of Radioengineering, Electronics and Automation, Moscow, Russia

E-mail: sigov@mirea.ru

The current-voltage (*I-V*) characteristics of some ferroelectric thin films frequently exhibit regions with an apparent negative differential conductivity [1]. To describe this phenomenon Dawber and Scott have suggested the diffusion current model [2]. However this model does not fully describe real *I-V* characteristics [3].

In this report we consider *I-V* dependences taking into account the polarization relaxation. The polarization relaxation in thin ferroelectric films can reach about tens percent [4]. Thus, in spite of the pre-polarization of the ferroelectric structure before the measurement, the total current in the structure consists of the the leakage current and the polarization recovery current components.

We have shown that the probability density of the Weibull distribution simulates well the polarization recovery current. A maximum value of the polarization recovery current is observed in the vicinity of the coercive field.

A technique that enables to exclude a polarization recovery current component from the *I-V* data is proposed. A method of recovery charge determination at different voltage ramp speed is discussed as well.

It should be noted that for the films with high charge carrier concentrations the polarization recovery current is observed as well. But it is masked by the real big leakage current and as a result the areas with a negative slope or plateau are absent near coercive field region. Therefore, the phenomenon of negative conductivity is relatively frequent in polycrystalline films, and it is relatively rare in epitaxial films with lower traps concentration density [1,5].

[1] JF Scott, BM Melnick, JD Cuchiario, R Zuleeg, CA Araujo, LD McMillan, MC Scott. *Integr Ferroelectr.* 4(1), 85-92 (1994).

[2] M Dawber, JF Scott . *J Phys: Condens Matter.* 16, L515-L521 (2004).

[3] Yu. Podgorny, A. Sigov, A. Vishnevskiy, K. Vorotilov. *Ferroelectrics.* in the press (2014).

[4] Yu. Podgorny , D. Seregin , A. Sigov, K. Vorotilov. *Ferroelectrics.* 439 (1), 56-61 (2012).

[5] L. Pentile, I, Vrejoiu, D. Hesse, G. Lerhun, M. Alexe. *Physical Revue.* B 75, 104103, 1-14 (2007).

Electro-optic and converse piezoelectric coefficients of highly polar epitaxial films: GaN grown on Si, and (Sr,Ba)Nb₂O₆ (SBN) grown on Pt coated MgO.

M. Cuniot-Ponsard¹, I. Saraswati^{2,4}, S. M. Ko³, M. Halbwx², Y. H. Cho³, N. R. Poespawati⁴, E. Dogheche²

1- Laboratoire Charles Fabry (LCF), IOGS, CNRS, Univ Paris-Sud, 2 Avenue Augustin Fresnel, 91127 Palaiseau cedex, France

2- Institut d'Electronique, Microelectronique et Nanotechnologie, Department Optoelectronics, IEMN UMR 8520 CNRS, Avenue Poincaré, 59652 Villeneuve d'Ascq, France

3- Department of Physics and KI for the NanoCentury, Korea Advanced Institute of Science and Technology (KAIST), Daejeon 305-701, South Korea

4- Electrical Engineering Dept., Faculty Eng., Universitas Indonesia, 42435, Depok, Indonesia

Mireille.Cuniot-Ponsard@institutoptique.fr

The preparation of nonlinear optical materials in the form of thin films opens the path to the realization of very new and attractive photonic components (low power, small size, and low cost electro-optic light modulators, miniaturized electric field sensors or second harmonic generators, electrically tunable photonic crystals,...). The ferroelectric (Sr,Ba)Nb₂O₆ (SBN) crystalline niobate is of special interest because it exhibits an exceptionally high electro-optic coefficient ($r_{33} = 237$ pm/V for SBN:60 at $\lambda=633$ nm). The nonlinear optical semiconductor GaN is of special interest because of its unique optoelectronic properties and its ability to grow epitaxially on silicon, that is to be integrated in a mature Si-based technology.

We have prepared epitaxial thin films (about 1 μm thick) of these two materials: SBN is deposited by RF magnetron sputtering on (001)Pt / (001)MgO substrates [1], and GaN is deposited by MOCVD on (111)Si substrates buffered with (Al,Ga)N layers [2]. The electro-optic coefficients have been measured by using an original method that enables to determine simultaneously and analytically the sign and amplitude of the electro-optic, converse-piezoelectric and electro-absorptive coefficients of the film [3]. Figure 1a describes the principle of this method: the measured variation in reflectivity $\Delta R(\theta)$ results from the three above mentioned electric-field-induced effects. Figure 1b shows the agreement obtained for GaN/Si between the experimental $\Delta R(\theta)$, and the $\Delta R(\theta)$ calculated using the values determined for the above mentioned coefficients.

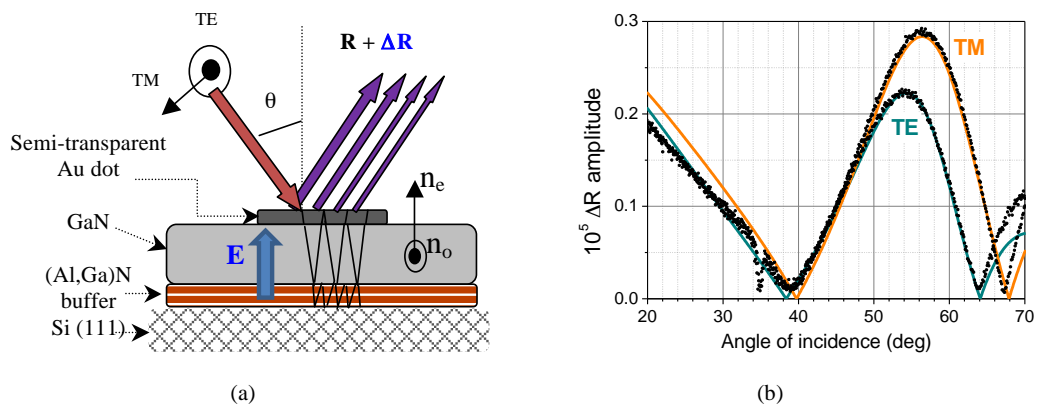


Figure 1 (a) Principle of the electro-optic measurement. The reflectivity (R), and its variation (ΔR) induced by an ac modulating voltage (E), are measured versus incident angle (θ), successively for transverse electric (TE) and transverse magnetic (TM) light polarizations. (b) Electric-field-induced variation in the reflectivity of a GaN/Si sample, for TE and TM polarizations. Calculated data (using the determined coefficients -continuous lines) and experimental data (black dots) are compared.

We report, to our knowledge, the first measurement of the (r_{13} , r_{33}) electro-optic coefficients in a SBN thin film and the first measurement of these two coefficients in a GaN film grown on Si (one measurement has been reported in the literature for GaN grown on sapphire). Converse-piezoelectric and electro-absorptive coefficients have never been measured before neither in SBN nor in GaN thin films.

[1] M. Cuniot-Ponsard, *Ferroelectrics - Material Aspects* (InTech, www.intechopen.com), Chap. 23, p 497-518 (2011)

[2] Hwa-Mok Kim, D. S. Kim, D. Y. Kim, T. W. Kang, Yong-Hoon Cho and K. S. Chung, *Appl. Phys. Lett.* **81**, 2193 (2002)

[3] M. Cuniot-Ponsard, J.M. Desvignes, A. Bellemain, F. Bridou, *J. Appl. Phys.* **109**, 014107 (2011).

PZT film thickness dependence on the structural, microstructural and electrical properties

M. Bousquet¹, B. Viala¹, J. Mouchot¹, H. Achard¹, E. Nolot¹, G. Le Rhun¹, E. Defay¹

1- CEA, LETI, MINATEC, 17 Rue des Martyrs, F38054 Grenoble, France

Main author email address: marie.bousquet@cea.fr

Lead zirconate titanate $\text{Pb}(\text{Zr}_x\text{Ti}_{1-x})\text{O}_3$ (PZT) thin films have been widely used in various microelectronic devices such as ferroelectric memories, capacitors and microelectromechanical systems (MEMS) etc. In particular, PZT thin films near the morphotropic phase boundary with $x \approx 52/48$ are of great interest owing to their high dielectric constants ($\epsilon_r = 730 - 1180$), high remanent polarization ($P_r = 20 - 97 \mu\text{C}/\text{cm}^2$), and high piezoelectric coefficients ($d_{33} = 223 \text{ pC}/\text{N}$, $e_{31,f} = -18.7 \text{ C}/\text{m}^2$) [1, 2].

However, the continuous trend towards miniaturization requires scaling down the thickness of ferroelectric system below $\sim 500 \text{ nm}$. Thus, an understanding of the influence of film thickness on the electrical properties is of primary importance for integration, functionality and reliability of the applications [3].

For such purpose, the present work is devoted to the thickness dependence of the structural, microstructural, and electrical properties of (100)-oriented PZT thin films.

PZT thin films with thickness ranging from 50 to 600 nm are prepared on 8 inch-diameter platinumized silicon (Pt/Si) substrates by sol-gel method. Structural, microstructural and chemical analyses are carried out by means of X-Ray Diffraction (XRD), Scanning Electron Microscopy (SEM), and Atomic Force Microscopy (AFM). In all cases, a highly (100)-textured, dense and crack-free PZT films are obtained. An increase in the mean grain sizes with the film thickness is also observed. We develop an original method based on wavelength-dispersive X-ray fluorescence spectrometry (WD-XRF) in order to determine the composition and the film thickness. WDXRF and ellipsometry measurements confirm the presence of a chemical composition gradient within the film thickness, which is characteristic of sol-gel deposited PZT film. The residual stress in the PZT films, determined by means of the wafer curvature method, are found to be tensile and decrease when the film thickness increase.

Finally, polarization-electric field (P-E) ferroelectric hysteresis, low-field dielectric permittivity, and nonlinear dielectric response as well as converse longitudinal piezoelectric response ($d_{33,d}$) of the PZT films, are systematically investigated as a function of the film thickness. The obtained results are explained based on film orientation, grain size, domain structure, domain wall motion, and non-switching interface layers.

[1] S. Trolier-McKinstry and P. Muralt, *J. Electroceram.* **12**, 7 (2004).

[2] N. Izyumskaya, Y. -I. Alivov, S. -J. Cho, H. Morkoç, H. Lee, and Y. -S. Kang, *Crit. Rev. Solid State Mater. Sci.* **32**, 111 (2007).

[3] N. Setter, D. Damjanovic, L. Eng, G. Fox, S. Gevorgian *et al.*, *J. Appl. Phys.* **100**, 051606 (2006).

Coupling between Polarization and Spin Transport in Multiferroic Tunnel Junctions

prof dr Marin Alexe, mr Andy Quindeau, mr Daniele Preziosi, dr Ignasi Fina

Email: malexe@mpi-halle.mpg.de

Traditionally spin polarized transport, or more general spintronics, and ferroelectricity have been largely two independent research areas. Only recently, a new dimension was added to spintronic devices, such as magnetic tunnel junction (MTJ), by adopting ferroelectric layers, which possess permanent dielectric polarization switchable between two stable states, as active materials. The resulting multiferroic tunnel junction (MFTJ) is in principle a non-volatile memory device with four states given by two ferroelectric polarization directions in the barrier and two different magnetization alignments of the electrodes.

At a more general level the coupling between ferroelectric polarization and magnetization, especially at the interface between the two materials, may result in new effects and rich physics. The present talk will address this interface mediated coupling showing, for instance, how the ferroelectric switching can induce a reversible and remanent *inversion* of the spin polarization in MTJ [1], or a massive modulation of the magneto-resistance in certain correlated electron oxides.[2]

[1] D. Pantel, S. Goetze, D. Hesse and M. Alexe, Nature Materials 11, 289 (2012)

[2] D. Preziosi et al, unpublished.

Lattice dynamics of bismuth ferrite revisited

J. Hlinka¹, J. Pokorný¹, F. Borodavka¹, P. Ondrejko¹

1- Institute of Physics, Academy of Sciences of the Czech Republic, Prague, Czech Republic

pokorny@fzu.cz

Characterisation of phonon modes in ferroelectric materials is essential for quantitative insight into their dielectric and electromechanical properties as well as magnetoelectric coupling in multiferroics. BiFeO₃ is a prototypical rhombohedral (*R3c*) multiferroic system, simultaneously ferroelectric and antiferromagnetic at room temperature ($T_C \sim 1100$ K, $T_N \sim 640$ K). Despite numerous studies, assignment of its polar phonon modes remains a controversial issue. Several mode-assignment strategies have been suggested with mutually contradicting results [1-4].

In the past, we carried out a series of micro-Raman experiments on bulk ceramics, single-crystal and films. We employed precise focusing capabilities and high signal throughput of current spectrometers for collecting large sets of Raman spectra at different geometries as well as sophisticated numerical processing for quantitative analysis. We numerically analysed the trends in curve-fitted frequencies [1] and intensities to obtain dispersion curves which served as a basis for mode assignment.

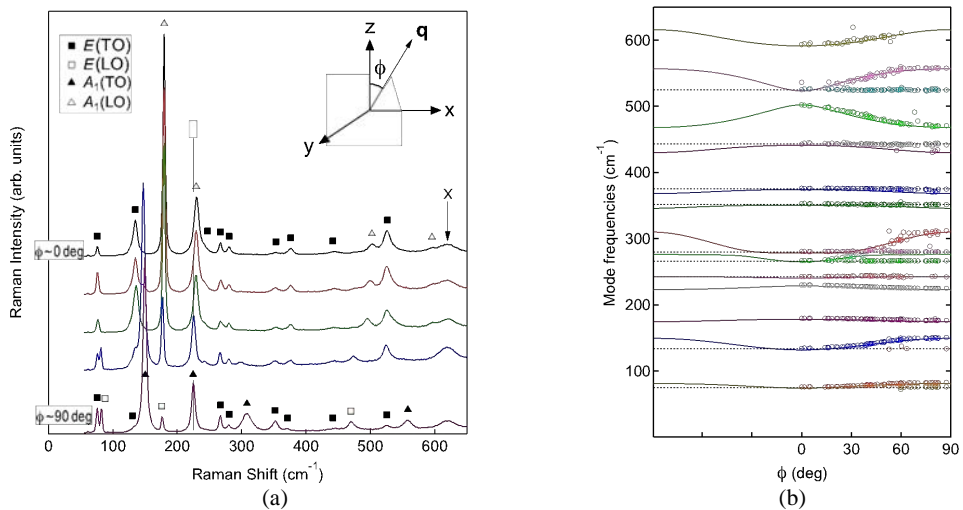


Figure 1 Micro-Raman spectra of BiFeO₃ bulk ceramics as an example of the experimental data: (a) Raman spectra from within different grains. (b) Angular dispersion of the phonon modes in BiFeO₃. Open circles represent the experimental fitted mode frequencies as a function of grain orientation, solid lines are the computed angular dispersion curves [1].

In this contribution, we will revisit the Raman results of our previous studies [1] as well as of the works published by other authors [2-3]. We will discuss both the conventional polarisation analysis of the spectroscopic data obtained on high-symmetry crystal facets and the alternative approach based on angular dispersion of oblique phonon modes. Possible sources of the reported disagreements will be discussed, including challenges connected with the rhombohedral structure and crystal twinning. We will try to resolve the controversies and demonstrate consistency of the raw spectroscopic data obtained by different authors.

[1] J. Hlinka, J. Pokorný, S. Karimi and I. M. Reaney, Angular dispersion of oblique phonon modes in BiFeO₃ from micro-Raman scattering, *Phys. Rev. B*, 83, 020101, pp. 1-4, (2011).

[2] C. Beekman, A. A. Reijnders, Y. S. Oh, S. W. Cheong and K. S. Burch, Raman study of the phonon symmetries in BiFeO₃ crystals, *Phys. Rev. B*, 96, 020403, pp. 1-5, (2012).

[3] R. Palai, H. Schmid, J. F. Scott and R. S. Katiyar, Raman spectroscopy of single-domain multiferroic BiFeO₃, *Phys. Rev. B*, 81, 064110, (2010).

[4] R. P. S. M. Lobo, R. L. Moreira, D. Lebeugle and D. Colson, Infrared phonon dynamics of a multiferroic BiFeO₃ single crystal, *Phys. Rev. B*, 76, 172105, pp. 1-4, (2007).

Magnetolectric Imaging at Buried Interfaces

O. Vlasin, B. Casals, N. Dix, F. Sánchez, G. Herranz

Institute of Materials Science of Barcelona ICMA-B-CSIC, Campus de la UAB, 08193 Bellaterra, Catalonia, Spain

gherranz@icmab.es

The electric-field control of data stored in magnetic units offers clear-cut advantages in terms of low-energy consumption and fast information processing [1]. These features prefigure a promising alternative to the nowadays conventional electronics, and foretell a future technology in which nonvolatile memory and data processing elements can be dynamically controlled by external fields. In composite magnetolectric systems, applied electric fields can modulate the magnetic properties either by mechanical means or by purely electrostatic effects. The thorough development of such novel electronics demands a complete understanding of the dynamics of the cross-coupling and its response mapped at the microscopic scale. Recent spectacular advances enable the direct visualization of magnetolectric domains in single crystals [2]. Yet, for room-temperature applications, the most promising approach is based on ferromagnetic/ferroelectric composite systems, where the magnetolectric coupling occurs deeply underneath any surface, making extremely difficult to have a simultaneous access to both magnetism and ferroelectricity.

Here we present a comprehensive experimental methodology that exploits optics as a probe of the magnetic and ferroelectric properties and that overcomes such limitations [3]. More specifically, we used the effects that ferroelectricity and magnetism exert on the light polarization, i.e., birefringence induced by electro-optic and magneto-optic effects, respectively. The analysis was performed at room temperature in a Pt(10 nm)/BaTiO₃ (120 nm)/La_{2/3}Sr_{1/3}MnO₃ (40 nm) trilayer, where the magnetolectric coupling emerges about 150 nm below the surface. By analyzing the evolution of the light polarization we have measured how the ferroelectric-induced electro-optic signal was changed under the application of magnetic fields. Additionally, we have measured the spatial distribution of this magnetolectric coupling strength with diffraction-limited resolution (< 500 nm for red light). A remarkable large effect was found, in which the ferroelectric-related birefringence was modulated by about 50% on average. A largely non-uniform distribution of the local magnetolectric response was found, which we assign to a mesoscopic texturing of electronic phases at the BaTiO₃/La_{2/3}Sr_{1/3}MnO₃ interface.

These results demonstrate the outstanding potential of optical microscopy to image simultaneously ferroelectricity and magnetism. In particular, the possibility of probing the magnetolectric coupling deeply buried at interfaces makes this a unique technique, providing novel clues for the dynamic analysis of magnetolectric coupling in multiferroic systems. Not the least, the observed large effects poise strongly correlated electronic systems as a suitable platform for large room-temperature magnetolectric responses.

[1] M. Bibes and A. Barthélémy, Multiferroics: towards a magnetolectric memory. *Nat. Mater.* 7, 425–426 (2008).

[2] Geng, Y. et al., Direct visualization of magnetolectric domains, *Nature Mater.* Published online 1st december 2013, doi:10.1038/nmat3813.

[3] O. Vlasin et al., in preparation.

Stress-induced phase transition in a poled KNbO_3 crystal: Micro-thermal expansion and micro-Raman study

Ph. Colomban^{1,2}, A. Ślodziak^{1,2}, G. Gouadec^{1,2}, M. Pham Thi³

1- Sorbonne Universités, UPMC Univ Paris 06, UMR 8233, MONARIS, F-75005, Paris, France

2- CNRS, UMR 8233, MONARIS, F-75005, Paris, France

3- THALES Research & Technology France, 91767 Palaiseau, France

philippe.colomban@upmc.fr

Piezoelectric ceramics of complex (KNbO_3 (KN) and $(\text{K}/\text{Na}/\text{Li})(\text{Nb}/\text{Sb}/\text{Ta})\text{O}_3$ (KNL-NST) compositions are non-toxic environment-friendly alternatives to lead-based relaxor ferroelectrics¹. A 30 MHz linear array transducer prototype based on a KN single crystalline 1-3 piezocomposite presents a thickness coupling factor of 50 %². Its high sensitivity, spatial resolution and depth-of-field confirm the high potential of this new generation of probes. In this study, KN behaviour was investigated as a function of temperature, applied stress and poling. Monocrystalline platelets of different sizes (FEE GmbH, Germany), poled along the [001] direction (perpendicularly to their flat surface) were studied by microdilatometry under axial loads varying from 0.2MPa to 15MPa at the measurement point ($<10 \times 10 \mu\text{m}^2$). Each sample was probed before and after the runs by micro Raman scattering, in different light polarization setups.

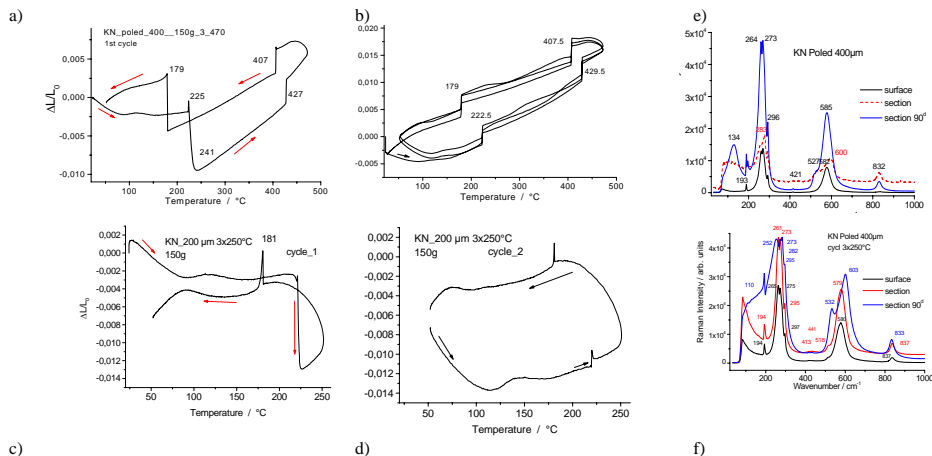


Figure 1: a) to d) Micro thermal expansion curves along the [001] direction of a poled KN single crystal stressed to ~ 15 MPa. a) 1st cycle up to 470°C ; b) 4th to 6th cycles up to 470°C ; c) and d) show details of the first and second cycles when heating is limited to 250°C ; e) and f) show the R.T. Raman spectra of a poled crystal, before (orthorhombic symmetry) and after (tetragonal symmetry) three cycles up to 250°C.

The 1st order phase transitions observed at $\sim 225/179^\circ\text{C}$ and $427/407^\circ\text{C}$ in Fig. 1 (a-d) were previously reported but we showed that their amplitude strongly depends on the applied stress and thermal history. Besides, we evidenced a stress-dependant contraction event occurring on heating the samples from R.T. up to 100°C . The Curie transition ($T_c \sim 428^\circ\text{C}$) is almost the same in poled and depoled samples (Figs 1a&b) whereas the swelling accompanying the 223°C transition of a depoled sample is replaced in a poled sample by a sharp expansion step at 225°C , followed by a contraction up to $\sim 240^\circ\text{C}$ (Figs 1a&c). This contraction almost disappears in case of a second thermal cycle (Fig. 1d), in relation with domains/twins formation, but it takes 6 cycles above T_c for dilatometry curves to become reproducible (Fig. 1b). It appears that the symmetries/structures are modified by crystal poling and stress (Figs 1e&f), with a remnant effect after heating above T_c . Poling the sample forces it to adopt orthorhombic R.T. symmetry and the tetragonal to rhombohedral transition that is normally observed around 223°C on cooling the high temperature phase can be hindered by the appropriate choice of thermal path and sample loading. The resulting domain/twinning and nano-heterogeneity most likely explains the high piezo properties, as observed for relaxors. However, the relative phase proportion is hard to anticipate because it will depend on the sample geometry and the poling, thermal and stress histories altogether.

1. Y. Saito, H. Takao, T. Tani, T. Nonoyama, K. Takatori, T. Homma, T. Nagaya & M. Nakamura, Lead-free piezoceramics, *Nature*, 2004, 432, 84–87.

2. E. Filoux, C. Bantignies, R. Rouffaud, M. Pham Thi, J.M. Grégoire, F. Levasort; *IEEE Int. Ultrasonics Symp.*, (2013).

Ferroelectric Properties of the Potassium Sodium Niobate-Based Ceramics

G.M. Kaleva¹, V.S. Akinfiyev², A.V. Mosunov¹, S.Yu. Stefanovich^{1,2}, E.A. Fortalnova³, E.D. Politova¹

¹L.Ya. Karpov Institute of Physical Chemistry, Obukha s.-st. 3-1/12, b. 6, Moscow, 105064, Russia

² Faculty of Materials Science, Lomonosov Moscow State University, Leninskie gory, 1, Moscow, 119992, Russia,

³ Peoples' Friendship University of Russia, Ordzhonikidze st., 3, Moscow, 117198, Russia

politova@cc.nifhi.ac.ru

Both ecological problems and demands of various industries simulate search for new lead-free piezoelectric materials for high temperature applications. Perovskite structure solid solutions on the base of $K_{0.5}Na_{0.5}NbO_3$ (KNN) composition close to Morphotropic Phase Boundary (MPB) with high Curie temperature $T_C \sim 700$ K may be used as basic oxide for the development of new piezoelectric materials [1]. However, K and Na oxides loss in course of high temperature sintering stage make the preparation of dense ceramics rather difficult task, and their piezoelectric properties depend on method of preparation [2, 3]. To improve sintering, various additives with low melting temperatures may be used, however, till now functional properties of these materials can not compete with those of the PZT-based materials.

We studied ceramic solid solutions $(K_{0.5}Na_{0.5})NbO_3$ modified by various overstoichiometric additives (KCl, NaCl, $CaCl_2$, LiF and MnO_2). The samples were prepared by the solid-state reaction method [4].

The phase formation, structure, microstructure, dielectric and ferroelectric properties were studied using the X-ray Diffraction, DSC/DTA, Scanning Electron Microscopy (SEM), Second Harmonic Generation (SHG), and Dielectric Spectroscopy methods.

The formation of solid solutions with relative content of tetragonal and rhombohedral phases depending on composition and preparation conditions was observed. The influence of additives on dielectric properties and Curie temperature T_C was revealed.

Temperature dependences of dielectric permittivity of initial KNN samples are characterized by maxima near 700 K. It was found out that T_C value increased to ~ 100 K in compositions modified by KCl or LiF additives. The increase in both T_C and dielectric permittivity values observed for doped ceramics pointed to the presence of Li ions in A-sites of the perovskite lattice. Moreover, significant decreasing of electric conductivity was typical for modified compositions that favored to effective poling of ceramics.

High values of the SHG signal confirmed polar nature of the samples, and high spontaneous polarization P_s value made them promising for the development of new functional materials.

[1] Y. Saito, H. Takao, T. Tani Tatsuhiko Nonoyama, Kazumasa Takatori, Takahiko Homma, Toshiatsu Nagaya & Masaya Nakamura Lead-free piezoceramics, Nature. 2004, vol. 432, pp. 84–87.

[2] J. Bernard, A. Bencan, T. Rojac, J. Holc, B. Malic, and M. Kosec, Low temperature sintering of $(K_{0.5}Na_{0.5})NbO_3$ ceramics J. Am. Ceram. Soc. 2008, vol. 91, pp. 2409–2411.

[3] M.S. Yoon, N.H. Khansur, W.J. Lee, L.Y. Geun, S.C. Ur, Effects of $AgSbO_3$ on the Piezoelectric/Dielectric Properties and Phase Transition of Li_2O Doped NKN Lead-Free Piezoelectric Ceramics, Journal Advanced Materials Research. 2011, V. 287–290, p. 801–804.

[4] G. M. Kaleva, A. V. Mosunov, S. Yu. Stefanovich, and E. D. Politova, Preparation and Dielectric Properties of Potassium Sodium Niobate-Based Solid Solutions, Inorganic materials, 2013, Vol. 49, No. 8, pp. 826–833.

The work was supported by the Russian Fund for Basic Research (Grant 12-03-00388).

Phase Transitions Dynamics in $\text{Ag}_{1-x}\text{Li}_x\text{NbO}_3$

J. Macutkevic¹, J. Banys¹, I. Gruszka², A. Kania²

1- Faculty of Physics, Vilnius university, Saulėtekio al. 9, LT-10222 Vilnius, Lithuania

2- Institute of Physics, University of Silesia, ul. Uniwersytecka 4, PL-40-007 Katowice, Poland

Main author email address: jan.macutkevic@gmail.com

X-ray, electron diffraction, dielectric, Raman, and domain structure studies showed that in silver niobate (AgNbO_3) the following phase transitions are observed at temperatures: 340 K—from the orthorhombic M_1 to the orthorhombic M_2 , 540 K—from the orthorhombic M_2 to the orthorhombic M_3 , 626 K—from the orthorhombic M_3 to the orthorhombic O_1 , 634 K—from the orthorhombic O_1 to the orthorhombic O_2 , 660 K—from the orthorhombic O_2 to the tetragonal T, 852 K—from the tetragonal T to the cubic C [1-3]. The M_1 phase exhibits ferroelectric properties, the phases M_2 and M_3 are antiferroelectric and phases O_1 , O_2 , T and C are paraelectric. All phase transitions are mostly related to Nb ions dynamics, however the role of Ag and O ions should not be neglected [2]. Therefore it is very interesting to investigate dielectric properties of various mixed systems like $\text{Ag}_{1-x}\text{Li}_x\text{NbO}_3$ (ALN) in wide frequency range. In this work results of dielectric investigations in very wide frequency range (20 Hz -3 THz) of $\text{Ag}_{1-x}\text{Li}_x\text{NbO}_3$ solid solutions, for Li concentration range $0 < x < 0.1$, are reported. These materials of a perovskite structure and exhibit the orthorhombic symmetry at room temperature. Several important aspects of Li substitution were found. The first one is associated with a shift of M_1 - M_2 anomaly to lower temperatures, an appearance of low frequency dielectric dispersion in the region of anomaly, finally the M_1 - M_2 anomaly vanishes for $\text{Ag}_{0.94}\text{Li}_{0.06}\text{NbO}_3$. The second one is related to a gradual increase of the broad $\epsilon(T)$ maximum associated with the transition between disordered antiferroelectric M_2 and

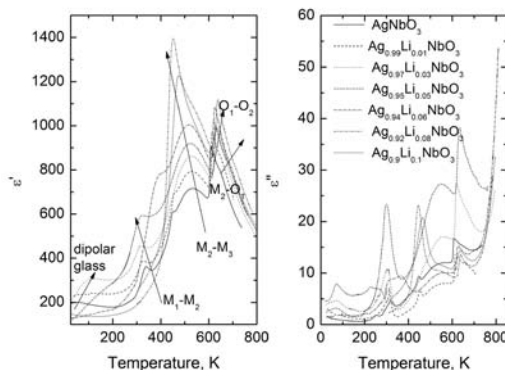


Fig. 1 Temperature dependence of complex dielectric permittivity of $\text{Ag}_{1-x}\text{Li}_x\text{NbO}_3$ at 1 MHz.

M_3 phases. The third one is related with appearance of dipolar glass behaviour at low temperatures for ceramics with $0.01 \leq x \leq 0.5$. No low frequency dielectric dispersion was observed below room temperature for $x \geq 0.6$. The fourth one is related with electrical conductivity behaviour of the system, which is observed at higher temperatures (above 600 K). Activation energy of DC electrical conductivity has pronounced minimum for $x=0.1$. The Li substitution influence is discussed in terms of the appearance of electric dipole moments linked with the occupation of the off-centre positions by Li ions.

This research is funded by the European Social Fund under the Global Grant measure.

1. H. U. Khan, I. Sterianou, S. Miao, J. Pokorny and I. M. Reaney, The effect of Li substitution on the M-phases of AgNbO_3 . J. Appl. Phys. 111, pp. 024107 (2012).
2. A. Kania, S. Miga, Preparation and dielectric properties of AgLiNbO_3 solid solutions ceramics. Material Science and Engineering B 86, pp. 128-133 (2001).
3. I. Levin, V. Krayzman, J. C. Wojcik, J. Karapetrova, T. Proffen, M. Tucker, I. M. Reaney, Structural changes underlying the diffuse dielectric response in AgNbO_3 . Phys. Rev. B 79, pp. 104113 (2009).

Effects of Na excess on dielectric and electrical properties of $(\text{Na}_{0.53+x}\text{K}_{0.47})(\text{Nb}_{0.55}\text{Ta}_{0.45})\text{O}_3$ ceramics

M. S. Kim, J. S. Kim, M. H. Kim*

School of Advanced Materials Engineering, Changwon National University, Gyeongnam 641-773, Republic of Korea

* E-mail address: mhkim@changwon.ac.kr

$(\text{Na}_{0.5}\text{K}_{0.5})\text{NbO}_3$ (NKN) has been considered as one of the superior lead-free candidate materials to replace PZT ceramics because of its good piezoelectric properties and high curie temperature [1]. Recently, we have investigated a new lead-free Ta-substituted $(\text{Na}_{0.53}\text{K}_{0.47})(\text{Nb}_{0.55}\text{Ta}_{0.45})\text{O}_3$ (NKNT) ceramic having high piezoelectric coefficient $d_{33} = 284$ pC/N. Additionally, piezoelectric coefficient of Na excess $(\text{Na}_{0.545}\text{K}_{0.47})(\text{Nb}_{0.55}\text{Ta}_{0.45})\text{O}_3$ ceramics increase from 284 pC/N to 333 pC/N [2]. Due to volatile nature in NKN ceramics, Na and K ion create the alkali-ion vacancies during sintering process. To retain the charge neutrality, the alkali vacancies make the oxygen vacancy which affect electrical conductivity. However, few dielectric and electrical properties have been reported on changes in NKN based ceramics with frequency and temperature. The low-frequency dielectric dispersion was investigated in wide frequency range (0.1 Hz ~ 10 MHz). In addition, complex impedance analysis permits the contribution of the bulk, the grain boundary and the interfacial effect to be separated [3]. So, we have investigated the electrical properties of $(\text{Na}_{0.53+x}\text{K}_{0.47})(\text{Nb}_{0.55}\text{Ta}_{0.45})\text{O}_3$ ($x=0.0$ - 0.015) ceramics on the complex impedance spectroscopy.

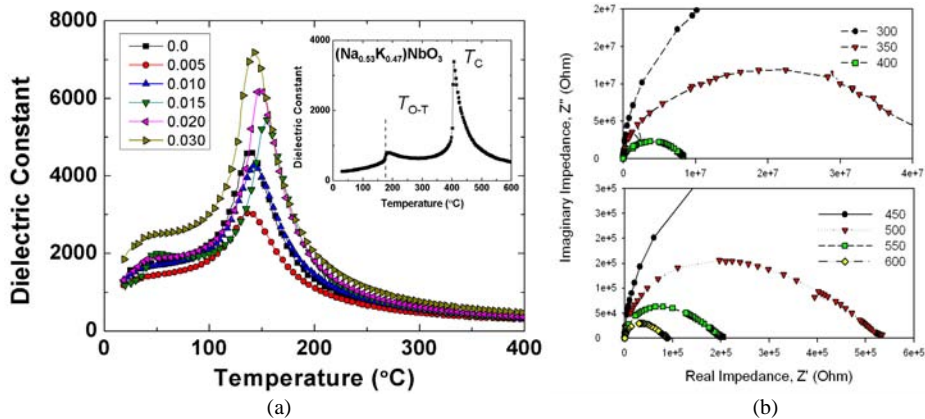


Figure (a) Temperature dependences of the dielectric constant Na-excess NKNT ceramics at various frequency. (b) Complex Impedance plot of the Na-excess NKNT ceramics at $x=0.015$.

Figure (a) shows the temperature dependences of the dielectric constant of the ceramics measured at 100 kHz. The inset shows the results of NKN ceramics. It is found that Na excess and Ta substitution increased the dielectric constant and decreased the loss tangent at the boundary of T_{O-T} and T_C . On the other hand, the electric conductivity (σ) obtain by using the imaginary dielectric constant (ϵ'') which is associated with the conductivity $\sigma(\omega) = \epsilon_0 \omega \epsilon''$. With increasing frequency (f), the ac conductivity (σ) increases and obeys the power law $\sigma(\omega) = \sigma_{dc} + A\omega^s$. Compared to the ac electrical conductivity of stoichiometry NKNT, that of Na-excess NKNT was slightly lower, which is due to decrease of charge carriers. With increasing temperature over T_C , the ac conductivity is independent on the low frequency, which is corresponds to dc conductivity. Figure (b) shows the complex impedance plots of the Na-excess NKNT ceramics. The dc conductivity is given by the points of intersection of the x -axis in the corresponding complex impedance semicircular arcs. Due to Na and K volatilization, defects such as oxygen and alkali-ion vacancies will be created. However, Na excess NKNT compensates for defects and decreases the formation of vacancies. Therefore, Na excess on NKNT ceramics decreases electrical conductivity, which will enhance the poling process and the piezoelectric properties.

[1] Li et al, "(K, Na)NbO₃-Based Lead-Free Piezoceramics : Fundamental Aspects, Processing Technologies, and Remaining Challenges", J. Am Ceram. Soc, 96[12], 3677-3696 (2013).

[2] Y. S. Sung et al, "Enhanced piezoelectric properties of $(\text{Na}_{0.5+y+z}\text{K}_{0.5-y})(\text{Nb}_{1-x}\text{Ta}_x)\text{O}_3$ ceramics", Appl. Phys. Lett, 101, 012902 (2012).

[3] J. S. Kim et al, "Effects of Tungsten Doping on Dielectric and Impedance Spectroscopy of Bismuth-Lanthanum-Titanate (BLT) Ferroelectrics", J. Korean Phys. Soc. 53[3], 1617-1621 (2008).

High strain effect on the soft mode, ferroelectricity and phase transition in lead-free $[\text{BaTiO}_3]_{(1-x)\Lambda}/[\text{BaZrO}_3]_{x\Lambda}$

M. El Marssi¹, J. Belhadi¹, Y. Gagou¹, F. de Guerville¹, Yu. I. Yuzyuk², I. Raevski²

¹Université de Picardie Jules Verne, LPMC, 33 rue Saint-Leu, F-80039 Amiens, France

²Rostov State University, Faculty of Physics, Zorge 5, Rostov-on-don 344090, Russia

* E-mail: mimoun.elmarssi@u-picardie.fr

We present X-ray diffraction and Raman spectroscopy measurements studies of artificial superlattices (SLs) consisting of ferroelectric BaTiO_3 (BT) and paraelectric BaZrO_3 (BZ) and compared their proprieties to the individual thin films BT and BZ. All samples were grown by pulsed laser deposition technique onto (100) MgO substrates buffered with an electrode of $\text{La}_{0.5}\text{Sr}_{0.5}\text{CoO}_3$ (LSCO). We have growth five different SLs of the type $\text{BT}_{(1-x)\Lambda}/\text{BZ}_{x\Lambda}$, where $x=0.15, 0.30, 0.50, 0.70,$ and 0.85 , the modulation period Λ is approximately 100 \AA , and the total thickness of each SL was approximately 3000 \AA . We have varied the BT and BZ layers thickness with the aim to change the epitaxial strains in $\text{BT}_{(1-x)\Lambda}/\text{BZ}_{x\Lambda}$ SLs, while the number of the interfaces was constant.

The out-of-plane lattice parameters of the SLs constituents were determined by modeling of the x-ray diffractograms. The results indicate that the polar c -axis of the BT layers lies in the plane of the substrate and BZ layers exhibit enhanced tetragonal distortion which is induced by the large mismatch between the alternating BZ and BT layers. The variation of the soft mode as a function of the modulation period shows a partial relaxation at the critical period Λ_c above which it is energetically more favorable to relax the strain in the SLs due to misfit dislocations. We discuss the coupling between the constituents of the SLs and the reduction of the disorder in ATiO_3 perovskite due to the strain in SL's. The results will be compared to those obtained on the less constrained $\text{BaTiO}_3/\text{BaTi}_{0.68}\text{Zr}_{0.32}\text{O}_3$ superlattices [1,2].

We discuss the strain-induced ferroelectricity in BZ layers of the large constrained SL's. Temperature dependence of Raman spectra of BT/BZ SLs shows a huge shift of the phase transition in BT layers and the stabilisation of ferroelectric phase in BZ up to very high temperature.

[1] F. De Guerville, M. El Marssi, I. P. Raevski, M.G. Karkut, Yu. I. Yuzyuk

Phys. Rev. B **74**, 064107 (2006).

[2] M. El Marssi, Y. Gagou, J. Belhadi, F. de Guerville, Yu. I. Yuzyuk, I. P. Raevski,

J. Appl. Phys. **108**, 084104 (2010).

Thickness dependent stress relaxation, twinning and thermal expansion of epitaxial LiNbO_3 and LiTaO_3 thin films on C-sapphire

A. Bartasyte^{1,2}, V. Plausinaitiene³, A. Abrutis³, S. Stanionyte³, S. Margueron⁴, V. Kubilius³, P. Boulet², S. Huband⁵, and P.A. Thomas⁵

1- Femto-ST Institute, University of Franche-Comté and CNRS (UMR 6174), 32 avenue de l'Observatoire, Besançon, France, 25044

2- Jean Lamour Institute, Lorraine University and CNRS (UMR 7198), Parc du Saurupt, Nancy, France, 54011

3- Department of General and Inorganic Chemistry, Vilnius University, Naugarduko 24, Vilnius, Lithuania, LT-03225

4- Laboratoire Matériaux Optiques, Photonique et Systèmes, EA 4423, Lorraine University and Supelec, 2 rue Eduard Belin, Metz, France, 57070

5- Department of Physics, University of Warwick, Gibbet Hill Road, Coventry, UK, CV4 7AL

Main author email address: ausrine.bartasyte@femto-st.fr

LiNbO_3 (LN) and LiTaO_3 (LT) are two of the most important crystals in the field of optics, nonlinear optics, optoelectronics and acoustics. Thus, LN and LT thin films are attracting interest due to miniaturization and integration of devices into silicon technologies. The deposition of LN and LT thin film by different techniques has been studied for more than twenty years. However, the high quality LN films suitable for acoustic and optic applications are not available at present. First of all, alternative methods to standard $\Theta/2\Theta$ spectra of X-ray diffraction (XRD) have to be used to identify the presence of parasitical phases in the films [1], which were rarely considered in the literature. One more difficulty is the estimation and control of Li concentration, the key parameter determining the physical and structural properties of LN and LT, within the films. The methods for the identification of parasitical phases and the estimation of residual stress and Li stoichiometry by means of Raman scattering have been reported [1, 2]. It is known that the structural quality of the films highly affects the physical properties of the films. The most complicating structural factors are twinning and cracking of LN and LT films, which induce high acoustical and optical losses and contribute to the degradation of physical properties. The appearance of in-plane epitaxial variant was reported in numerous literature works. However, only a few groups studied the $\{011\bar{2}\}$ twinning system in LN films, which presence cannot be identified in standard $\Theta/2\Theta$ spectra of XRD. Thus, very little known effects of deposition and annealing conditions, non-stoichiometry and residual stresses on the mechanical twin structure in thin films, which might degrade the physical properties considerably, were investigated. It was shown that the $\{011\bar{2}\}$ twinning contributed significantly to the stress relaxation in the thick films. The stresses in thin films can alter the mechanical, optical, structural, and electrical properties, which play a direct part in the reliability of devices. Many literature works report high residual stresses in the epitaxial LN and LT films, but the effect of stresses on the physical and structural properties remains not well understood. The significant changes of the in-plane and out-of-plane thermal expansions of LN films due to the clamping by the substrate, which could be useful in the creation of thermally stable surface acoustic wave devices, was recently reported [2]. To be able to tune the thermal expansion of LN films in a controlled way, the relationships between the thermal expansion and the thickness of the film/residual stresses/clamping were studied. Moreover, the inelastic deformation and elastic hysteresis of lattice parameters during the heating-cooling cycles were observed. The residual stresses and thermal expansion of films were highly thickness dependent.

[1] A. Bartasyte, V. Plausinaitiene, A. Abrutis, et al., J. Phys.: Condens. Matter 25, 205901(2013).

[2] A. Bartasyte, V. Plausinaitiene, A. Abrutis, et al., Appl. Phys. Lett. 101, 122902 (2012).

Electrochemical instability at PZT/electrode interfaces during polarisation reversal

F. Chen^{1,2}, A. Klein¹

¹ Technische Universität Darmstadt, Institute of Material Sciences, Surface Science, Jovanka-Bontschits-Str. 2, 64287 Darmstadt, Germany

² High Magnetic Field Laboratory, Chinese Academy of Sciences (CAS), and Hefei National Laboratory for Physical Sciences at Microscale, University of Science and Technology of China, Hefei 230026, China

aklein@surface.tu-darmstadt.de

Electrical fatigue corresponds to a decrease of switchable polarisation during cycling. In particular for thin film materials, this prevented application as non-volatile memories until the discovery of stable operation with oxide electrodes. Upon the suitable electrode materials are RuO₂ and IrO₂ as well perovskites like SrRuO₃ or (La,Sr)MnO₃. With Pt electrodes, a phase decomposition of PZT to the pyrochlore structure at the interface, which can lead to fatigue, has been identified using Raman spectroscopy by Lou et al. [1]. Charge injection during initial domain switching has been suggested to be the microscopic origin of the phase decomposition. Based on X-ray photoelectron spectroscopy (XPS) measurements, we suggest a different electrochemical mechanism as origin for the decomposition of PZT at electrode interfaces in this presentation.

We have performed XPS measurements of the interfaces of PZT with different electrode materials during polarisation switching. Such measurements are sensitive not only to chemical changes of the interface but also to the changes of the Schottky height. Recent measurement of BaTiO₃ single crystals have revealed changes of the ferroelectric/electrode Schottky barrier height of up to 1 eV [2]. Here we present measurements of polycrystalline ceramic PZT samples. Commercial PZT with morphotropic composition (PIC151 from PI ceramics, Lederhose, Germany) have been polished to 150 μm thickness. To avoid chemical reactions with the PZT substrate during metal deposition [3], metallic RuO₂ and Sn-doped In₂O₃ (ITO) were used as electrode materials. Both were deposited by magnetron sputtering. Polarisation measurements exhibit almost rectangular hysteresis loops with remanent polarisation $P_r=0.33$ C/m² and coercive fields of $E_c=1$ kV/cm for both electrode materials. The samples were inserted and electrically connected in the XPS system allowing for XPS measurements with applied electric field. XP spectra of the PZT and electrode species were recorded in the unpolarised state and subsequently with saturation ($U = 300$ V) and remanent polarisation ($U=0$ V) conditions. Significant changes of the Schottky barrier height in dependence on polarization are observed. Due to the polycrystalline nature of the ferroelectric, the barrier heights become strongly inhomogeneous, as evident from the reversible asymmetric broadening of the PZT related core-level emissions. Most strikingly, a metallic Pb species appears with ITO electrodes. This is accompanied by a higher Fermi level position compared to the RuO₂ electrode, which is in good agreement with different Schottky barrier heights for the high work function material RuO₂ and the low work function material ITO [4]. The formation of metallic Pb with the ITO electrode, which indicates a chemical decomposition of PZT, is therefore explained by a fundamental electrochemical process. The decomposition is related to the intrinsic defect properties of the compound: When the Fermi level is raised above a critical value, which happens during polarisation reversal when the polarisation charge is incompletely screened by the electrode, the formation energies for certain defects may become negative (see e.g. [5]). The defects, in this case Pb vacancies, should then form spontaneously.

- [1] X.J. Lou, M. Zhang, S.A.T. Redfern, and J.F. Scott, *Local phase decomposition as a cause of polarization fatigue in ferroelectric thin films*, Phys. Rev. Lett. **97** (2006), 177601.
- [2] F. Chen, and A. Klein, *Polarization dependence of Schottky barrier heights at interfaces of ferroelectrics determined by photoelectron spectroscopy*, Phys. Rev. B **86** (2012), 094105.
- [3] F. Chen, R. Schafrank, W. Wu, and A. Klein, *Reduction induced Fermi level pinning at the interfaces between Pb(Zr,Ti)O₃ and Pt, Cu and Ag metal electrodes*, J. Phys. D: Appl. Phys. **44** (2011), 255301.
- [4] F. Chen, R. Schafrank, S. Li, W. Wu, and A. Klein, *Energy band alignment between Pb(Zr,Ti)O₃ and high and low work function conducting oxides - from hole to electron injection*, J. Phys. D: Appl. Phys. **43** (2010), 295301.
- [5] A. Klein, *Transparent Conducting Oxides: Electronic Structure – Property Relationship from Photoelectron Spectroscopy with in-situ Sample Preparation*, J. Am. Ceram. Soc. **96** (2013), 331.

Electrode and interface influences on ferroelectric properties of BaTiO₃ single crystals

A. Hubmann¹, S. Li¹, E. Sapper¹, M. Coll², T. Puig², A. Klein¹

¹ Technische Universität Darmstadt, Institute of Material Sciences, Jovanka-Bontschits-Straße 2, 64287 Darmstadt, Germany

² Institut de Ciència de Materials de Barcelona (ICMAB-CSIC), Campus UAB, 08193 Bellaterra, Spain

sli@surface.tu-darmstadt.de

BaTiO₃ is one of the most extensively investigated ferroelectrics and serves as a prototypical model for studying perovskite ferroelectric materials. Compared to ceramics and thin films, BaTiO₃ single crystals exhibit unique orientation and no strain. Ferroelectric domain formation and its switching behaviour should therefore be best studied using such materials. According to literature, BaTiO₃ (100) single crystals exhibit a spontaneous polarization up to 26 $\mu\text{C}/\text{cm}^2$ and a coercive field strength around 1 kV/cm [1,2]. However, up to now not much attention has been paid to the choice of the electrode material and its influence on the ferroelectric properties, especially for single crystals. In this contribution we present the study of polarization of BaTiO₃ single crystals using different metals and conductive oxides as electrode material.

It is well known, that the existence of screening charge is necessary for the formation of a stable polarization in a ferroelectric material. The formation of defects and dead layers affects the charge distribution and can therefore strongly affect the overall ferroelectric properties. We have used Pt, RuO₂ and (La,Sr)MnO₃ as electrode materials and studied the polarisation characteristics of BaTiO₃ single crystals. Depending on the electrode material, clear differences in spontaneous polarization (P_s) and coercive field strength (E_c) have been observed. In general, the crystals with oxide electrodes exhibit considerably higher P_s and lower E_c . The highest polarization of $>30 \mu\text{C}/\text{cm}^2$ has been observed with (La,Sr)MnO₃, which exceeds the highest values reported for BaTiO₃ single crystals. In comparison, crystals with Pt electrode show much lower P_s and higher E_c . Clear improvements in the polarization can be achieved by performing post-growth annealing on the samples with Pt electrode. It is evident, that the oxide electrodes form a better interface to BaTiO₃ directly after deposition with much lower defect concentration, whereas defects are created at the interface during the contact formation with Pt. It is evident, that even in single crystals, the ferroelectric properties do not only depend on the bulk of the ferroelectric material. The electrode materials and their interface conditions significantly influence the measured polarisation properties.

[1] B. Jaffe, W. R. Cook, H. Jaffe, Piezoelectric Cramics (Academic Press), (1971).

[2] A. J. Moulson, J. M. Herbert, Electroceramics (Wiley), Chapter 2, (2003).

Multiferroic Antipolar and Polar Phases in Metastable Perovskite $\text{BiFe}_{0.5}\text{Sc}_{0.5}\text{O}_3$

**A.N. Salak¹, D.D. Khalyavin², N.M. Olekhovich³, A.V. Pushkarev³, Yu.V. Radyush³,
I.P. Raevski⁴, M.L. Zheludkevich¹, M.G.S. Ferreira¹**

1- Department of Materials and Ceramic Engineering/CICECO, University of Aveiro, 3810-193 Aveiro, Portugal

2- ISIS Facility, Rutherford Appleton Laboratory, Chilton, Didcot OX11 0QX, UK

3- Scientific-Practical Materials Research Centre of NAS of Belarus, Minsk, 220072, Belarus

4- Faculty of Physics and Research Institute of Physics, Southern Federal University, 344090, Rostov-on-Don, Russia

salak@ua.pt

Effects of substitutions in both *A*- and *B*-sublattices on crystal structure and multiferroic properties of the perovskite systems based on BiFeO_3 are widely studied. A variety of phases has been revealed in those systems. However, in spite of a great number of publications, the conclusions on both crystal structure and the related properties of some phases are still ambiguous. Extended studies have been conducted only for few systems which can be prepared by the conventional methods. Studies of the systems obtained in specific conditions (e.g., under high pressure) are scarce [1].

This work was launched aiming to obtain a perovskite ceramics of the $\text{BiFe}_{0.5}\text{Sc}_{0.5}\text{O}_3$ composition, which is actually the equimolar solid solution in the BiFeO_3 - BiScO_3 system. Preliminary study showed that the desired composition cannot be prepared at ambient pressure: the product of a solid-state reaction turned out to be a phase mixture, where the rhombohedral phase based on bismuth ferrite with maximum 15 at.% Sc substitution was the only perovskite phase.

Single-phase perovskite $\text{BiFe}_{0.5}\text{Sc}_{0.5}\text{O}_3$ ceramics was synthesized at 6 GPa and 1500 K. It was revealed from joint refinement of x-ray and neutron diffraction data that at room temperature the as-prepared samples have the orthorhombic *Pnma* symmetry with the $\sqrt{2}a_p \times 4a_p \times 2\sqrt{2}a_p$ superstructure resulted from antiferroelectric displacements of Bi^{3+} along the $[101]_p$ pseudocubic direction and associated unusual (++--) oxygen octahedra tilting. Temperature XRD measurements showed that the antipolar phase transforms into the polar *R3c* phase on heating (Fig. 1). The transformation occurs in the temperature range of 700-750 K, where both phases coexist. This high-temperature *R3c* phase is isostructural with the polar phase of undoped BiFeO_3 . The *Pnma*→*R3c* transition was revealed to be irreversible at ambient pressure: subsequent cooling below 670 K resulted in appearance of an orthorhombic phase with the *Ima2* symmetry and the $2a_p \times \sqrt{2}a_p \times \sqrt{2}a_p$ supercell. This orthorhombic modification of $\text{BiFe}_{0.5}\text{Sc}_{0.5}\text{O}_3$ is a new type of a polar perovskite structure, where ferroelectric-like displacements of Bi^{3+} cations along the $[110]_p$ direction are combined with the antiphase octahedral tilting about the polar axis. Besides, the primary distortions couple antiferroelectric displacements of Bi^{3+} along the $[1-10]_p$ direction as well, resulting in a canted ferroelectricity. Analysis of the neutron diffraction and magnetization data has shown that both the polar *Ima2* and antipolar *Pnma* polymorphs exhibit a long-range *G*-type antiferromagnetic order with a weak-ferromagnetic component below $T_N \sim 220$ K. The weak-ferromagnetism in both phases was suggested to be

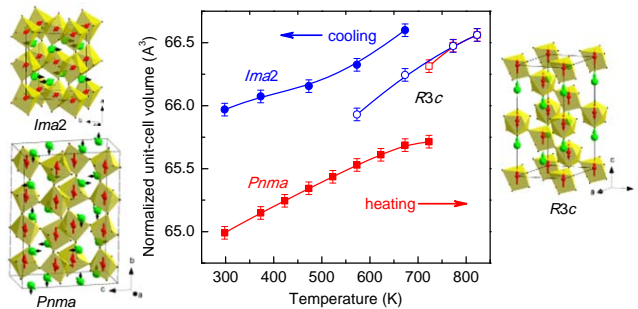


Figure 1. Temperature dependence of the normalized unit-cell volume (V/Z) of the metastable perovskite $\text{BiFe}_{0.5}\text{Sc}_{0.5}\text{O}_3$ (on heating and cooling). Polyhedral representations of the crystal structures corresponding to the observed phases (*Pnma*→*R3c*→*Ima2*) are shown.

mainly caused by the presence of the antiphase octahedral tilting whose axial nature directly represents the relevant part of Dzyaloshinskii vector. Existence of two multiferroic polymorphs (*Pnma* and *Ima2*) in $\text{BiFe}_{0.5}\text{Sc}_{0.5}\text{O}_3$ provides a unique opportunity to study the relations between (anti)ferroelectric, (anti)ferromagnetic and ferroelastic order parameters which all are present in these phases.

This work was supported by the EU Program 'NANEL' PIRSES-GA-2011-295273, the Russian Foundation for Basic Research (projects 12-02-90019 Bel-a and 12-08-00887-a), and the Belarussian Republican Foundation for Basic Research (project T12R-077).

[1] A. Belik, Polar and nonpolar phases of BiMO_3 : A review, Journal of Solid State Chemistry 195, 32-40 (2012).

Polar properties and phase diagram of the magnetoelectric $Gd_{1-x}Y_xMnO_3$ system

dr Rui Vilarinho, dr Abílio Almeida, dr Pedro Tavares, dr Joaquim Agostinho

IFIMUP-IN, Faculty of Sciences, University of Porto

ruivilarinhosilva@gmail.com

This work reports on magnetic, dielectric, thermodynamic and magnetoelectric properties of $Gd_{1-x}Y_xMnO_3$, $0 \leq x \leq 0.4$, with emphasis on the (x,T) phase diagram, towards unraveling the role of the driving mechanisms in the scope of available theoretical models.¹ The (x,T) phase diagram reflects the effect of lattice distortions induced by the substitution of Gd^{3+} ion by smaller Y^{3+} ions, which gradually unbalances the antiferromagnetic against the ferromagnetic exchange interactions, enabling the emergence of ferroelectricity for higher concentrations of yttrium.² For $x < 0.1$, the paramagnetic phase is followed by a presumably incommensurate collinear antiferromagnetic phase, then a weak ferromagnetic canted A-type antiferromagnetic ordering. An electric field applied in the temperature range of stability of the magnetic phase enhances the ferromagnetic character, pointing out for a magnetoelectric coupling. For $0.1 \leq x \leq 0.4$, a different phase sequence is obtained. The canted A-type antiferromagnetic arrangement is no more stable, and instead a pure antiferromagnetic ordering emerges. The antiferromagnetic spin arrangement strengthens as Y-concentration increases. On cooling, the collinear-sinusoidal incommensurate antiferromagnetic phase is followed by an antiferromagnetic phase, stable between $T_1 \approx 22 - 28$ K and $T_2 \approx 14 - 17$ K, depending on the Y-concentration. This magnetic phase does not allow a spontaneous electric polarization to be stabilized. Below T_2 is established a magnetic phase with spontaneous electric polarization. An applied electric field enhances its antiferromagnetic character, suggesting a magnetoelectric coupling due to the cycloidal modulated spin arrangement, accordingly to the predictions of the inverse Dzyaloshinskii–Moriya model.¹

¹ M. Mochizuki and N. Furukawa, Phys. Rev. B **80**, 134416 (2009).

² T. Goto et al, Phys. Rev. Lett. **92**, 257201 (2004).

Dielectric and non-linear properties of SrTiO₃@BaTiO₃ core-shell ceramic

Cristina E. Ciomaga¹, Mirela Airimioaei¹, Lavinia P. Curecheriu¹, Maria Teresa Buscaglia², Vincenzo Buscaglia², and Liliana Mitoseriu¹

¹Dept. of Physics, Alexandru Ioan Cuza University, Blv. Carol I, nr.11, 700506, Iasi, Romania

²Institute for Energetics & Interphases IENI-CNR Genoa, Via de Marini 6, 116149, Genoa, Italy

Main author email address: cristina.ciomaga@uaic.ro

The idea of this work was to investigate the dielectric and non-linear properties of the composite ceramic with the paraelectric phase (SrTiO₃) fully isolated by the ferroelectric phase (BaTiO₃). The ceramic composite with the 0-3 connectivity have been prepared by spark plasma sintering of the composite powders formed by SrTiO₃@BaTiO₃ core-shell particles. In order to prepare SrTiO₃@BaTiO₃ core-shell particles we have used a multistep process: (i) synthesis of the SrTiO₃ cores; (ii) coating the SrTiO₃ cores with a shell of amorphous TiO₂; (iii) transformation of SrTiO₃@TiO₂ core-shell particles into SrTiO₃@BaTiO₃ core-shell particles. The phase formation and morphologies have been investigated by using X-ray diffraction (XRD) and scanning electron microscopy (SEM).

The dielectric properties measure from (25-200)°C temperature and in a broad frequency range (20Hz-1GHz) were investigated and discussed. From temperature dependence on dielectric permittivity it was observed a giant relaxation effect, after reoxidation process, with a strong shift of T_m with frequency (to above ~80°C when $f \in (1, 10^6)$ Hz), which cannot be related to the relaxor state (Fig. 1(a)). The observed relaxation is an extrinsic effect most probably related to the oxygen deficiency and not to the relaxor behaviour of this system. The complex impedance showed that only one single component in the complex impedance plot found, after first step of reoxidation. Thus, the annealing process allowed the homogenization of the oxygen level within the ceramic grains, but dielectric relaxation (ϵ'') proposed the existence of 2 regions with different oxygen vacancies concentration – boundary/bulk or other effects. The frequency and temperature dependence of dielectric characteristics have been also investigated and discussed in correlation with the microstructural data perform by TEM and SEM analysis.

The non-linear investigation revealed a strong variation of permittivity vs. electrical field (Fig. 1(b)). The obtained results can be correlated with the peculiar microstructure of the present sample.

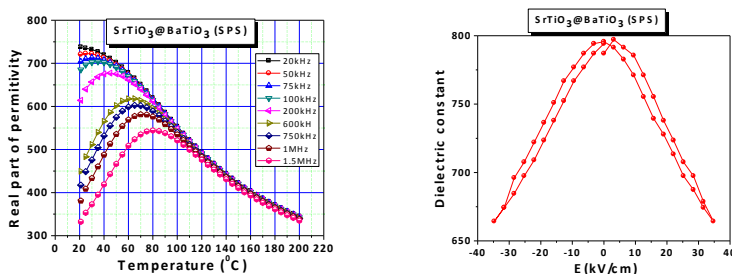


Figure 1. (a) Temperature dependence of dielectric permittivity at different frequency, (b) dielectric permittivity vs. electric field.

Acknowledgements: The financial support of the CNCS-UEFISCDI project PNII-RU-TE-2012-3-0150 is highly acknowledged. The collaboration in frame of Romania - Italy bilateral project 643/1.01.2013 (MULTIFER) is highly acknowledged.

Real-time Dynamics of Nano-domains: Effect of Cylindrical "hoop" Stresses

J. F. Scott

Cavendish Laboratory, Department of Physics, Cambridge University

jfs32@cam.ac.uk

Together with Ray McQuaid and Marty Gregg in Belfast, Alexei Gruverman in Nebraska, and Ashok Kumar in Delhi, we have measured some new nano-domain dynamics via HRTEM and PFM techniques. We observe vertex-vertex collisions in ferroelectric films and show that these satisfy the Maxwell-Voigt-Kelvin model (Standard Linear Model) with $v(x)$ proportional to x down to 200 nm separation over 24 hours. We also study domains within domains in multiferroics. We measure faceting in thin-film disks: Usually these are hexagonal but sometimes pentagonal or rectangular; under TEM irradiation the facets oscillate on 10-20 s cycles. In submicron-diameter ceramics we show that the domain stripe width w varies linearly with grain diameter d , unlike the Arlt modification of the square-root dependence of Landau-Lifshitz-Kittel or Roytburd and argue that this is due to hoop stress (previously ignored), which varies as $1/d$, unlike axial or radial stress, which varies as $1/d$ -squared.

Lattice modes of antiferroelectric PbZrO_3

J. Hlinka

Institute of Physics, Academy of Sciences of the Czech Republic, Prague 8, Czech Republics

hlinka@fzu.cz

Lead zirconate is probably the best known example of an antiferroelectric oxide. Its parent, paraelectric phase is a simple cubic perovskite with a 5-atom unit cell ($Pm\bar{3}m$, $Z=1$). Below the antiferroelectric phase transition point (~ 500 K), it turns into an orthorhombic $Pbam$ ($Z=8$) structure. This phase transition can be understood as a result of the condensation of two order parameters, one at the wave vector $Q_\Sigma = (0.25, 0.25, 0)$, and the other at the wave vector $R = (0.5, 0.5, 0.5)$, see Fig. 1a. Due to the multiplication of the unit cell, numerous phonon modes become active in the infrared and Raman spectra below the phase transition point. Most of these modes have been well identified in our recent low-temperature spectroscopic studies of PbZrO_3 single crystals, and in particular, those with low frequencies [1].

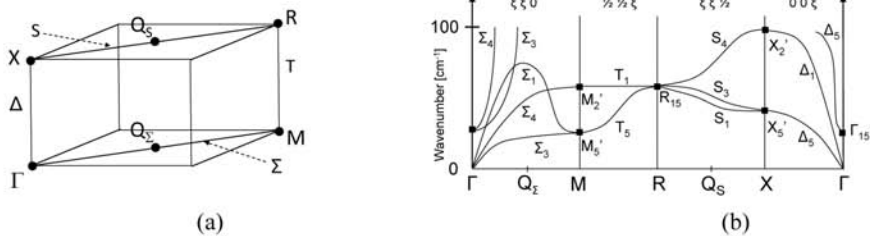


Figure 1 Schematic diagram showing the Brillouin zone points important for the discussion of the phase transition of lead zirconate (a) and the chart of the low frequency phonon branches (b), as estimated from available cubic-phase measurements.

We shall discuss three main issues. First, we tried to relate the optically active modes to the phonon modes at special Brillouin zone points of the parent, high temperature cubic phase (at Brillouin zone points Q_Σ and R , for example). We shall also briefly comment on the macroscopic symmetry of the ferroelectric and antiferroelectric modes [2]. Second, since there are no direct experimental measurements of phonon dispersion curves available to date, we tried to reconstruct some of them from our data, similarly as it was often done for incommensurate dielectrics in the past (see Fig. 1b). Third, our measurements revealed surprisingly strong anisotropy of the low-frequency permittivity. This has interesting consequences for the antiferroelectric switching.

[1] J. Hlinka, T. Ostapchuk, E. Buixaderas, C. Kadlec, P. Kuzel, I. Gregora, J. Kroupa, M. Savinov, J. Drahokoupil and J. Dec, *Multiple soft-mode vibrations of lead zirconate*, J. Hlinka, arXiv:1401.3730 [cond-mat.mtrl-sci] (2014).

[2] J. Hlinka, arXiv:1312.0548 [physics.class-ph] (2014).

The Role of Pseudosymmetry in the Functional Properties of Perovskite Structured Ceramics

Ian M. Reaney

Materials Science and Engineering, Mappin St., University of Sheffield, Sheffield, S13JD

I.M.Reaney@sheffield.ac.uk

The average structure and symmetry is no longer sufficient to interpret functional properties and a new concept, 'pseudosymmetry', has emerged which can rationalise the superior performance of many known materials. Pseudosymmetry refers to local distortions away from the macroscopic average structure that are correlated over only a few tens of unit cells. Historically, relaxor ferroelectrics such as $\text{PbMg}_{1/3}\text{Nb}_{2/3}\text{O}_3$ (PMN) may be considered the first class of materials whose properties were derived from pseudosymmetry but it has been shown that the enhancement of the properties at the morphotropic phase boundary in piezoelectrics also arises from a local intermediate monoclinic structure between rhombohedral (R) and tetragonal (T) phases. More recently, $\text{Na}_{1/2}\text{Bi}_{1/2}\text{TiO}_3$ (NBT) has been shown to exhibit a plethora of short range interactions involving local cation displacements and octahedral rotations in addition to the average pseudo-rhombohedral distortion. These local distortions contribute to the ability of NBT based compositions to undergo field induced structural phase transitions that give rise to high effective piezoelectric coefficients. They also facilitate a temperature stable plateau in permittivity for the fabrication of high temperature (up to 250 °C) capacitors in automotive applications. These newly emerging concepts have transformed the study of pseudosymmetry from a purely academic pursuit to one that is at the heart of materials discovery and development for 21st century electronics.

Further insights into the mesoscopic-scale atomic arrangements in perovskite-type relaxor ferroelectrics from x-ray absorption spectroscopy

T. Vitova¹, S. Mangold², C. Paulmann,³ V. Marinova,⁴ B. Mihailova³

1- Institut für Nukleare Entsorgung, Karlsruher Institut für Technologie, Hermann-von-Helmholtz-Platz 1, D-76344 Eggenstein-Leopoldshafen, Germany

2- ANKA Synchrotronstrahlungsquelle, Karlsruher Institut für Technologie, Hermann-von-Helmholtz-Platz 1, D-76344 Eggenstein-Leopoldshafen, Germany

3- Fachbereich Geowissenschaften, Universität Hamburg, Grindelallee 48, 20146 Hamburg, Germany

4- Institute of Optical Materials and Technologies, Bulgarian Academy of Sciences, Acad. G. Bonchev Str. 109, 1113 Sofia, Bulgaria

e-mail: boriana.mihailova@uni-hamburg.de

The search for advanced materials with high response functions over the past two decades has spotted complex perovskite-type relaxor ferroelectric materials of the general formula ABO_3 with Pb^{2+} on the A site and various transition elements on the B site. Lead is however environmentally undesirable, which has been stimulating considerable efforts to synthesize Pb-free perovskite-type relaxors with properties comparable to those of Pb-based relaxors. To achieve this goal in the most efficient way, one should have deep understanding of the mesoscopic-scale structural phenomena in the "etalon" Pb-based relaxors. On the other hand, the perovskite-type structure is very flexible and can adopt a large variety of chemical elements that may improve the multifunctionality of relaxor ferroelectrics. Ruthenium is a mixed-valence photochromic element and its incorporation into the structure of perovskite-type ferroelectrics leads to higher photosensitivity and stronger photorefractive effect close to the red and near-infrared spectral range, which is of significant interest for optical memories. Hence, the incorporation of Ru into relaxor-ferroelectric host matrices has the potential to induce new properties, which in turn is a strong motivation for fundamental structural studies of Ru-doped relaxor ferroelectrics. Thus the aim of this study was two-fold: (i) to analyze the way of incorporation of Ru into $PbSc_{0.5}B''_{0.5}O_3$ with $B'' = Ta, Nb$ as well as into $0.9PbZn_{1/3}Nb_{2/3}O_3-0.1PbTiO_3$ and its influence on the optical properties by x-ray absorption near-edge structure (XANES) and extended x-ray absorption fine structure (EXAFS) spectroscopy at the Ru K-edge and complementary optical spectroscopy, resonance Raman spectroscopy and synchrotron x-ray single-crystal diffraction, and (ii) the shed light on the short- and intermediate-range atomic arrangements in perovskite-type (ABO_3) relaxor ferroelectrics by applying EXAFS at the core-electron transition of the major ferroelectrically active B-site cations in $PbSc_{0.5}B''_{0.5}O_3$. The results show that Ru is octahedrally coordinated in all three relaxor host matrices but the average oxidation state of Ru in $PbSc_{0.5}Ta_{0.5}O_3-Ru$ and $PbSc_{0.5}Nb_{0.5}O_3-Ru$ is ~ 4.4 , whereas it is ~ 3.8 in PZN-0.1PT-Ru. In $PbSc_{0.5}B''_{0.5}O_3$ ($B'' = Ta, Nb$) Ru substitutes for the B'' cations in the form of isolated point defects, whilst in PZN-0.1PT-Ru Ru replaces adjacent A and B sites, forming a chain-like structural species of face-sharing elongated octahedra. Chemical 1:1 B-site order as well as dynamic BO_6 tilting is observed around both the Ru dopant and the major B'' cation in $PbSc_{0.5}Ta_{0.5}O_3-Ru$ and $PbSc_{0.5}Nb_{0.5}O_3-Ru$ regardless of the fact that according to x-ray diffraction at ambient conditions, the average structure is cubic with weak or none long-range chemical order. Pb cations are off-center displaced from the prototypic cubic A site for all three compounds and in Ru-doped $PbSc_{0.5}B''_{0.5}O_3$ the BO_6 tilt angle correlates with the degree of coherent B-Pb distances.

Relationship between Structural Characteristics and Polar Properties of Nonstoichiometric Silver Niobate



A. Kania¹, S. Miga², A. Niewiadomski¹, I. Jankowska-Sumara³, J. Dec²

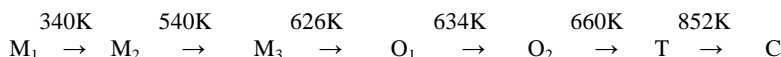
1- A. Chelkowski Institute of Physics, University of Silesia, Uniwersytecka 4, Katowice, Poland

2- Institute of Materials Science, University of Silesia, Chorzow, Poland

3- Institute of Physics, Pedagogical University, Krakow, Poland

Main author email address: antoni.kania@us.edu.pl

Silver niobate-tantalate $\text{AgNb}_{1-x}\text{Ta}_x\text{O}_3$ and silver-lithium niobate $\text{Ag}_{1-x}\text{Li}_x\text{NbO}_3$, solid solutions are promising candidates for high-permittivity microwave dielectrics ($\epsilon \approx 400$, $\Delta\epsilon/\epsilon < 0.04$, $Q \cdot f = 860$ GHz) and lead-free piezoelectrics ($d_{33} = 210$ pN/C), respectively [1,2]. These excellent characteristics are related to Nb/Ta ion dynamics and appearance of structural disorder in the antiferroelectric Nb/Ta ion displacement array. The disorder phenomenon is most significantly seen in pure silver niobate AgNbO_3 (AN) and seems to be unique among the simple perovskite oxides. AgNbO_3 undergoes the complex sequence of phase transitions:



where M_1 is disordered ferrielectric, M_2 , and M_3 are disordered antiferroelectric, and O_1 , O_2 , T and C are paraelectric phases. Different polar states appear due to the Ag and Nb ion displacements and interactions between appearing dipole moments [3-5]. Therefore, significant influence of the Ag deficiency or excess on physical properties of AgNbO_3 is expected. Moreover, these studies may also exclude the silver deficiency as an origin of structural disorder appearance in silver niobate based compounds.

Non-stoichiometric $\text{Ag}_x\text{NbO}_{2.5+x/2}$ ceramics with x equal 0.95, 0.98, 1, 1.02 and 1.05 were studied. Their quality and structure were examined by SEM and X-ray diffraction. Rietveld analysis showed that the orthorhombic lattice parameter b and orthorhombicity defined as $(b - a)/(a + b)$ increase significantly with increase of x. Linear and nonlinear dielectric and DSC studies showed that temperature of the M_1 - M_2 , M_2 - M_3 , M_3 - O_1 , O_1 - O_2 and O_2 -T phase transitions significantly increase with the increase of Ag concentration. Basing on structural characteristics the relationship between Ag content, and consequently the number and value of interacting dipole moments, and the appearance of polar ferrielectric and antiferroelectric states in AN is discussed.

[1] Petzelt J, Kamba S, Buixaderas E, Bovtun V, Zikmund Z, Kania A, Koukal V, Pokorny J, Polivka J, Volkov A, Pashkov V and Komandin G: Infrared and microwave dielectric response of the disordered antiferroelectric $\text{Ag}(\text{Ta,Nb})\text{O}_3$ system. *Ferroelectrics.*, vol. 223, pp. 235-246 (1999).

[2] Fu D, Endo M, Taniguchi H, Taniyama T, Koshihara S and Itoh M: Piezoelectric properties of lithium modified silver niobate perovskite single crystals. *Appl. Phys. Lett.*, vol. 92, pp. 172905 (2008).

[3] Kania A: Dielectric properties of $\text{Ag}_{1-x}\text{A}_x\text{NbO}_3$ (A: K, Na and Li) and $\text{AgNb}_{1-x}\text{Ta}_x\text{O}_3$ solid solutions in the vicinity of diffuse phase transitions. *J. Phys. D: Appl. Phys.*, vol. 34, pp. 1447 – 1455 (2001).

[4] Levin I, Krayzman V, Woicik JC, Karapetrova J, Proffen T, Tucker MG and Reaney IM: Structural changes underlying the diffuse dielectric response in AgNbO_3 . *Phys. Rev. B.*, vol. 79, pp. 104113 (2009).

[5] Yashima M, Matsuyama S, Sano R, Itoh M, Tsuda K, Fu D. Structure of Ferroelectric Silver Niobate AgNbO_3 . *Chem Mater.*, vol.23, pp. 1643–1645 (2011).

Lead-free bismuth-based relaxor ferroelectric composites

J. Rödel, H. Zhang, C. Groh and W. Jo.

Institute of Materials Science, TU Darmstadt, Alarich-Weiss-Straße 2, 64287 Darmstadt, Germany

roedel@ceramics.tu-darmstadt.de

Incipient piezoceramics [1] provide very large strain through a reversible field-induced phase transformation from ergodic relaxor to ferroelectric structure. This transition has been monitored with in-situ synchrotron, in-situ neutron and in-situ electron diffraction. While it provides normalized strain values, d_{33} , of more than 600 pm/V the required fields are usually in excess of 4 kV/mm, and the hysteresis is broad with large energy loss. A viable approach to produce materials with application-relevant properties has been developed through the use of a composite architecture with ferroelectric seeds and ergodic matrix [2]. These materials require a strongly reduced driving field but maintain high unipolar strain.

In this presentation the role of the ferroelectric seed will be described as a combination of polarization and strain coupling of ferroelectric and relaxor during electric loading. Composites with BNT-BT seeds and BNT-BT-KNN matrix have been prepared [3,4] to determine the optimum in seed content as a function of temperature and frequency. Further, model laminate structures were produced and compared under axial and serial loading to separate the impact of strain and polarization loading.

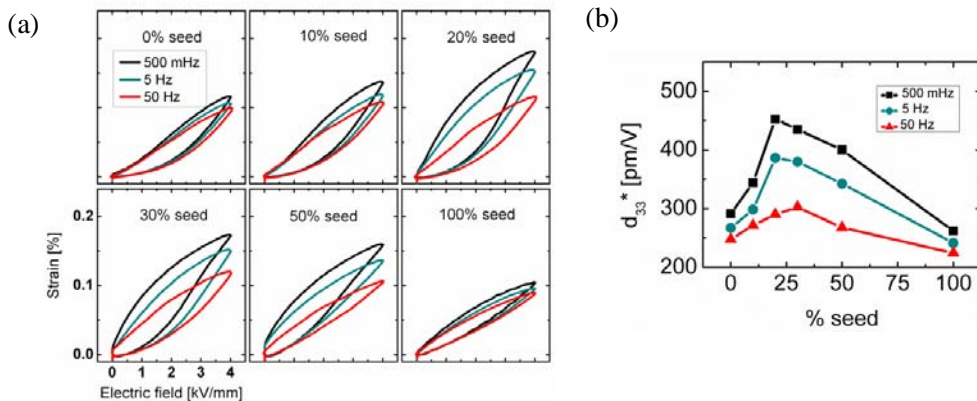


Figure 1 (a) Unipolar strain hysteresis and (b) normalized strain d_{33}^* (S_{max}/E_{max}) at $E_{max}=4$ kV/mm for various composites, measured at frequencies of 500 mHz, 5 Hz and 50 Hz.

[1] W. Jo, R. Dittmer, M. Acosta, J. Zang, C. Groh, E. Sapper, K. Wang, J. Rödel, "Giant electric-field-induced strains in lead-free ceramics for actuator applications", *J. Electroceram*, 29, 71-93, (2012).

[2] D.-S. Lee, D.-H. Lim, M.-S. Kim, K.-H. Kim, S.-J. Jeong, "Electric field-induced deformation behavior in mixed $\text{Bi}_{0.5}\text{Na}_{0.5}\text{TiO}_3$ and $\text{Bi}_{0.5}(\text{Na}_{0.75}\text{K}_{0.25})_{0.5}\text{TiO}_3\text{-BiAlO}_3$ ", *Appl. Phys. Lett.*, 99, 062906:3pp, (2011).

[3] C. Groh, D.J. Franzbach, W. Jo, K.G. Webber, J. Kling, L.A. Schmitt, H.-J. Kleebe, S.-J. Jeong, J.-S. Lee, J. Rödel, "Relaxor/Ferroelectric Composites: A Solution in the Quest for Practically Viable Lead-Free Incipient Piezoceramics", *Adv. Funct. Mat.*, 24, 356-362, (2014)

[4] C. Groh, W. Jo, J. Rödel, "Tailoring (94-x) $\text{Bi}_{1/2}\text{Na}_{1/2}\text{TiO}_3$ -6% BaTiO_3 -x $\text{K}_{1/2}\text{Na}_{1/2}\text{NbO}_3$ Ferroelectric/Relaxor Composites", *J. Amer. Ceram. Soc.*, in print (2014).

Performance of thin film polyvinylidene fluoride for pyroelectric energy harvesting

D. Zabek¹, J. Taylor², E. LeBoulbar¹ and C.R. Bowen¹

¹*Department of Mechanical Engineering, University of Bath, Bath, BA2 2ET, UK.*

²*Department of Electrical and Electronic Engineering, University of Bath, Bath, BA2 2ET, UK.*

D.Zabek@bath.ac.uk

When employing oscillating temperatures for pyroelectric energy transformation and harvesting, the short circuit pyroelectric current is defined by $I = p * A \frac{dT}{dt}$. Considering a time and space variant temperature profile, thermal wave effects take place. For multilayer electrode-pyroelectric-electrode compositions, interferences between heat absorption and diffusion disturb the thermal wave with increasing material thickness and therefore the energy transformation procedure [1].

A 2D modelling approach is considered in this work which demonstrates that polyvinylidene fluoride (PVDF) develops different heat transfer rates with increasing material thickness under constant thermal boundary conditions. The thin film temperature profile developed for different heating rates shows over a wide range of temperature oscillating frequencies acceptable pyroelectric transformation efficiencies.

Heating measurements for thin film PVDF films of 28, 53 and 100 μm thickness demonstrate that PVDF performs under practical oscillation frequencies of 1 Hz as good as widely employed lead zirconate titanate (PZT) [2]. PVDF has the potential as an energy harvesting material for a wider range of applications and compared to conventional ferroelectric ceramics [3] like PZT or BaTiO_3 it is flexible, light, cheap and easy to manufacture.

[1] G. Chen; “Wave effects on radiative transfer in absorbing and emitting thin-film media”; *Microscale Thermophysical Engineering*; vol. 1-3; pp 215–224, (1997).

[2] Huesgen, T., Ruhhammer, J., Biancuzzi, G. and Woias, P.; “Detailed study of a micro heat engine for thermal energy harvesting”; *J. Micromech. Microeng.*; vol. 20; pp. 1-9; (2010).

[3] D. Lingam, A- R. Parikh, J. Huang, A. Jain, M. Minary-Jolandan; “Nano/microscale pyroelectric energy harvesting: challenges and opportunities”; *International Journal of Smart and Nano Materials*; vol. 1; pp. 1-17; (2013).

Acknowledgement:

The research leading to these results has received funding from the European Research Council under the European Union's Seventh Framework Programme (FP/2007-2013) / ERC Grant Agreement no. 320963 on Novel Energy Materials, Engineering Science and Integrated Systems (NEMESIS).

High frequency dielectric characterization of high-k functional thin films

K. Nadaud¹, H.W. Gundel¹, R. Gillard², C. Borderon¹, E. Fourn²

1- IETR UMR CNRS 6164, Lunam Université, Université de Nantes, 2 rue de la Houssinière, 44322 Nantes Cedex 3, France

2- IETR UMR CNRS 6164, INSA Rennes 20 avenue des Buttes de Coësmes CS 70839 35708 Rennes Cedex 7

email: kevin.nadaud@univ-nantes.fr

Ferroelectric thin films are widely studied for their non constant dielectric permittivity which allows realization of electrically tunable components and devices like microwave filters, reflectarray antennas, resonators or phase shifters. Depending on the component architecture, the material might be elaborated on a conducting or an insulating substrate. Thin film synthesis and hence the dielectric properties strongly depend on the substrate type and more especially on its crystalline structure. Therefore, only a characterization method using a topology identical to this of the final component, guarantees reliable determination of the material's properties.

Most commonly, a MIM (Metal Insulator Metal) topology is used for thin film characterization [1- 3]. At high frequencies or in the case of a high permittivity, however, propagation phenomena reduce the apparent permittivity. Characterization methods relying on CoPlanar Waveguide (CPW) technology are mainly based on the measurement of the propagation constant or the effective permittivity. In this case, the obtained accuracy is usually poor because the thin film permittivity only little contributes to the overall effective permittivity as the film thickness is rather small in comparison to the spacing between the coplanar conductors. In the present paper we report on a method which allows characterization of the complex permittivity of a ferroelectric thin film in the microwave range using a coplanar capacitance with a narrow gap.

In the proposed CPW topology (Fig. 1a), the capacitor is formed in the central transmission line by the gap S_{capa} - W_{capa} [4]. Insertion into the two lateral ground lines allows the use of GSG (Ground Signal Ground) probes. The measurement does not disturb the capacitance and the high frequency (300 MHz to 10 GHz) permittivity can be extracted with the help of a mathematical model, improved from this initially proposed by Vendik [4]. The dielectric characteristics of the thin films without and with bias electric field in the large frequency range from 100 Hz to 10 GHz are shown in Fig. 1b. Up to 300 MHz, characterization has been performed using a MIM topology and an impedance analyzer (below 10 MHz) or a network analyzer (10 MHz to 300 MHz) and the technique reported by [1]. From 300 MHz to 10 GHz, the above described topology has been used.

Except little discontinuity at the frequency limits of each measurement method, a continuous evolution of the relative permittivity can be seen. The oscillations of the dielectric losses at high frequencies around a mean value of about $2 \cdot 10^{-2}$ are mainly due to calibration problems of the network analyzer. A tunability of the thin film above 50% has been obtained in the whole frequency range.

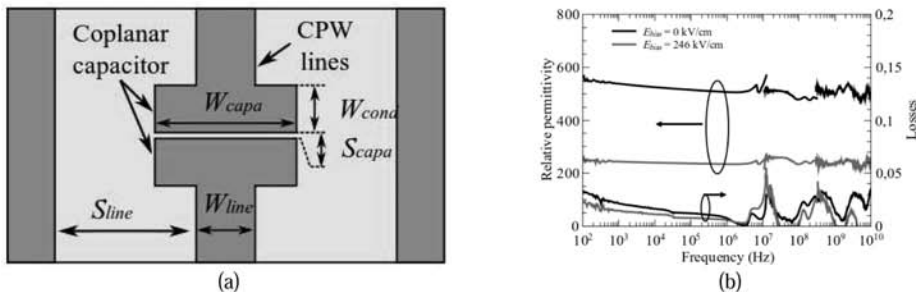


Figure 1 Proposed topology of the capacitor (a). Measured complex permittivity of BaSrTiO₃ thin film (b).

- [1] Z. Ma, A. J. Becker, P. Polakos, H. Huggins, J. Pastalan, H. Wu, K. Watts, Y. H. Wong, and P. Mankiewich, RF measurement technique for characterizing thin dielectric films, *IEEE Trans. Electron Devices*, vol. 45, pp. 1811-1816, (1998).
- [2] M. P. J. Tiggelman, K. Reimann, J. Liu, M. Klee, W. Keur, R. Mauczock, J. Schmitz, and R. J. E. Huetting, Identifying dielectric and resistive electrode losses in high-density capacitors at radio frequencies, in *Proc. IEEE ICMTS*, pp. 190-195 (2008).
- [3] W. Chen, K. G. McCarthy, A. Mathewson, M. Copuroglu, S. O'Brien, and R. Winfield, Capacitance and S-parameter techniques for dielectric characterization with application to high-k PMNT thin-film layers, *IEEE Trans. Electron Devices*, vol. 59, no. 6, pp. 1723-1729, (2012).
- [4] K. Nadaud, H. W. Gundel, C. Borderon, R. Gillard, E. Fourn, A New Method of Dielectric Characterization in the Microwave Range for High-K Ferroelectric Thin Films, *Proc. Joint UFFC, EFTF and PFM Symp. Prague, Czech Republic, 2013*, UFFC2013-001362.PDF, Paper ID: 1362.
- [5] O. G. Vendik, S. P. Zubko, and M. A. Nikolskii, Modeling and calculation of the capacitance of a planar capacitor containing a ferroelectric thin film, *Technical Physics*, vol. 44, no. 4, pp. 349-355, (1999).

Simultaneous Monitoring of the Electromechanical Coupling Coefficients and Domain Structural Changes of the PMN-32%PT Crystals during Poling Process

R. J. Kazys, R. Sliteris, J. Sestoke

Prof. Kazimieras Barsauskas Ultrasound Research Institute, Kaunas University of Technology
Studentų St. 50, Kaunas, Lithuania, LT-51368

justina.sestoke@ktu.lt

The discovery of high piezoelectric properties for lead magnesium niobate-lead titanate (PMN-PT) enables to develop ultrasonic transducers with significantly improved performance. This is due to high electromechanical coupling coefficients of the PMN-PT crystals which may be enhanced using domain engineering. Therefore monitoring of piezoelectric properties and domain structure of the crystals during poling process starts to be of a major importance.

Objective of this research was development of a novel measurement technique which enables simultaneous monitoring of the variations of the domain structure and piezoelectric coefficients during poling process of the PMN-32%PT crystals. The method is based on simultaneous measurement of the input electric impedance of the crystal versus frequency and optical observation of the crystal's domain structure. In order to get optical images of the domain structure inside PMN-32%PT single crystal plates they were coated by optically transparent electrodes using iridium tin oxide (ITO) technology. The PMN-32%PT single crystal plates with $\langle 001 \rangle$ and $\langle 011 \rangle$ cuts with sputtered ITO electrodes were prepared for monitoring of poling process. The ITO layer electrodes have resistivity ($R = 59 \div 105 \text{ } \Omega/\text{cm}$) which is similar or less then the resistivity of transparent platinum electrodes usually used in domain engineering. The functional diagram of the proposed method is shown in Figure 1.

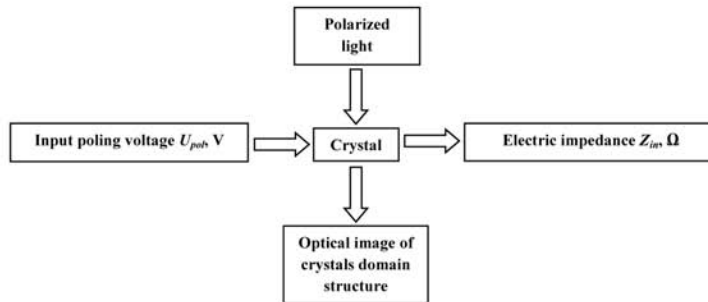


Figure 1 PMN-32%PT single crystal poling process.

Poling was performed using the high voltage power supply SRS PS350 and measurements of the electric impedance (Z_{in}) using the impedance analyzer Wayne Kerr 65120B. Optical observation of domain structure was performed using a polarized light and the optical microscope Olympus SZX16. Variations of electromechanical coupling coefficient k_{31} were obtained from the measured electrical input impedance at different poling voltages. The optical images of crystals during poling process were simultaneously recorded by the optical microscope's camera and transferred to a personal computer.

As a result the monitoring of variations of the piezoelectric properties and domain structure of the PMN-32%PT single crystal plates of $\langle 011 \rangle$ and $\langle 001 \rangle$ cuts during poling process was successfully performed. It enables to control the domain engineering process.

STUDY OF THE DOMAIN STRUCTURE OF $\text{Bi}_4\text{Ti}_3\text{O}_{12}$ CERAMICS BY RAMAN CONFOCAL SPECTROSCOPY AND ITS INFLUENCE ON THE ELECTRICAL POLARIZATION

A. Moure¹, M.G. Navarro-Rojero², F. Rubio-Marcos¹, A. del Campo¹, J.F. Fernández¹

1 - Ceramics for Smart Systems Group, Electroceramic Department, Instituto de Cerámica y Vidrio, CSIC, Kelsen 5, 28049 Madrid, Spain

2 - CIATEQ A.C. Av. Manantiales No. 23-A. Parque Industrial Bernardo Quintana. El Marqués, C.P. 76246, Querétaro (México)

Author email address: alberto.moure@icv.csic.es

Ferroelectric domain structure in Bismuth Layer-Structured Ferroelectric (BLSF) has been observed for the first time in ceramics with $\text{Bi}_4\text{Ti}_3\text{O}_{12}$ (BIT) composition by means of Raman Confocal Spectroscopy. This is a powerful tool that allows measuring particular modes that depends on the crystalline orientation when polarized laser light is used. Thus, chemical etching (as needed when the study is carried out by SEM) or the need of having transparent samples (as when they are observed by polarized light) can be avoided to characterize the domains distribution. A stripe 90° domains configuration appears for large platelet-like grains in BIT ceramics. The smallest grains with a more equiaxial shape show a needle-like domain structure that has an influence on the ferroelectric properties of the ceramics. The observed hysteresis loop indicates that the polarization is clamped due to a lower mobility of those domain walls and the remnant polarization is lower when grain size decreases. The domain structure is shown to be related with the stress within the grains and the presence of defects (oxygen vacancies) at the domain walls. All these factors are shown to determine the ferroelectric activity of the ceramics with such crystalline structure.

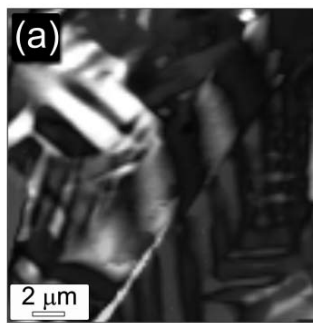


Figure 1. Confocal Raman Spectroscopy image of BIT ceramic exhibiting the domain structure. The Raman image resulted from mapping the different single Raman spectra collected from each pixel.

[1] F. Rubio-Marcos, A. Del Campo, R. López-Juárez, J.J. Romero, and J. F. Fernández. High spatial resolution structure of (K,Na)NbO₃ lead-free ferroelectric domains. *J. Mater. Chem.*, 22, 9714-9720, 2012.

Electrical Activity of Ferroelectric Biomaterials

P. Vaněk¹, J. Petzelt¹, Z. Kolská², T. Luxbacher³

1- Institute of Physics ASCR, Na Slovance 2, CZ-18221 Prague, Czech Republic
2- Jan Evangelista Purkyně University, České mládeže 8, CZ-40096 Ústí nad Labem, Czech Republic
3- Anton Paar GmbH, Anton-Paar-Straße 20, A-8054 Graz, Austria

vanek@fzu.cz

The bone is electrically active under mechanical loading, due to the piezoelectric collagen and moving ionic fluids within the bone structure. Electrical potentials in the bone have been linked to the adaptation of the bone in response to loading, leading to the suggestion that an electrically active implant material may improve healing. Ferroelectrics (i.e. also piezoelectrics) have been among others studied as electroactive implant materials. In vivo and in vitro investigations have indicated that such implants induce improved bone formation. The results are somewhat ambiguous. Mostly, a negative charge on the surface is preferred for cell growth but in some cases a positive charge is preferred.

Previous studies have not taken into account the fact that the charge at the surface of ferroelectrics is always quickly compensated by the opposite charge from the surroundings [1]. If a ferroelectric is immersed in a liquid (e.g. tissue fluid) an electric double layer and a diffusion layer are formed in a nano-region at its surface which is decisive for protein adsorption and bioactive behavior. Recent paper [2] studied the influence of spontaneous polarization in PZT ferroelectric films on the electric double layer in adjacent liquid using colloidal probe force microscopy. This influence is significant at low ionic strength and very low roughness of the PZT film.

The charge distribution in an electric double layer and diffusion layer can be characterized in a simplified way by zeta potential – potential at a slipping plane. The dependence of zeta potential on the polarity of the surface of poled ferroelectrics has not been measured until now. We measured the zeta potential in dependence on the surface polarity and pH on poled single crystalline plates of ferroelectric LiNbO₃ in two laboratories using Anton Paar SurPASS electrokinetic analyzer (Figure 1).

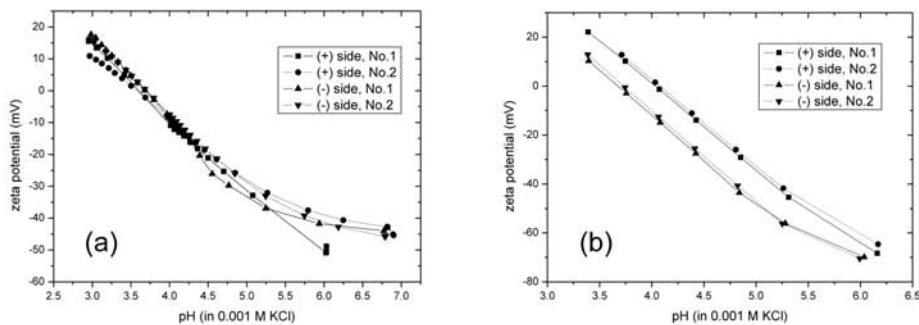


Figure 1 Zeta potential measurements on (+) or (-) sides of Z-cut single crystalline poled ferroelectric LiNbO₃ plates. (a) Measured at J.E. Purkyně University, Ústí nad Labem. (b) Measured at Anton Paar, GmbH, Graz.

The results from Anton Paar, GmbH, show clear reproducible influence of zeta potential on the ferroelectric surface polarity. However, the results from J.E. Purkyně University show no significant influence. The possible contamination of samples or of an instrument can play role. Therefore a standard polypropylene foil will be used to check the SurPASS analyzer and additional measurements will be performed at Tomáš Baťa University in Zlín. Both our results and results of [2] indicate that charge distribution at the surface can be influenced by the surface polarity of ferroelectrics at certain „ideal“ conditions (low ionic strength, non-contaminated surface, very low roughness). However, suggested ferroelectric coatings on the surface of implants for solid tissues are far from „ideality“, they are rough, polycrystalline, the body fluid is complex and has large ionic strength (0.15 M). Therefore, in this real case it can be expected that the influence of the sign of surface polarity on the electric diffusion layer and thus on the specific adsorption of proteins is low.

[1] S.V. Kalinin and D.A. Bonnell, Local potential and polarization screening on ferroelectric surfaces, *Physical Review B*, 63, 125411(1)-125411(13), (2001).

[2] R.J. Ferris, S. Lin, M. Therezien, B.B. Yellen and S. Zauscher, Electric double layer formed by polarized ferroelectric thin films, *ACS Applied. Materials and Interfaces*, 5, 2610-2617, (2013).

About the relaxor behaviour in TTBs: a crystal-chemical viewpoint

M. Josse^{*1}, P. Heijboer¹, M. Albino¹, F. Porcher², P. Veber¹, S. Pechev¹, M. Velazquez¹, Mario Maglione¹

¹ Université de Bordeaux, CNRS, ICMCB, 87 av. dr. A. Schweitzer, 33600 Pessac, France

² Laboratoire Léon Brillouin, CE Saclay CNRS-UMR12, 91191 Gif-Sur-Yvette Cedex, France

^{*}josse@icmcb-bordeaux.cnrs.fr

Niobates crystallizing in the Tetragonal Tungsten Bronze (TTB) structure [1] form a large class of ferroelectric materials, of which the "BaNaNb" ($\text{Ba}_2\text{NaNb}_5\text{O}_{15}$ [2]) can be regarded as the archetype. Many TTB structured compound also display a relaxor behaviour [3]. While the existence of a spontaneous polarization in many TTBS is clearly established, its origin and the microscopic mechanism(s) ruling their dielectric behaviour are not yet fully understood. If the displacive nature of ferroelectricity in TTBS gathers a general consensus, the crystal chemistry underlying the occurrence of ferroelectric or relaxor behaviour seems to bear a respectable degree of complexity. Many crystal-chemical parameters have been found to affect the dielectric behaviour of TTBS [4-10], and some attempts to rationalize the crystal chemistry of TTB ferroelectrics and relaxors have been made [11, for a recent example]. The frequent presence of modulations in the TTB structure, and their influence on physical properties, has been known for more than three decades [12-23], although structure-properties relationships are not yet fully clear. Deciphering the correlations between chemical composition, crystal structure (including disorder(s)), incommensurate modulations (described using 5-dimensional structural models), domain states (ferroelectric, but also ferroelastic...), microstructure (in ceramics) and finally dielectric properties, may take a few more decades...

Thus we will not put forth any claim of a solution to the crystal chemistry of TTBS in the present communication, but will rather highlight, through experimental results, some tracks that may be worth following. For this we will rely on a family of materials in which many original behaviours, from room-temperature composite multiferroics [24], to ferroelectric to relaxors crossovers [25-27], have been evidenced: the $\text{Ba}_2\text{LnFeNb}_4\text{O}_{15}$ (Ln = rare earth) TTBS.

We will present an empirical crystal chemistry approach specifically aiming at a better understanding of the ferroelectric to relaxor crossovers. The study of ceramics from several solid solutions, essentially based on the $\text{Ba}_2\text{NdFeNb}_4\text{O}_{15}$ ferroelectric TTB, by diversifying compositions and chemical substitutions patterns, underline a potential driving force of these crossovers.

To go further with the fundamental understanding of this system, we will present our development of crystal growth processes [28-30] which will allow for deeper insights on the microscopic mechanisms underlying original behaviours in TTBS.

Emphasis will be put on the role of the anionic sublattice in $\text{Ba}_2\text{LnFeNb}_4\text{O}_{15}$ TTBS crystal chemistry, and the eventual anion-driven properties it may be related to. The nature of the polar orders in $\text{Ba}_2\text{LnFeNb}_4\text{O}_{15}$ TTBS, and the influence of the aperiodic modulations on these polar orders, will be briefly discussed. Finally, the opportunity to take advantage of these original behaviours for the design of functional materials will be discussed, as well as their potential existence in most materials based on a TTB structure.

[1] A. Magneli et al, Ark. Kemi 1, 1949, 213.

[2] J.J. Rubin & al, J. Cryst Growth, 1967, 1, 315.

[3] J. Ravez & al, J. Solid State Chem., 2001, 162, 260.

[4] A.M. Glass, J. Appl. Phys. 1969, 40, 4699.

[5] K. Kakimoto & al, J. Eur. Ceram. Soc. 2001, 21, 1569.

[6] Li, K & al, Appl. Phys. Lett. 2012, 100, 012902.

[7] X. L. Zhu & al, J. Mater. Res. 2008, 23, 3112.

[8] A. Rotaru & al, Phys. Rev. B, 2011, 83, 184302.

[9] Y.B. Yao & al, J. Eur. Ceram. Soc. 2012, 32, 4353.

[10] M. Prades & al, Inorg. Chem. 2013, 52, 1729.

[11] X. L. Zhu & al, J. Am. Ceram. Soc., 2014, 97(2), 329

[12] J. Schneck & al, Phys. Rev. B (1981) 23(1), 383.

[13] J. Schneck & al, Phys. Rev. B (1982) 25(3), 1766.

[14] C. Manolikas & al, Phys. Rev. B (1987) 35(16), 8884.

[15] N. Mori & al, Phys. Rev. B (1997) 55(17), 11212.

[16] J.F. Scott & al, J. Phys. Cond. Mat. (2005) 17, 5911.

[17] H.Y. Lee & al, J. Appl. Cryst. (1998) 31, 683.

[18] T. Woike & al, Acta Cryst. (2003) B59, 28.

[19] I. Levin, & al, Appl. Phys. Lett. (2006) 89, 122908.

[20] M. Prades & al, J. Appl. Phys. (2008) 104, 104118.

[21] X.L. Zhu & al, Appl. Phys. Lett. (2010) 96, 032901.

[22] H.A. Graetsch & al, Acta Cryst. B, (2011) 68, 101.

[23] H.A. Graetsch & al, J. Solid State Chem., (2012) 196, 255.

[24] M. Josse & al, Solid State Sci., 2009, 11(6), 1118.

[25] E. Castel & al, J. Phys. Cond. Mat., 2009, 21(45), 452201.

[26] F. Roulland & al, Solid State Sci., 2009, 11(9), 1709.

[27] M. Albino & al, and P. Heijboer & al, in preparation.

[28] E. Castel & al, J. Cryst Growth, 2012, 340, 156.

[29] M. Albino & al, Eur. J. Inorg. Chem., 2013, 15, 2817.

[30] M. Albino & al, Cryst. Growth Des., 2014, 14, 500

Polymorphism Peculiarities of Bi_2WO_6 and Bi_2MoO_6 Aurivillius Phases

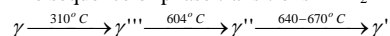
V.I. Voronkova, E.P. Kharitonova

M.V. Lomonosov Moscow State University, Faculty of Physics, Leninskie gory, 119991, Moscow, Russia

voronk@polly.phys.msu.ru

The isostructural Bi_2WO_6 (BW) and Bi_2MoO_6 (BM) are the simplest members of layered perovskite-related compound family with general formula $(\text{Bi}_2\text{O}_2)(\text{A}_{n-1}\text{B}_n\text{O}_{2n+1})$ (Aurivillius phases). These compounds are ferroelectrics, oxygen ionics, catalysts. The phase transitions of BW and BM have been studied for more than four decades, but the number of transitions and their detailed nature are not yet fully clear.

The sequence of phase transitions in Bi_2MoO_6 can be represented by the following scheme:



The first three phases (γ , γ'''' , γ'') are orthorhombic, last phase (γ') is monoclinic. γ and γ'''' are polar, γ'' and γ' are nonpolar phases. Next methods were used to identify of these phases: X-ray, DTA, DSC, thermo-Raman spectroscopy. γ'''' -phase was found in the early works by DTA and X-ray methods [1].

As for Bi_2WO_6 , there are disagreements concerning to its polymorphism. Bi_2WO_6 was found in orthorhombic ferroelectric γ -phase at room temperature, which transformed into ferroelectric γ'''' -phase at 660 °C. γ'''' -phase exists up to temperatures near 900-960 °C.

In most of the works made in the present moment and earlier, believe that near 900-960 °C orthorhombic polar phase γ'''' transforms to the monoclinic phase γ' . This transition is defined as simultaneously ferroelectric and reconstructive. The possibility of such transition to be ferroelectric with change of symmetry $\text{B2cb} \rightarrow \text{A2/m}$ is doubtful. In this connection, Rae [2] has assumed that in BW before the monoclinic phase a nonpolar orthorhombic phase Fmmm exists, which is similar to the γ'' - Bi_2MoO_6 . Any experimental evidences of the existence of γ'' -phase in BW were lacking. We revealed the existence of nonpolar phase γ'' - Bi_2WO_6 between γ'''' and γ' by measuring of dielectric permittivity temperature dependence and DSC [3]. So, the temperature dependence of permittivity showed ferroelectric λ -anomaly at 930 °C, and DSC-event associated with reconstructive phase transition was observed at 960 °C. This allowed to argue that in Bi_2WO_6 between γ'''' and γ' phases nonpolar γ'' -phase exists, as in the case of BM. It should be noted, that in the case of Bi_2MoO_6 γ'' -phase limited by two DSC-events associated with the $\gamma'''' \rightarrow \gamma''$ and $\gamma'' \rightarrow \gamma'$ transitions, while for BW only one DSC-event, associated with reconstructive $\gamma'''' \rightarrow \gamma'$ transition, is observed (Figure 1).

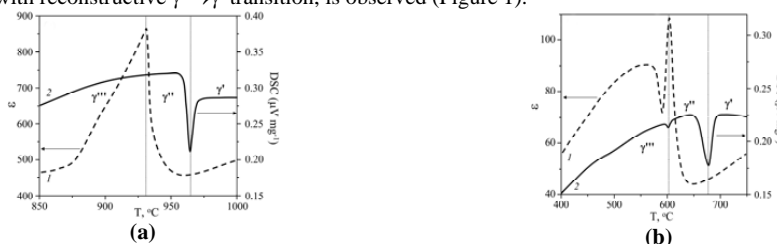
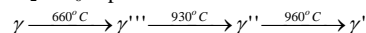


Figure 1 DSC heating scans and permittivity as function of temperature for Bi_2WO_6 (a) and Bi_2MoO_6 (b) ceramic samples at high temperatures [3].

A small region of existence of the γ'' -phase in pure BW (about 30 degrees) can be extended with doping. So, in BW doped with niobium ($\text{Bi}_2\text{W}_{0.9}\text{Nb}_{0.1}\text{O}_6$) the γ'' -phase exists from 700 °C to melting point. This makes it possible to investigate the atomic structure of γ'' -phase of Bi_2WO_6 , which has not been previously studied owing to small range and high temperature of its existence. Experimental detection of γ'' -phase in Bi_2WO_6 leads to the conclusion about the similarity of polymorphism in BW and BM. The scheme of polymorphism in pure Bi_2WO_6 is presented below:



[1] A. Watanabe, H. Kodama, Polymorphic transformations of Bi_2MoO_6 , J. Solid State Chem., vol. 35, pp. 240-245, (1980).

[2] A. Rae, J. Thomson, R. Withers, Structure refinement of commensurately modulated Bismuth tungstate, Bi_2WO_6 , Acta Cryst., vol. B47, pp. 870-881, (1991).

[3] V.I. Voronkova, E.P. Kharitonova, O.G. Rudnitskaya, Refinement of Bi_2WO_6 and Bi_2MoO_6 polymorphism. J. Alloys and Compounds, vol. 487, pp. 274-279, (2009).

Incipient ferroelectric-like behavior of langasites

E. Smirnova¹, **A. Sotnikov**^{1,2}, **H. Schmidt**², **M. Wehnacht**², **O. Buzanov**³, **S. Sakharov**³

¹ Saint-Petersburg, Russia, Ioffe Physical-Technical Institute

² Dresden, Germany, IFW Dresden

³ Moscow, Russia, JCS Fomos - Materials

esmirnoffa@gmail.com

Crystals of the langasite family $\text{La}_3\text{Ga}_5\text{SiO}_{14}$ (LGS), $\text{La}_3\text{Ga}_{5.5}\text{Ta}_{0.5}\text{O}_{14}$ (LGT), $\text{Ca}_3\text{TaGa}_3\text{Si}_2\text{O}_{14}$ (CTGS) demonstrate very promising properties for applications such as moderately high electromechanical coupling, low acoustic loss, absence of phase transition in a wide temperature range up to their melting points. The crystals belong to the same trigonal crystal class 32 as quartz (SiO_2) but compared with quartz they have two-three times higher piezoelectric coefficients (and hence, higher electromechanical coupling). In contrast to elevated temperatures and high temperature behavior [1] low temperature properties of the family founding father - langasite LGS as well as LGT and CTGS, are not studied up to now. In this communication, we report on dielectric measurements of LGS, LGT and CTGS single crystals at temperatures from 4.2 K to 300 K.

LGS, LGT and CTGS single crystals were grown by the well-developed Czochralski technique. Transparent boules up to approximately 70 - 100 mm in length and 90 - 102 mm in diameter were obtained.

The components of the dielectric tensor were determined using X-, Y-, and Z - cut plates of 10 x 10 mm in size and about 0.5 mm thick with evaporated gold electrodes. Dielectric spectra were obtained using a Solartron SI 1260 Impedance/Gain-Phase Analyzer at frequencies between 10 Hz and 1 MHz. The amplitude of the AC measurement electric field was 2 V/cm. The measurements were performed in an Oxford Instruments continuous-flow cryostat in the temperature range from 4.2 K to 300 K with an accuracy and stability of 0.1 K.

The experimental data for the temperature dependence of the real part of the relative dielectric permittivity $\epsilon'_{33}(T)$ show an unconventional behavior for dielectrics. The dielectric constant increases with temperature decreasing and saturates at low temperatures. According to this behavior, LGS, LGT and CTGS have been classified as incipient ferroelectrics or quantum paraelectrics similar to SrTiO_3 , KTaO_3 , CaTiO_3 and TiO_2 . The members of this family have a polar soft mode, but do not exhibit a ferroelectric phase transition. This effect is explained by the stabilization of their paraelectric phase due to the effect of quantum fluctuations.

In relation with the temperature dependence of the dielectric constant in incipient ferroelectrics, it is worthwhile to remember that in conventional dielectrics such as oxides, alkali halides and others with low frequency dielectric constant between 5 and 10, dielectric constants decrease very slowly with decreasing temperature, with the slope $(1/\epsilon)/d\epsilon/dT$ in the order of 10^{-4} K^{-1} .

The first and simplest approach to this problem was developed by Barrett [1]. The dielectric behavior of the incipient ferroelectrics at low-temperatures should be treated by taking quantum effects into account [1, 2]. The Barrett parameters of langasites and the well known incipient ferroelectrics are compared.

As follows from our measurements of langasites in the frequency range of 10 Hz–1 MHz, there is no dispersion of the dielectric constant as in the case of the other members of incipient ferroelectrics family. It was shown that though the low-temperature values of dielectric constant are very different, the general behavior of $\epsilon(T)$ is very similar. Thus, according to the data obtained, it might be concluded that LGS, LGS, LGT and CTGS belong to the group of incipient ferroelectrics or quantum paraelectrics.

[1] Barrett J.H., Dielectric constant in perovskite type crystals, *Phys. Rev.* **86**, 118-120, 1952

[2] Muller K.A., Burkard H., SrTiO_3 : an intrinsic quantum paraelectric below 4 K, *Phys. Rev. B* **19**, 3593- 3602, 1979

Growth of Large Diameter YCOB and LGS Crystals for Nonlinear Optical and Piezoelectric Applications

Yanqing Zheng¹, Xiaoniu Tu¹, Kainan Xiong¹, Erwei Shi¹

¹Shanghai Institute of Ceramics, Chinese Academy of Sciences, Jiading, Shanghai/P. R. China

Email: zyq@mail.sic.ac.cn

$\text{YCa}_4\text{O}(\text{BO}_3)_3$ (YCOB) and langasite (LGS) are two non-central symmetry crystals which are apt to grow into large diameter boules. YCOB is not only a nonlinear optical crystal which can be used in the optical parametric chirped-pulse amplification (OPCPA) but also a piezoelectric crystal which could be used as sensitive elements at temperature as high as 900°C. LGS is also used in high temperature piezoelectric devices and used as electro-optical switches.

Piezoelectric acceleration sensors that could stand environment temperature above 645°C (1200°F) are of great important to the field of vibration monitoring of aviation and aerospace engine. The traditional piezoelectric materials used in this area include lithium niobate crystal, bismuth layer structure system piezoelectric ceramics. But the issue of the lower electric resistivity limits their application of temperature higher than 645 °C.

ReCOB (Re= La, Y, Sm, Nd, Lu) crystals and LGX crystals including LGT, LGN and LGS are piezoelectric crystals with high melting points above 1400°C and without phase transition from room temperature to their melting points. They are all good candidates for high temperature application. YCOB and LGS crystals were grown in our laboratory by common Czochralski method up to 4 inches.

The optical homogeneity of YCOB and LGS crystals was tested by optical interferometer. The rocking curves of high-resolution X-ray diffraction (HRXRD) of these crystals were characterized to reveal the crystal quality. Piezoelectric acceleration sensors used the X-cut rings of 10 mm diameter based on these crystals were fabricated and tested. It was shown that YCOB crystal could be used up to 800°C after overcoming the issue of pyroelectric effect. YCOB element with aperture of 68 mm × 63 mm were characterized with the optical homogeneity of 1.6×10^{-6} and was used in OPCPA experiment to produce femtosecond pulse with energy larger than 3 J and conversion efficiency larger than 20%.



References:

[1] S.J. Zhang, X. N. Jiang, M. Lapsley, et al, Piezoelectric acelerometers for ultrahigh temperature application, Appl. Phys. Lett., vol. 96(1), p.013506, 2010.

[2] L. Yu, X. Liang, et al, Experimental demonstration of joule-level non-collinear optical parametric chirped-pulse amplification in yttrium calcium oxyborate, Optics Letters, Vol. 37, Issue 10, pp. 1712-1714 (2012)

Fig. 1: 4 inches YCOB and 4 inches LGS crystals grown in SICCAS .

Resonant Raman scattering in LiNbO_3 and LiTaO_3

A. Bartasyc^{1,2} and S. Margueron³

1- Femto-ST Institute, University of Franche-Comté and CNRS (UMR 6174), 32 avenue de l'Observatoire, Besançon, France, 25044

2- Jean Lamour Institute, Lorraine University and CNRS (UMR 7198), Parc du Saurupt, Nancy, France, 54011

3- Laboratoire Matériaux Optiques, Photonique et Systèmes, EA 4423, Lorraine University and Supelec, 2 rue Eduard Belin, Metz, France, 57070

Main author email address: ausrine.bartasyc@femto-st.fr

LiNbO_3 (LN) and LiTaO_3 (LT) have been the subject of intense studies because of their applications in electro-optic, nonlinear-optic, photo-refractive, and acoustical devices. Their dynamical properties have also been intensively studied. Nevertheless, only recently all nine E-symmetry optical phonons were experimentally resolved in Raman and IR spectra [1]. The frequencies, damping parameters, and intensities of the first and the second order phonons are of particular interest in studies of nonlinear optical properties, phase transitions, symmetry, effect of pressure, stress, composition and heterogeneities in thin films, integrated structures, nano and bulk materials.

In this work, the identification of Raman modes of the second order modes in LN and LT has been revisited. The observed second order modes in Raman spectra were attributed to the combinations of the first order modes. Moreover, using the incident photon energy close to the band gap, the harmonics of the longitudinal modes were excited. This multi-phonon phenomenon is similar to the resonance, observed in the semiconductors with excitonic transitions. The efficiency of resonance is a direct indication of the modulation of the induced polarization by phonons (both optical and acoustic). The intensity of the resonant Raman scattering in LN and LT were highly dependent on the Li_2O non-stoichiometry, which directly affected the band gap of these materials.

[1] S. Margueron, A. Bartasyc, A. M. Glazer, E. Simon, J. Hlinka, and I. Gregora, J. Appl. Phys. 111, 104105 (2012).

Photorefractive properties probed by Raman spectroscopy in ferroelectric materials.

**Marc D. Fontana^{1,2}, Ninel Kokanyan^{1,2}, David Chapron^{1,2}, Anna Zaltron³, Nicola Argiolas³
and Marco Bazzan³**

¹Université de Lorraine, Laboratoire Matériaux Optiques, Photonique et Systèmes, 2 Rue E. Belin 57070 Metz (France)

²Supélec, Laboratoire Matériaux Optiques, Photonique et Systèmes, 2 Rue E. Belin 57070 Metz (France)

³Università di Padova, Physics and Astronomy Department, Via Marzolo 8, 35131 Padova (Italy)

marc.fontana@supelec.fr

Lithium niobate (LN) is a well known material for its piezoelectric, ferroelectric, non linear (NL) optical and electro-optical properties [1]. In particular photorefractive (PR) properties can be enhanced by appropriate Fe or Mn doping, which is suitable for holographic recording [2]. By contrast, the PR effect which can lead to an irreversible damage is the main drawback for the use of LN in frequency conversion and electro-optical devices within the visible frequency range [3]. The PR effect arises from the inhomogeneous illumination of the material which gives rise to a space charge field and can be generally evidenced by the measurement of the photo-induced birefringence change or the two-wave mixing gain [3, 4]. The PR efficiency depends on the space charge field and the electro-optic coefficient which both can change with the nature and the concentration of dopant ion.

We have recently shown that the Raman spectroscopy can be also used to probe PR properties [5].

In fact the space charge field induces via the reciprocal piezoelectric effect, a local deformation which in turn gives rise to a shift of the frequency of vibrational modes. The time dependence of this frequency shift is analogous to the PR induced birefringence change.

Another phenomenon can be used to detect PR properties by means of Raman spectroscopy. The focused laser beam in the PR material is accompanied by a NL polarization giving rise to an additional component in the Raman tensor which in turn leads to the activation of some lines in a configuration where they are in principle forbidden by selection rules and the group theory. The ratio between the intensities of activated and expected Raman lines can be used to estimate the PR efficiency.

Here we report on Raman data in congruent LN crystals doped with different dopant ions, Zr, Zn, Mg, Fe, Cr...and several concentrations. Measurements have been performed as a function of the wavelength and power of the exciting laser line. Raman lines are analysed in terms of NL activated-intensity and piezo-induced frequency change.

Results are compared, in order to achieve in a same scale the PR efficiency of the investigated crystals. The threshold corresponding to the minimum of photorefractivity is deduced from these results for each series of doped crystals. The role of laser wavelength and the nature and concentration of dopant are underlined.

[1] T. Volk and M. Wöhlecke, Lithium Niobate: Defects, Photorefractive and Ferroelectric Switching, Springer Series in Materials Science (Springer, Berlin, Heidelberg) (2008)

[2] K. Buse, Light-induced charge transport processes in photorefractive crystals I : Models and experimental methods, Applied Physics B, 64, 273–291, (1997)

[3] M.D. Fontana, K. Chah, M. Aillierie, R. Mouras and P. Bourson, Optical damage resistance in undoped LiNbO3 crystals, Optical Materials 16, 111-117 (2001)

[4] E. Krätzig and F. Schirmer, Photorefractive Materials and Their Applications I, ed. by P. Günter and J.P. Huignard (Springer-Verlag, Berlin), (1988)

[5] M. Bazzan, N.Kokanyan, A. Zaltron, N. Argiolas, D. Chapron and M.D. Fontana, Raman frequency shift induced by photorefractive effect on Fe-doped lithium niobate, Journal of Applied Physics 114, 163506-13 (2013)

Synthesis, Structure and Properties of $\text{Pb}(\text{Zr}_{1-x}\text{Ti}_x)\text{O}_3$ Single Crystals

Zuo-Guang Ye^{1,2}

1- Department of Chemistry and 4D LABS, Simon Fraser University, Burnaby, British Columbia, V5A 1S6, Canada

2- Electronic Mater. Res. Lab. & Intl. Center for Dielectric Research, Xi'an Jiaotong University, Xi'an, 710049, China

zgye@sfu.ca

Lead zirconate-titanate solid solution, $\text{PbZr}_{1-x}\text{Ti}_x\text{O}_3$ (PZT), has been studied extensively over the past decades for both industrial applications and fundamental research, but almost exclusively in the forms of ceramics and thin films. On the other hand, the microstructure of this class of materials and the atomistic phenomena that cause the outstanding performance have not been thoroughly understood yet.

In this talk, we present our recent successful growth of $\text{PbZr}_{1-x}\text{Ti}_x\text{O}_3$ single crystals with a wide composition range across the morphotropic phase boundary (MPB) ($0.20 \leq x \leq 0.65$) by a top-seeded solution growth (TSSG) technique. The growth conditions are optimized in terms of the chemical, thermodynamic and kinetic parameters. The growth temperature is found to be a key factor for controlling the composition of the grown crystals. The availability of PZT single crystals makes it possible to systematically investigate the correlation between structural evolution and electrical properties in the PZT system.

The crystal structure, domain structure and phase transitions of PZT single crystals are studied by X-ray and neutron diffraction, polarized light microscopy (PLM) and dielectric/piezo-/ferroelectric measurements. PZT crystals with composition from $x = 0.42$ to $x = 0.47$ show characteristic ferroelectric-to-ferroelectric phase transitions due to the presence of a curved MPB. The crystals of MPB composition, $x = 0.46$, are found to exhibit the best properties, with a piezoelectric coefficient $d_{33} = 1223$ pC/N, an electromechanical coupling factor $k_{33} = 0.8$, a large coercive field $E_c = 7$ kV/cm and a high Curie temperature $T_C = 386$ °C, making PZT single crystals a high-performance and high- T_C piezoelectric material potentially useful for high temperature and high power electromechanical transducer applications.

The local polar domain structure and properties of PZT single crystals are studied by means of piezoresponse force microscopy (PFM), PLM and dielectric measurements. It is found that in samples with MPB compositions obtained by cooling through the second order phase transition, the ferroelectric phase is unstable, i.e. the state is optically isotropic. The fractal domain arrangement of the scale starting from several nm is observed by PFM. The ferroelectric phase can be stabilized by a large enough external electric field. These results suggest that quenched random fields play an important role in the formation of nanodomain state in PZT, which is discussed in the framework of the behaviour and mechanisms of relaxor ferroelectrics.

The atomic structure of PZT crystals with $x=0.42$ is imaged by means of high-resolution aberration-corrected transmission electron microscopy. The accurate Pb displacements and their directions are successfully determined relative to the centre of the four B-cations, on the $\langle 110 \rangle$ monoclinic mirror plane. The orientation and distribution of local polarizations indicate a mixture of rhombohedral, tetragonal and (possibly) monoclinic local symmetry. This result is in agreement with the neutron powder diffraction analysis of the rhombohedral phase of PZT system.

The work was supported by the U.S. Office of Naval Research (Grants No. N00014-11-1-0552 and No. N00014-12-1-1045) and the Natural Science & Engineering Research Council of Canada (NSERC). Part of this work was conducted at the Center for Nanophase Materials Sciences at Oak Ridge National Lab., which was sponsored by the Scientific User Facilities Division, Office of Basic Energy Sciences, U.S. Department of Energy, and at the International Centre for Dielectric Research at Xi'an Jiaotong University, China, with the support from the «Qianren Program».

GRAIN SIZE EFFECT ON DIELECTRIC PERMITTIVITY OF 0.36BiScO₃ – 0.64PbTiO₃ PEROVSKITE CERAMICS

M. Ivanov¹, S. Balčiūnas¹, H. Amorin², A. Castro², M. Algueró², J. Banys¹

1- Faculty of Physics, Vilnius University, Sauletekio 9/3 817k., LT10222 Vilnius, Lithuania
2- Instituto de Ciencia de Materiales de Madrid, CSIC, Cantoblanco, 28049 Madrid, Spain

maksim.ivanov@ff.vu.lt

Ferroelectric materials are of high interest for both researchers and engineers due to their remarkable properties. Their high dielectric permittivity allows us to make smaller capacitors and their switchable electric polarization can be used for memory storage. We should note that all ferroelectrics have piezoelectric properties [1] and can be used, for example, in piezoelectric motors [2]. In recent decades electronic devices tend to nanoscale, this brings the necessity to research ceramics grain size effects. Although ferroelectric PZT has taken almost all piezoelectric market due to its high piezoelectric coefficient [3], BSPT has ~ 100 K higher Curie temperatures than PZT, this allows making piezoelectric devices for higher temperatures.

In this presentation dielectric properties and grain size effect on dielectric permittivity of xBiScO₃-(1-x)PbTiO₃ (BSPT) where x=0.36 ceramics will be presented. Usually dielectric permittivity in ceramics should decrease as its grains get smaller, since the effective volume of grain boundaries grow (grain boundaries has lower permittivity). Effective permittivity of ceramics can be approximated with coated shell model [4]:

$$\varepsilon = \varepsilon_2 \left(\frac{x-n}{1-x} \right) + \left(\frac{1-x}{1-n} \right) \frac{\varepsilon_1 \varepsilon_2}{(1-n)\varepsilon_2 + n\varepsilon_1}, \quad (1)$$

where ε , ε_1 , ε_2 are complex dielectric permittivities of ceramics, grain core and grain shell respectively, x – grain shell volume and n – free parameter, characterizing the particle shape and topology. As we see in figure 1 (a) this model is accurate in low grain size region. The decrease of dielectric permittivity in high grain size region can be explained by Kittel's law which states that reducing crystallites size will decrease domain thickness, thus increasing wall count and in result dielectric permittivity (2). In figure 1 (b) coated shell model with Kittel's law correction fit curves correspond all experimental data.

$$\varepsilon_1 = \varepsilon_{c0} + \frac{C}{\sqrt{D}}, \quad (2)$$

where C – constant, D – grain diameter ε_{c0} – dielectric permittivity without domains.

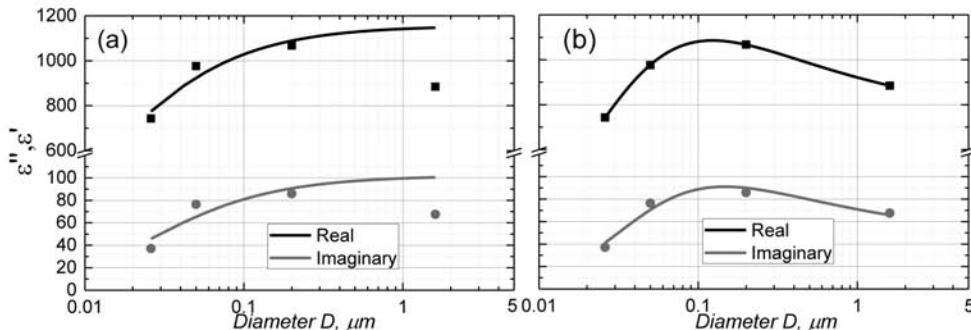


Figure 1 Dielectric permittivity dependence from crystallites size at 333kHz frequency and 300K temperature. Coated shell model fit curves: (a) without Kittel law correction (b) with Kittel law correction.

- [1] G. H. Haertling, "Ferroelectric ceramics: history and technology," Journal of the American Ceramic Society, vol. 82, pp. 797-818, (1999).
[2] T. Morita, "Miniature piezoelectric motors," Sensors and Actuators A: Physical, vol. 103, pp. 291-300, 2/15/ (2003).
[3] R. Guo, L. Cross, S. Park, B. Noheda, D. Cox, ir G. Shirane, "Origin of the high piezoelectric response in PbZr 1-x Ti x O 3," Physical Review Letters, vol. 84, p. 5423, (2000).
[4] J. Petzelt, I. Rychetsky, ir D. Nuzhnyy, "Dynamic Ferroelectric-Like Softening Due to the Conduction in Disordered and Inhomogeneous Systems: Giant Permittivity Phenomena," Ferroelectrics, vol. 426, pp. 171-193, 2012/01/01 (2012).

Electroluminescence studies of the polarization switching in PLZT relaxor ceramics

S.A. Sadykov¹, S.N. Kallaev², K. Bormanis³

1 - Daghestan State University, 367000 Makhachkala, Daghestan, Russia

2 - Institute of Physics, Daghestan Scientific Center, Russian Academy of Sciences, 367003 Makhachkala, Russia

3 -Institute of Solid State Physics, University of Latvia, LM-1063 Riga, Latvia

The results of an investigation of the temperature dependence of the intensity and its relationship with integral characteristics of the polarization switching in lanthanum doped lead zirconate titanate (PLZT 9/65/35) relaxor ceramics in fast raising strong electric fields are presented. The measurements were performed with 0,1 kV/(mm· μ s) electric field rise rates at sample temperatures in the 0–60°C interval, which included the point ($T_m \approx 60^\circ\text{C}$) corresponding to the maximum permittivity of ceramics.

It is shown that the typical waveforms of emission from PLZT ceramics has two distinctive features: the emission exhibits a pronounced discrete character, which is manifested by a large number of sequential flashes, and the integral emission intensity significantly increases with the temperature, i.e., with increasing volume fraction of nonpolar regions in a heterophase sample. A growth in the integral emission intensity with the temperature is related to the increase in both the amplitudes of separate flashes and their number during the switching time. The duration of each emission peak is about 0.1–0.5 μ s.

Similarly to the case of classical ferroelectrics, a critical field E_c (dynamic coercive field) for the start of domain reorientation in PLZT ceramics decreases with increasing temperature, which is indicative of a decrease in the internal bias fields. An increase in the integral emission intensity is not proportional to a change in the value. Moreover, the time of establishment of a polarized state in a strong field (at a switching time of $t_s \approx 50 \mu$ s) determined from the duration of emission decreases with increasing temperature, which is evidence for intensification of the formation and evolution of the domain structure (accounting for the increase in the emission intensity).

It is supposed that the discrete character of emission from PLZT in the entire temperature interval studied is related to temperature induced variations in the dimensions and number of the nanopolar regions. With increasing temperature, macroscopic polar domains in the volume of ceramics are subdivided into fine nanopolar regions with an increase in the number of charged interphase boundaries. Under the action of a rapidly growing external field, separate microscopic regions with individual characteristic critical start fields E_c are sequentially involved in the process of domain structure formation and rearrangement. The spread of these regions with respect to the internal and coercive fields determines the temporal scatter of separate emission peaks.

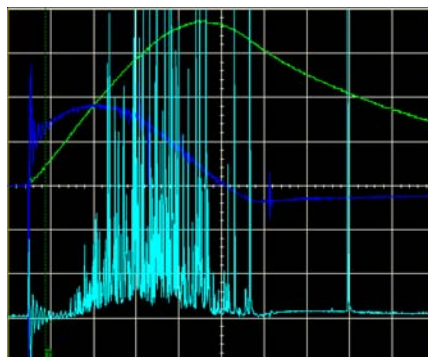


Figure 1. Waveforms showing correlation of the electroluminescence pulses (lower curves) with the applied voltage (upper curves- green) and switching current (middle curves- blue) for PLZT ceramics at 40°C.

Variation of Piezoelectric Properties and Mechanisms Across the Relaxor-Ferroelectric Continuum in BiFeO_3 - $(\text{K}_{1/2}\text{Bi}_{1/2})\text{TiO}_3$ - PbTiO_3 Ceramics

Andrew J Bell, Tim Comyn, Tim Stevenson, James Bennett and Anton Goetzee-Barral

Institute for Materials Research, University of Leeds, Leeds, UK

A.J.Bell@leeds.ac.uk

The mechanisms of electromechanical coupling in true ferroelectrics and relaxors are shown to exhibit both similarities and differences in terms of comparisons between direct and converse effects, the scaling of maximum strain with the weak field piezoelectric charge coefficient, and the observance of the Rayleigh law. This is demonstrated using materials from the BiFeO_3 - $(\text{K}_{1/2}\text{Bi}_{1/2})\text{TiO}_3$ - PbTiO_3 ternary system. Both the BiFeO_3 - PbTiO_3 and BiFeO_3 - $(\text{K}_{1/2}\text{Bi}_{1/2})\text{TiO}_3$ binaries exhibit morphotropic phase boundaries, but where the former is characterised by large spontaneous strain and strong macroscopic domains patterns indicative of strong long range order, the latter lead-free system possess vanishing spontaneous strain and nanoscale domains. Whilst both can exhibit large field-induced strains, their weak-field properties contrast markedly. Neither of these binaries are useful as commercial piezoelectrics, however exploration of the quaternary solid solutions along the line joining the two MPBs demonstrates a range of useful compositions intermediate to the two extremes of the ferroelectric and relaxor behaviours.

Insights into Analyzing the Electric Field Cycling Behavior of Ferroelectric Doped Hafnium Oxide

Tony Schenk¹, Milan Pešić¹, Uwe Schroeder¹, Mihaela Popovici², Christoph Adelman², Thomas Mikolajick^{1,3}

1- NaMLab gGmbH, Noethnitzer Str. 64, D-01187 Dresden, Germany

2- Imec, Kapeldreef 75, B-3001 Leuven, Belgium

3- Chair of Nanoelectronic Materials, University of Technology Dresden, D-01062 Dresden, Germany

tony.schenk@namlab.com

Recently, HfO_2 with various dopants [1, 2] and in a solid solution with ZrO_2 [3] was introduced as a new ferroelectric. Its serious potential for future ferroelectric random access memories (FeRAM) was proven by integrating Si:HfO₂ into 28 nm technology devices [4]. However, in contrast to e.g. lead zirconate titanate, many questions concerning the roles of defects and how to tune the ferroelectric characteristics are far less studied.

This work is dedicated to the electric field cycling behavior of Sr:HfO₂. Harmonic analysis [5] was adapted in a purely calculational approach to study the kinetics of 1) the conditioning behavior of a pristine sample, 2) polarization fatigue and 3) the split-up and merging of peaks in transient currents I by cycling the electric field E . The latter phenomenon is reported for the first time and appears to be of analog nature as shown in Figure 1: split-ups into multiple peaks are possible at any desired position. The split-up occurs exactly at the field used as cycling amplitude and the number of cycles defines the clarity of the split-up, i.e. the depth of the minimum between the split-up peaks. Additionally, different explanations for the observed behavior are discussed including a qualitative model of static domains as preferential sites for defect accumulation (Figure 2) as well as a charge trapping model.

All three phenomena were studied by dynamically measuring the polarization hysteresis after a continuously increasing number of field cycles. The hystereses were expanded into a Fourier series to monitor the evolution of amplitude and phases of the different harmonics. Phase jumps were observed most prominently for the 5th, 7th and 9th harmonic. The lower the temperature the higher was the number of cycles (or the cycling time) after which these jumps occurred. The corresponding Arrhenius-plots allowed determining activation energies for the respective phenomena in order to compare them with respect to possible reasons like e.g. the abovementioned charge trapping or typical fatigue mechanisms like seed inhibition or domain wall pinning [6].

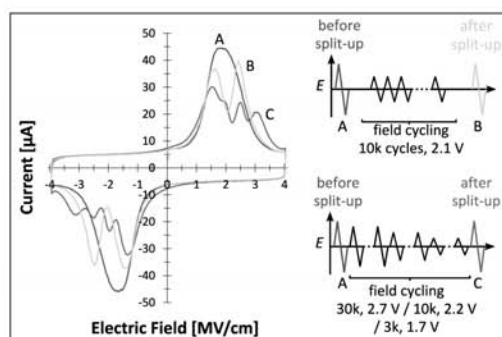


Figure 1: Multiple peak split-ups in transient currents (left) at any desired position via field cycling with lower amplitude. Corresponding cycling sequences are indicated with A, B and C (right).

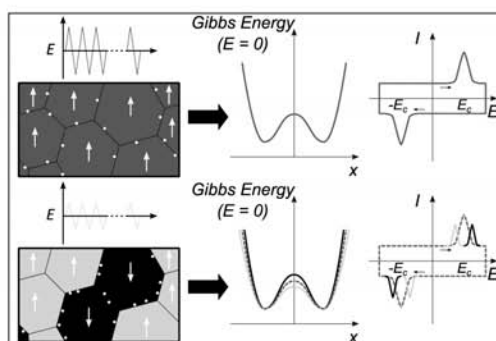


Figure 2: Qualitative model to explain: Defects accumulate preferably at domains not switched at lower fields. Their switching is increasingly impaired in favor of the non-static domains.

- [1] T. S. Böске, J. Müller, D. Bräuhäus, U. Schröder, U. Böttger, Ferroelectricity in hafnium oxide thin films, *Appl. Phys. Lett.*, 99, pp. 102903-1-102903-3, (2011).
- [2] U. Schroeder, S. Mueller, J. Mueller, E. Yurchuk, D. Martin, C. Adelman, T. Schloesser, R. van Bentum, T. Mikolajick, Hafnium Oxide Based CMOS Compatible Ferroelectric Materials, *ECS J. Solid State Sci. Technol.*, 2, pp. N69-N72, (2013).
- [3] J. Müller, T. S. Böске, U. Schröder, S. Mueller, D. Bräuhäus, U. Böttger, L. Frey, T. Mikolajick, Ferroelectricity in Simple Binary ZrO₂ and HfO₂, *Nano Lett.*, 12, pp. 4318-4323, (2012).
- [4] J. Müller, E. Yurchuk, T. Schlösser, J. Paul, R. Hoffmann, S. Mueller, D. Martin, S. Slesazek, P. Polakowski, J. Sundqvist, M. Czernohorsky, K. Seidel, P. Kücher, R. Boschke, M. Trentzsch, K. Gebauer, U. Schröder, T. Mikolajick, Symposium on VLSI Technology, (2012).
- [5] M. I. Morozov and D. Damjanovic, Hardening-softening transition in Fe-doped Pb(Zr,Ti)O₃ ceramics and evolution of the third harmonic of the polarization response, *J. Appl. Phys.*, 104, pp. 034107-1- 034107-8, (2008).
- [6] A. K. Tagantsev, I. Stolichnov, E. L. Colla, N. Setter, Polarization fatigue in ferroelectric films: Basic experimental findings, phenomenological scenarios, and microscopic features, *J. Appl. Phys.*, 90, pp. 1387-1402, (2001).

Evolution of dielectric hysteresis loops in alternating field of constant amplitude

O. Malyshkina, A. Eliseev

Tver State University, Tver, Russia

Olga.Malyshkina@mail.ru

The dielectric hysteresis loops of ceramic samples of lead titanate-zirconate samples were studied by the method of Sawyer-Tower [1] in alternating electric field at a frequency of 50 Hz in the field range of 400 to 1500 V/mm. The time changes of the hysteresis loop shape were registered simultaneously with temperature measurements performed distantly by thermographic camera (Testo-875-1). In fields lower than 1500 V/mm (Fig. 1a) minor hysteresis loops not reaching saturation are observed regardless of the exposure time under the action of the field. As an example Fig. 1b demonstrates the evolution of the loop observed in a field of 600 V/mm in a period of 0 to 12 minutes. It was possible to obtain the saturated dielectric loop only after the exposure to the field of 1500 V/mm (Fig. 1c). Attention should be paid to the fact that connection to the voltage of 826 V results in a voltage at the sample (fixed by the oscilloscope) exceeding the voltage taken from the generator through a step-up transformer with isolated windings. Elevation of this value results in a voltage at the sample lower than supplied one (Fig. 1). The effect of increasing the voltage at the sample during AC measurements was mentioned earlier for pure SBN crystals [2, 3].

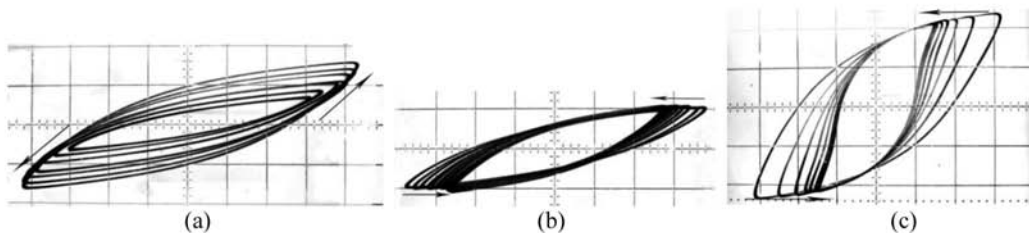


Figure 1 Dielectric hysteresis loops (a) at the initial moment of time for the field intervals from 400 to 1000 V/mm; (b) exposure in a field of 600 V/mm; (c) – 1500 V/mm. Arrows indicate the direction of the changes. X axis scale: (a, b) 200 V/div, (c) 300 V/div.

It was shown that the formation of the hysteresis loop is accomplished due to sample heating. Fig. 2 demonstrates the temperature dependence of the sample behaviour on the exposure time starting from the moment of field connection. The time for achieving saturation decreases with the increase of the field (shown in the figure by dashed line).

Exposing of the samples to constant fields gave no indication of their heating, so it follows that it is not related to the joule effect. The heating is also not observed with the application of alternating field of small amplitude when the minor loops are absent.

So since the effect of heating exists only in fields corresponding to either minor or full hysteresis loops, apparently it is related to alternating mechanical stresses arising in the samples during the polarization switching in alternating fields.

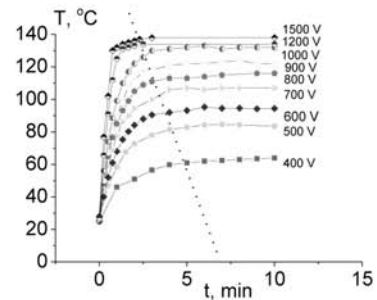


Figure 2 Dependence of the sample temperature on time for different amplitudes of the applied field

- [1] C.B. Sawyer, C.H. Tower, Rochell salt as a dielectric, *Phys. Rev.*, vol. 35, pp. 269-273, (1930).
- [2] O.V. Malyshkina, I.L. Kislova, B.B. Ped'ko, *Izvestiya Vuzov, Effect of an external electric field on the dielectric properties of strontium barium niobate single crystals of congruent composition, Materialy elektronnoi tekhniki.* N.4, pp. 40-42. (2004).
- [3] O.V. Malyshkina, B.B. Ped'ko, A.A. Movchikova and I.V. Morgushka, *Effect of External Forces on the Dielectric and Pyroelectric Properties of Strontium-Barium Niobate Crystals, Crystallography Reports.* V. 50, pp. S28-S31. 2005.

Antiferroelectricity: competing instabilities and domain walls

prof Alexander Tagantsev

École Polytechnique Fédérale de Lausanne, Switzerland

alexander.tagantsev@epfl.ch

Antiferroelectrics can be viewed as systems where a competition between two structural instabilities results in wide range of physical phenomena in the bulk of the material [1], including a strong dielectric anomaly at the high temperature side of the transition. A proper insight into the phenomenon can be gained by identifying the antiferroelectricity as a result of the interruption of an imminent ferroelectric phase by a structural phase transition [1,2]. This interruption occurs due to a repulsive interaction between the polarization and the structural order parameter. This approach not only provides a simple explanation of the bulk properties of antiferroelectrics, it also enables the identification of antiphase boundaries resulting from the antiferroelectric phase transition as promising candidates for the occurrence of ferroelectricity in domain boundaries of a non-polar material.

This paper addresses properties of the classical antiferroelectric – lead zirconate - in the context of the aforementioned approach. The data of the comprehensive experimental characterization (X-ray inelastic and diffuse scattering, Brillouin scattering and electron microscopy) of the material are presented and analyzed in view of the results of Landau theory and first principals calculations [2,3].

[1] E. V. Balashova. and A. K. Tagantsev, Physical Review B 48, 9979 (1993).

[2] A. K. Tagantsev et al, Nature Communications 4, 2229 (2013).

[3] X.-K. Wei, et al, Nature Communications 5, 3031 (2014).

Microscopic model of polarization switching

A. Leschhorn, S. Djombou, H. Kliem

Institute of Electrical Engineering Physics, Saarland University, 66041 Saarbruecken, Germany

h.kliem@mx.uni-saarland.de

Polarization switching is simulated using a model based on a sequence of single dipole flips. The dipoles (dipole moment p) fluctuate thermally activated in double well potentials with transition rates depending on the activation energy W_0 and on the local field. The local field at dipole i is the sum of all fields acting on this individual dipole, i.e. the applied field E_a , the fields E_{ij} of all other dipoles and charges in the system and the fields E_j^{im} of the images in the electrodes:

$$E_i^{\text{loc}} = E_a + \sum_{j \neq i} E_{ij} + \sum E_j^{\text{im}} .$$

The time t_i to switch a single dipole depends on the deterministic transition rate

$$w_i = \frac{1}{\tau_0} \exp\left(-\frac{W_0 + p_i E_i^{\text{loc}}}{k_B T}\right)$$

and on a probabilistic factor $\xi \in]0;1[$. The flip time t_i is calculated with a dynamic Monte-Carlo step [1,2]

$$t_i = -\frac{1}{w_i} \ln(\xi) .$$

In each step, the dipole with the shortest flip time is switched.

We investigate one dimensional dipole chains as well as two and three dimensional systems based on the barium titanate structure that comprises single charges fluctuating in double well potentials and induced dipoles. The two and three dimensional simulations yield intrinsic dead layers close to the electrodes that can not be switched even in very strong fields. These non switchable layers are nuclei for the reversal of dipole chains. The highest probability to form a stable nucleus of reverted dipoles is found at the edge of the sample. Having formed such a nucleus the reversal starts at this edge where a first chain is reversed. The neighboured chain is switched next. Thus a domain wall propagates perpendicular to the applied field (Fig.1). The switching time of the system decreases faster than exponential for low fields with increasing field (Fig.2). This decrease slows down for higher fields. Furthermore we found non switchable dipoles at defects which also act as nuclei for the polarization reversal (Fig.1).

A movie of the switching process according to Fig.1 is produced.

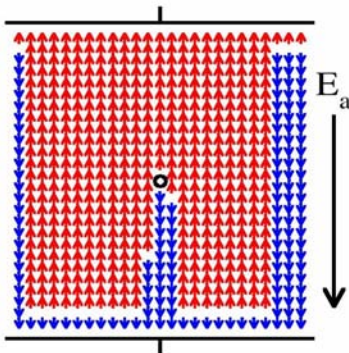


Figure 1 Snapshot of the permanent dipole moments in a dipole plane during a polarization reversal. Non switchable layers at electrodes and defects (circle in the center) are nuclei for new domains pointing downwards to the new direction of the applied field.

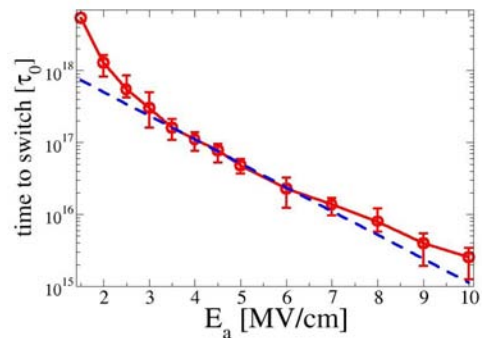


Figure 2 Switching time of a 2-dimensional system without defect as a function of the applied field. For comparison an exponential decrease is plotted also.

[1] A. Bortz, M.Kalos, J.Lebowitz, A new algorithm for Monte Carlo simulation of Ising spin systems, J. Comp. Phys., 17, pp. 10, (1975).
 [2] M. Kühn, H. Kliem, Monte Carlo simulations of ferroelectric properties for PVDF and BaTiO₃, Ferroelectrics, 370, pp. 207-218, (2008).

First principles investigation of 2-dimensional electron gases in ferroelectric thin films

N. C. Bristowe^{1,2}, P. Aguado-Puente³, R. Shirasawa⁴, B. Yin^{3,5}, P. B. Littlewood⁶, Ph. Ghosez¹ and E. Artacho^{2,3,7}

1- Département de Physique, Université de Liège, B-4000 Sart-Tilman, Belgium

2- Theory of Condensed Matter, Cavendish Laboratory, University of Cambridge, J. J. Thomson Av. Cambridge CB3 0HE, UK

3- CIC NanoGUNE and DIPC, Tolosa Hiribidea 76, 20018 San Sebastián, Spain

4- Advanced Materials Laboratories, Sony Corporation, 4-14-1 Asahi-Cho, Atsugi-Shi 243-0014, Japan

5- Department of Engineering Mechanics, Zhejiang University, Hangzhou 310027, China

6- Physical Sciences and Engineering, Argonne National Laboratory, Argonne, Illinois 60439, USA

7- Basque Foundation for Science Ikerbasque, 48011 Bilbao, Spain

Main author email address: paguado@nanogune.eu

Since the discovery of the 2-dimensional electron gas (2DEG) that forms at the interface between LaAlO₃ and SrTiO₃ [1], two band insulators, the research on this and similar systems has been very active. This activity has result in the discovery of a vast amount of different properties with potential practical applications [2]. Although the formation of a 2DEG has been observed in other oxide heterostructures, the prototypical system for these studies is still the LaAlO₃/SrTiO₃ interface where it was originally discovered. However great efforts are also being devoted to devise systems where the 2DEG couples with other functional properties such as magnetism or strain.

Very early after the discovery of this system, the use of a ferroelectric substrate was proposed as a way to tune the population of the 2DEG. Since the ferroelectric material possess a non-volatile polarization, its switching with the application of an external electric field could be used to increase or decrease the polar discontinuity with the polar LaAlO₃ and consequently turn on and off the 2DEG. First principles simulations shown that this was physically feasible [3] and later manipulation of the electronic properties of the LaAlO₃/SrTiO₃ interface through a ferroelectric was experimentally achieved [4, 5]. Nevertheless one could think of a more radical approach to this problem: the spontaneous polarization of a ferroelectric material could play the same role as the formal polarization of the centrosymmetric LaAlO₃, suggesting that a 2DEG should also form in ferroelectric thin films due to a polarization discontinuity with a dielectric substrate or vacuum. If this was achieved a number of possible applications can be envisioned, such as the already mentioned non-volatile manipulation of the metallic interface.

Even though an electronic reconstruction similar to the one observed in the LaAlO₃/SrTiO₃ is predicted using very simple macroscopic models [6], and despite the vast amount of experiments where ferroelectric thin films are grown on top of insulating substrates, there are no experimental evidences of the formation of 2DEG in these systems. The reason for this is that alternative screening mechanisms compete with this phenomenon. Formation of polarization domains, ubiquitous in ferroelectric thin films, prevents the appearance of the 2DEG. Avoiding polydomain phases is difficult because domains are an intrinsic screening mechanism that is always available, regardless of the growth conditions. The only way to obtain the 2DEG in a ferroelectric thin films is to find a right combination of materials and boundary conditions such that due to the different interactions involved the electronic reconstruction scenario becomes more favorable than the breaking into domains.

Here we present a combination of macroscopic models and first principles simulations aimed at explaining the precise conditions under which the formation of a 2DEG in a ferroelectric thin films might be viable and what the properties of the system would be. We study the competition between the electronic reconstruction and typical alternative screening mechanisms, paying special attention to the formation of polydomain structures. These results are used to propose routes to favor the formation of the 2DEG. The properties of the 2DEG formed at realistic ferroelectric surfaces or interfaces are analyzed using first principles simulations, taking explicitly into account the interaction with the substrate, the external fields, strain, and other instabilities present in the materials.

[1] A. Ohtomo and H. Y. Hwang, Nature 427, 423 (2004)

[2] J. Manhart and D. G. Schlom, Science 327, 1607 (2010)

[3] M. Niranjan *et al.*, Phys. Rev. Lett. 103, 016804 (2009)

[4] C. W. Bark *et al.*, P. Nat. Acad. Sci. USA 108, 4720 (2011)

[5] V. T. Tra *et al.*, Adv. Mater. 25, 3357 (2013)

[6] Bristowe *et al.*, accepted for publication in J. Phys.: Condens. Matter.

Piezoelectric and dielectric properties of doping and A-site non-stoichiometric effect on $(\text{Na}_{0.5}\text{K}_{0.5})\text{NbO}_3$ ceramics

S.Y. Lim, G.H. Ryu M.H. Kim*

1- School of Advanced Materials Engineering, Changwon National University Gyeongnam 641-773, Korea

syylim@changwon.ac.kr

Lead-based ceramics are widely used for piezoelectric and ferroelectric devices such as sensors, motors and transducers because of its good piezoelectric properties. However, these materials have problems that pollute the environment and harm the human health [1, 2]. Therefore, to replace lead-based piezoelectric materials, many lead-free candidate materials were studied. Among them, $(\text{Na}_{0.5}\text{K}_{0.5})\text{NbO}_3$ (NKN) based ceramics are regarded as most promising candidates for lead-free applications because of their good piezoelectric constant and high curie temperature. The high piezoelectric properties of NKN could be obtained by controlling the phase coexistence region [3-6]. To control phase coexistence region, many studies have been devoted to substitute NKN with Li, Sb, Ta. Dopants such as Li, Ta, Sb have been proved to increase the piezoelectric and dielectric properties [7-10]. In 2012, we reported Ta modified KNN ceramics which show high piezoelectric properties [10]. However, volatility of A-site ions make it difficult to prepare high density ceramics. To compensate this problem, A-site excess compositions were investigated which increase density and piezoelectric constant. Ag doping has been also reported to increase the piezoelectric and dielectric properties. However, there are few reports of Ag effect on KNN based ceramics [11, 12]. In this study, dopants effects were studied to improve the densification behavior and the piezoelectric properties of lead-free $(\text{Na},\text{K})(\text{Nb},\text{Ta})\text{O}_3$ ceramics.

- [1] Haertling G.H, Ferroelectric Ceramics: History and Technology, J.Am. Ceram. Soc. 82(4):797 (1999)
- [2] B.Jaffe, R.S. Roth, S. Marzullo, J.Appl.Phys, 25 809-19 (1954)
- [3] G.H. Haertling, Properties of Hot-Pressed Ferroelectric Alkali Niobate Ceramics, J.Am. Ceram. Soc. 50. 329 (1967)
- [4] P. Kumar, M. Pattanaik, Sonia, Synthesis and characterization of KNN ferroelectric ceramics near 50/50 MPB, Ceram. Int. 39, pp. 65-69 (2013)
- [5] Jaeger R. E and Egerton. L. J.Am. Ceram. Soc. 45 209 (1962)
- [6] Dungan R.H, Golding R.D. J.Am. Ceram. Soc. 48 601 (1965)
- [7] E.K. Akdogan, K. Keraman, M. Abazari, A. Safari, Origin of high piezoelectric activity in ferroelectric $(\text{K}_{0.44}\text{Na}_{0.52}\text{Li}_{0.04})\text{-(Nb}_{0.84}\text{Ta}_{0.16}\text{Sb}_{0.06})\text{O}_3$ ceramics, Appl.Phys.Lett. 92, 112908 (2008)
- [8] Ruzhong Zuo, Jian Fum Danya Lv, Phase transformation and Tunable Piezoelectric properties of Lead-free $(\text{Na}_{0.52}\text{K}_{0.48-x}\text{Li}_x)(\text{Nb}_{1-x-y}\text{Sb}_y\text{Ta}_x)\text{O}_3$ System, J. Am. Ceram. Soc., 92 [1] 283-285 (2009)
- [9] Yuanyu Wang, Jiagang Wu, Dingquan Xiao, Piezoelectric properties of $(\text{Li},\text{Ag},\text{Sb})$ modified $(\text{K}_{0.50}\text{Na}_{0.50})\text{NbO}_3$ lead-free ceramics, Journal of Alloys and Compounds 462, 310-314 (2008)
- [10] Y.S. Sung, S. Baik, J.H. Lee. Appl. Phys. 101, 012902 (2012)
- [11] Jiagang Wu, Yuanyu Wang, Effects of Ag content on the phase structure and piezoelectric properties of $(\text{K}_{0.44-x}\text{Na}_{0.52}\text{Li}_{0.04}\text{Ag}_x)(\text{Nb}_{0.91}\text{Ta}_{0.05}\text{Sb}_{0.04})\text{O}_3$ lead-free ceramics Appl.Phys.Lett 91, 132914 (2007)
- [12] Chao Lei, Zuo-Guang Ye, Lead-free piezoelectric ceramics derived from the $\text{K}_{0.5}\text{Na}_{0.5}\text{NbO}_3\text{-AgNbO}_3$ solid solution system, App.Phys.Lett 93, 042901 (2008)

Processing-Dependent Dielectric and Ferroelectric Properties of BST Ceramics

J. Ćirković, K. Vojisavljević, N. Nikolić, N. Tasić, Z. Branković, T. Srećković, G. Branković

Institute for multidisciplinary research, University of Belgrade, Kneza Višeslava 1, 11030 Belgrade, Serbia

jovana.cirkovic@gmail.com

Barium strontium titanate, $\text{Ba}_x\text{Sr}_{1-x}\text{TiO}_3$ (BST) ceramics have been extensively used as in a microelectronics due to its excellent ferroelectric, dielectric, piezoelectric, and pyroelectric properties [1–3]. At room temperature BST is ferroelectric when x is in the range of 0.7–1, and has a maximum dielectric constant around $x = 0.8$ [4]. Characteristics of BST powders strongly depend on their synthesis. To achieve the desired properties and practical application, BST powder needs to be free of intermediate phases, with a defined stoichiometry and homogenous microstructure.

The commonly used techniques to produce BST powders are conventional solid state processing, complex polymerization method, and hydrothermal method. The solid state reaction is most common technique for preparation of BST powders, but it is faced with several disadvantages such as large particle size distribution, non-homogeneity and presence of impurities, which can negatively affect the properties of BST ceramics. Hydrothermal technique is able to produce uniform, nanosized, low agglomerated BST particles at low temperature, but it is hard to control the stoichiometry of the final products. In this study, BST powder $\text{Ba}_{0.8}\text{Sr}_{0.2}\text{TiO}_3$ was obtained by hydrothermal treatment of precursor solution containing titanium citrate, barium and strontium acetates, previously prepared by complex polymerization method. By combining the advantages of both methods a fine, nanosized BST powder was synthesized with homogeneous particle size distribution [5]. The calcined BST powders were pressed into pellets and sintered at 1280°C with different dwelling times, from 1 to 32 h. The phase compositions of the sintered samples were determined by X-ray diffraction (XRD) and EDS analysis. Microstructural properties were investigated by scanning electron microscopy. The phase transitions and dielectric properties were investigated by measuring dielectric permittivity (ϵ) and dielectric losses ($\tan\delta$) as a function of temperature. Ferroelectric properties such as remanent polarization (P_r) and coercive field (E_c) were determined by polarization-electric field (P-E) measurements.

The main objective of this work was to investigate the changes in the phase composition, structural parameters and microstructure of BST ceramics and their influence on dielectric and ferroelectric properties. XRD analysis of BST ceramics showed that crystallite size and phase composition varied with different sintering times. It was found that the sintering process leads to a formation of secondary phases; $\text{Ba}_6\text{Ti}_{17}\text{O}_{40}$, BaTi_2O_5 and $\text{SrTi}_{21}\text{O}_{38}$ on Ti-rich side, and Ba_2TiO_4 on Ba-rich side. The sintered samples underwent an abnormal grain growth, whereby some grains grew faster than others due to the presence of multi-phase structure. It was found that dielectric and ferroelectric properties of BST ceramics strongly depended on grain size, density, phase compositions and defects.

- [1] S. Agarwal, G.L. Sharma, Humidity sensing properties of (Ba, Sr) TiO_3 thin films grown by hydrothermal–electrochemical method, *Sensor Actuat B-Chem*, vol. 85, pp. 205–211 (2002).
- [2] M.W. Cole, C. Hubbard, E. Ngo, M. Ervin, M. Wood, R.G. Geyer, Structure–property relationships in pure and acceptor-doped $\text{Ba}_{1-x}\text{Sr}_x\text{TiO}_3$ thin films for tunable microwave device applications, *J Appl Phys*, vol. 92, pp. 475–483 (2002).
- [3] S. Ezhilvalavan, T.Y. Tseng, Progress in the developments of (Ba,Sr) TiO_3 (BST) thin films for Gigabit era DRAMs, *Mater Chem Phys*, vol. 65, pp. 227–248 (2000).
- [4] S. Lahiry, A. Mansingh, Dielectric properties of sol–gel derived barium strontium titanate thin films, *Thin Solid Films*, vol. 516, pp. 1656–1662 (2008).
- [5] J. Ćirković, K. Vojisavljević, M. Šćpanović, A. Rečnik, G. Branković, Z. Branović, T.Srećković, Hydrothermally assisted complex polymerization method for barium strontium titanate powder synthesis, *J Sol-Gel Sci Technol*, vol. 65, pp. 121–129 (2013).

PHASE TRANSITIONS, FERROELECTRIC AND PIEZOELECTRIC PROPERTIES OF BISMUTH-BASED PEROVSKITE CERAMICS

E.D. Politova¹, G.M. Kaleva¹, A.V. Mosunov¹, S. Yu. Stefanovich¹, A.H. Segalla²

¹*L.Ya.Karpov Institute of Physical Chemistry, Obukha s.-st., 3-1/12, b.6, 105064, Moscow, Russia*

²*ELPA Company, Panfilovsky pr. 10, Zelenograd, 124460, Moscow, Russia*

politova@cc.nifhi.ac.ru

Perovskite-like bismuth containing ceramics have real prospects for the development of materials with Curie temperatures $T_C > 700$ K for high temperature applications.

In this work, ferroelectric and piezoelectric properties on oxides based on $\text{BiScO}_3 - \text{PbTiO}_3$ (BSPT) compositions were studied. In order to regulate functional properties of BSPT-based ceramics complex approach was used that included modification of compositions in A- and B-sublattices, addition of overstoichiometric additives, and optimization of preparation conditions [1].

Ceramic samples $(1-x)\text{BiScO}_3 - x\text{PbTiO}_3$ (BSPT) with $x = 0.63 - 0.65$ close to Morphotropic Phase Boundary (MPB) were prepared by the solid state reaction method and were characterized by the X-ray diffraction, Scanning Electron Microscopy (SEM), Second Harmonic Generation (SHG), DTA/DSC, and Dielectric Spectroscopy methods. Piezoelectric parameters d_{33} and k_t of the preliminary poled samples were determined.

Optimal sintering conditions of dense and textured ceramics preparation were determined. Dense single-phase ceramic samples with different microstructure were obtained by using overstoichiometric additives (chlorides KCl, NaCl, CaCl_2 and fluoride LiF) [2].

Variations in phase content, structure parameters, dielectric and piezoelectric properties were observed depending on both composition and thermal treatment conditions. The 1st order ferroelectric-paraelectric phase transitions were observed for all samples at high temperatures of 650 – 1000 K. The changes of the T_C values observed correlated with the unit lattice parameters and relative content of the rhombohedral and tetragonal phases caused by doping. Effects of dielectric relaxation were observed in samples prepared at high sintering temperatures. A microscopic mechanism of such behaviour is related to the presence of vacancies in A- and oxygen sublattices due to inevitable lead and/or bismuth oxide loss during the high-temperature sintering process. Suppression of relaxation effects was observed in modified samples sintered at lower temperatures characterized by the marked decrease of total conductivity values to more than one order. High piezoelectric coefficients d_{33} up to ~ 500 pC/N and $k_t \sim 0.65$ values were measured in ceramics prepared. Enhancement of piezoelectric properties is discussed in relation to the preparation conditions, type and content of dopants.

[1] E.D. Politova, G.M. Kaleva, A.V. Mosunov, N.V. Sadovskaya, A.G. Segalla, and A.A. Bush, Influence of Complex Additives on Morphology, Phase Transitions, and Dielectric Properties of $0.36\text{BiScO}_3 - 0.64\text{PbTiO}_3$ Ceramics, *Ferroelectrics*, 2013, vol. 440, pp. 105-112.

[2] E. D. Politova, G. M. Kaleva, A. V. Mosunov, A. H. Segalla, A. E. Dosovitskiy and A. L. Mikhlin, Processing, phase transitions, and dielectric properties of BSPT ceramics, *Journal of Advanced Dielectrics*, 2013, vol. 3, No. 4, 1350024 (5 pages).

Atomic-scale determination of spontaneous polarization in the antiphase boundary of antiferroelectric PbZrO₃

Xian-Kui Wei^{1,2}, Chun-Lin Jia^{2,3}, Hong-Chu Du^{2,4}, Alexander K. Tagantsev¹, Alexander Kvasov¹, Krystian Roleder⁵ & Nava Setter¹

1-Ceramics Laboratory, Swiss Federal Institute of Technology Lausanne (EPFL), Lausanne CH-1015, Switzerland.

2-Peter Grünberg Institute and Ernst Ruska Center for Microscopy and Spectroscopy with Electrons, Research Center Jülich, 52425 Jülich, Germany.

3-International Centre of Dielectric Research, The School of Electronic and Information Engineering, Xi'an Jiaotong University, Xi'an 710049, China.

4- Gemeinschaftslabor für Elektronenmikroskopie (GFE) RWTH Aachen, Ahornstraße 55, 52074 Aachen, Germany.

5-Institute of Physics, University of Silesia, Katowice 40007, Poland.

Correspondence author email address: xiankui.wei@epfl.ch

The exceptional property of domain boundary against domains brings in promising potentiality in designing novel electronic devices [1, 2]. Here, using negative spherical-aberration imaging (NCSI) technique in an aberration-corrected transmission electron microscope [3], we report on the development of spontaneous polarization in the antiphase domain boundary of antiferroelectric PbZrO₃ single crystal. Associate with breaking of the normal cation arrangements and the antiphase rotation of the octahedra, our picometer-precision measurements on the basis of an atomic-resolution image reveal that the polarization vectors essentially lie in the antiphase boundary plane. In addition to the Pb atoms, displacements of Zr atoms with respect to centers of the distorted octahedra also contribute equally to the developed electric polarizations [4]. It is believed that the spontaneous polarization observed within the antiphase boundary will stimulate further interests of both fundamental and applied researches on novel electronic devices.

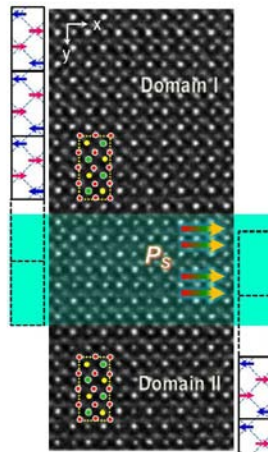


Figure 1 Atom-resolved structure of the antiphase boundary in PbZrO₃. The schematic unit cells are overlapped on the image. Lead-yellow circles, zirconium-green circles, oxygen-red circles. The schematic unit cells at both sides shows the phase shift of this antiphase boundary.

- [1] T. Sluka, A.K. Tagantsev, P. Bednyakov, N. Setter, Free-electron gas at charged domain walls in insulating BaTiO₃, *Nature Communications*, 4, 1808, (2013).
- [2] S.Y. Yang, J. Seidel, S.J. Byrnes, P. Shafer, C.H. Yang, M.D. Rossell, P. Yu, Y.H. Chu, J.F. Scott, J.W. Ager, L.W. Martin, R. Ramesh, Above-bandgap voltages from ferroelectric photovoltaic devices, *Nature Nanotechnology*, 5, 143-147 (2010).
- [3] C.L. Jia, M. Lentzen, K. Urban, Atomic-resolution imaging of oxygen in perovskite ceramics, *Science*, 299, 870-873, (2003).
- [4] X.-K. Wei, A.K. Tagantsev, A. Kvasov, K. Roleder, C.L. Jia, N. Setter, Ferroelectric translational antiphase boundaries in nonpolar materials, *Nature Communications*, 5, 3031, (2014).

Response of a ferroelectric to an electric field: the Rayleigh law and its extensions

R. Renoud¹, C. Borderon¹, M. Ragheb¹, H.W. Gundel¹

¹- Institut d'Electronique et de Télécommunication de Rennes, University of Nantes, Nantes, France

raphael.renoud@univ-nantes.fr

The response of a ferroelectric to the application of an electric field at low amplitudes is generally depicted by the empirical Rayleigh law. This one indicates a linear variation of the permittivity with the amplitude of the applied electric field. It is well admitted that this behavior is due to the pinning of the domain walls on defects. The Rayleigh law is only valid in a limited amplitudes region and for hard ferroelectrics.

Recently, we have proposed to extend the Rayleigh law to very low field amplitudes by including the effect of the domain wall vibrations in pinning centers [1,2]. This more general approach, called the hyperbolic law, also permit us to describe the behavior of the soft ferroelectric materials [1].

In this paper, we propose to study the deviation of the hyperbolic law at higher amplitudes. The value of the amplitude for which a deviation from the hyperbolic law is significant strongly depends on the frequency. In this region, the dominant mechanism is the switching of the domains. We propose here again a hyperbolic correction. Our approach is compared with experimental data available in literature and the frequency dependence is discussed.

Our approach is illustrated by figures 1 and 2. In the figure 1 is reported the real part of the permittivity ϵ' of a lead zirconate titanate thin films (PZT) measured by Khodorov *et al.* as a function of the amplitude E_0 of the electric field and for several frequencies f [3]. The hyperbolic law (lines on figure 1) well fits the experimental points at low amplitudes E_0 but a discrepancy is observed at high values. The figure 2 corresponds to the correction function ξ' applied to the hyperbolic law to take into account the effect of the domains switching.

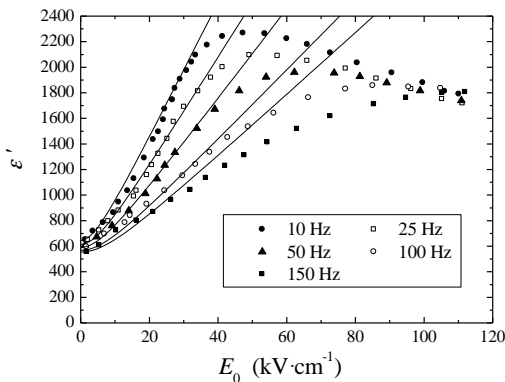


Figure 1: Variation of the real part of the permittivity of thin film of PZT as a function of the amplitude of the applied field E_0 and for various frequencies. Experimental data are from [3].

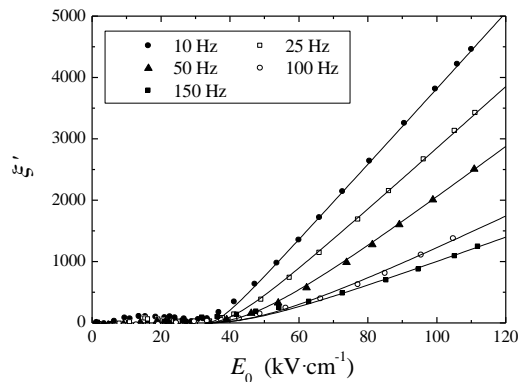


Figure 2: Correction to the hyperbolic law as a function of the amplitude E_0 for various frequencies.

[1] C. Borderon, R. Renoud, M. Ragheb, H.W. Gundel, Description of the low field nonlinear dielectric properties of ferroelectric and multiferroic materials, *Applied Physics Letters*, **98**, pp. 112903-1-3 (2011).

[2] R. Renoud, C. Borderon, H.W. Gundel, Measurement and Modeling of Dielectric Properties of Pb(Zr,Ti)O₃ Ferroelectric Thin Films, *IEEE Transactions on Ultrasonics, Ferroelectrics, and Frequency Control*, **58**, pp.1975-1980 (2011).

[3] A. Khodorov, S.A.S. Rodrigues, M. Pereira, M.J.M. Gomes, Dielectric nonlinearity in a compositionally graded lead zirconate titanate structure, *Journal of Applied Physics*, **104**, pp. 126102-1-4 (2008).

Dielectric losses due to domain walls in ferroelectric materials

C. Borderon¹, R. Renoud¹, H. W. Gudel¹

*1- Institut d'Électronique et de Télécommunications de Rennes, University of Nantes, Nantes, France
Caroline.Borderon@univ-nantes.fr*

Ferroelectric thin films are attractive materials for tunable microwave devices such as electrically tunable filters, capacitors, oscillators, resonators or phase shifters. For this type of applications, the material needs to have a high dielectric permittivity and low losses ($\tan \delta < 10^{-2}$). However, the dielectric properties, in ferroelectric materials, are very sensitive to domain wall motions. This process produces many losses since the domains walls interact with lattice defects such as vacancies, charged defects or dislocations.

In the present work, the losses due to domain walls motion are studied. At low field, the domains walls move on a randomly varying force and several types of domains walls displacements can be occurred. When a domain wall is trapped in a pinning point, it can "jump" to another pinning center only if the field is sufficiently high. This irreversible phenomenon induces a variation of the global polarization since the domain wall doesn't return to its origin position. In contrast, if the field is too weak, the domain wall only vibrates around its equilibrium position. Thus, these two events contribute to the value of the permittivity which can be described by a hyperbolic law [1]:

$$\epsilon_r = \epsilon_{rl} + \sqrt{\epsilon_{r-rev}^2 + (\alpha_r E_0)^2}.$$

This law is based on reversible and irreversible domain wall motions and allows us to dissociate the domain wall and lattice contributions. ϵ_{rl} is due to intrinsic lattice and ϵ_{r-rev} to reversible domain wall vibrations and can be associated to a measure of domain wall mobility [2]. The parameter α_r represents domain wall pinning and is related to an irreversible modification of the local polarization [2,3]. Both parameters depend on the crystal structure, but α_r also reflects the presence of impurities, dopants or defects [4]. This law is valid for the real and imaginary part of the permittivity and it is possible to evaluate the part in dielectric losses which is due to domain walls motion.

For this study, the real and imaginary parts of the permittivity of different types of ferroelectric thin films were measured as a function of a DC bias field. For each value of DC bias field, the coefficients of the hyperbolic were determined (Figure 1). This allows calculation of the dielectric losses of domain wall movements.

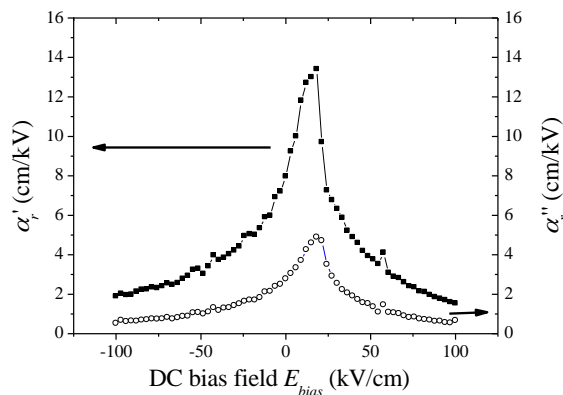


Figure 1: Variation of the real and imaginary part of the coefficient due to irreversible domain wall motion of PZT thin film as a function of the amplitude of the DC applied field E_{bias}

- [1] C. Borderon, R. Renoud, M. Ragheb et al., "Description of the low field nonlinear dielectric properties of ferroelectric and multiferroic materials," *Appl.Phys.Lett.* **98** (1), 112903-112901-112903 (2011).
- [2] D.V. Taylor and D. Damjanovic, "Evidence of domain wall contribution to the dielectric permittivity in PZT thin films at sub-switching fields," *Journal of Applied Physics* **82** (4), 1973-1975 (1997).
- [3] J. E. García, R. Perez, and A. Albareda, "Contribution of reversible processes to the non-linear dielectric response in hard lead zirconate titanate ceramics," *Journal of Physics: Condensed Matter* **17** (44), 7143-7150 (2005).
- [4] O. Boser, "Statistical theory of hysteresis in ferroelectric materials," *Journal of Applied Physics* **62** (4), 1344-1348 (1987).

Geometric Ferroelectricity in Fluoro-Perovskites

A. C. Garcia-Castro^{1,2}, N. A. Spaldin³, Ph. Ghosez¹, A. H. Romero⁴ and E. Bousquet¹

¹Physique Théorique des Matériaux, Université de Liège, B-4000 Sart Tilman, Belgium.

²Materials Department, CINVESTAV, Querétaro, Qro. 76230, México.

³Materials Department, ETH-Zurich, Zurich, CH-8093, Switzerland.

⁴Physics Department, West Virginia University, Morgantown, WV 26506-6315, USA.

Eric.bousquet@ulg.ac.be

Because of its large polarizability, the metal-oxygen bond in perovskite oxides ABO_3 is particularly favorable for promoting a transition-metal off-centering in the MO_6 octahedra. This property has been identified to be the key mechanism for ferroelectricity in ABO_3 perovskites such as $BaTiO_3$ [1, 2]. Ferroelectrics also exist, in several other material chemistries that do not contain oxygen, such as fluorine-based compounds, including polymers [3] and ceramics and thus in many crystal classes and stoichiometries [4]. Given the low polarizability of M-F bond, we can expect the mechanism for ferroelectricity in fluorine-based crystals to be distinct from the one found in oxides. For example, it has been observed that molecular reorientations is the main mechanism of ferroelectricity in polymers [5] or that geometric reconstructions can induce ferroelectricity in ceramics [6]. These alternative mechanisms are of particular interest because, unlike the oxides, they are not contra-indicated by partially filled transition metal d -orbitals, and so they have a high potential in having simultaneous ferroelectric and magnetic ordering (multiferroicity). Interestingly, however, none of the known perovskite-structure fluorides has been reported to be ferroelectric.

Here we would like to present the first-principles calculations we performed in order to investigate the possible existence and the origin of a ferroelectric instability in the ABF_3 fluoro-perovskites. Interestingly, we find that several fluoro-perovskites have a ferroelectric instability in their high symmetry cubic structure, which is of similar amplitude to that commonly found in oxide perovskites. In contrast to the oxides, however, the fluorides have close to nominal Born effective charges, indicating a different mechanism for the ferroelectric instability. We will show that the ferroelectric instability in ABF_3 actually originates from an ionic size effect and is thus related to a geometric-like ferroelectricity with A-site dominated eigendisplacements. In most of the cases, the ferroelectric instability in ABF_3 is slightly sensitive to pressure and strain, again in contrast to the oxide perovskites.

Going beyond, we will also show that in $NaMnF_3$ coherent epitaxial strain matching to a substrate with equal in-plane lattice constants allows to destabilize the bulk $Pnma$ ground state structure toward a ferroelectric ground state and, thus, making it multiferroic. The induced polarization is not large (though of several $\mu C/cm^2$), as expected from nominal Born effective charges, but we found a polarization/strain response that does not follow the usual linear dependence observed in ferroelectric ABO_3 perovskites. All of that makes the fluorides of large interest in the understanding of the physics of ferroelectrics as well as in their possible technological applications.

References:

- [1] G. Sághi-Szabó, R. E. Cohen, and H. Krakauer, Phys. Rev. Lett. 80, 4321 (1998).
- [2] N. A. Hill, J. Phys. Chem. B 104, 6694 (2000).
- [3] A. J. Lovinger, Science 220, 1115 (1983).
- [4] J. F. Scott and R. Blinc, J. Phys. Condens. Matter 23, 113202 (2011).
- [5] D. Guo and N. Setter, Macromolecules 46, 1883 (2013).
- [6] C. Ederer and N. A. Spaldin, Phys. Rev. B 74, 020401 (2006).
- [7] N. Benedek and C. Fennie, J. Phys. Chem. C 117, 13339 (2013).
- [8] P. Ghosez, X. Gonze, and J. Michenaud, Europhys. Lett. 713, 713 (1996).

Local field engineering for designing tunable composite materials

L. Padurariu¹ and L. Mitoseriu¹

1-Faculty of Physics, Alexandru Ioan Cuza University, 11 Bv. Carol I, 700506 Iasi, Romania

Main author email address: leontin.padurariu@uaic.ro

One of the most important properties of ferroelectric materials is the ability to modify their permittivity with increasing the applied electric field values (tunability) which makes them applicable for tunable microwave devices such as oscillators, phase shifters and varactors. The requirements for a good tunable materials are: high tunability, low losses (below 3%) and moderate dielectric constant (below 1000). The first two requirements are easily accomplished in single phase ferroelectric materials, but they are always accompanied by a high permittivity. In the last years, the materials scientists attention has been focused in searching of new tunable materials with required properties. The most tried solution was to create composites materials based on BaTiO₃ or its based solid solution and a low permittivity phase. Unfortunately, in this case the reduced permittivity was always accompanied by a reduced permittivity.

The aim of this work is to investigate the tunable composites materials in terms of local electric field inhomogeneity, and to show how the desired tunable properties can be reached by controlling the microstructure features (local field engineering). Finite Element Method (FEM) was employed to compute local electric fields distribution in composites materials.

The simulations explained the reduction of the tunability in the case of randomly mixed phase composites through the suppression of the electric field on the nonlinear component. A worse situation is in the case of the nonlinear phase included in the low permittivity matrix for which an almost zero tunability is obtained. These results were confirmed experimentally in the case of BaTiO₃ ceramics (composite with nonlinear grain core and linear grain boundary) [1] with reduced grain size (below 100 nm). Conversely, in the case of low permittivity phase included in a nonlinear matrix the simulations showed a reduced permittivity and still a high tunability. The results were confirmed by the particular case of porous Nb-doped PZT ceramics with various levels of porosity [2]. Another promising solution to reach the required properties in tunable applications is to develop composites materials based on polar dielectric matrix (with permittivity below 100 and weak tunability). By adding the conductive or high permittivity inclusions the tunability of the system is increased due to the enhanced field on the matrix. This FEM result was confirmed experimentally in the case of Chitosan with Gold nanoparticles inclusions [3].

Acknowledgements: The support of the project POSDRU/159/1.5/S/137750 is highly acknowledged.

[1] L. Padurariu, L. Curecheriu, V. Buscaglia, L. Mitoseriu, Phys.Rev.B 85, pp. 224111-9 (2012)

[2] L. Padurariu, L. Curecheriu, C. Galassi, L. Mitoseriu, Appl.Phys.Lett. 100, pp. 252905-5 (2012)

[3] A. Cazacu, L. Curecheriu, A. Neagu, L. Padurariu, A. Cernescu, I. Lisiecki, L. Mitoseriu, Appl. Phys. Lett. 102, pp. 222903-5 (2013)

Phase transition properties of Bell-Lavis model

M.Šimėnas, A. Ibenskas, E. E. Tornau

Semiconductor Physics Institute, Center for Physical Sciences and Technology, Goštauto 11, LT-01108 Vilnius, Lithuania

et@et.pfi.lt

Self-assembly of molecular nanostructures is often due to cooperativity, selectivity, and directionality of H-bonds. One of the most popular patterns found in an assembly of H-bonded molecular arrays is a two-dimensional honeycomb (HON) pattern. For description of the ordering of H-bonded molecules into the HON and some other phases the statistical models of phase transitions might be used. The HON structure is represented then as the phase on a tripartite lattice in which the sites of each sublattice are occupied by occupation variables +1, -1 and 0, respectively. For example, the ordering of triangular trimesic acid molecules [1] might be described by the antiferromagnetic (AFM) triangular nearest neighbour (1NN) 3-state model [2] which was originally created to describe the ordering of lattice fluids, water in particular, and is called Bell-Lavis (BL) model [3]. This model with some modifications can be mapped into better known triangular AFM models: Blume-Capel, Blume-Emery-Griffiths and Ising.

It is assumed in the 1NN BL model [2,3] that each molecule has three bonding directions at 120° angle to each other. The molecule has two non-zero states and a vacancy state. In each of non-zero states the molecule has bonding directions pointing towards three of the six 1NN sites of triangular lattice. The H-bond is formed if two NN molecules point towards each other. The interaction energy of a pair of molecules at 1NN sites is $-\varepsilon_H$ and $-\varepsilon_{vdW}$ for H-bonded and unbonded pair, respectively, and the subscripts H and vdW denote H-bond and van der Waals interactions, respectively.

Here we present Monte Carlo simulations of phase transitions at $\xi = \varepsilon_{vdW}/\varepsilon_H = 0$ and 0.1 for two BL-type models: 1NN and 3NN1. In a latter model it is assumed (i) H-bond interactions between molecules on third nearest neighbour sites and (ii) molecular size-induced infinite repulsion (exclusion) between molecules on 1NN sites.

Our results demonstrate that in the 1NN model the phase transitions from disordered to HON phase are either of the second ($0 < \mu' < \mu'_i$) or the first order ($\mu'_i < \mu' < 1.5$) with the value of tricritical point at $\mu'_i = 1.48$ ($\mu' = \mu/\varepsilon_H$ is the normalized chemical potential) for $\xi = 0$. Finite size scaling and reweighted histograms calculations show that the second order transitions belong to the 3-state Potts universality class in almost all interval of μ' values except for the HON phase boundaries. Close to the boundary $\mu' \rightarrow 0$ the BL model resembles triangular AFM Ising model and might be attributed to the Ising universality class. At low temperature and $\mu' \rightarrow 0$ we find Shottky anomaly in specific heat, analogous to that found in 1D Ising model, and originating from scarcity and proximity of energy levels.

In temperature dependences of the 3NN1 model we find either one or two phase transitions. When $\xi = 0$ and molecular density is small ($\mu' > \mu'_i = 0.8$), one first order phase transition from disordered to HON phase is obtained. At higher densities ($\mu'_i < 0.8$) the model shows the sequence of phase transitions: disordered - intermediate - HON. We performed combined finite size scaling and reweighted histogram analysis to find if the intermediate phase has some features of the Kosterlitz-Thouless planar ordering characteristic to some frustrated structures. However, we could not give a definite answer. Most likely, the intermediate phase in the 3NN1 model is a frustrated phase with domains of the HON phase partly diluted by vacancies. Its occurrence might be related to the fact that exclusions create inhomogeneous distribution of particles in disordered phase and make the energy and other thermodynamic functions more abrupt, thus inducing the phase transition at higher temperature.

[1] M. Lackinger, S. Griessl, W.M. Heckl, M. Hietschold, and G.W. Flynn, Self-assembly of trimesic acid at the liquid-solid interface - a study of solvent-induced polymorphism, *Langmuir*, v. 21, pp. 4984-4988, (2005).

[2] T. Misiūnas and E. E. Tornau, Ordered assemblies of triangular-shaped molecules with strongly interacting vertices: phase diagrams for honeycomb and zigzag structures on triangular lattice, *J. Phys. Chem. B*, v. 116, pp. 2472-2482, (2012).

[3] G. M. Bell and D. A. Lavis, Two-dimensional bonded lattice fluids. II. Orientable molecule model, *J. Phys. A: Gen. Phys.*, vol. 3, pp. 568-581, (1970).

Application of the matrix homogenization method for calculation of effective properties of laminated composites

A. Starkov¹, I. Starkov²

1- Institute of Refrigeration and Biotechnology, National Research University of Information Technologies, Mechanics and Optics, Kronverksky pr. 49, 197101 St. Petersburg, Russia

2- SIX Research Centre, Department of Radio Electronics, Brno University of Technology, Technicka 12, 616 00 Brno, Czech Republic

ferroelectrics@ya.ru

In recent years, new composite dielectric materials have been intensively developed to meet the requirements of modern technology. As a consequence, approximate analytical methods for analysis and description of laminated and block systems play nowadays a very important role. The most apparent approach to this problem is to replace such a structure on an effective medium with constant material parameters. This approximation limits the applicability of the model but greatly simplifies the procedure for calculating electromagnetic fields. As an efficient approach to address those issues, in this work we propose to use a variant of the matrix homogenization method [1].

Let us consider a stratified medium $0 \leq z \leq h$ consisting of n layers with boundaries $z = z_i$ ($i=1, 2, \dots, n$). Thickness of the i -th layer is denoted by $h_i = z_{i+1} - z_i$, and the relative thickness by $\theta_i = h_i/h$. We assume that the equations describing the system behaviour can be written as

$$dU/dz = AU, \quad V = BU. \quad (1)$$

Here $U = (u_1, u_2, \dots, u_m)^T$, $V = (v_1, v_2, \dots, v_l)^T$ are column matrices representing the unknown variables (polarization, magnetization, etc.) and tr indicates transposition. The operator matrices A and B may contain other variables (coordinates) and derivatives thereof. As a result of application of the developed homogenization method, we have

$$A^{eff} = \sum_{i=1}^n A_i \theta_i \equiv \bar{A}, \quad B^{eff} = \sum_{i=1}^n B_i \theta_i \equiv \bar{B}. \quad (2)$$

The bar above the quantity means the weighted average of its value. The relations (2) determining the effective parameters of the system have a simple structure. Therefore, the main challenge of our approach is the reduction of the initial equations to the form (1).

As an example of the model applicability, we have considered the electromagnetoelastic equations for transversely isotropic medium [2]. In this case, the matrices U and V have the form

$$U = (u_1, u_2, u_3, \sigma_{13}, \sigma_{23}, \sigma_{33}, D_3, B_3, \varphi, \psi)^T, \quad V = (\sigma_{11}, \sigma_{12}, \sigma_{22}, D_1, D_2, B_1, B_2)^T.$$

Here u_i are components of the displacement vectors, $\{D_i, B_i\}$ the electric and magnetic induction, σ_{ij} the components of the stress tensor ($i, j = 1, 2, 3$), $\{\varphi, \psi\}$ the electric and magnetic field potentials. The separation of variables into two groups is conducted in the following order. The column U includes those quantities that are continuous at the boundaries of the layers. In turn, the variables of column V may be discontinuous at interfaces. The explicit formulas for the matrices A (of size 10×10) and B (7×10) are not presented here because of their cumbersome form. To describe the results of the homogenization method, let Q be the following matrix

$$Q = \begin{pmatrix} c_{33} & e_{33} & f_{33} \\ e_{33} & -\epsilon_{33} & -g_{33} \\ f_{33} & -g_{33} & -\mu_{33} \end{pmatrix}.$$

Here c_{33} , e_{33} and f_{33} are the elastic, piezoelectric and piezomagnetic modules; $\{\epsilon_{33}, \mu_{33}\}$ the electric and magnetic permeabilities, g_{33} magnetolectric coefficient. For the effective parameters of Q , according to the scheme described above, we obtain $Q^{eff} = (\bar{Q}^{-1})^{-1}$. It should be noted that all quantities in Q influence each other in the

averaging operation. Even in the absence of magnetolectric interaction in layers, the averaged magnetolectric coefficient will be nonzero due to the elastic interaction. This fact describes the main advantage of the composite materials: the system exhibits properties that are absent in their constituent components.

In conclusion, the proposed approach can be rigorously justified in contrast to the existing models. More precisely, we have systematized and generalized method presented in [1]. The homogenization procedure is extremely simple, but possible only for equations of the form (1). That is, the main computational effort is to reduce the problem to the form given as (1). The similar approach can be used for block and cylindrical structures.

[1] V.Z. Parton, Electromagnetoelasticity of piezoelectrics and electrically conductive solids (Moscow, Nauka), Chapter II, (1988).

[2] X. Wang, Y.P. Shen, The general solution of three-dimensional problems in magnetoelctroelastic media, Int. J. Eng. Sci., vol.40, pp. 1069-1080, (2002).

Polarization Switching Phenomena in the Polymer Ferroelectrics at the nanoscale

Bystrov V.S.⁽¹⁾, Paramonova E.V.⁽¹⁾, Gevorkyan V.E.⁽²⁾, Avakyan L.A.⁽²⁾

1- The Institute of Mathematical Problems of Biology RAS (IMPB RAS), Russia

2- Southern Federal University, Russia

Email: vsbys@mail.ru

Piezoelectricity in polyvinylidene fluoride (PVDF) is well known, and has been investigated by many authors [1-3]. Nevertheless, the nature of the piezoelectric effect in these PVDF materials is still not clear, although several attempts have been made to solve this problem. In this work, several versions of molecular models for PVDF ferroelectrics were developed and investigated using HyperChem 8.0 [1]. We studied the dependence of the main PVDF electrical properties (dipole momentum, polarization, atomic charges and bond lengths, energies of electron subsystems as well as the total energy of the systems), both without and under an applied electrical field. We explored molecular models of PVDF ferroelectrics with different lengths of the molecular chain. We consider the molecular model of ferroelectric polymer polyvinylidene fluoride (PVDF) film, consisting from one, two chains $[-CH_2-CF_2-]_n$. First principle calculations were employed, using various quantum-chemical methods (QM), including semi-empirical (PM3) and density functional theory (DFT) approaches. The first model, is limited by $n = 6$ elementary units CH_2CF_2 . The first principle approach PM3 and molecular dynamic run were applied for investigation of the switching and its kinetics for these models. Two types of 2 PVDF chains behavior were established: simultaneous and consequence rotation in low and high electric field for two chains model. Obtained results are compared with experimental data at the nano-scale level by the atomic force microscopy. These data are related also with arisen of the PVDF piezoelectric effect. This computational study is corroborated by measured nanoscale data obtained by atomic force and piezo-response force microscopy (AFM / PFM). This study could be useful as a basis for further insights into organic and molecular ferroelectrics.

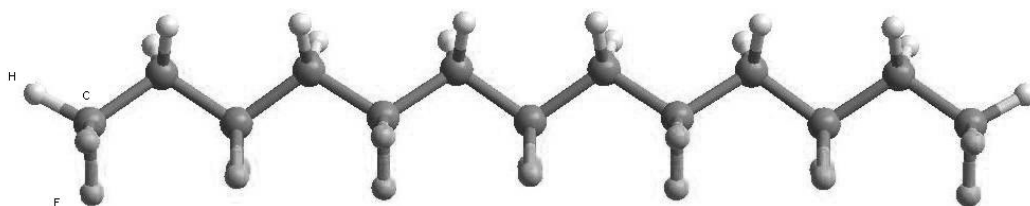


Figure 1 PVDF chain consisting of 6 $[-CH_2-CF_2-]$ units

[1] Furukawa T// Ferroelectric properties of vinylidene fluoride copolymers. -1989. -Phase Transit 18:143–211.

[2] Bune AV, Fridkin VM, Ducharme S, Blinov LM, Palto SP, Sorokin AV, Yudin SG, Zlatkin A.// Two-dimensional ferroelectric films. -1998. -Nature 391:874–877.

[3] Bystrov V, Bystrova N, Paramonova E, Saponova A.// Computational nanostructures and physical properties of the ultra-thin ferroelectric Langmuir-Blodgett films. -2006. -Ferroelectr Lett 33:153–162.

[4] HyperChem, Tools for Molecular Modeling, FL, Hypercube, Inc., Gainesville, 2002.

Domain Nanotechnology in Uniaxial Ferroelectrics of Lithium Niobate and Lithium Tantalate Family

V.Ya. Shur

Ferroelectrics Laboratory, Institute of Natural Sciences, Ural Federal University, 51 Lenin Ave., 620000 Ekaterinburg, Russia

vladimir.shur@urfu.ru

The recent achievements in domain nanotechnology in single crystals of lithium niobate and lithium tantalate family have been reviewed. We have demonstrated the synergetic effect of joint usage of optical, confocal Raman, scanning electron and piezoelectric force microscopy, which provide extracting of the unique information about appearance and evolution of the nanodomain structures. The physical basis of the domain nanotechnology based on the role of nanoscale domains in formation of various quasi-regular nanodomain structures in highly non-equilibrium switching conditions has been considered [1,2]. The obtained knowledge has been used for manufacturing of the highly efficient periodically poled crystals for laser light frequency conversion in wide spectral range.

Domain nanotechnology is the important target of the ferroelectric science and technology nowadays. The stable tailored domain structures with micron-scale periods are used for spatial modulation of the electro-optic and nonlinear optical properties in devices with upgraded performance. The further development of the poling process for fabrication of sub-micron-pitch gratings and precise engineered structures for the photonic applications needs the domain visualization with submicron spatial resolution.

The application of the modern experimental methods for domain visualization in nanoscale has allowed to reveal and to investigate the important role of the self-assembled nanodomain structures appeared at the initial stage of the domain evolution. The reviewed recent achievements in research of the nanodomain kinetics in highly non-equilibrium switching conditions discovered the crucial role of the “earlier invisible” interacting nanodomains [3,4].

The single crystals of lithium niobate and lithium tantalate family have been chosen for investigation as the most important for application nonlinear optical materials [2]. These crystals have been considered also as the model ferroelectrics as they possess comparatively simple domain structure and ability to change drastically the rate and anisotropy of the bulk screening effect by heating.

The evolution of the nanodomain structures has been studied under application of the uniform field in the plates with the surface layer modified by proton exchange or covered by dielectric layer. The formation of the quasi-regular and self-assembled (fractal) nanodomain structures has been investigated during switching by pyroelectric field during cooling after fast pulse laser heating [5,6]. Various types of nanoscale domain structures and scenarios of their evolutions have been singled out. The unique analysis of the nanodomain images at the different depth in the bulk obtained by confocal Raman microscopy allows us to extract the unique information about formation of the nanodomain structures [7]. The unique properties of lithium tantalate crystals for creation of the tailored short-pitch domain structures with sub-micron period have been demonstrated.

The obtained knowledge opens the new approach to the nanodomain engineering. The high-efficient periodically poled lithium niobate and lithium tantalate crystals for laser light frequency conversion in wide spectral range have been manufactured.

The equipment of the Ural Center for Shared Use “Modern Nanotechnology”, Institute of Natural Sciences, Ural Federal University has been used. The research was made possible in part by RFBR and the Government of Sverdlovsk region (Grant 13-02-96041-r-Ural-a), and by RFBR (Grants 13-02-01391-a, 14-02-01160-a).

[1] V.Ya. Shur, Nano- and Micro-domain Engineering in Normal and Relaxor Ferroelectrics, in Handbook of advanced dielectric, piezoelectric and ferroelectric materials. Synthesis, properties and applications, Ed. by Z.-G. Ye (Woodhead Publishing Ltd.), pp.622–669, (2008).

[2] V. Ya. Shur, Kinetics of Ferroelectric Domains: Application of General Approach to LiNbO₃ and LiTaO₃, J. Mater. Sci. vol.41, pp.199–210 (2006).

[3] V.Ya. Shur, D.K. Kuznetsov, E.A. Mingaliev, E.M. Yakunina, A.I. Lobov, and A.V. Ievlev, In situ Investigation of Formation of Self-assembled Nanodomain Structure in Lithium Niobate after Pulse Laser Irradiation, Appl. Phys. Lett., 2011, V.99, No.8, pp.082901-1-3.

[4] A.V. Ievlev, S. Jesse, A.N. Morozovska, E. Strelcov, E.A. Eliseev, Y.V. Pershin, A. Kumar, V.Ya. Shur, and S.V. Kalinin, Intermittency, Quasiperiodicity, and Chaos during Scanning Probe Microscopy Tip-induced Ferroelectric Domain Switching, Nature Physics, vol.10, pp.59-66, (2014).

[5] V.Ya. Shur, E.A. Mingaliev, V.A. Lebedev, D.K. Kuznetsov, and D.V. Fursov, Polarization Reversal Induced by Heating-Cooling Cycles in MgO Doped Lithium Niobate Crystals, J. Appl. Phys., vol.113, pp.187211-1-5, (2013).

[6] V.Ya. Shur, D.S. Chezganov, M.S. Nebogatikov, I.S. Baturin, and M.M. Neradovskiy, Formation of Dendrite Domain Structures in Stoichiometric Lithium Niobate at Elevated Temperatures, J. Appl. Phys., vol.112, pp. 104113-1-6, (2012).

[7] V.Ya. Shur, P.S. Zelenovskiy, M.S. Nebogatikov, D.O. Alikin, M.F. Sarmanova, A.V. Ievlev, E.A. Mingaliev, and D.K. Kuznetsov, Investigation of the Nanodomain Structure Formation by Piezoelectric Force Microscopy and Raman Confocal Microscopy in LiNbO₃ and LiTaO₃ Crystals, J. Appl. Phys., vol.110, pp.052013-1-6, (2011).

Single crystals versus polycrystals of $K_{0.5}Na_{0.5}NbO_3$ towards optimized electromechanical performance

Paula Maria Vilarinho, Muhammad Asif Rafiq, Rui Manuel Pinho, Maria Elisabete Costa

Department of Materials and Ceramics Engineering, CICECO, University of Aveiro, 3810-193 Aveiro, Portugal

paula.vilarinho@ua.pt

This talk intends to contribute to the answer to the following question: will compositions in the $NaNbO_3 - KNbO_3$ system ever be substitutes for lead based piezoelectrics?

Within this context, this talk is about the comparison between the electromechanical properties of single crystals and polycrystals of sodium potassium niobate (KNN), towards the development of materials with improved electromechanical performance able to substitute lead based compositions.

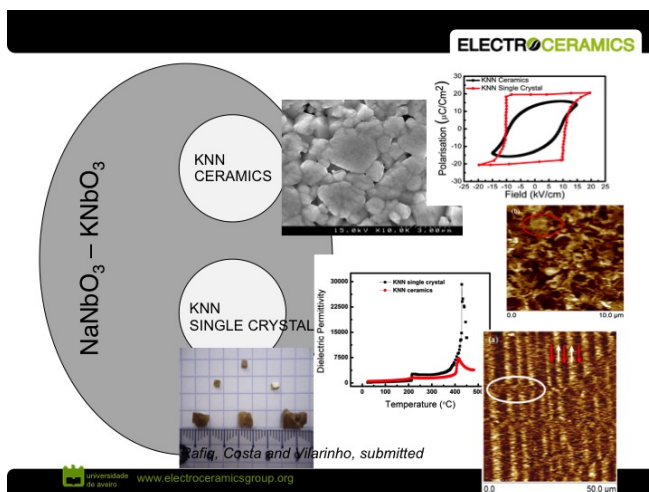
Piezoelectrics and ferroelectrics are currently the basis of the most important smart materials used in micro-electromechanical systems (MEMS), for applications as optical displays, acceleration sensing, radio-frequency switching, drug delivery, chemical detection, and power generation and storage. The increasing importance of MEMs in microelectronics industry has also been addressed by the International Road Map for Semiconductors (ITRS) within the concept of functional diversification called "More than Moore" [1].

Compositions in the solid solution of $PbZrO_3 - PbTiO_3$ ($Pb(Zr_xTi_{1-x})O_3$ (PZT)) [2] and $PZN-PbTiO_3$ [3] exhibit some of the highest electromechanical coupling coefficients, being consequently key materials for these applications. However, environmental restrictions are requiring the rapid substitution of lead based compounds. Though a substitute for the lead based compounds is yet to be found, compositions in the $NaNbO_3 - KNbO_3$ system are leading candidates for some of these applications.

This talk will revise the state of the art on $NaNbO_3 - KNbO_3$ materials. The different strategies to improve the performance of KNN based materials will be addressed. To support this discussion we will present the results of our systematic studies on the comparison between the performance of single crystals and polycrystalline $K_{0.5}Na_{0.5}NbO_3$ (Figure 1) [4-6]. From the domain structure to the charge transport we will establish the differences between KNN single crystals and ceramics. Based on the striking behavior differences we will try to contribute to the discussion: will compositions of the system $NaNbO_3 - KNbO_3$ ever be the substitutes for lead based piezoelectrics?

References:

- [1] International Technology Roadmap For Semiconductors 2012.
- [2] Y. Saito, H. Takao, T. Tani, T. Nonoyama, K. Takatori, T. Homma, T. Nagaya, M. Nakamura, Lead-free piezoceramics, *Nature*, 432, 84-87, 2004.
- [3] H. Dammak, A. E. Renault, P. Gaucher, M. P. Thi, Origin of the Giant Piezoelectric Properties in the [001] Domain Engineered, *Japanese Journal of Applied Physics, Part 1*, 42, 10, 6477-6482, 2003.
- [4] Muhammad Asif Rafiq, M. Elisabete V. Costa, Paula M. Vilarinho, Establishing the domain structure of $(K_{0.5}Na_{0.5})NbO_3$ (KNN) single crystals by piezoforce-response microscopy, accepted in *Science of Advanced Materials*.
- [5] Muhammad Asif Rafiq, M. Elisabete V. Costa, Paula M. Vilarinho, Defects and charge transport in Mn doped lead free $K_{0.5}Na_{0.5}NbO_3$, submitted.
- [6] Muhammad Asif Rafiq, Peter Supancic Elisabete Costa, Paula M. Vilarinho, Marco Deluca, Structure and orientation of KNN single crystals by polarized micro-Raman spectroscopy, submitted.



Design driven development of piezoelectric touch-sensitive luminous flexible plastics

D.B. Deutz¹, E. Tempelman², S. van der Zwaag¹, W.A. Groen³

1- Novel Aerospace Materials, Faculty of Aerospace Engineering, Delft University of Technology, Kluyverweg 1, 2629 HS Delft, The Netherlands

2- School of Industrial Design Engineering, Delft University of Technology, Landbergstraat 15, 2628 CE Delft, The Netherlands

3- Holst Centre, TNO, High Tech Campus 31, 5605 KN Eindhoven, The Netherlands

d.b.deutz@tudelft.nl

The combination of touch-sensitive flexible electronics with integrated light sources offers new opportunities for product designers to develop intuitive user interfaces. To meet both the mechanical and electrical requirements of the touch-sensitivity in these novel products, composites of piezoelectric particles in a polymer matrix may offer new opportunities.

Piezoelectric composites are valued for affordability, good mechanical properties and low temperature, easy processing. However, at low ceramic volume fractions, the electronic properties suffer due to limited connectivity, while high ceramic volume fractions have a detrimental effect on the failure strain. Due to this trade-off between mechanical flexibility and electronic sensitivity, various solutions to the electrical and mechanical requirements are presented. Composites balancing the conflicting requirements are obtained through in situ dielectrophoretic alignment of the particles during UV-curing of the polymer matrix. Further enhancements are implemented through refining of the piezoelectric powder processing.

Phase pure, monocrystalline bismuth ferrite nanoparticles for biomedical applications

G. Clarke¹, Y. Mugnier², R. Le Dantec², Y. Gunko³, D. Rytz⁴, C. Galez², Y. Volkov¹, A. Prina-Mello¹

1- Nanomedicine, Department of Clinical Medicine, Trinity College Dublin, Ireland

2- Laboratoire SYMME, Polytech'Amey-Chambéry, Université de Savoie, France

3- Department of Chemistry, Trinity College Dublin, Ireland

4- FEE GmbH, Struthstr 2, Idar-Oberstein, 55743, Germany

Corresponding author: clarke2@tcd.ie

We present two novel synthetic routes for phase-pure, monocrystalline bismuth ferrite (BFO). Both phase-pure and mixed phase BFO nanoparticles were produced by solvent evaporation and sol-gel combustion. In the synthesis, metal nitrates were dissolved with a series of dicarboxylic acids with and without NaCl and glycerol which were used to promote crystallisation and complexation. We have found that when the carbon backbone had a hydroxyl group attached to each carbon, BFO formed as the dominant phase at lower annealing temperatures.

Table 1: Structure, ratio of hydroxyl groups to carboxylic acids and lowest annealing temperature at which the dominant phase present was BiFeO₃ for each of the chelating agents used in this study

Chelating agent	Oxalic acid	Tartronic acid	Tartaric acid	Mucic acid
Structure				
-OH:-COOH	0	1:2	1:1	2:1
Lowest annealing temperature (30 min annealing)	750	550	450	350

Better crystallised nanoparticles were produced after annealing at low temperatures by adding glycerol. Results showed that nanocrystals more readily formed at a given temperature on increasing the salt concentration.

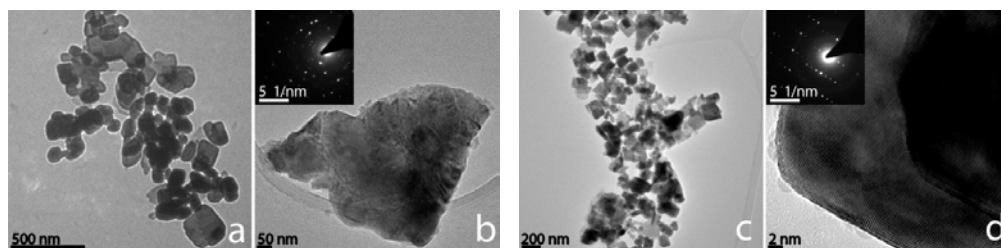


Figure 1 – a) SEM image showing panoramic view of aggregated BFO nanoparticles prepared without NaCl; **b)** HRTEM image showing amorphous surface of BFO nanoparticles prepared without NaCl; inset, Selected Area Electron Diffraction (SAED) patterns showing diffraction peaks of BFO. **c)** SEM image showing panoramic view of aggregated BFO nanoparticles prepared with NaCl; **d)** HRTEM image showing the lattice spacings of well-crystallised BFO NPs prepared with NaCl; inset, SAED patterns showing diffraction peaks of BFO.

This promotion of crystallisation was possibly associated with the formation of intermediate complexes with lower activation energies. The BFO nanoparticles have been characterised by temperature-dependent XRD, electron microscopy (SEM and TEM), zeta potential measurement and photon correlation spectroscopy techniques and the quantitative nonlinear optical response was measured through Hyper-Rayleigh Scattering measurements of colloidal suspensions of the nanoparticles. The nanoparticles were also dispersed in a biomimetic medium and imaged using a Second Harmonic microscope.

We believe that the development of simple, scalable synthesis routes which yield phase-pure and monocrystalline BFO nanoparticles is important for a range of bio-imaging applications based on second harmonic generation.

The authors would like to thank Jean-Christophe Marty, Clive Downing, Sarah McCarthy and Marc Dumbled for their support. This project was partly funded by the Irish Research Council Embark Award, by the EU FP7 NAMDIATREAM project and by the IRC Ulysses travel grant.

Stress induced structural transformation at the MPB of $\text{BiScO}_3\text{-PbTiO}_3$ solid solution

Lalitha.K.V., Rajeev Ranjan

Department of Materials Engineering, Indian Institute of Science, Bangalore, India

kvlalitha87@gmail.com

Ferroelectric materials exhibiting morphotropic phase boundary (MPB) are known to show high electromechanical response. Recent report [1] on a high Curie point MPB system $x\text{BiScO}_3\text{-}(1-x)\text{PbTiO}_3$ (BS-PT) suggests partial irreversible transformation of the monoclinic phase to tetragonal phase on application of strong electric field. In the present study, we have investigated the effect of pure stress on the stability of co-existing phases at the MPB of this system by undertaking a comparative structural analysis of (i) annealed and (ii) mechanically ground/crushed specimens.

Figure 1 compares the pseudocubic $\{200\}$ x-ray Bragg profiles of different MPB compositions. It was found that, upon crushing, the intensity of the monoclinic Bragg peak (marked by M) shows a marked decrease for $x=0.3725$, the composition which exhibits the highest piezoelectric response [1]. Rietveld analysis confirmed the reduction in monoclinic volume fraction to be $\sim 10\%$. This observation is similar to what has been reported for the specimen subjected to electric field [1]. For compositions outside the MPB region, mechanical grinding does not bring about any noticeable structural change. The result proves for the first time the equivalence of stress and electric field with regard to the nature of phase transformation in this MPB system.

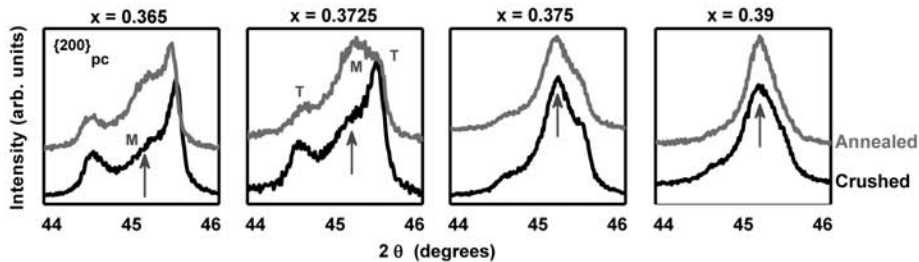


Figure 1 High resolution x-ray diffraction profiles showing $\{200\}$ pseudocubic reflections of crushed and annealed samples for different MPB compositions. The tetragonal peaks are marked as 'T' and the monoclinic peak is marked as 'M'.

[1] Lalitha K. V., Andy N. Fitch, and Rajeev Ranjan, Correlation between enhanced lattice polarizability and high piezoelectric response in $\text{BiScO}_3\text{-PbTiO}_3$, *Phys Rev B*, 87, 064106 (2013).

Templated Grain Growth of Textured (K,Na,Li)(Nb,Ta)O₃ Piezoelectric Ceramics

Jae-Ho Jeon

Korea Institute of Materials Science, 797 Changwondaero, Changwon, Korea

jhjeon2004@google.com

Over the past few decades, lead zirconate titanate (PZT) based piezoelectric ceramics have been used extensively for sensors, actuators and transducers owing to their excellent piezoelectric properties [1-2]. But the toxicity from lead and its compounds to human health and the environment gives rise to environmental regulations which restrict the use of PZTs by replacing them with lead-free piezoelectric ceramics while maintaining comparable piezoelectric properties. Lead-free piezoceramics are now being developed as potentially attractive alternatives to PZTs for specific applications [3-4]. Among them, alkaline niobates have been receiving especial attentions as promising piezoceramics to replace PZTs since Toyota reported that textured (K,Na,Li)(Nb,Ta,Sb)O₃ ceramics using plate-like NaNbO₃ (NN) templates improved piezoelectric properties drastically [5]. Since Toyota used NN templates which have different chemical composition with that of matrix material, there was a possibility to improve piezoelectric properties more if they used templates which have a similar chemical composition of matrix material.

We developed plate-like NaNb_{1-x}Ta_xO₃ (NNT) (x=0, 0.2, 0.5) templates by molten-salt reaction and followed by a topochemical process. NNT templates were aligned in (K_{0.47}Na_{0.51}Li_{0.02})(Nb_{0.8}Ta_{0.2})O₃ (KNLNT) matrix powders using tape casting process and then heat-treatment for burning-out binders and sintering were carried out. The phase structure and the degree of grain orientation of textured samples were determined by X-ray diffraction. Cross-sectional microstructures were examined using optical and scanning electron microscopes. Temperature dependent dielectric constants were measured with an impedance analyzer. Piezoelectric coefficient d₃₃ was measured with a d₃₃ meter. Among three kinds of NNT templates, NaNb_{0.8}Ta_{0.2}O₃ template was most effective to improve the degree of grain orientation and d₃₃ of KNLNT ceramics presumably due to the same content of Ta in both matrix powders and NNT templates. The relationship between microstructure and piezoelectric properties were investigated in terms of Ta content in NNT templates and the amount of template addition.

- [1] Jaffe B, Roth RS, Marzullo S, Piezoelectric properties of lead zirconate-lead titanate solid-solution ceramics. *J. Appl. Phys.*, 25, 809-810 (1954).
- [2] A. Author, B. Author, C. Author, Title of paper, *Journal Name*, vol., pp. start-end, (year). Guo R, Cross L E, Park S E, Noheda B, Cox DE, Shirane G, Origin of the high piezoelectric response in PbZr_{1-x}Ti_xO₃. *Phys. Rev. Lett.*, 84, 5423-5426 (2000).
- [3] Shrout TR, Zhang SJ, Lead-free piezoelectric ceramics: Alternatives for PZT?, *J. Electroceram.*, 19, 111-124 (2007).
- [4] Panda PK, Review: environmental friendly lead-free piezoelectric materials, *J. Mater. Sci.*, 44, 5049-5062 (2009).
- [5] Saito Y, Takao H, Tani T, Nonoyama T, Takatori K, Homma T, Nagaya T, Nakamura M, Lead-Free Piezoceramics, *Nature*, 432, 84-87 (2004).

Sensing complicated motion of human body using piezoelectric chiral polymer fiber

Y. Tajitsu

Kansai University, Electrical Engineering Department, 3-3-35 Yamate Suita, Osaka 564-8680, Japan

tajitsu@ipcku.kansai-u.ac.jp

The demand for smart phones and tablet personal computers with a touch panel has expanded at an incredible pace. This suggests a growing need for human-machine interfaces [1]. Toward sensing the complicated motion of the human body, we have been continuously attempting to develop a new soft and flexible fiber sensor assembled from piezoelectric poly-L-lactic acid (PLLA) fibers [2,3]. As an early stage of this study, we attempted to detect the pulse rate and observe the motion of a human arm using a PLLA fiber sensor [4]. First, we prepared a left-hand helical torsion coil (PLLA fiber left-hand coil), which was

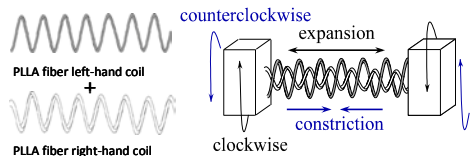


Figure 1 PLLA fiber coil.

formed by drawing a PLLA fiber ten times. It was observed that, when twisted and released suddenly, the coil exhibited a torsion vibration, and we confirmed that a piezoelectric response signal followed the torsion vibration. Next, we developed an experimental system for simultaneous sensing using two PLLA fiber coils. Both ends of the PLLA fiber left-hand coil and those of a PLLA fiber right-hand coil were bonded to an epoxy-plastic block in tight contact, as shown in Fig. 1. By simultaneously measuring the peak signals generated by the two coils, four types of motion, constriction, expansion, clockwise twisting, and counterclockwise twisting, can be distinguished simultaneously, as shown in Fig. 2. The

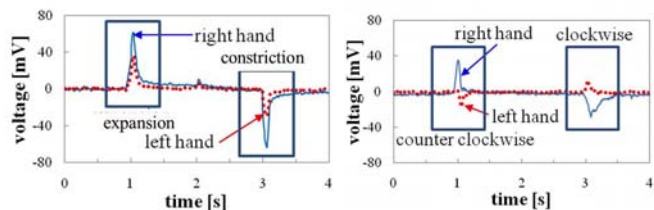


Figure 2 Signals from PLLA fiber coils.

Table 1 Signs of response signals from PLLA fiber coils.

displacement	largest peak sign	
	left-hand coil	right-hand coil
expansion	+	+
contraction	-	-
clockwise twisting	+	-
counterclockwise twisting	-	+

signals of the two coils differed in sign. The results are summarized in Table I. Then, using the PLLA fiber coils, we attempted to simultaneously detect each pulse rate and human arm motion. We prepared a PLLA fiber sensor system in which a PLLA fiber coil was linked to a personal computer (PC) used for simple image processing, as shown in Fig. 3. Still images of various types of motion of the arm of a subject were prepared in advance. The response signal generated by each PLLA fiber coil was processed by the PC to determine which of the still images most closely matched the motion of the arm. As shown in Fig. 3, the PLLA fiber left-hand and right-hand coils were placed on the wrist and the arm of a subject, respectively. One was used to measure the pulse rate and the other was used to observe the motion of arm. We found that the pulse rate could be measured by the PLLA fiber sensor, and extremely accurate measurements were made, as shown in the left of Fig. 3. Furthermore, using the PLLA fiber sensor system, the most appropriate still image could be selected from the signal from the PLLA fiber coils induced by the motion of the arm. We emphasize here that the PLLA fiber sensor system functioned as designed. Our experimental results indicate the strong possibility of realizing a new soft sensor using biodegradable chiral piezoelectric polymers such as PLLA fibers.

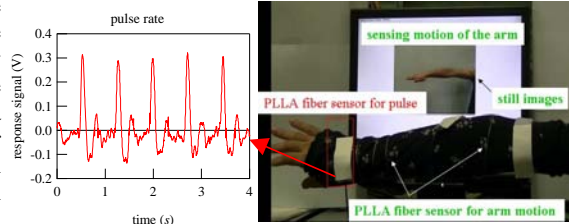


Figure 3 Demonstration of simultaneous detection of pulse rate and human arm motion using PLLA fiber coils.

This work was supported in part by a Grant-in-Aid for Scientific Research (No. 2528059) from the Ministry of Education, Culture, Sports, Science and Technology, Japan, and a COE grant from Kansai University.

[1] F. Carpi and E. Smela, Eds., *Biomedical Applications of Electroactive Polymer Actuators* (Wiley), (2009). [2] Y. Tajitsu, *IEEE Trans. Ultrason. Ferroelectr. Freq. Control*, vol. 55, pp.1000-1008, (2008). [3] Y. Tajitsu, *IEEE Trans. Ultrason. Ferroelectr. Freq. Control*, vol. 60, pp.1625-1629, (2013). [4] S. Ito, M. Date, E. Fukada and Y. Tajitsu, *Jpn. J. Appl. Phys.*, vol. 51, 09LD16 (2012).

Smart Microsystems based on Piezoceramic Thick Films – Application Overview

A. Schönecker, S. Gebhardt, D. Ernst, B. Bramlage

Fraunhofer IKTS, 01277 Dresden, Winterbergstraße. 28, Germany

Andreas.Schoenecker@ikts.fraunhofer.de

Piezoceramic thick films based on lead zirconate titanate (PZT) offer the possibility of integrated electromechanical transducers in microsystems applications. In the here considered technology, the films are screen printed directly on ceramic substrates (LTCC, Al_2O_3) and Si – wafer with high accuracy and reproducibility. Compared to conventional assembling techniques the fired PZT thick films show strong bonding to the substrate and high interface reliability under operation.

We developed a screen printable PZT thick film paste which shows after sintering excellent dielectric and electromechanical properties like dielectric constant value of $\epsilon_{33}^T/\epsilon_0 = 1900$ and piezoelectric coefficient of $d_{33} = 210$ pC/N. Depending on the envisaged application, different types of electrodes (film electrodes, IDT electrodes) and structural integration designs (bender, array) have been developed.

The paper gives an overview on exemplary device developments of the recent past [1]. Special emphasis is given to force sensor for axial load measurement (Fig. 1a), bending actuator array for active optics (Fig. 1b) [2] and ultrasound transducer array for cell manipulation (Fig. 1c).

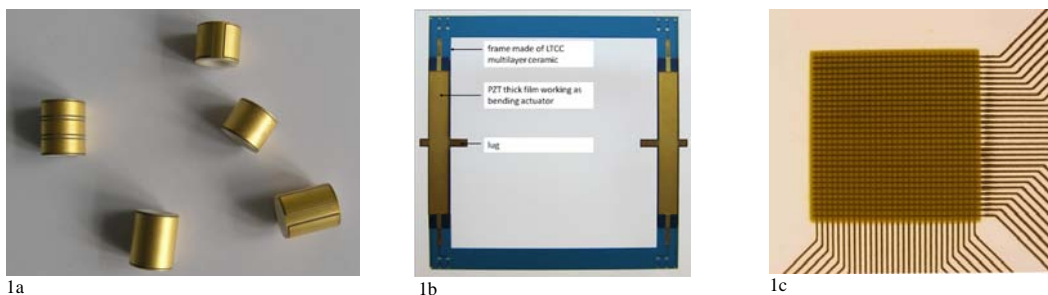


Figure 1 : Examples of PZT thick film devices: 1a Axial force sensing transducer with PZT film on the hollow cylinder surface, 1b actuator frame for positioning purposes and 1c screen printed ultrasound transducer array

Based on comprehensive experimental data we are now able to derive general process and design recommendations for technical and commercial device developments. Major technological progress has been obtained by combining PZT thick film technology with advanced packaging steps, like in jet printing, Laser cutting and multilayer technology, and introduction of simulation methods concerning the mechanics of materials. The presentation reviews the attained progress over the last 5 years.

[1] A. Schönecker, IEEE International Ultrasonics Symposium, IUS, 2012, Article number 6562220, Pages 2122-2128

[2] C. Reinlein, M.Appelfelder, S. Gebhardt, E. Beckert, R. Eberhardt, A. Tünnermann, Journal of Micro/ Nanolithography, MEMS, and MOEMS, Vol. 12, Issue 1, 2013, Article number 013016

Air-coupled Ultrasonic Transducers based on an Application of the PMN - 32% PT Single Crystals

R. J. Kazys, R. Sliteris, J. Sestoke, A. Vladisauskas

Prof. K. Barsauskas Ultrasound Research Institute of Kaunas University of Technology
Studentu St. 50, Kaunas, Lithuania, LT-51368

reimondas.sliteris@ktu.lt

Development of efficient air-coupled ultrasonic transducers is problematic due to a very big difference between acoustic impedances of the used piezoelectric materials and air. The manufactured crystals of the lead magnesium niobate-lead titanate (PMN-PT) possess very high piezoelectric properties and specific acoustic impedance lower than of the conventional piezoceramics. The electromechanical coupling factor for the longitudinal extension mode is $k_{33} > 0.90$, for the transverse extension mode- $k_{31} = 0.84 \sim 0.90$ and for the transverse shear mode- $k_{15} > 0.95$. Those parameters are higher than the parameters of most piezoceramics existing in the market and used for manufacturing of ultrasonic transducers.

The objective of this work was investigation of possibilities of application of the PMN – 32% PT single crystal plates for development of novel effective air-coupled ultrasonic transducers. The high effectiveness of such transducers can be achieved due to a lower acoustic impedance of PMN – PT crystals ($Z_a \approx 13$ MRayl) and higher electromechanical coupling factor in comparison with piezoceramic materials.

The set of PMN – 32% PT single crystals of $\langle 011 \rangle$ cut and $[011]$ poling directions with dimensions of $(15 \times 15 \times 1.0)$ mm³ were investigated. This type of crystal plates possesses anisotropy of piezoelectric parameters such as d_{31} , d_{32} and k_{31} , k_{32} . The existing vibration modes in the crystals were determined and measured. The main transverse extension mode resonant frequency in the direction 1 is 70 kHz and in the orthogonal direction 2 is 45 kHz.

The prototype of an ultrasonic array consisting of the 6 single crystal plates operating in the transverse extension mode was designed and manufactured. The acoustic properties of this transducer were investigated (Figure 1) and compared with the acoustical properties of analogous ultrasonic transducer with PZT type piezoceramic elements. It was found that performance of the array with PMN – 32% PT crystals was a few times better than of the PZT based array.

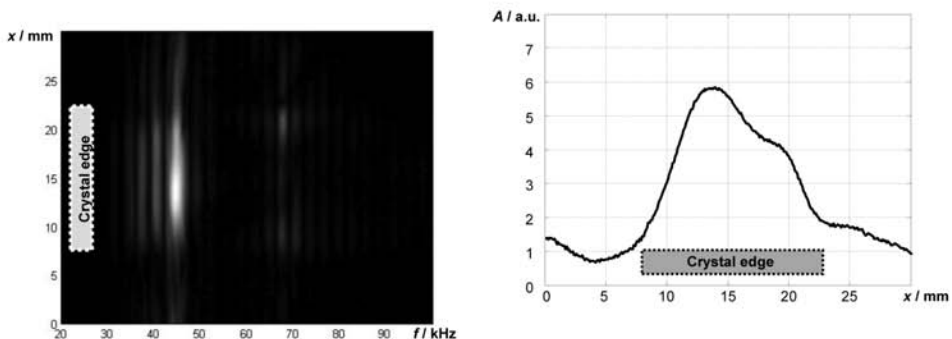


Figure 1 The 45 kHz ultrasonic signal radiated to air by a single PMN – 32% PT crystal plate: (a) spatial distribution of the ultrasonic signal spectrum along the crystal edge. (b) spatial distribution of the ultrasonic signal along the crystal edge at the distance 1mm from the edge.

PyzoFlex[®] - a novel, ferroelectric Human Machine Interface for flexible Electronics

M. Zirkl¹, G. Scheipl¹, A. Tschupp¹, C. Rendl², P. Greindl², B. Stadlober¹, M. Haller², P. Hartmann¹

1- Institute of Surface Technologies and Photonics, JOANNEUM RESEARCH Forschungsgesellschaft mbH, Weiz, Austria
2- Media Interaction Lab, University of Applied Sciences Upper Austria, Hagenberg, Austria

martin.zirkl@joanneum.at

Ferroelectric material supports both pyro- and piezoelectric effects that can be used for sensing pressures on large, bended surfaces [1]. Within this work we present PyzoFlex[®], a pressure-sensing input device that is based on a ferroelectric material. It is constructed as a sandwich structure of four layers that can be printed easily on any material. The PyzoFlex[®] foil is bendable, energy-efficient, and it can easily be produced in a printing process (Screen Printing or Roll to Roll). Even a pyroelectric hovering mode is feasible due to its pyro electric effect.

In organic and large-area printed electronics smart sensors for detection of physical forces are very promising with respect to novel user interface applications. Over the last decade, touch sensing devices have become more and more important [2-4]. Multi-touch screens are now the de-facto standard in mobile devices such as phones and tablets, depth cameras are increasingly being used to capture gestural input in the living room and beyond. This rise in adoption of such ‘natural’ user interfaces shows there is a great deal of user demand for simpler ways of navigating information and content, where the computer interface is not a barrier, but enables them to accomplish tasks more quickly and easily.

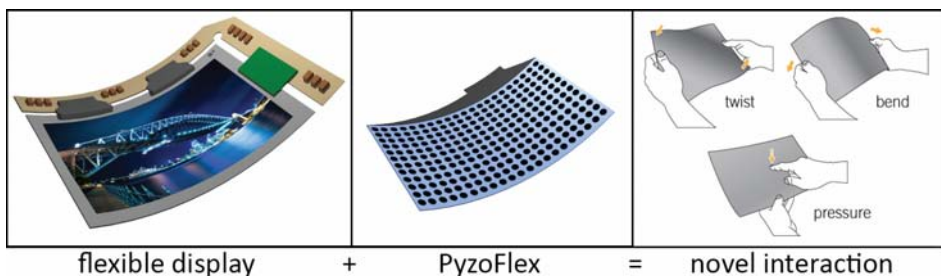


Figure 1 : Illustration of novel, three-dimensional user interaction techniques by combining a flexible display with a printed, ferroelectric PyzoFlex[®] sensor.

We present the development of a printable sensor technology – PyzoFlex[®]. Such a PyzoFlex[®] sensor is based on the ferroelectric material PVDF:TrFE which supports both – the pyro- and the piezoelectric effect that can be used for sensing pressures on large, bended surfaces. The sensor foil is constructed as a sandwich structure of four layers that can easily be printed onto any substrate (e. g. plastic foils, paper, and textiles). The resulting PyzoFlex[®] sensors are sensitive to pressure and temperature changes, bendable, energy-efficient, and they are realized sheet to sheet by a screen-printing routine. Even a hovering input-mode is feasible due to the pyroelectric effect within the sensor material. Since the PyzoFlex[®] sensor acts as a piezoelectric energy converter; any deformation of the sensor foil caused by – e.g. a touch of a human finger – is converted into electric energy. The charges being generated by such a deformation can be measured as a voltage between the electrodes of the sensor setup. An important advantage of the PyzoFlex[®]-technology is its energy self-sufficient sensing principle. The sensor can be driven in a passive (high impedance) mode and any user interaction directly generates electric charges indicating the pressure being applied. On this account the PyzoFlex[®] sensing concept can also be used for energy harvesting purposes.

Acknowledgement: The research leading to these results has received funding from the European Union’s Seventh Framework Programme FP7 / 2007-2013 under grant agreement n° 611104

[1] Rendl, C., Greindl, P., Haller, M., Zirkl, M., Stadlober, B., & Hartmann, P. (2012). PyzoFlex: Printed Piezoelectric Pressure Sensing Foil. In *Proceedings of the 25th annual ACM symposium on User interface software and technology - UIST '12* (pp. 509–518). New York, New York, USA: ACM Press.

[2] Buxton, W., Hill, R. and Rowley, P. 1985. Issues and techniques in touch-sensitive tablet input. In *Proc. SIGGRAPH 1985*, 215-224.

[3] Rekimoto, J. 2002. SmartSkin: an infrastructure for freehand manipulation on interactive surfaces. In *Proc. CHI 2002*, 113-120.

A. Author, Title of book (Publisher), Chapter, (year).

[4] Rosenberg, I. and Perlin, K. 2009. The UnMousePad: an interpolating multi-touch force-sensing input pad. In *Proc. SIGGRAPH 2009*, 65:1-65:9

Manufacture and characterisation of piezoelectric broadband energy harvesters based on asymmetric bistable laminates

C. R. Bowen, P. Harris, D. N. Betts and H. A. Kim

Department of Mechanical Engineering, University of Bath, Bath, BA2 7AY, UK

c.r.bowen@bath.ac.uk

Piezoelectric energy harvesters that convert mechanical vibration into electrical energy are potential power sources for systems such as wireless sensor networks or safety monitoring devices [1]. However, ambient vibrations generally exhibit multiple time-dependent frequencies which can include components at relatively low frequencies. This can make typical linear systems inefficient or unsuitable; particularly if the resonant frequency of the device is higher than the frequency range of the vibrations it is attempting to harvest. To broaden the frequency response of energy harvesters a variety of researchers have introduced elastic non-linearity; for example by designing bistable harvesters with two energy wells [2]. Researchers have considered inducing bistability through magnetic interactions, axial loading, and buckling of hinge-like components. An alternative method has been recently found where a piezoelectric element is attached to bistable laminate plates with two plies of $[0/90]_T$ layup to induce large amplitude oscillations [3,4,5]. Such harvesting structures have been shown to exhibit high levels of power extraction over a wide range of frequencies. This arrangement can be designed to occupy a smaller space and is potentially more convenient and portable for broadband energy harvesting.

In this paper we will manufacture and characterise the energy harvesting capability of bistable asymmetric laminates coupled to piezoelectric materials. Cantilever configurations [6] will be explored to determine power levels as a function of load impedance, frequency and amplitude; in addition to the application of white noise. Harvested power levels, natural frequency and mode shapes will be compared with monostable cantilevers of the same geometry and stiffness to assess the benefits of using bistable configurations.

Acknowledgement

Chris Bowen acknowledges funding from the European Research Council under the European Union's Seventh Framework Programme (FP/2007-2013) / ERC Grant Agreement no. 320963 on Novel Energy Materials, Engineering Science and Integrated Systems (NEMESIS). Alicia Kim acknowledges support from the Engineering and Physical Science Research Council (EPSRC) for Project Reference: EP/J014389/1 "Optimisation of Broadband Energy Harvesters Using Bistable Composites".

- [1] C.R. Bowen, H.A. Kim, P.M. Weaver, S. Dunn, Piezoelectric and ferroelectric materials and structures for energy harvesting applications, *Energy & Environmental Science*, 7, 25-44, (2014).
- [2] R.L. Harne, K. W. Wang, A review of the recent research on vibration energy harvesting via bistable systems, *Smart Materials and Structures*, 22, 023001, (2013).
- [3] A.F. Arrieta, P. Hagedorn, A. Erturk, D. J. Inman, A piezoelectric bistable plate for nonlinear broadband energy harvesting, *Applied Physics Letters* 97, 104102, (2010).
- [4] D.N. Betts, C.R. Bowen, H.A. Kim, N. Gathercole, C.T. Clarke, D. J. Inman, Nonlinear dynamics of a bistable piezoelectric-composite energy harvester for broadband application, *European Physical Journal* 222, 1553-15, (2013).
- [5] D.N. Betts, H.A. Kim, C.R. Bowen, D.J. Inman, Optimal configurations of bistable piezo-composites for energy harvesting, *Applied Physics Letters*, 100, 114104 (2012).
- [6] A. F. Arrieta , T. Delpero, A. Bergamini, P. Ermanni, A cantilevered piezoelectric bi-stable composite concept for broadband energy harvesting, *Proceedings of the SPIE 8688, Active and Passive Smart Structures and Integrated Systems*, 86880G, (2013).

E-beam recording of regular domain structures on the nonpolar surface of LiNbO₃ crystals and their investigations by PFM and SHG microscopy

L.S. Kokhanchik¹, R.V. Gainutdinov², S.D. Lavrov³, E.D. Mishina³, T.R. Volk²

1- Institute of Microelectronics Technology and High Purity Materials, Chernogolovka, Moscow region, 142432, Russia

2- Shubnikov Institute of Crystallography, Moscow 119333, Russia

3- Moscow State Technical University of Radioengineering, Electronics and Automation, 119454, Moscow, Russia

e-mail: mlk@iptm.ru

Periodically poled lithium niobate (PPLN) is a highly efficient medium for nonlinear quasi-phase matching (QPM) wavelength conversion processes. Electron-beam recording is a promising method of PPLN fabrication. In particular, local polarization reversal under e-beam irradiation of the nonpolar faces can be applied for recording of planar regular domain structures on XZ and YZ faces in LiTaO₃ and LiNbO₃ crystals [1, 2]. Planar domain gratings are promising for wavelength conversion processes in integrated optical devices, particularly in optical waveguides. This work presents the results of studies of planar single microdomains and microdomain gratings recorded by e-beam irradiation on the Y-cut LiNbO₃ crystals. For the first time the combined investigations of these structures were performed with the use of PFM technique, nonlinear confocal microscopy (in second harmonic generation mode), optical interference microscopy and chemical etching. The combination of these methods provides full characterization of the fabricated domain arrays.

Domain recording was performed in a SEM equipped with the NanoMaker lithography system. The nonpolar Y-cut of LiNbO₃ crystal was irradiated by e-beam with varied SEM accelerated voltages $U_0 = 5, 10, 15$ and 25 kV. E-beam irradiation of a small surface area results in a domain nucleation and subsequent domain growing along the polar axis Z within a thin surface layer. The length L_d of this planar extended domain depends on the introduced e-beam charge and the thickness along the Y-axis is controlled by the electron penetration depth, i.e. by U_0 . Planar domain gratings with varied parameters were constructed using the original procedure presented for the first time in [1]. The main advantage of this procedure is the possibility of fabrication of domain gratings with specified shapes on rather large areas of nonpolar faces without masks or coatings. The periods of recorded gratings were varied from 4 to 30 μm , the linear sizes were $X \times Z = 650 \times 750 \mu\text{m}^2$, the thickness along the Y axis of about microns.

The examination of recorded single domains and domain gratings was carried out with a SOLVER P47 AFM (NT-MDT, Moscow) using the lateral PFM regime and the contact regime (topography). The regularities in the domain formation were discussed in terms of the current approach to the processes of electron-beam dielectric charging [3]. The revealed dependence of the domain growth kinetics on the e-beam energy was accounted for by an impact of the surface layer on the domain nucleation.

For imaging the domain gratings by SHG confocal microscopy, a Ti:Sapphire femtosecond laser with average power of 360 mW (100 fs, 80 MHz) at wavelength of 800 nm was used. The intensity of SHG converted on the recorded domains exceeds essentially the value calculated based on the nonlinear coefficients of LiNbO₃, which evidences of a specificity of the nonlinear-optical conversion on planar domain arrays.

The combination of PFM and SHG methods detected the fine structure of the recorded structures, especially in the domain boundary region.

The scope of data obtained allowed us to select the optimal exposure conditions for recording the gratings with specified design at different SEM accelerated voltages.

We conclude that the planar domain gratings fabricated by the electron-beam method have a real good perspective for applications in optical-frequency conversion

[1] L. S. Kokhanchik and D. V. Punegov, *Ferroelectrics*, **373**, 69-76 (2008)

[2] L.S. Kokhanchik, V. Borodin, S.M. Shandarov, N.I. Burimov, V.V. Shcherbina, T.R. Volk, *Physics of the Solid State*, **52**(8), 1722-1729 (2010)

[3] L.S. Kokhanchik, T. R. Volk, *Appl. Phys. B*, **110**, 367 - 373 (2013)

Towards Devices Based on Charged Domain Walls in Ferroelectrics

T. Sluka^{1,2}, P. Bednyakov¹, A. Crassous¹, L. Feigl¹, C. Sandu¹, A. Tagantsev¹, N. Setter¹

1- Ceramics Laboratory, EPFL Swiss Federal Institute of Technology, Lausanne, CH-1015 Switzerland

2- DPMC-MaNEP, University of Geneva, 24 Quai Ernest-Ansermet, 1211 Geneva 4, Switzerland

tomas.sluka@epfl.ch

Domain walls in ferroics display uniquely distorted electronic structures and ionic displacements due to the local transition of a ferroic order parameter. Their intrinsic properties may therefore be fundamentally different from those of their parent matrices. Indeed, intriguing phenomena like elevated photoactivity [1] and conductivity [2] were reported at neutral (multi-)ferroic domain walls. The conductivity however represents rather a quantitative change from the bulk properties. In contrast, qualitatively different properties were predicted [3-5] and recently experimentally verified [6] at so-called Charged Domain Walls (CDWs) in ferroelectrics. CDWs have rare head-to-head (or tail-to-tail) configuration of spontaneous polarization and form a quasi Two-Dimensional Electron Gas (q2DEG) which is a sheet of free electrons confined in a narrow 2D potential well. Artificially engineered CDWs in a prototypical ferroelectric BaTiO₃ displayed steady metallic-like conductivity up to 10⁹ times that of the insulating bulk [6].

q2DEG is in current industrial applications created only at fixed heterointerfaces between two distinct materials. Its high electron mobility is exploited in transistors and rectifiers for ultra high frequency operation such as in cell phones, radars, microwave and millimeter wave receivers. Properties of q2DEG in these heterostructures are however strongly sensitive to the interface quality which makes its production technologically challenging.

Unlike heterointerfaces, CDWs are compositionally homogeneous and therefore naturally “perfect” boundaries between domains with differently oriented spontaneous polarization. q2DEG at CDWs has therefore a potential to approach the upper theoretical limits of electron mobility and can be created, displaced and erased repetitively inside a functioning devices which represents an additional degree of freedom to q2DEG properties.

We will introduce current theory, engineering, control and characteristics of CDWs in crystals and thin films and properties of their junctions with electrodes. These studies head towards assembly of a transistor-like structure (Fig. 1) that may have unique characteristics due to the gate control of the local “doping” by polarization charges of CDWs in a wide-bandgap semiconductor.

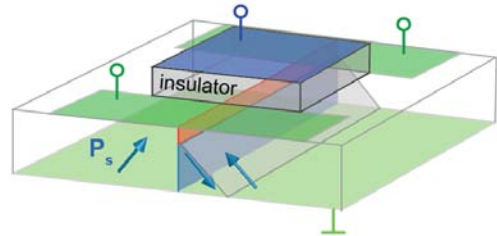


Figure 1 Illustration of a field effect transistor-like structure with a charged domain wall in a ferroelectric crystal or a thin film. The green electrodes on the top of a ferroelectric layer represent source and drain, the blue electrode is a gate separated by a dielectric layer, the red plane is a charged domain wall intersecting two neutral domain walls and arrows represent the spontaneous polarization P_s .

[1] S. Y. Yang et al., Above-bandgap voltages from ferroelectric photovoltaic devices, *Nat. Nanotechnol.*, 5:143, (2010).

[2] J. Seidel et al., Conduction at domain walls in oxide multiferroics, *Nat. Mater.*, 8:229 (2009).

[3] B. M. Vul, G.M. Guro and I. I. Ivanchik, Encountering domains in ferroelectrics, *Ferroelectrics*, 6:29, (1973).

[4] M. Y. Gureev, A. K. Tagantsev and N. Setter, Head-to-head and tail-to-tail 180 degrees domain walls in an isolated ferroelectric, *Physical Review B*, 83, (2011).

[5] T. Sluka, A. K. Tagantsev, D. Damjanovic, M. Gureev and N. Setter, Enhanced electromechanical response of ferroelectrics due to charged domain walls, *Nat. Commun.*, 3:748, (2012).

[6] T. Sluka, A. K. Tagantsev, P. Bednyakov and N. Setter, Free-electron gas at charged domain walls in insulating BaTiO₃. *Nat. Commun.*, 4, (2013).

Investigation of Domain Kinetics in MgO Doped Stoichiometric Lithium Tantalate

V. Shur, A. Akhmatkhanov, M. Chuvakova, I. Baturin

Ferroelectrics Laboratory, Institute of Natural Sciences, Ural Federal University, 51 Lenin Ave., 620000 Ekaterinburg, Russia

Andrey.Akhmatkhanov@urfu.ru

The polarization reversal process and the bulk screening of the depolarization field were studied in 1 mol.% MgO doped stoichiometric lithium tantalate single crystal (MgOSLT), which is very promising nonlinear optical material for high power second harmonic generation. The creation of stable precise periodical domain structure for nonlinear application requires deep knowledge of the domain evolution.

The 1-mm-thick Z-cut optical grade polished samples of MgOSLT (Oxide Corp., Japan) have been studied. The used experimental setup allowed to apply the external voltage pulses of arbitrary shape with simultaneous recording of switching current and visualization of domain kinetics using polarizing optical microscope. The uniform liquid electrodes of saturated aqueous solution of LiCl have been used.

Two shapes of external field pulses were used. (1) The rectangular pulses allowed to analyze the polarization reversal in constant field and important for classical periodical poling technique by single poling pulse. (2) The triangular pulses allowed to measure the dependence of the coercive field on the external field ramping rate. The extracted parameters are important for multi-pulse poling technique, which are used frequently for ferroelectric crystals with high leakage currents such as MgO doped lithium niobate (MgOLN).

The domain structure evolution was visualized during application of rectangular field pulses with amplitude ranged from 0.8 to 2 kV/mm. It was shown that the main mechanism of domain kinetics in MgOSLT with liquid electrodes represents the motion of small number of Y-oriented plane domain walls appeared at the electrode edge or at the macroscopic surface defects. The arising of isolated domains occurs under the whole electrode in the applied field range. The observed continuous domain wall motion caused by wall merging with isolated domains leads to the smooth switching current shape. The activation-type field dependence of the switching time had been observed with activation field equal to (3.2 ± 0.1) kV/mm.

The polarization reversal by application of the triangular field pulses (linear increasing field) allowed to measure the dependence of the coercive field on the external field ramp rate (E_{ex}/dt). The coercive field in MgOSLT is twice lower than in 7 mol.% MgO doped congruent lithium tantalate for the same external field ramp rate [1]. However these values are still 7 times larger than that for stoichiometric lithium tantalate crystals prepared by vapor transport equilibration (VTE-SLT) [2,3]. The value of exponent 0.18 is approximately equal to that of VTE-SLT in high-field range [2]. The lowest coercive field in MgOSLT (about 150 V/mm) was estimated for quasi-static limit (for dE_{ex}/dt approaching to zero).

The bulk screening process in MgOSLT was studied by measurement of the backswitching characteristics with variable delay time and the temporal resolution about 20 ms [4]. The bulk screening process with characteristic time about 1.7 s has been revealed.

The equipment of the Ural Center for Shared Use “Modern Nanotechnology”, Institute of Natural Sciences, Ural Federal University has been used. The research was made possible in part by RFBR and the Government of Sverdlovsk region (Grant 13-02-96041-r-Ural-a), by RFBR (Grants 13-02-01391-a, 14-02-01160-a) and with the financial support of young scientists in terms of Ural Federal University development program.

[1] H. Ishizuki and T. Taira, Study on the field-poling dynamics in Mg-doped LiNbO₃ and LiTaO₃, *Nonlinear Opt. Mater. Fundam. Appl.* (OSA, Washington, D.C., 2007), p. WE35.

[2] V.Ya. Shur, A.R. Akhmatkhanov, I.S. Baturin, and E.V. Shishkina, Polarization reversal and jump-like domain wall motion in stoichiometric LiTaO₃ produced by vapor transport equilibration, *J. Appl. Phys.*, 111, 014101-1-8 (2012).

[3] D.S. Hum, R.K. Route, G.D. Miller, V. Kondilenko, A. Alexandrovski, J. Huang, K. Urbanek, R.L. Byer, and M.M. Fejer, Optical properties and ferroelectric engineering of vapor-transport-equilibrated, near-stoichiometric lithium tantalate for frequency conversion, *J. Appl. Phys.*, 101, 93108- (2007).

[4] V.Y. Shur, A.R. Akhmatkhanov, I.S. Baturin, M.S. Nebogatikov, and M.A. Dolbilov, Complex study of bulk screening processes in single crystals of lithium niobate and lithium tantalate family, *Phys. Solid State*, 52, 2147- (2010).

Optical properties near neutral and charged ferroelectric domain walls

P. Mokrý and K. Steiger

Regional Centre for Special Optics and Optoelectronic Systems (TOPTeC), Institute of Plasma Physics, Academy of Sciences of the Czech Republic, Sobotická 1660, CZ-51101 Turnov, Czech Republic

pavel.mokry@tul.cz

It is known that the existence of domain walls in ferroelectric samples tremendously affects their macroscopic properties, including dielectric, electromechanical, elastic, optical, etc. [1] Nowadays, this effect is employed in a controlled manner and methods for the preparation of domain patterns to intentionally enhance particular physical properties of a ferroelectric sample are developed in the research field called domain engineering. Illustrative examples of novel methods for increasing the piezoelectric response of ferroelectrics using domain engineering have been introduced in the works by Wada et al. [2]. Then, as one can expect, this breakthrough discovery initiated lively discussions in the scientific community and stimulated an intense theoretical investigation to identify the phenomenon standing behind such experimental observations. As usual, several theoretical models have been presented: domain wall broadening [3, 4], high domain wall permittivity and piezoelectricity [5], the stress-assisted enhancement of piezoelectric properties due to mechanically incompatible domain structures [6], or enhanced electromechanical response of ferroelectrics due to charged domain walls [7]. Unfortunately, all the aforementioned models suffer some weak points and the definite answer is not absolutely clear after several years from the first experimental observation. Identification of the relevant physical phenomenon, which stands behind particular observations, is often limited due to the lacking knowledge on the exact domain pattern geometry that takes place in the particular experiments with a ferroelectric sample. Without detailed experimental knowledge of the spatial 3D distribution of domain walls within the ferroelectric sample, one cannot further progress in answering fundamental questions on the effect of domain patterns to macroscopic properties of ferroelectric samples.

In this work, we present the theoretical study of optical properties near ferroelectric domain walls. We are focused on the computation of refractive index in the regions near neutral and charged domain walls. Since it is known that the refractive index depends on the configuration of the crystal lattice within a particular domain and on the internal and external electric fields, the obtained results will be used for a suggested method of 3D imaging of ferroelectric domain walls and internal electric fields using digital holographic tomography.

- [1] A. K. Tagantsev, L. E. Cross, J. Fousek, *Domains in Ferroic Crystals and Thin Films*. (Springer, 2010).
- [2] S. Wada, K. Yako, T. Muraishi, H. Kakemoto, and T. Tsurumi, Development of Lead-free Piezoelectric Materials Using Domain Wall Engineering, *ELECTRO CERAMICS IN JAPAN IX*, 320:151–154, (2006).
- [3] R. Ahluwalia, T. Lookman, A. Saxena, and W. Cao, Domain-size Dependence of Piezoelectric Properties of Ferroelectrics, *Physical Review B* 72, no. 1 (2005).
- [4] J. Hlinka, P. Ondrejčokovic, and P. Márton, The Piezoelectric Response of Nanotwinned BaTiO₃, *Nanotechnology* 20(10) 105709 (2009).
- [5] Y. Xiang, R. Zhang, and W. Cao, “Piezoelectric Properties of Domain Engineered Barium Titanate Single Crystals with Different Volume Fractions of Domain Walls.” *Journal of Applied Physics* 106(6) 064102 (2009).
- [6] T. Sluka, D. Damjanovic, A. K. Tagantsev, E. Colla, M. Mtebwa, and N. Setter, The Stress-assisted Enhancement of Piezoelectric Properties Due to Mechanically Incompatible Domain Structures in BaTiO₃, *Proc. ISAF*, 1–4, (2010).
- [7] T. Sluka, A. K. Tagantsev, D. Damjanovic, M. Gureev, and N. Setter, “Enhanced Electromechanical Response of Ferroelectrics Due to Charged Domain Walls.” *Nature Communications* 3, 748 (2012).

Charged Domain Walls in Lithium Niobate with Inhomogeneous Modification of Bulk Conductivity

V.Ya. Shur, D.O. Alikin, V.I. Pryakhina, I.S. Palitsyn, N.A. Besedina, S.A. Negashev

Ferroelectrics Laboratory, Institute of Natural Sciences, Ural Federal University, 51 Lenin Ave., 620000, Ekaterinburg, Russia

vladimir.shur@urfu.ru

The formation of the charged domain walls during polarization reversal in the single crystalline lithium niobate plate with essentially increased bulk conductivity in the vicinity of the polar surfaces have been investigated. Two alternative methods have been used for inhomogeneous modification of the bulk conductivity.

The recent interest to creation of the charged domain walls (CDW) in ferroelectrics is stimulated by possibility to enhance the piezoelectric properties, to develop the emerging oxide electronics and high-density ferroelectric memory [1]. The fabrication of the tailored stable charged domain walls with proper geometry and reproducible properties in various ferroelectric crystals important for application is a new useful tool for the domain wall engineering.

Polarization reversal has been studied in modified congruent (CLN) and magnesium doped (MgO:LN) lithium niobate single crystals by vacuum annealing and by low energy plasma ion irradiation [2,3]. It is known that the vacuum annealing of LN crystals at the temperatures above 600°C leads to sufficient increase of the bulk conductivity caused by out-diffusion of the oxygen from the sample surface. We have studied the formation of the charged domain walls in LN crystals with inhomogeneous modification of the bulk conductivity produced by two methods: (1) high temperature annealing in vacuum, (2) irradiation of the crystal polar surface by glow discharge in plasma of Ar⁺ ions.

The investigated samples represented 0.5-mm-thick plates of CLN and 1-mm-thick plates of MgO:LN cut normal to the polar axis. The vacuum annealing was realized in furnace in a temperature range from 700 to 800°C. The ion irradiation of Z⁺ polar surface was done by glow discharge in Ar⁺ plasma with energy ranged from 2 to 5 keV in vacuum 10⁻⁴Torr during 2-8 min. The maximal crystal temperature induced by ion radiation ranged from 400 to 900°C. The sample was fixed on the metal substrate by silver paste to remove charge and to block out-diffusion at the opposite polar surface.

The spatial distribution of the bulk conductivity has been extracted from the surface conductivity values measured by two-probe method using repeated removal of the surface layer with thickness from 10 to 100 μm by precise polishing. The electric field distribution in the bulk had been measured by optical interferometry [4]. Application of the electric field in polar direction leads to inhomogeneous change of the interference pattern due to linear electro-optical effect. The local line shift is proportional to the local value of the electric field. The analysis of the recorded interference patterns allowed to extract the electrical field distribution.

The triangular or rectangular electric field pulses were applied by liquid electrodes. The optical microscopy was used for *in situ* observation of the domain kinetics. The charged domain walls have been visualized by optical microscopy on YZ cross-sections after selective chemical etching and by analysis of the set of domain images at different depth obtained by Raman confocal microscopy.

The formation of the charged domain walls by appearance and isotropic expansion had been revealed. The main stages of the domain evolution in the crystal bulk have been separated and studied. It was shown that the geometrical parameters (position, averaged period and aperture) of the stable charged domain walls are determined by the field distribution in the bulk. The studied formation of the charged domain walls in crystals with inhomogeneous modification of the bulk conductivity can be considered as a new area of the domain engineering in ferroelectrics.

The equipment of the Ural Center of Share Use “Modern Nanotechnology”, Institute of Natural Sciences, Ural Federal University has been used. The research was made possible in part by RFBR (Grants 13-02-01391-a, 11-02-91066-CNRS-a, 12-02-31377-mol-a), by RFBR and the Government of Sverdlovsk region (Grant 13-02-96041-r-Ural-a), by Ministry of Education and Science (Contracts 14.513.12.0006 and 16.740.11.0585).

[1] J. Seidel, L.W. Martin, Q. He, Q. Zhan, Y.-H. Chu, A. Rother, M.E. Hawkrige, P.Yu. Maksymovych, M. Gajek, N. Balke, S.V. Kalinin, S. Gemming, F. Wang, G. Catalan, J.F. Scott, N.A. Spaldin, J. Orenstein and R. Ramesh, Conduction at domain walls in oxide multiferroics, *Nature Materials*, vol. 8, pp. 229-234, (2009).

[2] V.Ya. Shur, D.O. Alikin, A.V. Ievlev, M.A. Dolbilov, M.F. Sarmanova and N.V. Gavrilov, Formation of nanodomain structures during polarization reversal in congruent lithium niobate implanted with Ar ions, *Transactions on Ultrasonics, Ferroelectrics, and Frequency Control (TUUFFC)*, vol. 30, pp. 1934-1941, (2012).

[3] V.I. Pryakhina, V.Ya. Shur, D.O. Alikin and S.A. Negashev, Polarization reversal in MgO:LiNbO₃ single crystals modified by plasma-source ion irradiation, *Ferroelectrics*, vol. 439, pp. 20-32, (2012).

[4] V.Ya. Shur, A.L. Gruverman, N.V. Korovina, M.Z. Orlova and L.V. Sherstobitova, Spatial distribution of the internal field in lead germanate having different types of domain structure, *Sov. Phys. Solid State*, vol. 30, pp. 299-302, (1988).

Ferroelectric properties and the Bulk Photovoltaic Effect at the Nanoscale

Vladimir Fridkin

Shubnikov Institute of Crystallography of the Academy of Sciences, Russia

Email: fridkin@ns.crys.ras.ru

Ferroelectric films at the nanoscale (1- 10nm) show very peculiar properties, including switching kinetics and coercive field scaling. These properties could be successfully explained by the Ginzburg-Landau phenomenology for the homogeneous (without domains) medium.

One of the most remarkable properties of the ferroelectrics at the nanoscale (10-100nm) is high efficiency of the bulk photovoltaic effect.

The experimental results are obtained for polymeric and perovskite ferroelectric films at the nanoscale.

References:

1. Vladimir Fridkin and Stephen Ducharme. *Ferroelectricity at the Nanoscale* (Springer, Berlin-Heidelberg, 2014)
2. Boris Sturman and Vladimir Fridkin. *The Photovoltaic and Photorefractive Effects in Noncentrosymmetric Materials* (Gordon and Breach Science Publishers, Philadelphia, 1992)

Fine tuning of the ferroelectric domain structure in La-doped BiFeO₃ towards domain wall based electronics

A. Crassous¹, C. Sandu¹, N. Setter¹

1- Ceramics Laboratory, Ecole Polytechnique Fédérale de Lausanne, CH1015-Lausanne, Switzerland

arnaud.crassous@epfl.ch

BiFeO₃ (BFO) is a multiferroic material extensively studied in the last years because of its high ferroelectric polarization and its G-type antiferromagnetism forming a spin cycloid. At room temperature, its rhombohedral symmetry allows the formation of 71°, 109° and 180° domain walls between two adjacent ferroelectric domains. Interestingly, it was shown for La-doped BFO films thicker than ~100nm that, grown on a low mismatch scandate substrate such as DyScO₃ (DSO), the domains could arrange into a 1 dimensional stripe array [1]. The type of domain walls between two stripes, 71° or 109°, was selected through electrostatic conditions by changing the thickness of the underlying electrode of SrRuO₃ (SRO).

Here, we show using piezoresponse force microscopy (PFM) that La-doped BFO films thinner than 100nm grown on DSO substrates exhibit a complex domain structure before forming the stripe array. By carefully selecting the thickness of the film and of the SRO electrode, it is possible to finely control the type of domain walls but also tune their density (Figure 1).

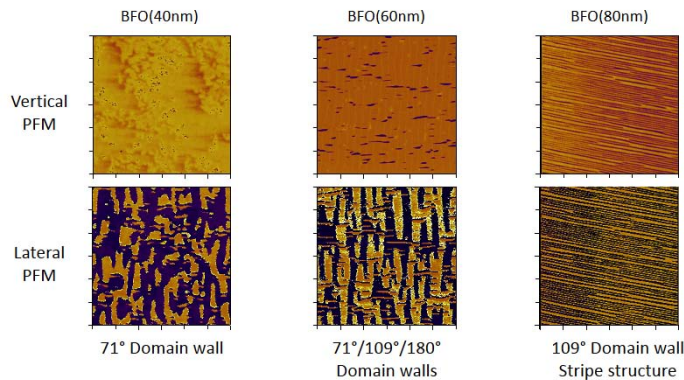


Figure 1: 3x3µm vertical (top line) and lateral (bottom line) PFM images of La-doped BFO.

Clear evolution can be seen from 71° domain walls to purely 109° domain walls with a strip structure (from left to right) with increasing BFO thickness. The intermediate thickness display a complex ferroelectric pattern that can be useful for the creation of charged domain walls.

Analysis of the PFM images combined with transmission electron microscope (TEM) revealed the possibility to control the ferroelectric domains in order to obtain wedge structures where ferroelectric vortices [2] are more likely to be created.

Fine tuning of the domain structure is a prerequisite to the promising electronics based on ferroelectric domain walls.

[1] Y-H. Chu, Q. He, C-H. Yang, P. Yu, L. W. Martin, P. Shafer, R. Ramesh, Nanoscale control of domain architectures in BiFeO₃ thin films, *Nano Letters*, 9, 1726-1729, (2009).

[2] Y. Qi, Z. Chen, C. Huang, L. Wang, X. Han, J. Wang, P. Yang, T. Sriharan, L. Chen, Coexistence of ferroelectric vortex domains and charged domain walls in epitaxial BiFeO₃ film on (110)_o GdScO₃ substrate, *J. Appl. Phys.*, 111, 104117, (2012).

Controlling ferroelectric domain wall motion

L. J. McGilly, L. Feigl, N. Setter

Ceramics Laboratory, Swiss Federal Institute of Technology (EPFL), CH-1015 Lausanne, Switzerland

leo.mcgilley@epfl.ch

Ferroelectric domain wall motion in thin films of tetragonal $\text{PbZr}_{0.1}\text{Ti}_{0.9}\text{O}_3$ has been investigated through use of patterned Pt top electrodes and piezoresponse force microscopy (PFM). The electron-beam deposited top electrodes can be fabricated with almost any desired 2D geometry (see Fig. 1a). Domain nucleation underneath the top electrode can be controlled through the position of the PFM tip (Fig. 1c) while still maintaining the ability to apply fields over a much larger area than what is typically possible with the probe tip alone. In practice this method offers the unique advantage of predetermined nucleation sites combined with a near-homogeneous applied electric field. Ways in which 180° domain wall motion can be studied and manipulated through engineering of the electrode geometry will be discussed and shown. It is hoped that this work shows the unprecedented control over individual 180° domain walls that is possible within this experimental framework.

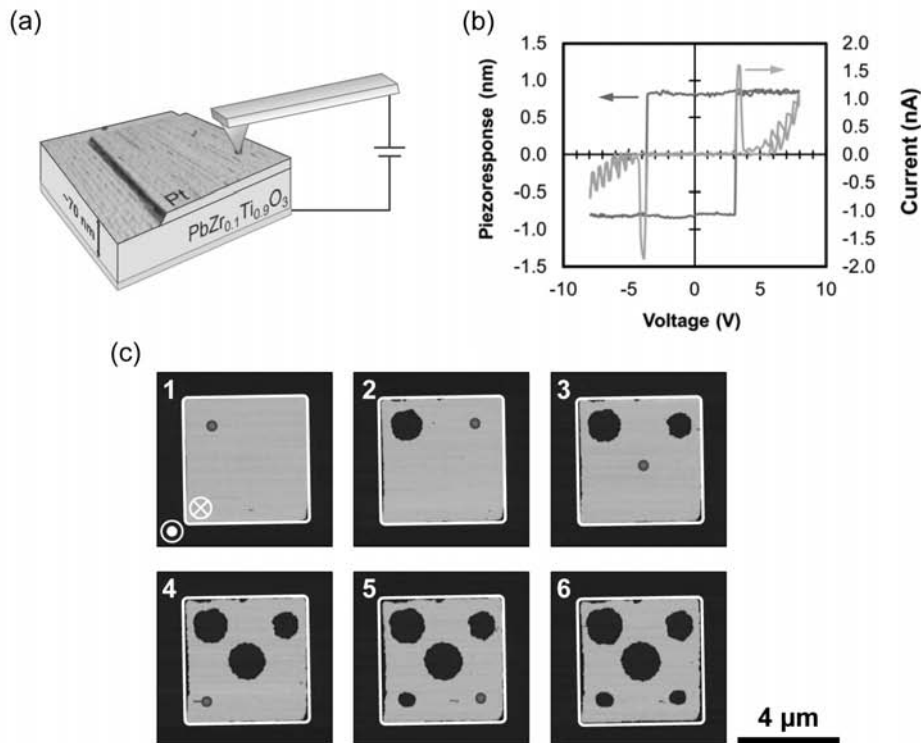


Figure 1 A schematic diagram of the experimental setup can be seen in (a). The 3D topography image shows the $8 \pm 1 \text{ nm}$ thick Pt electrode (orange) deposited on the PZT thin film (blue). The hysteresis profile and the current during switching by PFM can be seen in (b). This gives information on the coercive bias and demonstrates the sharp nature of the ferroelectric switching. In (c) PFM images show that the electroded area, as given by the white outline, is switched from the initial polarization state *i.e.* out-of-plane (OOP) upwards (purple), via the application of a suitable voltage pulse, to OOP downwards (yellow) as can be seen in image (1). In images (2)-(6) the tip is placed at the position given by the small red dot and a suitable voltage pulse applied to nucleate domains only underneath the tip as seen in each sequential image.

Orientation Effects in the Formation of Hydrostatic Piezoelectric and Energy-harvesting Parameters of Novel Composites Based on Relaxor-ferroelectric Single Crystals

V. Yu. Topolov^{1,2}, C. R. Bowen³, P. Biseegna⁴, A. V. Krivoruchko⁵, and A. A. Panich²

1- Department of Physics, Southern Federal University, 5 Zorge Street, 344090 Rostov-on-Don, Russia

2- Scientific Design & Technology Institute "Piezopribor", Southern Federal University, 10 Milchakov Street, 344090 Rostov-on-Don, Russia

3- Department of Mechanical Engineering, University of Bath, BA2 7AY Bath, United Kingdom

4- Department of Civil Engineering and Computer Science, University of Rome "Tor Vergata", 00133 Rome, Italy

5- Don State Technical University, Gagarin Place, 344000 Rostov-on-Don, Russia

vutopolov@sfned.ru

Composites based on highly piezoelectric single crystals (SCs) of relaxor-ferroelectric solid solutions of $(1-x)\text{Pb}(\text{Mg}_{1/3}\text{Nb}_{2/3})\text{O}_3-x\text{PbTiO}_3$, $(1-x)\text{Pb}(\text{Zn}_{1/3}\text{Nb}_{2/3})\text{O}_3-x\text{PbTiO}_3$ and $x\text{Pb}(\text{In}_{1/2}\text{Nb}_{1/2})\text{O}_3-y\text{Pb}(\text{Mg}_{1/3}\text{Nb}_{2/3})\text{O}_3-(1-x-y)\text{PbTiO}_3$ are important for modern piezo-technical, energy-harvesting, hydroacoustic, and other applications [1]. These SCs can be split into non-180° domains (mechanical twins) in different ways, be poled in various crystallographic directions and exhibit high piezoelectric activity that strongly depends of the domain orientations and contents. The aim of the present study is to consider a series of effective parameters concerned with the piezoelectric effect in the 2–2 and 1–3 SC / polymer composites (Figure 1) and to take into account

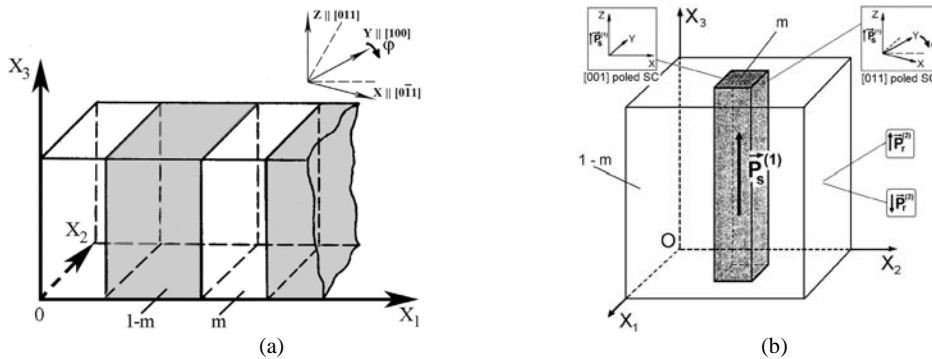


Figure 1 Schematics of the parallel-connected 2–2 SC / polymer composite (a) and the 1–3 SC / polymer composite (b) wherein the polarisation orientation effects [2] are studied. m is the volume fraction of SC, and X , Y and Z are its main crystallographic axes.

(i) the specifics of the domain structure, the orientation of the main crystallographic axes in the SC component and (ii) the characteristics of the polymer component, e.g. the orientation of the remanent polarisation vector and the Poisson's ratio.

Of interest for hydroacoustic applications are the following hydrostatic parameters [1, 2] of the 2–2 and 1–3 composites: piezoelectric coefficients $d_h^* = d_{33}^* + d_{32}^* + d_{31}^*$ and $g_h^* = g_{33}^* + g_{32}^* + g_{31}^*$, squared figure of merit (SFOM) $(Q_h^*)^2 = d_h^* g_h^*$ and electromechanical coupling factor k_h^* . Some energy-harvesting applications depend on large values of SFOM $(Q_{33}^*)^2 = d_{33}^* g_{33}^*$, the anisotropy of SFOMs $(Q_{33}^*)^2 / (Q_{3j}^*)^2$ and electromechanical coupling factors k_{33}^* / k_{3j}^* , where $j = 1$ and 2 .

Interrelations between the electromechanical properties of the SC component and the aforementioned parameters of the composite are revealed at the rotation of the main crystallographic axes. This orientation effect enables us to improve the hydrostatic and anisotropy parameters of the composites that comprise the SC component poled along a specific crystallographic direction and the auxetic polymer component [2]. Results of the study are compared to the hydrostatic performance of some conventional ceramic / polymer composites [1].

[1] V. Yu. Topolov and C. R. Bowen, *Electromechanical Properties in Composites Based on Ferroelectrics* (London: Springer, 2009).

[2] V. Yu. Topolov, P. Biseegna and C. R. Bowen, *Piezo-active Composites. Orientation Effects and Anisotropy Factors* (Berlin, Heidelberg: Springer, 2014).

Controlling domain dynamics in topographically engineered ferroelectric capacitors

J.R. Whyte¹, R.G.P. McQuaid¹, C.M. Ashcroft^{1,2}, J.F. Einsle¹, C. Canalias³, A. Gruverman⁴, J.M. Gregg¹

1- School of Mathematics and Physics, Queen's University Belfast, Belfast, U.K.

2- Department of Physics, Cavendish Laboratory, J. J. Thomson Avenue, Cambridge, CB3 0HE, U.K.

3- Department of Applied Physics, Royal Institute of Technology, Roslagstullsbacken 21, 10691, Stockholm, Sweden

4- Department of Physics and Astronomy, University of Nebraska Lincoln, Nebraska 68588-0299, USA

Main author email address: jwhyte05@qub.ac.uk

Exerting control over the spatial distribution of domains and domain walls is crucial for future nanoelectronic device applications. The prospect of utilising the conductive properties of domain walls displayed in specific oxide ferroelectrics has inspired new electronic devices such as a domain wall transistor and memristor. These devices rely upon the domain walls acting as conducting channels between electrodes, thus complete control over the domain wall nucleation and position is required.

Here we demonstrate, through FIB milled topographic features into the capacitor geometry, control of the domain wall nucleation and position realised through either engineered heterogeneity in the electric field or tailored geometric pinning centres. We further refine the electric field heterogeneity approach described in ref [1] to allow sequential domain wall injection as a function of voltage, by appropriate shaping of the low-permittivity holes in the capacitor or the local electrode geometry.

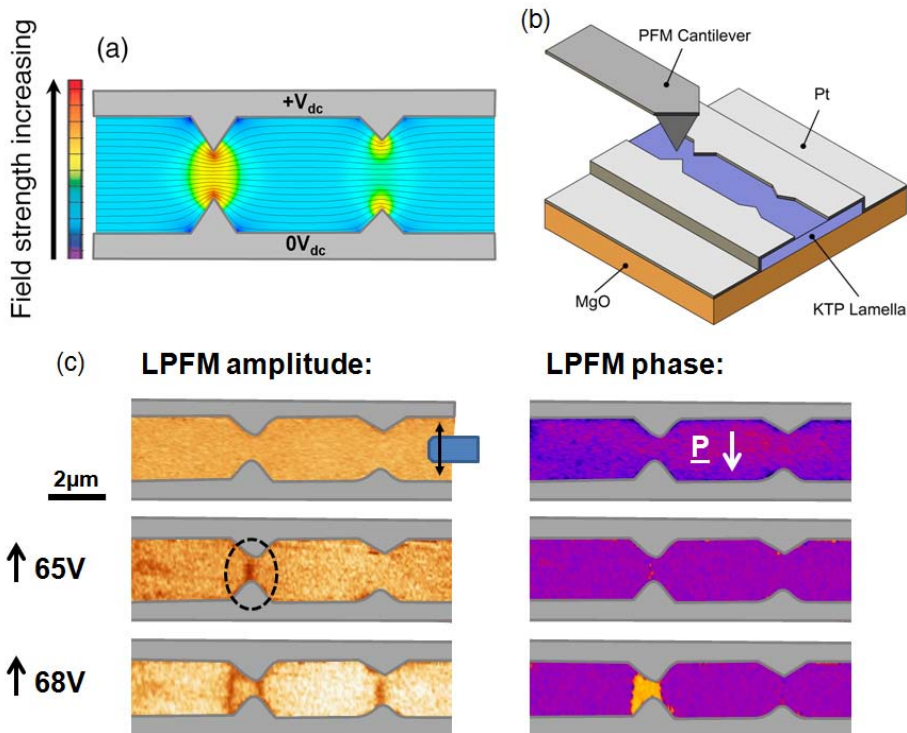


Figure 1(a) An electric field model for a KTP capacitor with notched electrodes where the left set of asperities are sharper than the right and the local electrode gap between opposing apices is closer. (b) A schematic of the experimental setup for PFM investigations. (c) The lateral-PFM amplitude and phase images showing the initial mono-domain state, one pair of injected domain walls after application of a 65V 100 μ s pulse then, after being reset back to a mono-domain state, two pairs of injected domain walls after a 68V 100 μ s pulse.

[1] J. R. Whyte, R. G. P. McQuaid, P. Sharma, C. Canalias, J. F. Scott, A. Gruverman, and J. M. Gregg, Ferroelectric Domain Wall Injection, *Advanced Materials*, 26: 293–298, (2014).

Oxygen ion and mixed conductivity in the Pr₂O₃-ZrO₂ system

A.V. Shlyakhtina¹, J.C.C. Abrantes^{2,3}, D.A. Belov^{1,4}, G.A. Gasyмова¹, L.G. Shcherbakova¹

¹*Semenov Institute of Chemical Physics, Russian Academy of Sciences, Moscow, 119991, Russia;*

²*UIDM, ESTG, Instituto Politécnico de Viana do Castelo, Apartado 574, 4901-908 Viana do Castelo, Portugal;*

³*Ceramics Dep., (CICECO), University of Aveiro, 3810 Aveiro, Portugal*

⁴*Faculty of Chemistry, Moscow State University, Moscow, 119991, Russia*

E-mail addresses: annash@chph.ras.ru; annashl@inbox.ru

In the Pr₂O₃-ZrO₂ (PrZrO) system we have studied the structure and transport properties of solid solutions with 18, 26.6, 30, 33.3, 35.5, 54, 60 Mol.% Pr₂O₃ synthesized through co-precipitation and high temperature annealing at 1550°C, 4 hrs. The X-ray data show the region of the homogeneous single phase pyrochlore-like solid solutions for compositions with 30% - 35.5 Mol.% Pr₂O₃. Maximum conductivity between pyrochlore-like solid solutions was observed in the oxygen interstitials conducting (Pr_{2-x}Zr_x)Zr₂O_{7+x/2} (x=0.15) and is 8.84×10^{-3} S/cm at 800°C (E_a=0.66 eV). Total conductivity maximum in the PrZrO system ~ 0.237 S/cm at 800°C (E_a=0.42 eV) was observed for single phase fluorite-like solid solution with 60% Pr₂O₃, but its conductivity has mixed oxygen ion - electronic type.

Conduction in nanodomain inversion dots in congruent lithium tantalate single crystal

Y. Cho¹

1- Research Institute of Electrical Communication, Tohoku University, Katahira, Aoba-ku, Sendai 980-8577, Japan

yasuocho@riec.tohoku.ac.jp

Conduction at domain walls has attracted much interest recently among researchers in the field of ferroelectric materials due to the possibility of applications to future nanosized electronic devices[1][2][3][4][5]. Although these studies were aimed at potential nanoelectronics applications, excluding one exception [5], the measured domains had micrometer dimensions and the widths of the domain walls and current pathways were also larger than 50 nm.

In this paper, the electrical current flow behavior was investigated for nanodomains formed in a thin congruent lithium tantalate (LiTaO₃) single-crystal plate. When the nanodomains were relatively large, with diameters of about 100 nm, current flow was detected along the domain wall as shown in Figure 1. However, when they were about 40 nm or smaller, the current flowed through the entire nanodomain as shown in Figure 2. We also investigated relationship between topographical changes (dents) on the nanodomain and the shapes of the current pathways. Schottky-like rectifying behavior was observed. Unlike the case of LiNbO₃[4], optical illumination was not required for current conduction in LiTaO₃. A clear temperature dependence of the current was found, indicating that the conduction mechanism for nanodomains in LiTaO₃ may involve thermally activated carrier hopping.

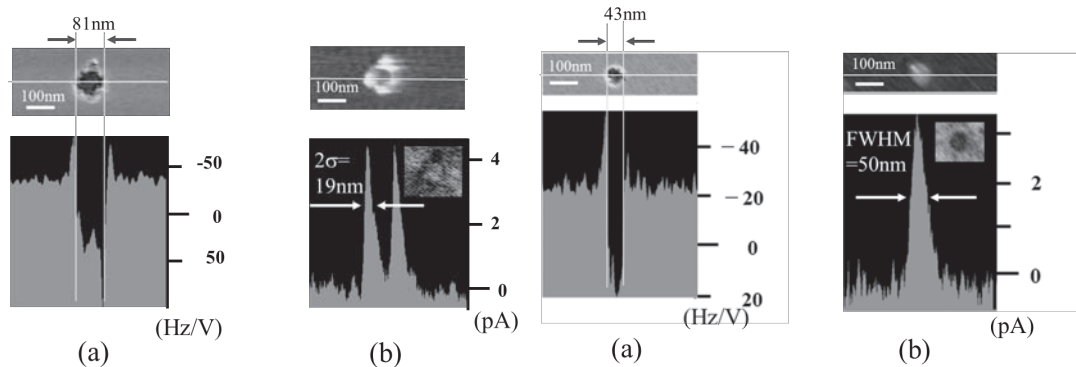


Figure 1 (a) SNDM image (upper panel) and one-dimensional profile of SNDM signal (lower panel) for large (ca. 100 nm) inverted nanodomain with positive polarization on negatively polarized surface of LiTaO₃ thin film. (b) c-AFM current image (upper panel) and one-dimensional current profile (lower panel) for same nanodomain. The inset shows a topography measured on the nanodomain. Very shallow dent with the depth of about 0.2nm was observed along the domain wall (or along current pathway).

Figure 2 (a) SNDM image (upper panel) and one-dimensional profile of SNDM signal (lower panel) for smaller (ca. 40 nm) inverted nanodomain with positive polarization on negatively polarized surface of LiTaO₃ thin film. (b) c-AFM current image (upper panel) and one-dimensional current profile (lower panel) for same nanodomain. The inset shows a topography measured on the nanodomain. Very shallow dent with the depth of about 0.1nm was observed on the entire nanodomain dot (or on the entire current pathway) differently from the result for the larger nanodomain shown in Figure 1.

- [1] J. Seidel, L. W. Martin, Q. He, Q. Zhan, Y.-H. Chu, A. Rother, M. E. Hawkrige, P. Maksymovych, P. Yu, M. Gajek, N. Balke, S. V. Kalinin, S. Gemming, F. Wang, G. Catalan, J. F. Scott, N. A. Spaldin, J. Orenstein, and R. Ramesh, "Conduction at domain walls in oxide multiferroics," *Nat. Mater.*, Vol.8, pp.229-234, (2009).
- [2] S. Farokhipoor and B. Noheda, "Conduction through 71° Domain Walls in BiFeO₃ Thin Films," *Phys. Rev. Lett.*, Vol. 107, pp.127601-1-4, (2011).
- [3] J. Guyonnet, I. Gaponenko, S. Gariglio, and P. Paruch, "Conduction at Domain Walls in Insulating Pb(Zr_{0.2}Ti_{0.8})O₃ Thin Films," *Adv. Mater.*, Vol.23, pp.5377-5382, (2011).
- [4] M. Schröder, A. Haubmann, A. Thiessen, E. Soergel, T. Woike, and L. M. Eng, "Conducting Domain Walls in Lithium Niobate Single Crystals," *Adv. Funct. Mater.*, Vol.22, pp.3936-3944, (2012).
- [5] P. Maksymovych, A. N. Morozovska, P. Yu, E. A. Eliseev, Y.-H. Chu, R. Ramesh, A. P. Baddorf, and S. V. Kalinin, "Tunable Metallic Conductance in Ferroelectric Nanodomains," *Nano Lett.*, Vol.12, pp.209-213, (2012).

Preparation and characterization of solid electrolytes based on TiP_2O_7 pyrophosphate

V. Venckutė^{1*}, V. Kazlauskienė², J. Miškinis², A. Dindune³, Z. Kanepė³, J. Ronis³, A. Maneikis⁴, M. Lelis⁵, V. Jasulaitienė⁶, P. Dobrovolskis¹, T. Šalkus¹, A. Kežionis¹, A.F. Orliukas¹

¹Faculty of Physics, Vilnius University, Saulėtekio av. 9/3, LT-10222 Vilnius, Lithuania

²Institute of Applied Research, Vilnius University, Saulėtekio av. 9/3, LT-10222 Vilnius, Lithuania

³Institute of Inorganic Chemistry, Riga Technical University, Miera iela 34, LV-2169 Salaspils, Latvia

⁴Semiconductor Physics Institute of Center for Physical Sciences and Technology, A. Goštauto 11, LT-01108 Vilnius, Lithuania

⁵Centre for Hydrogen Energy Technologies, Lithuanian Energy Institute, Breslaujos st. 3, LT-44403 Kaunas, Lithuania

⁶Institute of Chemistry of Center for Physical Sciences and Technology, A. Goštauto 9, LT-01108 Vilnius, Lithuania

vilma.venckute@ff.vu.lt

The lattice of TiP_2O_7 compound has a cubic superstructure ($3 \times 3 \times 3$) (space group $\text{Pa}\bar{3}$, the lattice parameter is $a = 23.5340(5) \text{ \AA}$) with $Z = 108$ formula units in the supercell [1]. It belongs to metal pyrophosphates $\text{M}^{4+}\text{P}_2\text{O}_7$ family [2]. The pyrophosphates based on TiP_2O_7 are suitable electrode materials for applications in lithium secondary batteries [3]. The theoretical reversible capacity of TiP_2O_7 reaches 121 mAh/g [5] and redox potential vs. Li^+/Li found to be $E = 2.62 \text{ V}$ [4]. At room temperature TiP_2O_7 superstructure consist of distorted TiO_6 octahedra and PO_4 tetrahedra sharing corners in a three-dimensional network [1]. In cells with such superstructures Li can be inserted down to 2.2 V vs Li^+/Li corresponding to the reduction of Ti^{4+} to Ti^{3+} [4]. According to [1, 2] TiP_2O_7 compound is proton conductor. At temperature $T = 770 \text{ K}$ in H_2O – containing atmosphere the value of electrical conductivity of TiP_2O_7 was found to be $\sigma \approx 1.6 \cdot 10^{-4} \text{ S/m}$ and increase with temperature in the range from 773 K to 947 K with activation energy $\Delta E = 0.7 \text{ eV}$, but in the range from 965 K to 1273 K the activation energy acquires the value 0.47 eV [2]. Authors [2] concluded that σ and ΔE anomalies can be caused by phase transition.

In the present work the powders of TiP_2O_7 and $\text{Li}_{0.24}\text{Ti}_{0.94}\text{P}_2\text{O}_7$ have been synthesized by solid state reaction. The powders were uniaxially pressed into pellets. TiP_2O_7 pellets were sintered at 1460 K temperature for 3 hours and ceramics of $\text{Li}_{0.24}\text{Ti}_{0.94}\text{P}_2\text{O}_7$ were sintered for 1 hour in air. The structure was studied by X-ray diffraction (XRD) of the powder and the results show that in the investigated temperature range 300 K to 1150 K they include phase transition. SEM/EDX and X-ray photoelectron spectroscopy (XPS) of the surface of the ceramics were investigated at room temperature. The results of the investigation of electrical properties of the ceramics in the frequency range ($10 - 3 \cdot 10^9$) Hz in the temperature range (300-780) K by impedance spectroscopy are presented in the paper.

Acknowledgement

This work was supported by Research Council of Lithuania Projects No TAP LLT 03/2012

[1]. S.T. Norberg, G. Svensson, J. Albertsson, A TiP_2O_7 superstructure, Acta Crystallogr C, 57, pp. 225-227, (2001).

[2]. V. Nalini, R. Haugsrud, T. Norby, High – temperature proton conductivity and defect structure of TiP_2O_7 , Solid State Ionics, 181, pp. 510-516, (2010).

[3]. Z. Shi, Q. Wang, W. Ye, Y. Li, Y. Yang, Synthesis and characterisation of mesoporous titanium pyrophosphate as lithium intercalation electrode materials, Micropor. Mesopor. Mat., 88, pp. 232-237, (2006).

[4]. S. Patoux, C. Masquelier, Lithium insertion into titanium phosphates, silicates, and sulfates, Chem. Mater., 14, pp. 5057-5068, (2002).

Dielectric, XRD and ultrasonic investigations of $\text{Cu}_{0.15}\text{Fe}_{1.7}\text{PS}_3$ mixed crystal

A. Dziaugys¹, J. Macutkevici¹, S. Svirskas¹, R. Juskenas², J. Banys¹, A.F. Orliukas¹, and Yu. Vysochanskii³

¹Faculty of Physics, Vilnius University, Saulėtekio al. 9/3, LT-10222 Vilnius, Lithuania

²Center for Physical Sciences and Technology, A. Gostauto 9, LT-01108 Vilnius, Lithuania

³Institute of Solid State Physics and Chemistry of Uzhgorod University, Ukraine

andrius.dziaugys@ff.vu.lt

Various ferroic phases were recently shown to occur in the layered compounds AMP_2S_6 (A= Cu, Ag; M= Cr, In;) at low temperatures [1-3]. These compounds consist of lamellae defined by a sulphur framework in which the metal cations and P - P pairs fill the octahedral voids; within a layer, the metal cations and P-P form triangular patterns [2]. In the low temperature phase metal cations sublattice exhibit some kind of ordering. Depending of the type of the ordering, phase transition can be ferroelectric as in CuInP_2S_6 [2], antiferroelectric and antiferromagnetic as in CuCrP_2S_6 [1]. In disorder (high temperature) phase metal cations exhibit high mobility and can migrate through the lattice. This is main cause of high ionic conductivity in these and similar compounds [4].

In this contribution the broadband dielectric spectra of newly synthesized $\text{Cu}_{0.15}\text{Fe}_{1.7}\text{PS}_3$ crystal are presented. No ferroelectric phase transition was detected by broadband dielectric investigations in the temperature range from 25 K to 300 K, however a possibly structural transition is placed near 125 K. The temperature dependence of the dielectric constant imaginary part reveals the presence of a loss peak at the low temperatures together with a strong dispersion at the low frequencies and at the highest investigated temperatures. While the loss peak presence is characteristic for dipolar polarization processes, the strong low frequency dispersion at not very high temperatures, observed also in the dielectric constant real part, is typical for system with hopping charge carriers. XRD investigations showed the crystal consisting of two phases: FePS_3 and $\text{Cu}_{0.5}\text{P}_{0.5}\text{S}$. The lattice parameters are as follows : $a = 5.977 \text{ \AA}$, $b = 10.304 \text{ \AA}$, $c = 6.724 \text{ \AA}$. The activation energy has been calculated from this DC conductivity and compared with pure FePS_3 , CuCrP_2S_6 and CuInP_2S_6 crystals. It was noticed, that magnetic field increases electric conductivity and dielectric permittivity, but at the same time it reduces the activation energy of the electric conductance.

[1] V. Maisonneuve, C. Payen, V. B. Cajipe. Chem. Mater. **5**, 758 (1993).

[2] V. Maisonneuve, V. B. Cajipe, A. Simon, R. Von der Muhll and J. Ravez, Phys. Rev. B **56**, 10860 (1997).

[3] J. Banys, J. Macutkevici, V. Samulionis, A. Brilingas and Yu. Vysochanskii, Phase Transitions **77**, 345 (2004).

[4] J. Macutkevici, J. Banys and Yu. Vysochanskii, phys. stat. sol. a **206**, 167 (2009).

Rare-Earth and Niobium ion substitution effects on the dielectric response of $\text{Ba}_2\text{REFeNb}_{4-x}\text{Ta}_x\text{O}_{15}$ (RE = Nd, Eu) ceramics

**D. Gabrielaitis¹, M. Kinka¹, M. Albino², M. Josse², V. Samulionis¹,
R. Grigalaitis¹, M. Maglione², J. Banys¹**

1- Faculty of Physics, Vilnius University, Vilnius, Lithuania

2- CNRS, Université de Bordeaux, ICMCB-CNRS, Bordeaux, France

Main author email address: dainius.gabrielaitis@ff.stud.vu.lt

The tungsten bronze ferroelectric family is one of the largest oxygen octahedral ferroelectric families next to the ferroelectric perovskites [1]. It attracted much attention in recent years as its unique structure makes it a better candidate in search of relaxors, ferroelectrics and multiferroics. Three types of open channels that develop within its octahedral framework constitutes an open crystalline network that makes TTB a more versatile material. Multiple substitutions of various cations are possible, thus opening up a wide range of interesting compositions [2, 3].

Dielectric measurements of three tetragonal tungsten bronze ceramic types $\text{Ba}_2\text{LnFeNb}_4\text{O}_{15}$ (Ln = Nd, Eu) and $\text{Ba}_2\text{NdFeNb}_{x-4}\text{Ta}_x\text{O}_{15}$ ($x = 0,3; 0,6; 2$) with general formula $\text{A}_1\text{A}_2\text{A}_4\text{C}_4(\text{B}_1\text{B}_2)_8\text{O}_{30}$ were performed. Experiments were carried in a frequency range from 20 Hz to 37 GHz, upon heating and cooling. Obtained temperature dependencies of complex dielectric permittivity for Nd, Eu pure and $\text{Ta}_{0,3}$ compounds exhibit anomalous behavior associated with ferroelectric phase transition. Unusual cooling-heating hysteresis, ranging over 50 K, was observed as well as a huge shifts of permittivity maxima towards lower temperatures while cooling. The shape of permittivity temperature behavior for all compounds remains very similar, this suggests same mechanisms behind observed processes. Results show that substitution of Nd by Eu in A2 cationic site shifts ferroelectric phase transition region about 100 K to higher temperatures while replacement of ferroelectrically active Nb in B1 site with Ta cations shifts transition region to lower temperatures by less than 20 K. Further increase of Ta amount in octahedral framework actively suppresses ferroelectric phase and compound exhibits classical relaxor behaviour. These three ceramics have a second „relaxor like” permittivity dispersion region at lower temperatures, which might indicate an appearance of a second phase. Furthermore, two separate, temperature dependent dielectric relaxation processes were distinguished in Nd, Eu pure and $\text{Ta}_{0,3}$ compounds. This was achieved by examining measured frequency dependences of complex permittivity. These effects, most likely, are associated with rare-earth content in A2 sites. Further investigation of these temperature dependent processes will be used to gain deeper understanding on the observed phenomena.

[1] R. Guo, H. T. Evans, A. S. Bhalla, Crystal Structure Analysis of Ferroelectric Tetragonal Tungsten Bronze $\text{Pb}_{0,596}\text{Ba}_{0,404}\text{Nb}_{2,037}\text{O}_6$, Applications of Ferroelectrics, vol 1., pp 241 - 244, (1996).

[2] A. Magneli, Ark. Kem, vol 24, pp 213, (1949).

[3] M. Pouchard, J-P. Chaminade, A. Perron, J. Ravez and P. Hagenmuller, Influence de divers types de substitutions cationiques sur les propriétés diélectriques de niobates de structure “bronzes oxygénés de tungstène quadratiques”, J. Solid State Chem. vol 14., pp 274-282, (1975).

Broadband dielectric spectroscopy of $x\text{Na}_{0.5}\text{Bi}_{0.5}\text{TiO}_3$ -(1- x) $\text{Sr}_{0.7}\text{Bi}_{0.2}\text{TiO}_3$ solid solutions

A. Olšauskaitė¹, Š. Svirskas¹, M. Ivanov¹, T. Šalkus¹, A. Kežionis¹, J. Banys¹, M. Dunce², E. Birks², M. Antonova², A. Sternberg²

1- Vilnius University, Faculty of physics, Saulėtekio av. 9, III b., LT-10222 Vilnius, Lithuania

2- Institute of Solid State Physics, University of Latvia, Kengaraga street 8, LV-1063 Riga, Latvia

Main author email address: sarunas.svirskas@ff.vu.lt

In this work we present the dielectric measurements of lead-free A-substituted $x\text{NBT}$ -(1- x) SBT . The measurements were performed in a broad frequency and temperature range from 10 mHz to 50 GHz and 30 – 800 K respectively. The samples with $x = 0.7, 0.5, 0.3, 0.1$ were measured.

Pure strontium bismuth titanate exhibits relaxor/glassy behaviour with dielectric anomaly around room temperature. The mean relaxation time follows Vogel-Fulcher law [1].

On the other hand, sodium bismuth titanate has very peculiar properties which are attributed to both normal ferroelectric and relaxor behaviour and even more solid solutions with NBT attract much attention due to its piezoelectric properties. Although there are several difficulties which prohibit this material from being used in the practical applications: (i) NBT itself has rather high conductivity which makes it difficult to pole (the poling of the sample requires rather huge coercive fields as well); (ii) it has peculiar dispersion around the room temperature [2].

The huge advantage of sodium bismuth titanate is that it can host various dopants to form solid solutions which in many cases can decrease the conductivity of NBT by few orders of magnitude. Also, these solid solutions exhibit morphotropic phase boundary (MPB) where the performance is expected to be significantly enhanced [3].

The dielectric investigation on the NBT-SBT solid solutions show that there is gradual cross-over from relaxor/glassy (SBT rich samples) state to the peculiar properties of NBT. It was observed that NBT related properties evolves gradually versus x in the system.

Dielectric spectra of the samples with various x show interesting behaviour which manifests in the occurrence of second relaxation process when the concentration of sodium bismuth titanate is increased.

[1] Š. Bagdzevičius, J. Banys, R. Grigalaitis, A. Sternberg, K. Bormanis, Dipolar Glass-Like Perovskite $\text{Sr}_{0.8}\text{Bi}_{0.2}\text{TiO}_3$ Ceramic, *Ferroelectrics*, vol. 400(1), pp. 434-440, (2010).

[2] S. Said and J. P. Mercurio, Relaxor behaviour of low lead and lead free ferroelectric ceramics of the $\text{Na}_{0.5}\text{Bi}_{0.5}\text{TiO}_3$ - PbTiO_3 and $\text{Na}_{0.5}\text{Bi}_{0.5}\text{TiO}_3$ - $\text{K}_{0.5}\text{Bi}_{0.5}\text{TiO}_3$ systems, *Journal of European Ceramic Society*, vol. 21(10-11), pp. 1333-1336, (2001).

[3] J. Roedel, W. Jo, K. T. P. Seifert, E. M. Anton, T. Granzow, D. Damjanovic, Perspective on the Development of Lead-free Piezoceramics, *Journal of American Ceramic Society*, vol. 92(6), pp. 1153-1177, (2009).

Dielectric spectroscopy of polymer based PDMS nanocomposites with ZnO nanoparticles

**J. Belovickis¹, J. Macutkevicius¹, Š. Svirskas¹, V. Samulionis¹,
J. Banys¹, O. Shenderova²**

1- Faculty of Physics, Vilnius University, Sauletekio 9/3, LT-10222 Vilnius, Lithuania

2- International Technology Center, Raleigh, NC 27715, USA

e-mail: jaroslavas.belovickis@ff.vu.lt

Adding nanoparticles to a polymer matrix can dramatically change its performance depending on the nature of nanofillers. Polydimethylsiloxane (PDMS) is one of the most used polymers in chemical and biological applications due to its optical transparency, mechanical compliance, chemical stability, bio-compatibility, and ease of fabrication [1]. PDMS is a non-conducting elastomer. However to become electrically conducting PDMS can be doped with conducting nanoparticles to broaden the range of electrical applications [2].

We investigated nanocomposite fabricated from PDMS and ZnO nanoparticles. Due to semiconducting and photoconducting properties ZnO nanomaterials have enhanced conductivity that allows to modify PDMS polymer. Although the electrical and mechanical properties of ZnO nanomaterials have been extensively investigated, the dielectric properties of polymer PDMS filled with ZnO nanoparticles have not been reported so far.

Investigation of dielectric relaxation in PDMS loaded with ZnO nanofillers of different concentration was performed in a wide frequency 20 Hz – 1 MHz and temperature 108 – 300 K range. Dielectric dispersion and the peak of dielectric losses have been observed near glass transition temperature (Figure 1a). Real and imaginary parts of dielectric permittivity depend on ZnO nanoparticle loading, similarly our former

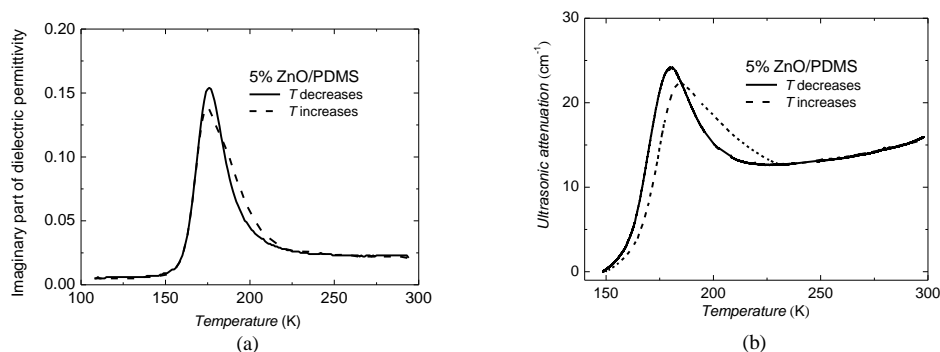


Figure 1. Experimental dependencies of imaginary part of dielectric constant (a) and ultrasonic wave attenuation (b) for 5% of ZnO in PDMS. Solid lines: on cooling, dashed lines: on heating.

investigation of PCL with MoSI nanowires [4]. It can be observed from Figure 1a that temperature dependencies of imaginary part of dielectric permittivity in heating and cooling runs does not coincide. This temperature hysteresis was showed to be dependent of ZnO nanoparticle loading. The behaviour of dielectric losses was compared with our measurements of temperature dependencies of ultrasonic attenuation (Figure 1b).

This research is funded by the European Social Fund under the Global Grant measure.

[1] K. M. Yamada, K. Olden, Fibronectins - adhesive glycoproteins of cell-surface and blood, *Nature*, vol.275, pp. 179-184, (1978).

[2] P. Du, X. Lin, X. Zhang, Dielectric constants of PDMS nanocomposites using conducting polymer nanowires, *Proceeding of the 16th International Conference on Solid-State Sensors, Actuators and Microsystems (Transducers '11)*, Beijing, China, pp. 645- 648, (2011).

[3] Y. Yang, W. Guo, X. Wang, Z. Wang, J. Qi, Y. Zhang, Size dependence of dielectric constant in a single pencil-like ZnO nanowire, *Nano Lett.*, vol.12, pp. 1919-1922, (2012).

[4] Š.Svirskas, D. Jablonskas, V. Samulionis, A. Kuprevičiūtė, J. Banys, S. Jecg Chin, T. McNally, Effect of Mo6S3I6 nanowires on the dielectric properties of poly(ϵ -caprolactone), *Phys. Status Solidi A*, vol.210, pp. 2272-2277, (2013).

The Alternative Expression of Lichtenecker's Mixing Formula and Its Application to the Broadband Dielectric Spectroscopy of BaTiO₃ – Ni_{0.5}Zn_{0.5}Fe₂O₄ Composites

A. Sakanas¹, R. Grigalaitis¹, J. Banys¹, L. Mitoseriu², V. Buscaglia³, P. Nanni⁴

1- Faculty of Physics, Vilnius University, Vilnius, Lithuania

2- Physics Department, University "Alexandru Ioan Cuza", Iasi, Romania

3- Institute of Energetics & Interphases, IENI-CNR, Genoa, Italy

4- Department Chemical & Process Engineering, University Genoa, Genoa, Italy

aurimas.sakanas@ff.vu.lt

Composite materials are valuable for the possibility to improve various properties of the final material by changing the composition of its constituents. In order to predict the properties of the final material, many theoretical approaches are taken. The most suitable approximation is called the effective medium approach (EMA), which considers that each inclusion grain is surrounded by a continuous media, which is assumed to be homogeneous. One of the most used EMA approximations is Lichtenecker's logarithmic mixture formula. Lichtenecker's formula was derived with differential analysis by applying Maxwell's equations and the principle of local charge conservation [1].

In the present contribution, barium titanate and nickel-zinc ferrite multiferroic composite ceramics ($x\text{BaTiO}_3 - (1-x)\text{Ni}_{0.5}\text{Zn}_{0.5}\text{Fe}_2\text{O}_4$), prepared by the coprecipitation method [2], with the volume fractions $x=0.466, 0.567$ and 0.67 , were investigated adapting the broadband dielectric spectroscopy methods in the frequency range of 20 Hz – 50 GHz and in the temperature range from 100 K to 500 K. The results indicate the properties of pure barium titanate to be preserved with the noticeable conductivity contribution, caused by the ferrite phase.

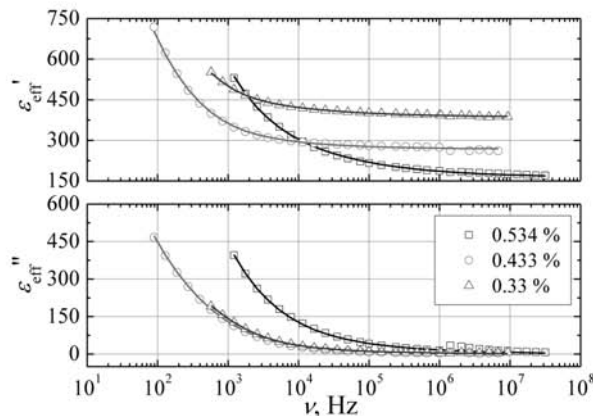


Figure 1. Frequency dependencies of the complex effective dielectric permittivity. Lines correspond to approximations using the alternative expression of Lichtenecker's mixing formula

Experimental effective permittivity data of the composite ceramics were approximated using classical Lichtenecker's mixing formula. The values of dielectric permittivity for both barium titanate and nickel-zinc ferrite were calculated at 100 MHz in the whole temperature range, and reasonable results were obtained. Furthermore, alternative expression of Lichtenecker's mixture formula, changing frequency with a fixed volume fraction will be presented (Fig. 1). This approach allows generalizing the composite having only one composition available, making it a very universal in various calculations. The usefulness of the alternative expression will be presented in the form of experimental data approximation.

[1] R. Simpkin, Derivation of Lichtenecker's Logarithmic Mixture Formula From Maxwell's Equations, IEEE Trans. Microw. Theory Techn., vol. 58, no. 3, p. 545-550 (2010).

[2] A. Testino, L. Mitoseriu, V. Buscaglia et al., Preparation of multiferroic composites of BaTiO₃-Ni_{0.5}Zn_{0.5}Fe₂O₄ ceramics, J. Eur. Ceram. Soc. 26, p. 3031-3036 (2006).

Dielectric spectroscopy characterization of 0.7BaTiO₃-0.3Ni_{1/2}Zn_{1/2}Fe₂O₄ composite ceramics

A. Sakanas¹, R. Grigalaitis¹, J. Banys¹, L. Mitoseriu², V. Buscaglia³, P. Nanni³

1- Faculty of Physics, Vilnius University, Sauletekio 9/3, LT-10222 Vilnius, Lithuania

2- University "Al. I. Cuza", Faculty of Physics, Bv. Carol nr. 11, Iasi 700506, Romania

3- Inst. for Energetics & Interphases IENI-CNR, Via de Marini 6, Genova I-16149, Italy

aurimas.sakanas@ff.vu.lt

Multiferroics and magnetoelectrics are multifunctional materials which are promising due to possibilities of using their combined properties for various practical applications. According to the definition, at least two of the main ferroic properties coexist in the same range of temperatures in multiferroics, and if the electric and magnetic properties are cross-coupled, then the material is considered magnetoelectric.

Core-shell structure barium titanate and nickel-zinc ferrite composites $x\text{BaTiO}_3 - (1-x)\text{Ni}_{0.5}\text{Zn}_{0.5}\text{Fe}_2\text{O}_4$, with $x=0.7$ volume part were investigated. Composites were prepared from the core-shell particles as precursors using cold isostatic pressing, followed by conventional sintering in air [1]. Two different samples, sintered at 1050 and 1150 °C temperatures (denoted as BT-NZF-1050 and BT-NZF-1150) are compared by the means of dielectric spectroscopy.

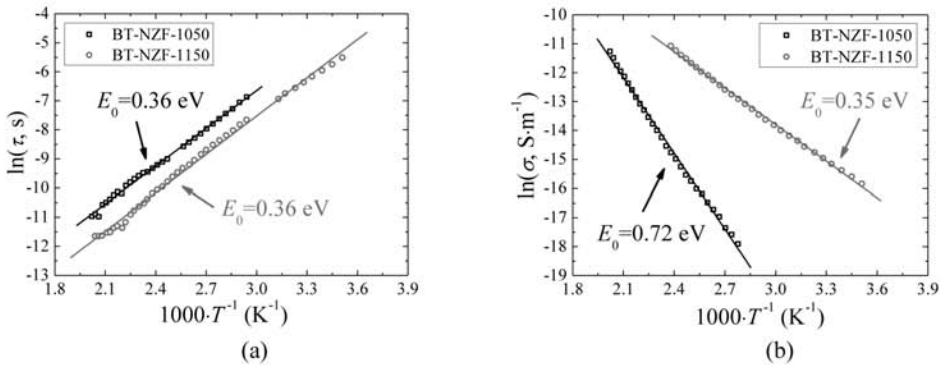


Figure 1. (a) Inverse temperature dependence of logarithmic average relaxation times, (b) inverse temperature dependence of logarithmic conductivity for the low frequency process. Solid lines correspond to Arrhenius approximations, E_0 designate the corresponding activation energies.

In order to investigate conductivity processes in both composites, complex dielectric modulus (reciprocal complex permittivity) data representation was used. The imaginary part of dielectric modulus reveals greatly asymmetric spectra, composed of two thermally activated conductivity processes. For the approximation of frequency dependencies of dielectric modulus in various temperatures Havriliak-Negami formula with the conductivity term was used [2]. Logarithmic average relaxation times and conductivity of the low frequency process vs. the inverse temperature, calculated from the spectra of complex dielectric modulus, are presented in Figure 1.

From the parameters obtained it was concluded that higher frequency conductivity mechanism is physically similar in both composites. On the other hand, the mechanism associated with low frequency peak is more active in BT-NZF-1150 composite, due to the reasons associated with higher density ceramics, courser grains and increased defectivity, which were caused by higher sintering temperature.

[1] M. T. Buscaglia, V. Buscaglia, L. Curecheriu et al., Fe₂O₃@BaTiO₃ Core-Shell Particles as Reactive Precursors for the Preparation of Multifunctional Composites Containing Different Magnetic Phases, Chem. Mater. 22, pp. 4740-4748 (2010).

[2] M. Wubbenhorst, J. van Turnhout, Analysis of complex dielectric spectra. I. One-dimensional derivative techniques and three-dimensional modelling, J. Non-Cryst. Solids 305, 40-49 (2002).

Dielectric properties of diammonium hypodiphosphate (NH₄)₂H₂P₂O₆ (ADhP)

R. Mackeviciute¹, J. Banys¹, P. Szklarz²

1-Vilnius University, Faculty of Physics, Saulėtekio av. 9, III b. 817, LT-10222 Vilnius, Lithuania
2-Faculty of Chemistry, University of Wrocław, Joliot Curie 14, 50-383 Wrocław, Poland

ruta.mackeviciute@ff.vu.lt

The connection between ferroelectricity and organic molecules started in 1920 with the discovery of the first ferroelectric crystal, Rochelle salt, containing organic tartrate ions [1]. Organic ferroelectrics, such as diammonium hypodiphosphate (ADhP) [2] or tris-sarcosine calcium chloride (TSCC) [3] crystals, could be important not only for fundamental approach but also for versatile technical applications. Despite the fact that investigations on KDP type ferroelectrics continue, but only a few novel crystals have been discovered in recent years. One of them is ADhP single crystal. So it is very important to investigate a dielectric permittivity in a wide temperature and frequency range.

Dielectric measurements were performed in 100 – 300 K temperature and 20 – 1 GHz frequency range. Frequency dependence of the real and imaginary parts of dielectric permittivity is shown in Fig. 1. Solid lines represent a fits of the complicated formula which consists of the Debye, Cole – Davidson and Cole – Cole equations (1).

$$\varepsilon^*(\omega) = \varepsilon(\infty) + \frac{\varepsilon_1(0) - \varepsilon(\infty)}{1 + i\omega\tau_1} + \frac{\varepsilon_2(0) - \varepsilon(\infty)}{(1 + i\omega\tau_2)^\gamma} + \frac{\varepsilon_3(0) - \varepsilon(\infty)}{1 + (i\omega\tau_3)^{1-\alpha}} \quad (1)$$

Here α is a parameter which indicates the width of the spectra; γ describes the asymmetry of the spectra; $\tau_{1,2,3}$ are the mean relaxation times for three different processes; $\varepsilon_{1,2,3}(0) - \varepsilon(\infty) = \Delta\varepsilon_{1,2,3}$ are static dielectric permittivities (the dielectric strength of the relaxations) and $\varepsilon(\infty)$ is the dielectric permittivity at high frequency. Frequency dependence of the real and imaginary parts of dielectric permittivity could be divided into three frequency ranges: the high frequency range (10⁶ Hz – 10⁹ Hz), the mid-frequency range (400 Hz – 10⁶ Hz) and the low frequency range (20 Hz – 400 Hz).

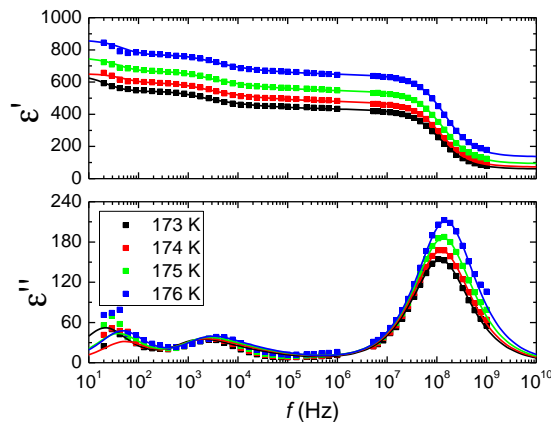


Fig. 1. Frequency dependence of the real and imaginary parts of dielectric permittivity of ADhP crystal

The Cole – Cole equation perfectly describes the relaxation process which is observed in the high frequency range and this process could be related to the ordering of NH₄ cations. The Cole – Davidson equation describes the dispersion at the mid-frequency range, which is related to the domain wall formation and motion. Despite the fact that we can only observe the end of the low frequency process, it is necessary to describe that process, due to the fact that all of the observed processes are overlapped together and they influence each other considerably in the whole frequency range. This process is described by the Debye equation and could be related to the other type of the domain wall motion.

[1] J. Valasek, Phys. Rev, Vol: 17, 475-481, (1921)

[2] P. Szklarz, M. Chanski, K. Slepokura, T. Lis, Chem. Mater.; 23; 1082-1084, (2011)

[3] S. P. P. Jones, D. M. Evans, M. A. Carpenter, S. A. T. Redfern, J. F. Scott, U. Straube, V. H. Schmidt, Phys. Rev. B.; 83; 094102, (2011)

Dielectric and pyroelectric properties of PMN-29PT single crystal near MPB

R. Mackeviciute¹, R. Grigalaitis¹, M. Ivanov¹, R. Sliteris², J. Banys¹

1-Vilnius University, Faculty of Physics, Saulėtekio av. 9, III b. 817, LT-10222 Vilnius, Lithuania
2- Ultrasound Institute of Kaunas University of Technology, Studentu St. 50, Kaunas LT-51368, Lithuania

ruta.mackeviciute@ff.vu.lt

Ferroelectric crystals find application in a variety of high tech devices that covers piezoelectric sensors and transducers, micro-electro-mechanical systems (MEMS), electro-optical wave guides, IR detectors and cameras based on the pyroelectric effect and many more. Single crystals based on solid solutions of lead-magnesium-niobate (PMN) and lead titanate (PT) have emerged as highly promising multifunctional systems combining piezoelectric, pyroelectric and electro-optic properties.

Lead-magnesium-niobate is a relaxor ferroelectric material, which has a very high dielectric constant (around 20000) [1]. With lead titanate (PT), PMN forms a solid solution known as PMN-PT. In this system, with the increase in PT content, T_c increases and relaxor behavior decreases and between PMN-30PT to PMN-50PT compositions, there exists a morphotropic phase boundary (MPB) [2]. The nature of the MPB is still debated in the literature, but a consensus seems to emerge as to the existence of a sequence of phase transitions (second order transitions) that accommodate the rhombohedral to the tetragonal transition thus allowing for easy rotation of the polarization vector [3].

Dielectric and pyroelectric properties of $0.71\text{Pb}(\text{Mg}_{1/3}\text{Nb}_{2/3})\text{O}_3\text{-}0.29\text{PbTiO}_3$ single crystal, oriented and poled along three different crystallographic directions, [001], [011] and [111], have not yet systematically investigated in a broad temperature range. The dielectric measurements were performed in 300 – 500 K temperature range. HP4284 LCR-meter was used to measure capacitance and loss tangent of the sample in 20 Hz – 1 MHz frequency range and a model of flat dielectric capacitor was used. Measurements were performed during cooling cycle with temperature variation rate of about 1 K/min. The pyroelectric properties of these crystals were performed in 220 – 430 K temperature range using a dynamic method. While changing the temperature the current flow through the sample was recorded. The pyroelectric coefficient was calculated using the following formula:

$$p \approx \frac{1}{A} \frac{I \Delta t}{\Delta T}$$

where I is the pyroelectric current, A is the area of the electrodes and $\frac{\Delta T}{\Delta t}$ is the rate of change of temperature. A more detailed discussion of dielectric and pyroelectric properties of PMN-29PT will be presented.

Acknowledgements

This work has been financed by the Lithuanian-Swiss cooperation programme "Research and development" joint research project "SLIFE", project code LSP-12 007

[1] L. E. Cross, *Ferroelectrics* 76 (1987) 241.

[2] M. Sepiarsky and R. E. Cohen, *J. Phys.: Condens. Matter* 23 (2011) 435902 (11pp).

[3] H. Fu and R. E. Cohen, *Nature* 403, 281-283 (2000)

Dielectric properties of $0.9\text{PbMg}_{1/3}\text{Ta}_{2/3}\text{O}_3 - 0.1\text{PbTiO}_3$ single crystals

E. Palaimiene¹, J. Macutkevicius¹, A. Kania², J. Banys¹

¹- Vilnius University, Faculty of physics, Saulėtekio av. 9, III b., LT-10222 Vilnius, Lithuania

²- A. Chelkowski Institute of Physics, University of Silesia, Uniwersytecka 4, 40-007 Katowice, Poland

Main author email address: edita.palaimiene@ff.vu.lt

The solid solutions formed between ferroelectric relaxor $\text{PbMg}_{1/3}\text{Nb}_{2/3}\text{O}_3$ (PMN) or $\text{PbZn}_{1/3}\text{Nb}_{2/3}\text{O}_3$ (PZN) and ferroelectric PbTiO_3 (PT), i.e. $\text{PbMg}_{1/3}\text{Nb}_{2/3}\text{O}_3 - \text{PbTiO}_3$ ((1-x)PMN – xPT) and $\text{PbZn}_{1/3}\text{Nb}_{2/3}\text{O}_3 - \text{PbTiO}_3$ ((1-x)PZN – xPT), have recently attracted [1]. Their crystal structure and nature of phase transitions strongly depend on composition[1]. The similar behaviour was also observed in (1-x) $\text{PbMg}_{1/3}\text{Ta}_{2/3}\text{O}_3 - \text{PbTiO}_3$ ((1-x)PMT-xPT) crystals [2]. With the increase in Ti content the ferroelectric—paraelectric phase transition changes gradually from relaxor to normal ferroelectric type and shifts towards higher temperatures [2].

In this work we present broadband dielectric spectroscopy results of 0.9PMT-0.1PT single crystals. Dielectric measurements were performed in wide temperature region (25 K – 500 K) at 20 Hz – 1 GHz frequencies. The 0.9PMT–0.1PT single crystals were grown by the flux method.

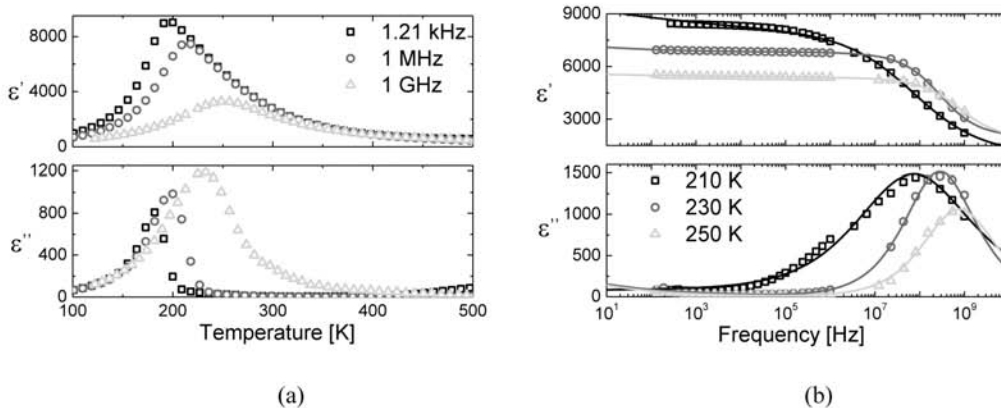


Figure 1. (a) Temperature dependences of the real (ϵ') and imaginary (ϵ'') parts of the dielectric permittivity of 0.9PMT–0.1PT at different frequencies. (b) Frequency dependence of the real (ϵ') and imaginary (ϵ'') parts of dielectric permittivity of 0.9PMT–0.1PT at different temperatures.

Fig. 1 (a) shows the temperature dependencies of real and imaginary parts of dielectric permittivity for investigated crystals. We observe the anomaly of dielectric permittivity which is typical for ferroelectric relaxors: peaks of complex dielectric permittivity move to higher temperature with increasing frequency. Fig. 1 (b) shows the frequency dependence of the real and imaginary parts of complex dielectric permittivity of 0.9PMT–0.1PT. The dielectric spectra look like symmetric at high temperatures, therefore for fitting was used the Cole-Cole equation. Solid lines represent a best fit. From broadband dielectric spectra were calculated distributions of relaxation times. Both the longest and most probable relaxation time diverge on cooling according to the Vogel-Fulcher law, however with different freezing temperatures. The effect is related with distribution of freezing temperatures phenomena and will be discussed in the presentation in details.

This research is funded by the European Social Fund under the Global Grant measure.

[1] J. M. Kiat, Y. Uesu, B. Dkhil, M. Matsuda, C. Malibert, G. Calvarin, Monoclinic structure of unpoled morphotropic high piezoelectric PMN-PT and PZN-PT compounds, *Phys. Rev. B* 65, 064106 (2002).

[2] A. Kania. Flux Growth and Dielectric Studies of (1-x) $\text{PbMg}_{1/3}\text{Nb}_{2/3}\text{O}_3$ -x PbTiO_3 Single Crystals, *Ferroelectrics*, 369, 141-148 (2008).

Broadband dielectric spectroscopy of NaNbO_3 ceramics

J. Macutkevic¹, A. Molak² and J. Banys¹

¹ Faculty of Physics, Vilnius university, Sauletekio al. 9, LT-10222 Vilnius, Lithuania

² Institute of Physics, University of Silesia, ul. Uniwersytecka 4, PL-40-007 Katowice, Poland

Main author email adress: jan.macutkevic@gmail.com

Sodium niobate (NaNbO_3) is an oxygen perovskite with the largest number of phase transitions [1]. The material gained new attention in the last years due the increased interest in environmental protection, since it is an end member of a number of solid solutions with good piezoelectric properties (for example $\text{Na}_{0.5}\text{K}_{0.5}\text{NbO}_3$) which could replace the widely used lead-based perovskites. In this presentation results of broadband dielectric investigations of sodium niobate in wide temperature region (25-730 K) are presented. In this temperature range three frequency independent dielectric anomalies were observed on cooling: one at 603 K, which corresponds to antiferroelectric P-R phase transition; the second at 406 K, which corresponds to P-Q antiferroelectric phase transition; and the third at 142 K, which corresponds to Q-N phase transition. All anomalies not indicate any significant dielectric dispersion in frequency range 20 Hz -1 GHz, therefore the dynamics of these phase transitions are related with soft modes, which frequencies are higher as 1 GHz. Below Q-N phase transition frequency dependent dielectric anomalies, at 116 K and 40 K, are related with domains dynamics. The P-R phase transition temperature demonstrate pronounced hysteresis between heating and cooling (about 40 K) while for P-Q hysteresis is lower (about 10 K), which indicate that both phase transitions are first order. At higher temperatures (above 650 K) and lower frequencies (below 11 kHz) the dielectric properties are mainly covered by high electrical conductivity. DC electrical conductivity follows the Arrhenius law with activation energy of 1.13 eV.

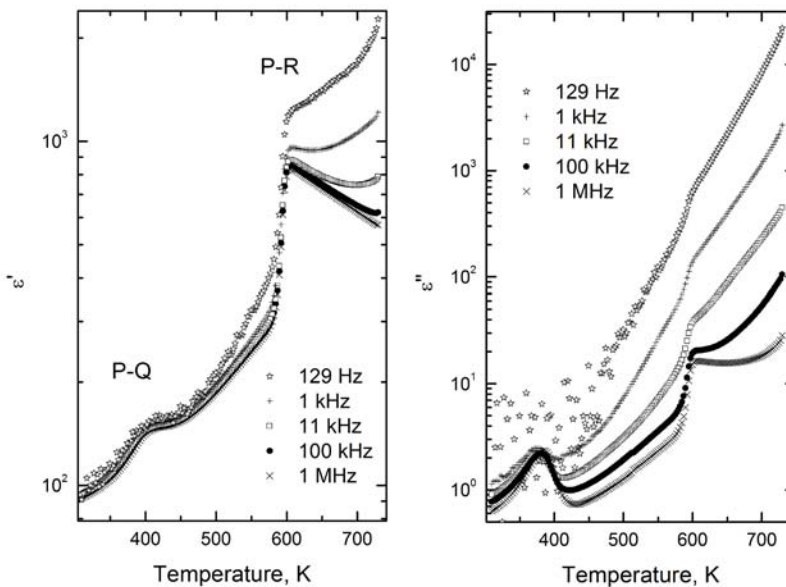


Fig. 1 Temperature dependence of complex dielectric permittivity of NaNbO_3 above room temperature on cooling.

[1] H. D. Megaw, 7 Phase of Sodium Niobate, *Ferroelectrics* 7, 87-89 (1974).

Broadband dielectric properties of carbon foams

J. Macutkevic¹, A. Paddubskaya², J. Banys¹, P. Kuzhir², S. Maksimenko², M. Letellier³, V. Fierro³, A. Celzard³

1- Vilnius university, Sauletekio al. 9 Vilnius, Lithuania

2- Research Institute for Nuclear problems of Belarussian State University, Bobruiskaya str., Minsk, Belarus

3- IJL-UMR Université de Lorraine – CNRS 7198, ENTSIB, 27 rue Philippe Seguin, CS 60036, 88026 Epinal Cedex, France

Main author email address: jan.macutkevic@gmail.com

Tannin-based rigid foams and their carbonaceous counterparts are new, easily prepared, cellular solids based on renewable resources [1]. Prepared from mimosa bark extracts as a major component, the interest for such cheap, lightweight, cellular materials is increasingly growing, given that they are able to compete with more expensive synthetic polymer foams. In this presentation, results of broadband dielectric/electric investigations of carbon foams in wide temperature (25-600 K) and frequency range (20 Hz – 3 THz) are reported. The value of complex dielectric permittivity of carbon foams is very high (more than 10^6 at low frequencies) in wide frequency range, it is higher than the value of complex dielectric permittivity of well known composites with carbon nanofillers (such as carbon nanotubes or carbon black). The complex dielectric permittivity increases with carbon foam density, however increasing saturates at densities higher as 0.075 g/cm^{-3} . The complex dielectric permittivity decreases with frequency according to the Jonsher universal power law. At higher frequencies, in microwave and terahertz frequency range, the real part of complex dielectric permittivity exceeds the imaginary part. At these frequencies, carbon foams properties are similar to dielectric. Carbon foams demonstrate anisotropic behaviour, the value of complex dielectric permittivity is lower in the growth direction in comparison with the one perpendicular to the growth direction. Anisotropy increases with carbon foam density. Foams dielectric permittivity decreases on cooling down to the lowest temperatures, however it is almost temperature-independent in heating (from room temperature to 600 K). On cooling, dc conductivity of carbon foams follows variable range hopping conductivity law and parameters of this law – Mott constant and hopping dimensionality are almost density-independent.

This research was partially supported by Lithuanian-French program Giliber, project Nr. TAP LZ 02/2013.

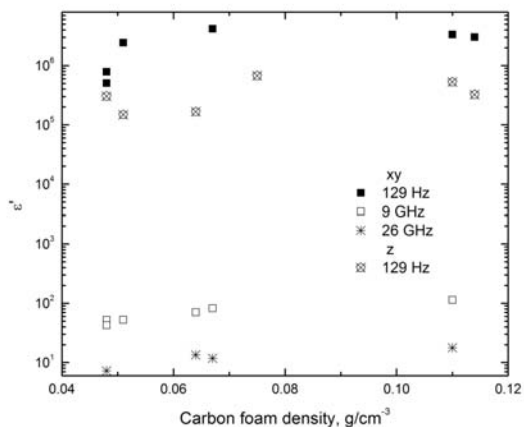


Fig. 1 Dielectric permittivity of carbon foams versus density at different frequencies (z is the growth direction, xy is the perpendicular to growth direction).

[1] W. Zhao, V. Fierro, A. Pizzi, G. Du, A. Celzard, Effect of composition and processing parameters on the characteristics of tannin-based rigid foams. Part II: Physical properties. *Material Chemistry and Physics* 123, 210-217 (2010).

Influence of carbon nanotube length on composite dielectric properties

I. Kranauskaite¹, J. Macutkevic¹, J. Banys¹, D. Krasnikov², S. Moseenkov², V. Kuznetsov²

1- Vilnius university, Sauletekio al. 9 Vilnius, Lithuania
2- Boreskov institute of Catalysis SB RAS, Novosibirsk, Russia

Main author email address: ieva.kranauskaite@ff.vu.lt

Dielectric properties of carbon nanotubes (CNT) composites were investigated very often, mainly in order to find an electrical percolation [1]. Indeed, above percolation threshold the values of dielectric permittivity and electrical conductivity for composites with CNT are very high in wide frequency range, including microwave and terahertz frequencies [2]. However, the relation between CNT microscopic parameters (like length or diameter), polymer matrix and percolation threshold in composites up to now is not clear [1]. Therefore, before experiment it rather impossible to predict dielectric properties of CNT composites. Generally, it expected that percolation threshold (f_c) is directly proportional to CNT length/diameter aspect ratio ($f_c \sim p=L/d$), however this relation experimentally was never observed and more complicated formula were used in order to establish influence of aspect ratio on percolation threshold in composites. In this presentation results of dielectric investigations of CNT composites in Polymethylmethacrylate (PMMA) matrix are presented in wide (20 Hz – 3 THz) frequency range. The mean diameter of all CNT used for composite preparation was 9 nm, while four different length CNT groups were used: 1) CNT with mean length about several tens micrometers, 2) CNT after oxidation with nitric acid, mean length 335 nm, 3) CNT after grinding in mill, mean length 438 nm, 4) CNT after grinding in mill, mean length 428 nm. It was establish that electrical percolation threshold in the first and second groups was 2 wt%, in the third 1 wt% and in the fourth 0.5 wt%. Thus is observed an inversion dependence as it would be expected from aspect ratio theory. According, to model of electrical percolation presented in [3] critical concentration f_c is:

$$f_c = 9H(1-H)/(-9H^2 + 15H + 2), \quad (1)$$

where H is the principal depolarisation factor, which takes into account influence of CNT aspect ratio on percolation threshold,

$$H(p) = 1/(p^2 - 1)[p(p^2 - 1)^{-0.5} \ln(p + (p^2 - 1)^{0.5}) - 1]. \quad (2)$$

For very high aspect ratio CNT (as in our case), H and f_c are inversely proportional to p^2 . Thus obtained results are in agreement with percolation theory presented in [3]. In heating both the complex dielectric permittivity and electrical conductivity rapidly increase above glass transition temperature, while on cooling they both are almost temperature independent. Thus, the percolation threshold further decreases after annealing above glass transition temperature (it is 390 K for PMMA). On cooling, down to lowest temperatures DC conductivity decreases according to tunneling model law, and influence of CNT length on this model parameters will be discussed in the presentation.

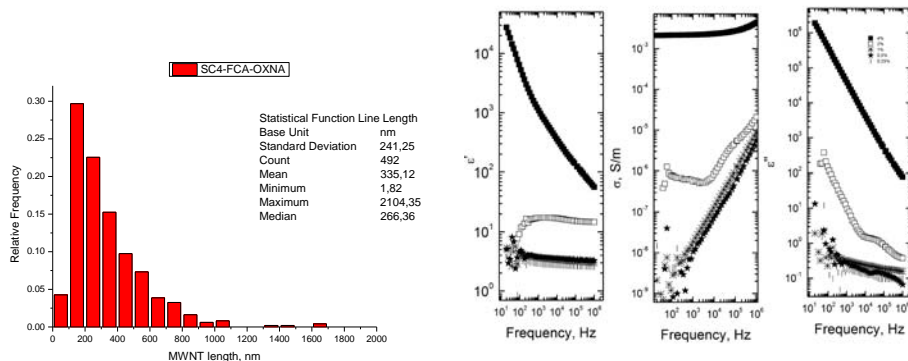


Fig. 1 Distribution of CNT lengths a) and dielectric/electric spectra at low frequencies b) in the second group of CNT/PMMA composites.

This research is funded by the European Social Fund under Global Grand measure.

[1] W. Bauhofer, J. Z. Kovacs, A review and analysis of electrical percolation in carbon nanotube polymer composite, Composite Science and Technology 69, 1486 (2009).

[2] D. Nuzhnyy, M. Savinov, V. Bovtun, M. Kempa, J. Petzelt, B. Mayoral, T McNally, Broad-band conductivity and dielectric spectroscopy of composites of multiwalled carbon nanotubes and poly(ethylene terephthalate) around their low percolation threshold, Nanotechnology 24, 055707 (2013).

[3] F. Dung, Q. S. Zheng, L. F. Wang, C. W. Nan, Effects of anisotropy, aspect ratio, and nonstraightness of carbon nanotube composites, Appl. Phys. Lett. 90, 021914 (2007).

Ultrasonic and Dielectric Studies of Polyurea Elastomer Composites with Inorganic Nanoparticles

V. Samulionis¹, Š. Svirskas¹, J. Banys¹, A. Sánchez-Ferrer², R. Mezzenga²

1- Vilnius University, Physics Faculty, 10222 Vilnius, Lithuania

2- Institute of Food, Nutrition & Health, ETH Zurich, 8092 Zurich, Switzerland

vytautas.samulionis@ff.vu.lt

Inorganic nanotubes can be used for fabrication of various composites based on polymer materials, because they exhibit a good homogeneity and solubility of the composite material. Multifunctional materials produced on composites of polymer containing inorganic nanotubes, which can be designed at the nanoscale, are expected to have great impact on industrial applications in the future. New family of such composites are polyurea elastomer composites with inorganic MoS₂ or MoSI nanotubes and nanowires [1]. Polyurea elastomers are a new kind of materials with higher performance than polyurethanes. The enhancement of mechanical, chemical and thermal properties is due to the presence of hydrogen bonds between the urea motives which can be erased at high temperature softening the elastomeric network. Thus, the final polymer network could be considered as a chemical and physical network at room temperature, and a chemical network above the temperature which breaks down such hydrogen bonds. Such materials are the combination of amorphous polymers above glass transition and crosslinkers which keep the chains into a single macromolecule. They are obtained by the rapid reactions of isocyanates (rigid molecules) with polyetheramines (flexible chains). Polyurea exhibits a phase separated structure with rigid urea domains (hard domains) embedded in a matrix of flexible polymer chains (soft domains) [2-3]. The elastic properties of polyurea can be tuned over a broad range by varying the molecular weight of the components, the relative amount of hard and soft domains, and the loading of nanoparticles.

Ultrasonic methods as non-destructive techniques can be used for elastomer characterization. In this way, we have studied the temperature dependencies of the longitudinal ultrasonic velocity and ultrasonic attenuation of these new polyurea elastomers and composites with inorganic nanoparticles. It was shown that in these polyurea elastomers large ultrasonic attenuation peak and corresponding velocity dispersion exists at 10 MHz frequency below room temperature and this behaviour is related to glass phase transition T_g of the soft segments in the polymer matrix. The relaxation parameters and T_g depend on the segmental molecular weight of the polymer chains between crosslinking points, the nature of the crosslinkers in the network and content of MoS₂ nanotubes or MoSI nanowires. The increase of ultrasonic velocity in composites with loading of nanoparticles has been observed [4]. In semicrystalline polyurea elastomer matrices above glass transition the first order phase transition from quasi crystalline to amorphous state exists. In this case the sharp ultrasonic velocity and attenuation anomalies were observed near the first order phase transition temperature T_C . Ultrasonic attenuation maximum related to glass transition was considerably smaller in quasicrystalline polyureas showing the decreased influence of soft domain segments is polymer matrix below T_C . The first order phase transition in semicrystalline polyurea elastomer samples has large temperature hysteresis (> 10 K). This was confirmed also by dielectric investigations, as well as by measurements of DC electric field induced piezoelectric sensitivity, as in case of the paraelectric phase of layered materials such as CuInP₂S₆ [5]. The addition of small amount of inorganic nanoparticles resulted in the decrease of the first order phase transition temperature in semicrystalline composites.

Acknowledgements This work was supported by the Lithuanian Research Council under project MIP-068/2012.

- [1] V. Samulionis, J. Banys, A. Sánchez-Ferrer and R. Mezzenga, Ultrasonic Characterization of Dynamic Elastic Properties of Polymer Composites with Inorganic Nanotubes, *Sensors & Transducers*. 12, 66 (2011).
- [2] A. Sánchez-Ferrer, D. Rogez and P. Martinoty, Synthesis and Characterization of New Polyurea Elastomers by Sol/Gel Chemistry, *Macromolecular Chemistry and Physics*. 211, 1712-1721 (2010).
- [3] A. Sánchez-Ferrer, M. Reufer, R. Mezzenga, P. Schurtenberger, H. Dietsch, Inorganic-Organic Elastomer Nanocomposites from Integrated Ellipsoidal Silica-Coated Hematite Nanoparticles as Crosslinking Agents. *Nanotechnology*. 21, 185603/1-7 (2010).
- [4] V. Samulionis, Š. Svirskas, J. Banys, A. Sánchez-Ferrer, S. Jecg Chin, and T. McNally, Ultrasonic Properties of Composites of Polymers and Inorganic Nanoparticles, *Phys.status solidi A*, 210, 2348-2352 (2013).
- [5] V. Samulionis, J. Banys, Yu. Vysochanskii, Piezoelectric and Elastic Properties of Layered Materials of Cu(In,Cr)P₂(S,Se)₆ System, *J. Electroceram*. 22, 192-197 (2009).

Phase Transitions in Polymers with Highly Ordered Liquid-Crystalline Phases

V. Samulionis¹, Š. Svirskas¹, J. Banys¹, A. Sánchez-Ferrer², R. Mezzenga², N. Gimeno³, M.B. Ros³

1- Vilnius University, Physics Faculty, 10222 Vilnius, Lithuania

2- Institute of Food, Nutrition & Health, ETH Zurich, 8092 Zurich, Switzerland

3- Materials Science Institute of Aragón (ICMA), University of Zaragoza, 50009 Zaragoza, Spain

vytautas.samulionis@ff.vu.lt

Bent-core liquid crystals (BCLC) are achiral molecules which contain aromatic rings disposed in a non-straight configuration, and are of interest in the field of liquid crystals because of their spontaneous segregation into chiral domains. These mesogens show ferro- [1], antiferro- [2] and piezoelectric [3] properties. Moreover, such molecules show nonlinear optical activity [4], optical biaxiality [5], or flexoelectric behavior [6] which are of high interest as potential new functional materials for the construction of electric or electrooptic devices.

The combination of such bent-core based molecules with polymers results on macromolecular structures which keep the properties of both components, and the chiral segregated domains contain the BCLC in a lamellar or columnar fashion. This combination enables to process the material, and brings mechanical and thermal stability. Recently, the synthesis and characterization of linear BCLC main-chain polymers have been published, showing the “dark conglomerate” mesophase (DC) [7], which showed interesting dielectric and polarization switching properties under electric field.

Herein, we report an example of BCLC main-chain polymer elastomer synthesized via one-pot reaction from hydrosilylation polyaddition. Dielectric studies on this material showed two maxima in the real and imaginary components of the dielectric permittivity at 365 K and 450 K (Figure 1), together with a temperature hysteresis showing the first order nature of the two phase transitions.

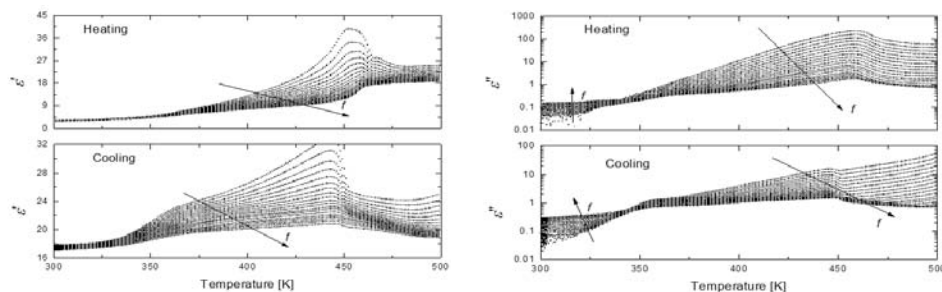


Figure 1. Temperature dependent real (left) and imaginary (right) components of the dielectric permittivity upon heating and cooling cycles at different frequencies ranging from 1.2 kHz to 1 MHz.

Longitudinal ultrasonic attenuation and velocity measurements at 10 MHz frequency showed anomalies at the phase transition temperatures respect to the dielectric results. Above room temperature, a large ultrasonic attenuation was observed which can be related to glass transition of this polymer network. The piezoelectric sensitivity in this BCLC main-chain polymer elastomer was determined using our ultrasonic method [8].

Acknowledgements This work was supported by the Lithuanian Research Council under project MIP-068/2012.

- [1] R.A. Reddy, C. Tschierske, Bent-Core Liquid Crystals: Polar Order, Superstructural Chirality and Spontaneous Desymmetrisation in Soft Matter Systems, *J. Mater. Chem.* 16, 907-961 (2006).
- [2] A. Jákli, C. Bailey, J. Harden, *Thermotropic Liquid Crystals: Recent Advances* (Springer), Chapter 2 (2007).
- [3] A. Jákli, I.C. Pintre, J.L. Serrano, M.B. Ros, M.R. de la Fuente, Piezoelectric and Electric-Field-Induced Properties of a Ferroelectric Bent-Core Liquid Crystal, *Adv. Mater.* 21, 3784-3788 (2009).
- [4] I.C. Pintre, J.L. Serrano, M.B. Ros, J. Martínez-Perdiguero, I. Alonso, J. Ortega, C.L. Folcia, J. Etxebarria, R. Alicante, B. Villacampa, Bent-Core Liquid Crystals in a Route to Efficient Organic Nonlinear Optical Materials, *J. Mater. Chem.* 20, 2965-2971 (2010).
- [5] C. Tschierske, D.J. Photinos, Biaxial Nematic Phases, *J. Mater. Chem.* 20, 4263-4294 (2010).
- [6] K. Van Le, F. Araoka, K. Fodor-Csorba, K. Ishikawa, H. Takezoe, Flexoelectric Effect in a Bent-Core Mesogen, *Liq. Cryst.* 36, 1119-1124 (2009).
- [7] N. Gimeno, A. Sánchez-Ferrer, N. Sebastián, R. Mezzenga, M.B. Ros, Bent-Core Based Main-Chain Polymers Showing the Dark Conglomerate Liquid Crystal Phase, *Macromolecules* 44, 9586-9594 (2011).
- [8] V. Samulionis, J. Banys, Y. Vysochanskii, Piezoelectric and Elastic Properties of Layered Materials of Cu(In,Cr)P₂(S,Se)₆ System, *J. Electroceram.* 22, 192-197 (2009).

Nonequilibrium effects near the Lifshitz point in $\text{Sn}_2\text{P}_2(\text{Se}_x\text{S}_{1-x})_6$ uniaxial ferroelectrics

A. Molnar¹, R. Bilanych¹, R. Yevych¹, A. Kohutych¹,

V. Samulionis², J. Banys², K. Rushchanskii³, Yu. Vysochanskii¹

1- Uzhgorod University, Uzhgorod, Ukraine

2- Vilnius University, Vilnius, Lithuania

3- Peter Grünberg Institut, Jülich, Germany

vytautas.samulionis@ff.vu.lt

For $\text{Sn}_2\text{P}_2(\text{Se}_x\text{S}_{1-x})_6$ proper uniaxial ferroelectrics with the incommensurate phase of type II at selenium content above the Lifshitz point concentration $x_{LP} \approx 0.28$ on the temperature – composition diagram, the nonequilibrium effects have been investigated by dielectric susceptibility measurements with cooling and heating speed within 0.002 – 0.1 K/min range, and also by high temperature resolution ultrasound measurements and hypersound Brillouin scattering studies. Clear anomalies at second order incommensurate transition (T_i) and at first order lock-in transition (T_c) are observed at low cooling rate for samples with $x > 0.28$ as well as for crystal with $x = 0.28$. It means that the incommensurate phase appears at smaller concentration of selenium.

By increasing of cooling rate the dielectric susceptibility anomaly near T_c smears and the intermediate IC phase doesn't appear for sample with $x = 0.28$ and 0.1 K/min rate. Such cooling rate dependence of lock-in transition is associated with transformation of the long wave modulated polarization into domain structure with wide enough domain walls, what is determined by strong nonlinear local potential [1, 2]. Smearing of dielectric susceptibility jump near lock-in transition by increasing of cooling speed could be related to the rise of the domain wall concentration n_w in the ferroelectric phase just below T_c . Such effect of nonequilibrium appearance near the Lifshitz point could be described within known Kibble - Zurek model [3, 4]. At this, for the uniaxial ferroelectrics the domain walls could be considered as scalar topological defects with concentration n_w related to the temperature change rate. After estimations by relations from [3, 4] it follows that n_w strongly increases when cooling rate increases from 0.002 K/min to 0.1 K/min. The largest value n_w gives the distance between domain walls about 50 nm. This value is comparable with modulation wavelength which is expected near the LP at concentration distance $x - x_{LP} \approx 0.01$ [5, 6].

- [1] K.Z. Rushchanskii, Yu.M. Vysochanskii, D. Strauch, Ferroelectricity, nonlinear dynamics, and relaxation effects in monoclinic $\text{Sn}_2\text{P}_2\text{S}_6$, Phys. Rev. Lett., vol. 99, pp. 207601-1–207601-4, (2007).
- [2] D.A. Kiselev, K.Z. Rushchanskii, I.K. Bdkin, M.D. Malinkovich, Y.N. Parkhomenko, Yu. M. Vysochanskii, Theoretical prediction and direct observation of metastable non-polar regions in domain structure of $\text{Sn}_2\text{P}_2\text{S}_6$ ferroelectrics with triple-well potential, Ferroelectrics, vol. 438, pp. 55 – 67, (2012).
- [3] A. del Campo, T.W.B. Kibble, W.H. Zurek, Causality and non-equilibrium second-order phase transitions in inhomogeneous systems, J. Phys.: Condens. Matter., vol. 25, pp. 404210-1 – 404210-10, (2013).
- [4] T.W. Kibble, G.E. Volovik, On phase ordering behind the propagating front of a second-order transition, *is'ma v ZhETF*, vol. 65, pp. 96 – 101, (1997).
- [5] T.K. Barsamian, S.S. Khasanov, V.Sh. Shekhtman, Diffraction analysis of incommensurate phases in crystals of quasi-binary system $\text{Sn}_2\text{P}_2(\text{S}_{1-x}\text{Se}_x)_6$, Ferroelectrics, vol. 138, pp. 63 - 77, (1993).
- [6] Yu.M. Vysochanskii, T. Janssen, R. Currat, R. Folk, J. Banys, J. Grigas, V. Samulionis, Phase transitions in ferroelectric phosphorous chalcogenide crystals (Vilnius University Publishing House: Vilnius, Lithuania), Chapter 2, (2008).

Dielectric and magnetic properties of (1-x)PZT-(x)PFW ceramics with $0.25 < x < 0.55$.

Ryszard SKULSKI^{1) a)}, Dariusz Bochenek¹⁾, Artur CHROBAK²⁾, Ewa NOGAS-ĆWIKIEL¹⁾, Przemysław NIEMIEC¹⁾

¹⁾University of Silesia, Materials Science Department, 2, Śnieżna Str., 41-200, Sosnowiec, Poland;

²⁾University of Silesia, Institute of Physics, 2, 4 Uniwersytecka Str. 40-007 Katowice, Poland;

^{a)} ryszard.skulski@us.edu.pl

Email: ryszard.skulski@us.edu.pl

We present the results of investigating of dielectric and magnetic properties of ceramic samples of solid solution $(1-x)(\text{PbZr}_{0.53}\text{Ti}_{0.47}\text{O}_3)-x(\text{PbFe}_{2/3}\text{W}_{1/3}\text{O}_3)$ [i.e. (1-x)PZT-xPFW] with $x=0.25, 0.35, 0.45$ and 0.55 . Samples have been obtained from oxides using conventional ceramic technology. Solid solution $(1-x)(\text{PbZr}_{0.53}\text{Ti}_{0.47}\text{O}_3)-x(\text{PbFe}_{2/3}\text{W}_{1/3}\text{O}_3)$ [i.e. (1-x)PZT-xPFW] generally belongs to materials known as multiferroics but some compositions of this solid solution belong to materials known as birelaxors in which can coexist short range order of electric and magnetic dipoles. Such materials are interesting due to their potential practical applications, and also because of the possibility to investigate the basics of physical phenomena occurring in them. We describe also the results of investigations of magnetic properties obtained using the SQUID magnetometer.

Keywords: multiferroics, birelaxor, PZT-PFW ceramics, phase transitions, dielectric properties

Multiferroic properties of lead iron niobate $\text{PbFe}_{1/2}\text{Nb}_{1/2}\text{O}_3$ ceramics and single crystals

I. Gruszka¹, A. Kania¹, S. Miga², E. Talik¹

1- A.Chełkowski Institute of Physics, University of Silesia, Katowice, Poland

2- Institute of Materials Science, University of Silesia, Chorzow, Poland

Main author email address: irena.gruszka@us.edu.pls

Lead iron niobate $\text{PbFe}_{1/2}\text{Nb}_{1/2}\text{O}_3$ is a multiferroic material of the disordered perovskite structure [1]. The Fe^{3+} and Nb^{5+} , which occupy the oxygen octahedron centre, are randomly distributed. This disorder strongly influence nature of structural and magnetic phase transitions. Two structural ferroelectric phase transitions are observed at 353 K and 376 K [2,3]. However, majority of dielectric studies of PFN ceramics point to one diffuse maximum of dielectric permittivity $\epsilon(T)$ function, characteristic for ferroelectric relaxors. Two magnetic transition are detected at 10 K and 156 K [3,5]. The microscopic origin of appearance of spin glass state below 10 K is not finally recognised. In addition, PFN crystals exhibit significant electro-magnetic coefficient [4]. These characteristics cause this compound interesting both for basic research and application interest. Crystal and ceramic technologies and their influence on physical properties of $\text{PbFe}_{1/2}\text{Nb}_{1/2}\text{O}_3$ are the main aims of the present study.

PFN single crystals were grown by the flux method. The $\text{PbO} - \text{PbF}_2 - \text{B}_2\text{O}_3$ mixture was used as a solvent. Black crystals of rectangular shape and dimensions up to 5 mm were grown. High quality, dense and brown ceramics were synthesized using two methods: two-step solid state reaction via “columbite” phase and by a new one-step synthesis from polymeric precursors. Precursor powders were obtained by a sol-gel method based on water solution of citric acid.

Dielectric measurements were performed using an Agilent E4980A Precision RLC meter for frequencies 100 Hz – 1 MHz in the temperature range 80 – 500 K. Magnetic studies were carried out using a Quantum Design MPMS SQUID magnetometer in the temperature range 2 – 400 K.

[1] M. Lampis et al., J.Phys.: Condens. Matter, **12**, 2367 (2000)

[2] S.A Ivanov et al., j. Phys.: Condens. Matter, **13**, 25 (2001)

[3] A.Falqui et al., J.Phys. Chem. B, **109**, 22967 (2005)

[4] W. Kleemann et al., Phys. Rev. Lett., **105**, 257202 (2010)

[5] S. Chillal et al., Phys. Rev. B, **87**, 220403 (R) (2013)

SrTiO₃ and Pr effects on structural, dielectric and ferroelectric properties of Na_{0.5}Bi_{0.5}TiO₃ ceramic

J.Suchanicz¹, G.Klimkowski¹, D.Sitko¹, M.Antonova², A.Sternberg²

¹Institute of Technics, Pedagogical University, 30-084 Krakow, ul Podchorazych 2, Poland

²Institute of Solid State Physics, University of Latvia, Kengaraga 8, LV-1063 Riga, Latvia

sfsuchan@up.krakow.pl

(Na_{0.5}Bi_{0.5})_{0.7}Sr_{0.3}TiO₃ (NBTS30) and (Na_{0.5}Bi_{0.5}TiO₃)_{0.7}Sr_{0.3}]_{1-x}Pr_xTiO₃ (NBTS30P) (0 ≤ x ≤ 0.025) ceramics were prepared by conventional fabrication process. Their crystal structure, microstructure dielectric and ferroelectric properties were studied. The data of XRD show that all ceramics possess a single perovskite phase. The SEM results confirm that ceramics are well sintered and exhibit relative densities higher than 97%. The results also reveal that the microstructure of the different compositions do not show a significant variation. The SrTiO₃ substitution to Na_{0.5}Bi_{0.5}TiO₃ was found to induce a transition from ferroelectric rhombohedral to relaxor pseudocubic phase. Electric permittivity increases and their maximum is shifted to lower temperature. Polarization and coercive field increases and decreases, respectively. The praseodymium (Pr) substitution to NBTS30 results in crystal structure change from pseudocubic to tetragonal at x=0.025. At the same time electric permittivity increases, their maximum is slightly shifted to higher temperature, polarization and coercive field increases and decreases, respectively. It is also found that frequency dependence of T_m (the temperature where electric permittivity is maximum) increases with increasing of Pr. Due to small polarizability and ionic size Sr²⁺ Ion A-site substitution of Na_{0.5}Bi_{0.5}TiO₃ weakened the long-range interaction between Na⁺ and Bi³⁺ ions and in consequence induced local internal fields. This caused relaxor ferroelectric behavior. Similar scenario are expected after Pr-doping of NBTS30. The results show that investigated ceramics are one of the promising lead-free materials for electronic applications.

Sb effect on structural, dielectric and ferroelectric properties of $\text{Na}_{0.5}\text{K}_{0.5}\text{NbO}_3$ ceramics

J.Suchanicz¹, K.Konieczny¹, I.Faszczowy¹, M.Karpierz², U.Lewczuk², B.Urban², G.Klimkowski¹, M.Antonova³, A.Sternberg³

¹Institute of Technology, Pedagogical University, 30-084 Krakow, Poland

²Institute of Physics, Pedagogical University, 30-084 Krakow, Poland

³Institute of Solid State Physics, University of Latvia, LV-1063 Riga, Latvia

Email address: kkoniec@up.krakow.pl

To date, lead-based materials are widely used in sensors, transducers, actuators and other electronic devices. However, the lead containing materials can cause an environmental pollution and a damage to the human body. Recently, it is desirable for applications to use lead-free materials [1-2]. Lead-free $\text{Na}_{0.5}\text{K}_{0.5}(\text{Nb}_{1-x}\text{Sb}_x)\text{O}_3$ ($0 < x < 0.06$) ceramics were fabricated by the solid-state reaction method. The materials with more than 95% densification were obtained. The microstructure study confirm that ceramics are well sintered. All compositions show complete perovskite solid solutions. The dielectric, heat capacity, Raman and ferroelectric investigations for these specimens were performed. Dielectric study revealed that the obtained ceramics are rather normal ferroelectrics. However some signs of diffuse phase transition were observed. The transition temperature, the maximum electric permittivity and dielectric loss were found to decrease with increasing Sb content in the system. The possible origin for effects observed was discussed. The results could point out a possibility of application of $\text{Na}_{0.5}\text{K}_{0.5}(\text{Nb}_{1-x}\text{Sb}_x)\text{O}_3$ as electronic ceramics.

[1] Y.M.Chiang, G.W.Farrey, A.N.Soukhajak, Appl.Phys.Lett., 73, 3683 (1998)

[2] R.Farhi, M.E.Marssi, A.Simon,, J.Ravez, Eur.Phys.J., B9, 599 (1999)

Effect of sintering temperature and time on dielectric properties of $\text{Ba}(\text{Ti}_{0.75}\text{Zr}_{0.15})\text{O}_3$ - $(\text{Ba}_{0.77}\text{Ca}_{0.23})\text{TiO}_3$ 50/50 ceramics

R. Boschilia¹, A.L. Boaventura¹, A.C. Hernandez², E. Antonelli¹

¹Instituto de Ciência e Tecnologia (ICT), Universidade Federal de São Paulo, 12231-280, São Jose dos Campos, SP, Brazil.

²Grupo Crescimento de Cristais e Materiais Cerâmicos, Instituto de Física de São Carlos (IFSC), Universidade de São Paulo (USP), São Carlos, SP, Brazil

Main author email address: antonelli@unifesp.br

The Lead has recently been expelled from many commercial applications and materials (for example, from solder, glass and pottery glaze) owing to concerns regarding its toxicity. Currently, piezoelectric ceramic materials in commercial use are based on lead titanate zirconate (PbZrO_3 - PbTiO_3 or PZT), which are widely used in sensors, actuators and other electronic devices. Although there has been a concerted effort to develop lead-free piezoelectric ceramics, no effective alternative to PZT has yet been found. The basic approach to achieving high piezoelectricity is to place the composition of the material to the proximity of a composition-induced phase transition between two ferroelectric phases [1]. Such a transition has been known as the morphotropic phase boundary (MPB) in the phase diagram. Therefore, in the present work, sintering temperature effect on $\text{Ba}(\text{Ti}_{0.85}\text{Zr}_{0.15})\text{O}_3$ (BTZ)/ $(\text{Ba}_{0.77}\text{Ca}_{0.23})\text{TiO}_3$ (BCT) 50/50 system has been studied. The studied materials were prepared through the conventional ceramic method, starting from high-purity precursor powders of BaCO_3 (99%), TiO_2 (99%), ZrO_2 (99%) and CaCO_3 (99%). These raw materials were mixed in stoichiometric proportions according to the nominal formulations: $(0.77) \text{BaO} + (0.23) \text{CaO} + \text{TiO}_2 \rightarrow (\text{Ba}_{0.77}\text{Ca}_{0.23})\text{TiO}_3$ (BCT) and $\text{BaO} + (0.85) \text{TiO}_2 + (0.15) \text{ZrO}_2 \rightarrow \text{Ba}(\text{Ti}_{0.85}\text{Zr}_{0.15})\text{O}_3$ (BZT). After homogenization for 24h, the mixtures were calcined at 1200°C for 2h. The powders were then mixed in the proportion of 50/50, ball-milled for 12h into fine powders, compacted into disk-shaped samples and then sintered at 1320°C for 1min/2h/10h and at 1270°C for 1 min. The final density of each sintered specimen was determined by the Archimedes method. The BZT/BCT phase and microstructure developments were followed by X-ray diffraction (XRD) using a Rigaku Geigerflex diffractometer (with a monochromatic CuK_α radiation, $\lambda=1.5406\text{\AA}$) and optical microscopy (Zeiss AX10), respectively. Grain size of the ceramics was evaluated by the intercept method on the optical images. Electrical measurements were carried out with a Solartron SI 1260 impedance/gain-phase analyzer over a wide temperature range from 25 to 200°C . Grain size, density and dielectric constant at room temperature increased with the increase of sintering time and temperature. The dielectric spectra are characterized by dielectric peaks that correspond to the ferroelectric-to-paraelectric phase transitions (Figure 1a).

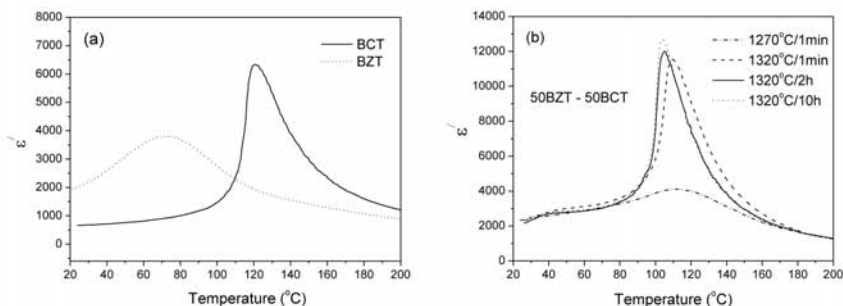


Figure 1 - (a) The figure, as well as each axis coordinates and titles must be large enough to be easily read. (b) Any micrographs being used

In addition, the nature of this transition is seen to change from normal (sharp-like dielectric peak) to diffuse (broad-like dielectric peak) when the temperature and time of sintering is decreased (Figure 1a and b). The conclusion is that with the increase in sintering temperature and time the competition between Ti and Zr ions decrease to occupy the same crystallographic site B, with leads to decrease in compositional fluctuations of different polar micro-regions.

Acknowledgments: This work was supported by CNPq, CAPES and FAPESP.

[1] W. Liu and X. Ren, Large Piezoelectric Effect in Pb-Free Ceramics, 103, 257602-1-4, (2009).

Organic one-dimensional photonic crystals with ferroelectric properties

Yu.A. Draginda, S.P. Palto, S. G. Yudin, V. V. Lazarev

Shubnikov Institute of Crystallography, Russian Academy of Sciences, Leninsky prosp. 59, Moscow 119333, Russia

E-mail: draginda@mail.ru

In the last several years, there has been much interest in physics and applications of tunable photonic crystals with different functional properties. In our case tunable one-dimensional photonic crystals consist of alternating organic molecular thin films of vinylidene fluoride copolymers P(VDF/TrFE) and azo-dye (4-(4'-nonilamino-phenilazo)benzoic acid). Our selected organic materials are of great interest because of their special properties: ferroelectricity in copolymer ultrathin films [1] and photoinduced optical anisotropy (POA) in azo-dye material [2]

Experimental samples were prepared using the well-known Langmuir-Blodgett technique, when thin films are transferred from the air-water interface onto a solid substrate. This method offers the possibility to fabricate highly ordered films with monolayer by monolayer control of thickness and structure. The manufactured "sandwich" heterostructures possess the photonic band gap at a wavelength of 780 nm.

We have observed the "quasi"-linear electrooptical effect that is due to the Stark effect in a spectral band of azo-dye absorption. This electrooptical effect is caused by "built-in" electric field that can be described in terms of electric induction continuity in the heterogeneous structure consisting of macroscopically polarized ferroelectric sub-system. At the same time the linear electrooptical effect that is due to piezoelectric properties of the copolymer P(VDF/TrFE) appears in the spectral range of the photonic band. It means that the photonic band is shifting under an electric field. After the repolarization using high-voltage pulses the linear electrooptical effect shows bistable switching, that results in the sign change of the spectral shift. The photonic band gap shift achieves a maximal value of 2.4×10^{-2} nm.

Thus the ferroelectricity of P(VDF/TrFE) sublayers allows both electric field control of the photonic band spectral position and the bistable switching of the linear electrooptical effect.

The financial support from the Russian Fund for Basic Research (grant No. 12-02-00214a) is acknowledged.

References

1. A. V. Bune, V. M. Fridkin, S. Ducharme, L. M. Blinov, S. P. Palto, A. V. Sorokin, S. G. Yudin & A. Zlatkin. Two-dimensional ferroelectric films// Nature 391, 874-877 (1998)
2. S. P. Palto, S. G. Yudin, C. Germain and G. Durand. Photoinduced Optical Anisotropy in Langmuir Blodgett Films as a New Method of Creating Bistable Anchoring Surfaces for Liquid Crystal Orientation// J. Phys. II France 5 (1995) 133-142

Effect of reoxidation annealing on electrical properties in ceramic composites

Cristina E. Ciomaga¹, Mirela Airimioaei¹, George Stoian², Marco Deluca^{3,4}, Carmen Galassi⁵ and

Liliana Mitoseriu¹

¹Faculty of Physics, "Al. I. Cuza" University of Iasi 700506, Romania

²National Institute of Research and Development for Technical Physics, Iasi 700050, Romania

³Institut für Struktur- und Funktionskeramik, Montanuniversität Leoben, Peter Tunner Str. 5, A-8700 Leoben, Austria

⁴Materials Center Leoben Forschung GmbH, Roseggerstr. 12, 8700 Leoben, Austria

⁵CNR -ISTEC, Via Granarolo no. 64, I-48018 Faenza, Italy

Corresponding author: cristina.ciomaga@uaic.ro

Analysis on phase transformation and the influence of annealing temperature on the morphological, structural and ferroelectric properties of multi-walled carbon nanotubes (MWCNTs) with $\text{Pb}(\text{Zr}_{0.47}\text{Ti}_{0.53})\text{O}_3$ (PZT) ceramic composites with different compositions $x=0, 0.5, 1$ and 2wt% CNTs were performed in this paper. The $(1-x)\text{PZT}-x\text{CNTs}$ ceramic composites were prepared by spark plasma sintering. By using Spark Plasma Sintering (SPS) we expect to obtain composites with new functional properties, which were previously not possible to fabricate using conventional processing routes, non-equilibrium composites. SPS can process the composites in very short intervals of time without structural or chemical degradation of the CNTs. Using this method can be developed ceramics with new electro-mechanical properties and applications, such as, heating elements, Electro Discharge Machinability (EDM), and high electrical and thermal anisotropy [1, 2].

Structural characterization performed by XRD analysis, after SPS and different reoxidation treatments of the samples, confirmed the formation of perovskite phase and small structural modification from possible tetragonal-rhombohedral structure due to the addition of CNTs. From TEM images the presence of CNTs in the powder composite was confirmed. The microstructural analyze by SEM on powder composite showed the good compatibility between MWCNTs and the PZT matrix. Raman analyze demonstrated that black spots in the powder composites are rich in carbon. The Raman study performed on the surface if the SPS samples after thermal treatment confirmed the presence of carbon on SPS.

We have studied the influence of addition of CNTs and the effect of reoxidation annealing on the dielectric properties of investigated ceramic composites. The ferroelectric measurements were also performed and a tendency to a more rectangular shape of the major hysteresis loop was observed. These results were correlated with the microstructure investigations, and explained or confirmed that the intragranular pores plays a dominant role on the ferroelectric properties. A detailed study of non-linear properties taking into account different thermal treatment steps for different applied electric field, after sintering process, was realized.

Acknowledgements: These works were financial supported by CNCSIS-UEFISCSU, project number PN-II-ID-PCE-2011-3-0745. The collaboration in frame of the COST Action MP0904 is highly acknowledgements.

References

- [1] Subhranshu Sekhar Samal and Smrutisikha Bal, Journal of Minerals & Materials Characterization & Engineering, pp 355-370, (2008).
- [2] Guo-Dong Zhan and Amiya K. Mukherjee, Reviews on advanced materials science, pp 185-196 (2005).

Elastic constants of $\text{GdCa}_4\text{O}(\text{BO}_3)_3$ single crystal in a wide temperature range

A. Sotnikov^{1,2}, H. Schmidt¹, M. Weihnacht¹, R. Möckel³, C. Reuther⁴, J. Götze⁴

1-IFW Dresden, Helmholtzstraße 20, Dresden, Germany

2-A.F. Ioffe Physical-Technical Institute, Polytekhnicheskaya 26, St.-Petersburg, Russia

3-Helmholtz Institute Freiberg for Resource Technology, Halsbrücker Straße 34, Freiberg, Germany

4-Freiberg University of Mining and Technology, Brennhausgasse 14, Freiberg, Germany

E-mail: A.Sotnikov@ifw-dresden.de

Piezoelectric crystals are key materials for various bulk- and surface acoustic wave devices and sensors. Of particular interest are crystals which possess a reasonable piezoelectric response at high temperatures. Among them, trigonal crystals of the langasite family (LGS, SNGS, STGS, CTGS, etc.), and monoclinic crystals of the oxoborate $\text{RCa}_4\text{O}(\text{BO}_3)_3$ (where R = rare earth) family are very promising. These crystals demonstrate a combination of moderately high electromechanical coupling coefficients and low acoustic loss. They can operate up to very high temperatures since their melting point is at about 1500°C. Large size high quality single crystals can be readily grown using the Czochralski technique at low cost.

Room temperature elastic compliances of Gadolinium oxoborate ('GdCOB'; $\text{GdCa}_4\text{O}(\text{BO}_3)_3$) single crystal were obtained previously using the resonance technique. Notice that constants available from literature are contradictory. In this communication, we report on the measurement of the elastic constants of GdCOB single crystal in a wide temperature range using the pulse-echo ultrasonic method.

GdCOB single crystals were grown using the Czochralski pulling technique at the Freiberg University of Mining and Technology, Freiberg, Germany. As grown colorless boules without cracks and macroscopic defects had a length up to approximately 65 mm and a cross-section of 18 mm x 15 mm. The elastic constants were obtained from the velocity data of bulk acoustic waves measured by the high-precision pulse-echo method at a frequency of 10 MHz. Crystals cubes (approximately 8 x 8 x 8 mm³) of the appropriate crystallographic orientations were used. Electromechanical coupling coefficients were obtained by the overtone ratio method on thin crystal plates (8 x 8 x 0.5 mm³) of the appropriate cuts.

Using the pulse-echo ultrasonic technique, the velocities of the longitudinal and the shear acoustic waves propagating in six crystallographic directions of GdCOB monoclinic single crystal were measured over the temperature range 22°C up to 950°C for the first time. The set of elastic constants for this crystal was derived and compared with published data. A strong piezoelectric excitation of the shear waves propagating along b- and c crystallographic axes was maintained up to 950°C. Temperature dependences of the electromechanical coupling coefficients for some crystallographic directions interesting for potential acoustic applications will be presented too.

Elastic and anelastic properties of the relaxor ferroelectric $0.55\text{SrTiO}_3\text{-}0.45\text{BiScO}_3$

Oleg Ivanov, Elena Danshina

Belgorod National Research University, Pobedy St., 15, 308015, Belgorod, Russia

Ivanov.Oleg@bsu.edu.ru

The $\text{SrTiO}_3\text{-BiScO}_3$ system is interesting system in order to examine new manner of lead-free ferroelectrics search based on possibility of forming a ferroelectric state in multicomponent systems consisting of nonferroelectric end components. In fact, the $\text{SrTiO}_3\text{-BiScO}_3$ system was recently found to be characterized by relaxor ferroelectric properties [1]. Relaxor properties of this system are rather unexpected. In fact, strontium titanate, SrTiO_3 , is known to be an incipient ferroelectric lying near the limit of its paraelectric phase stability. At room temperature pure SrTiO_3 is a cubic $Pm\bar{3}m$ crystal and it retains its nonpolar centrosymmetric structure undergoing a few structural nonferroelectric phase transitions upon cooling at $T \rightarrow 0$ K, while BiScO_3 is a nonpolar monoclinic $C2/c$ compound. Although it has been speculated that BiScO_3 may be ferroelectric, no experimental confirmations have been reported. So, the $\text{SrTiO}_3\text{-BiScO}_3$ system consisting of nonferroelectric end members can in the same time demonstrate a relaxor ferroelectric behavior. Relaxor behavior is usually originated from two phase's coexistence as polar nanoclusters distributed inside a nonpolar matrix [2]. Each of these polar clusters has own local Curie temperature. Preliminary results have allowed us to conclude that the coexistence of the polar tetragonal $P4mm$ phase and the nonpolar cubic $Pm\bar{3}m$ phase is responsible for relaxor properties of the $\text{SrTiO}_3\text{-BiScO}_3$ system [1]. Two-phase state of relaxors is formed just below some temperature called as the Burns temperature, T_d . A cluster structure of relaxors will give specific contributions to dielectric,

optical, mechanical properties. Elastic and anelastic properties of solids are known to be sensitive-to-structure properties. So, these properties can be sensitive to appearance and temperature evolution of the cluster structure during a transition from the paraelectric clusterless phase into the relaxor cluster state. The aim of this paper is to examine changes in elastic and anelastic properties during the transition from the paraelectric phase into the relaxor state of relaxor $(1-x)\text{SrTiO}_3\text{-}x\text{BiScO}_3$ system. Composition with $x=0.45$ was taken as a sample.

Elastic and anelastic properties of the lead-free relaxor $0.55\text{SrTiO}_3\text{-}0.45\text{BiScO}_3$ ceramics were studied at frequencies of 1, 10, 25, 50 and 100 Hz. Anomalous behavior of Young's modulus and internal friction were observed at cooling below the Burns temperature $T_d \approx 585$ K (Figure 1). Both elastic and anelastic anomalies were found to be frequency dependent. Elastic softening observed just below T_d is assumed to be due to electrostriction relationship between spontaneous polarization of polar tetragonal Pmm nanoclusters and strain of unit cell. It was found that the internal friction maximum observed below T_d is in fact superposition of two maxima. Higher temperature maximum is typical for relaxors. Using the special internal friction mechanism for the first order phase transition, size of the polar tetragonal nanoclusters was estimated to be equal to ~ 10 nm. Such sizes of tetragonal islands were found for the sample under study by using the electron backscattered diffraction method. Microscopic inhomogeneity of the sample is characterized by coexistence of ferroelectric ordered phase as large tetragonal domains and relaxor state as the polar tetragonal nanoclusters distributed inside the nonpolar cubic matrix.

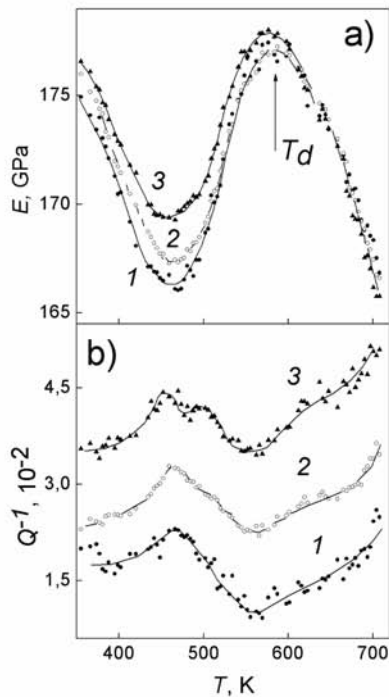


Figure 1 The temperature dependencies of Young's modulus (a) and internal friction (b) for the $0.55\text{SrTiO}_3\text{-}0.45\text{BiScO}_3$ sample taken at frequencies of 1 (curves 1), 50 (2) and 100 (3) Hz. T_d is the Burns temperature.

[1] Ivanov O. E. Danshina E, Tuchina Y and Sirota V 248 2011 Physica Stat. Sol. (b) 248 1006.

[2] Cross L E 1994 Ferroelectrics 151 305.

Relaxor properties of the KBiScNbO_6 double perovskite

Elena Danshina, Oleg Ivanov

Belgorod National Research University, Pobedy St., 85,3 08015, Belgorod, Russia

Danshina@bsu.edu.ru

At present, double perovskites with general formula MBiScNbO_6 ($M = \text{Na, K, and Rb}$) are considered as novel ferroelectric materials having interesting and potentially useful physical properties [1]. According to theoretical predictions these materials are characterized with different types of cation ordering leading to developing the ferroelectric structural instabilities and forming the various polar structures. To our knowledge, syntheses of the NaBiScNbO_6 , KBiScNbO_6 , and RbBiScNbO_6 have not been reported. So, theoretical predictions of the ferroelectric properties of these materials have no experimental evidences by now. The aim of this paper is to prepare the ceramic KBiScNbO_6 double perovskite and find out and analyze the peculiarities in its dielectric behavior characteristic for ferroelectric materials.

The ceramic KBiScNbO_6 samples were synthesized via solid-state processing technique. According to XRD data samples under study consist of mixture of two phases. Major phase has a perovskite structure. Amount of minor pyrochlore phase was estimated to be equal to ~ 10 vol. %. Perovskite phase can be satisfactory described as rhombohedrally distorted pseudocubic $Pm\bar{3}m$ structure with unit-cell parameter $a_c = 4.069 \text{ \AA}$.

Broad maxima centered at $T_m \approx 700 \text{ K}$ were observed in $\varepsilon'(T)$, and $\varepsilon''(T)$ dependences (Figure 1). These maxima are ones of the characteristics for relaxor ferroelectrics. Another feature of relaxors is the characteristic frequency dispersion their dielectric constant. It was found that the ε' and ε'' maxima are shifted to lower temperatures as the measuring frequency, f , decreases. Figure 2 shows the $T_m(f)$ dependence extracted from the $\varepsilon''(T)$ curves measured at frequencies between 15 Hz and 4.2 MHz. The $T_m(f)$ dependence was further used to recover of the temperature dependence of relaxation time, τ . The τ values were taken as $\tau = 1/2\pi f$ for each T_m value. It is known that for relaxors the $\tau(T)$ dependence obeys the Vogel-Fulcher law [2]

$$\tau = \tau_0 \exp\left(\frac{U}{k(T - T_f)}\right), \quad (1)$$

where τ_0 is the inverse of attempt frequency, U is an effective activation energy, k is the Boltzmann constant and T_f is the freezing temperature mentioned above. It was found the experimental $\tau(T)$ curve is satisfactory reproduced by the expression (1) as is shown by dashed line in Figure 2 inset. The τ_0 , U and T_f values were estimated to be equal to 10^{-12} s , 0.2 eV and 585 K, respectively. So, the peculiarities of dielectric properties of KBiScNbO_6 are characteristic for relaxor ferroelectrics.

It should be noted that the KBiScNbO_6 consists of the KNbO_3 and BiScO_3 perovskites. KBiScNbO_6 has the Nb^{5+} ions at the B -site which favors ferroelectricity, as in KNbO_3 . The BiScO_3 compound has a very small tolerance factor $t = 0.85$ and a stereochemically active Bi^{3+} at the A -site. These two factors can lead to strong lattice instabilities. That is why BiScO_3 is an interesting end member for fabrication of new ceramic solid solutions for ferroelectric and piezoelectric applications [3].

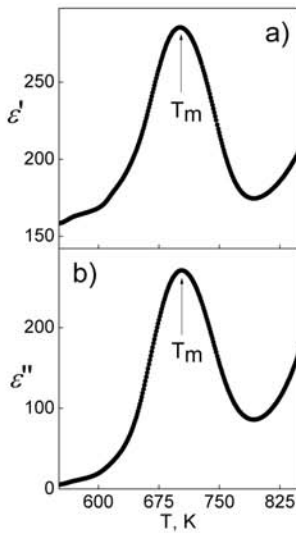


Figure 1 The $\varepsilon'(T)$ (a) and $\varepsilon''(T)$ (b) dependences for the KBiScNbO_6 sample

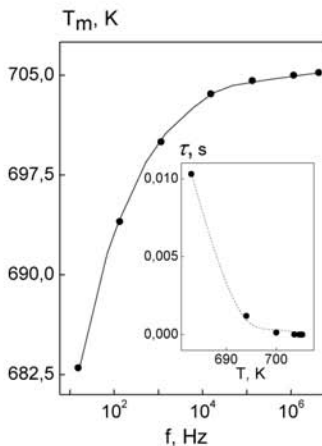


Figure 2 The $T_m(f)$ dependence for the KBiScNbO_6 sample. The inset is $\tau(T)$ dependence. Dashed line is the Vogel-Fulcher fit.

[1] S. Takagi, A. Subedi, V.R. Cooper, D.J. Singh. Phys. Rev. B. 82, 134108 (2010)

[2] V.V. Shvartsman and D.C. Lupascu. J. Am. Ceram. Soc. 95. 1 (2012).

[3] R.E. Eitel, C.A. Randall, T.A. Shrout and S.-E. Park. J. Soc. Appl. Phys. 41, 2009 (2002).

The vibronic-proton mechanism of the ferroelectric phase transition in the KH_2PO_4 -type systems

P. Konsin¹, B. Sorokin¹

1- Institute of Physics, University of Tartu, Riia 142, 51014 Tartu, Estonia

konsin@fi.tartu.ee

We present a vibronic-proton model of the KH_2PO_4 (KDP)-type ferroelectrics. In [1-5] the importance of the proton subsystem and the proton-phonon coupling was stressed in these systems. In this report it is shown that the electron-phonon (vibronic) interaction in the PO_4 groups (including also the K^+ ions) between the conduction electronic states and the valence states mixing these bands by the $[\text{K-PO}_4]$ dynamic displacements of the potential soft optic vibrations (the covalent hybridization) takes place. This interaction is the driving force in the mechanism of the KH_2PO_4 ferroelectric phase transition. The results of the *ab initio* calculations of the electronic band structure in KDP [6] are used. The tunneling of protons between the two equivalent positions in KH_2PO_4 (neutron Compton scattering measurements support the large value for the tunnel splitting [7]) interacts with the optic phonons corresponding to the dynamic displacements of the $[\text{K-PO}_4]$ cluster along the z direction. This coupling contributes also to the dynamic instability of the KDP-type crystals. The actual vibronic anharmonicity is produced by the electron-phonon couplings and the phonon-phonon anharmonicities are taken into account. The spontaneous polarization in the ferroelectric phase and the dielectric constants (including the anisotropy) in the paraelectric and ferroelectric phases are calculated. The spontaneous shear strain u_6 (ϵ_{xy}) is caused by the deformation potentials (the electron-phonon interactions with the acoustic vibrations) and it contributes essentially to the change of the symmetry of KDP systems at the ferroelectric transition which is also ferroelastic one. The influence of the isotope effects ($\text{H} \rightarrow \text{D}$ and $^{16}\text{O} \rightarrow ^{18}\text{O}$) on the ferroelectric properties of KDP systems are estimated.

[1] J. C. Slater, J. Chem. Phys. 9, 16 (1941).

[2] R. Blinc and S. Svetina, Phys. Rev. 147, 423 (1966).

[3] M. E. Lines and A. M. Glass, Principles and Applications of Ferroelectrics and Related Materials (Clarendon Press, Oxford, 1977).

[4] R. R. Levitskii and B. M. Lisnii, Phys. Stat. Sol. B 241, 1350 (2004).

[5] P. Konsin, Phys. Tverd. Tela. 16, 2337 (1974), Phys. Stat. Sol. B 70, 451 (1975).

[6] Q. Zhang, F. Chen, N. Kioussis, S. G. Demos, and H. B. Radousky, Phys. Rev. B 65, 024108 (2001).

[7] G. F. Reiter, J. Mayers, and P. Platzmann, Phys. Rev. Lett. 89, 135501-1 (2002).

The influence of microstructure on functional properties of $\text{Ba}(\text{Sn}_x\text{Ti}_{1-x})\text{O}_3$ ceramics

N. Horchidan¹, A. Ianculescu², H. Ursic^{3,4}, B. Malic³, M. Deluca^{5,6}, L. Curecheriu¹, L. Padurariu¹, L. Mitoseriu¹

¹Department of Physics, Alexandru Ioan Cuza University, Blv. Carol I, nr.11, 700506, Iasi, Romania

²Dept. of Oxide Materials Science & Eng., Polytechnics Univ. Bucharest, Romania

³Electronic Ceramics Department, Jožef Stefan Institute, Jamova cesta 39, SI-1000 Ljubljana, Slovenia

⁴CO NAMASTE, Jamova cesta 39, SI-1000 Ljubljana, Slovenia

⁵Institut für Struktur- und Funktionskeramik, Montanuniversität Leoben, Peter Tunner Str. 5, A-8700 Leoben, Austria

⁶Materials Center Leoben Forschung GmbH, Roseggerstr. 12, 8700 Leoben, Austria

Main author email address: NHorchidan@stoner.phys.uaic.ro (N. Horchidan)

The dielectric and ferroelectric properties of the $\text{Ba}(\text{Sn}_x\text{Ti}_{1-x})\text{O}_3$ ceramics are strongly dependent by the Sn addition, microstructure being another factor that influences these properties. The high permittivity combined with low losses makes this material as a valuable candidate for high permittivity applications, with similar performance with other known solid solutions. In the present work, the role of composition and sintering parameters (temperature and time) on the dielectric and ferroelectric properties of $\text{Ba}(\text{Sn}_x\text{Ti}_{1-x})\text{O}_3$ ceramics was analyzed. The ceramic compositions (in range $x = 0+0.20$) have been prepared using solid state method and different sintering treatment ($1300^\circ\text{C}/4\text{h}$, $1300^\circ\text{C}/8\text{h}$ and respectively $1400^\circ\text{C}/4\text{h}$) in order to generate different grain sizes and porosity in the final ceramics (Fig. 1). A transformation from normal ferroelectric to a relaxor state with diffuse phase transition is promoted by the increasing of Sn concentration, and the critical concentration corresponding to the ferroelectric-relaxor crossover is strongly dependent on the processing and sintering parameters. The present work contains the results of a combined field-induced dielectric and ferroelectric analysis with Raman spectroscopic investigations and PFM analysis in order to obtain new insights concerning the superposition of phases, evolution of ferroelectric domains with Sn addition and for the identification of composition-induced modification of the structural phase transitions. The sintering at higher temperature favours the stability of the ferroelectric state even for higher Sn addition x , fact confirmed by Raman results and empirical parameters calculated using fits of a modified Curie-Weiss law. PFM investigations revealed modifications of the domain structure and of local switching properties which confirm the ferroelectric-crossover induced by the Sn increasing, as resulted from the macroscopic and Raman investigations.

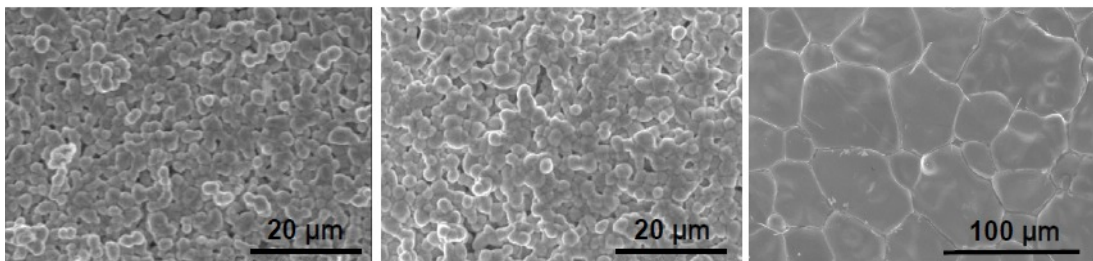


Figure 1 SEM images for BaTiO_3 normal sintered on: (a) $1300^\circ\text{C}/4\text{h}$, (b) $1300^\circ\text{C}/8\text{h}$ and (c) $1400^\circ\text{C}/4\text{h}$

Acknowledgements: This work was supported by PN-II-ID-PCE-2011-3-0745 and PN-II-ID-PCCE-2011-2-0006 grants.

[1] X. Wei, Y.J. Feng, X. Yao, Appl. Phys. Lett. 83, 2031–2033, (2003).

Combining antiferroelectric-ferroelectric in composite in searching new functional properties

L.P. Curecheriu¹, M.T. Buscaglia², V. Buscaglia², C. Padurariu¹, Mitoseriu¹

¹- Faculty of Physics, A.I. Cuza University, Iasi 700506, Romania

²-Institute for Energetics & Interphases - CNR, Via de Marini 6, Genoa I-16149, Italy

lavinia.curecheriu@uaic.ro

The interest in improving tunability properties or to modify permittivity in the range of desired values in various types of ceramics is related to the continuous growth of their use as tunable microwave devices. In order to fulfill technological requirements *e.g.* $\text{tg}\delta < 0.3\%$, $\epsilon_r \sim 1000$, the combination of ferroelectric (FE) BaTiO₃ with antiferroelectric (AFE) PLZT phases in ceramic composite structures is proposed in the present work.

AFE-FE di-phase composite powders with compositions 50% Pb_{1-x}La_xTi_{1-y}Zr_yO₃ - 50% BaTiO₃ have been prepared from powders produced by two different methods: (i) mixed powders realised by solid state reaction (PLZT_BT_SS) and (ii) core-shell composites (PLZT_BT_CS). The samples were obtained using two nominal different AFE compositions: Pb_{0.96}La_{0.04}Ti_{0.10}Zr_{0.90}O₃ (PLZT1) and Pb_{0.92}La_{0.08}Ti_{0.20}Zr_{0.80}O₃ (PLZT2). Dense ceramics with relative density of 95-98% and homogeneous microstructures have been obtained for all the compositions.

The dielectric properties were investigated in a large frequency and temperature range. An increase of the dielectric constant was observed at room temperature for PLZT_BT_SS and a reduction of permittivity was obtained in case of PLZT_BT_CS for both antiferroelectric phases. The tunability properties determined at room temperature showed a strong nonlinear character and a hysteretic behavior for all the composite ceramics and reduced permittivity, to be compared with almost zero tunability found in the pure PLZT ceramics. The P(E) loops showed unsaturated loops and a linear character even for very high applied fields ($E \sim 5$ kV/mm), due to fine microstructure of the composites materials. As a conclusion, the advantages of combining FE and AFE properties in composites towards a high tunability and lower permittivity properties of this kind of composite can be controlled by the preparation method and compositions.

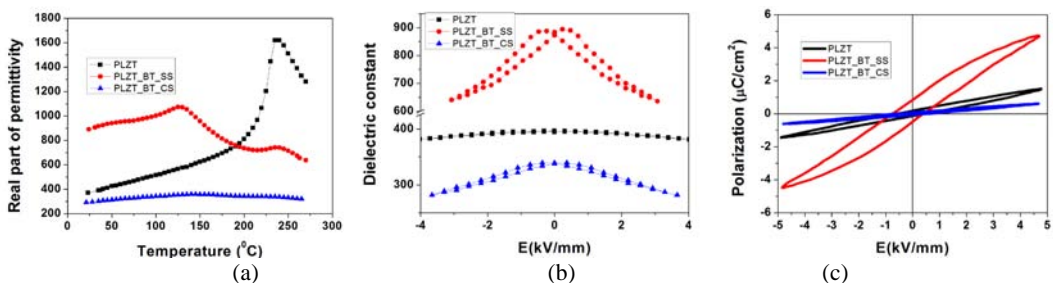


Fig.1 Dielectric constant vs. temperature at $f=20$ kHz for PLZT and PLZT-BT ceramics; (b) Dielectric constant vs. field for PLZT and PLZT-BT ceramics; (c) P(E) loops for PLZT and PLZT-BT ceramics

Acknowledgements: The financial support of the PNII-RU-TE-2012-3-0150 grant is acknowledged.

Local structural and electronic properties of chemically disordered ferroelectric relaxor $\text{PbMg}_{1/3}\text{Nb}_{2/3}\text{O}_3$

O. Kvyatkovskii

Ioffe Physical-Technical Institute of the Russian Academy of Sciences, 194021 St. Petersburg, Russia

e-mail: Kvyatkovskii@mail.ioffe.ru

Results of *ab initio* calculations of electronic structure and optimized geometry of $\text{PbMg}_{1/3}\text{Nb}_{2/3}\text{O}_3$ (PMN) crystal lattice fragments centered on lead, magnesium and niobium are presented.

The electronic problem was solved in terms of the density functional theory (DFT) with the B3LYP hybrid functional using the MO LCAO SCF method implemented in the GAUSSIAN 03 program package. The calculations were performed using the Gaussian Basis Sets of double-zeta or triple-zeta quality. Clusters $\text{PbO}_{12}\text{Mg}_n\text{Nb}_{8-n}\text{Pb}_6(\text{OH})_{24}$ ($n=0,1,2,3,4$), $\text{MgO}_6\text{Mg}_{n-1}\text{Nb}_{7-n}\text{Pb}_8(\text{OH})_{30}$ and $\text{NbO}_6\text{Mg}_n\text{Nb}_{6-n}\text{Pb}_8(\text{OH})_{30}$ ($n=1,2,3,4,5$) for modeling various environments of lead, magnesium and niobium atoms (at given n) are employed.

Most distributions of B -cations give rise to polar nanofragments with C_{3v} , C_{2v} , C_{3v} or C_{4v} symmetry and corresponding central atoms are shifted from average cubic positions. It is found that off-center shifts of Pb atoms are large (in the range from 0.1 to 0.4 Å), whereas Mg and Nb off-center shifts lie in the range from 0.01 to 0.1 Å. These results are consistent with the PDF measured for Pb ions [1] and are in a good agreement with rms displacements of Pb, Mg and Nb ions calculated by the alternative method in [2]. All these polar configurations are frozen in the temperature range in which atomic diffusion is hampered. At the same time, nonpolar distributions of cations are found which are unstable relative to off-center shift of central atom in several equivalent directions: one configuration with $n=4$ of D_{2h} symmetry for Pb and the other configuration with $n=2$ of D_{4h} symmetry for Nb. This brings about the formation of local switchable polar configurations in the system.

It is found that the gap in the electron spectrum between highest occupied and lowest unoccupied states (HOMO-LUMO) in the nano-fragments centered on lead atoms or on B -cations strongly depends on chemical composition and of B -cation distribution. In Pb-centered fragments the HOMO-LUMO gap lies in the range from 3.4 to 4.2 eV for the most configurations with the exception of several configurations with the HOMO-LUMO gap lying in the range from 2.2 to 3.0 eV. Whereas in B -centered fragments for the most of configurations with small deviation from 1:2 distribution of B -cations the HOMO-LUMO gap lies in the range from 1 to 2.6 eV, i.e. the HOMO-LUMO gap is far less than the experimental optical gap in PMN (≈ 3.2 eV).

The method of calculations in use (DFT/B3LYP/MOLCAO-SCF) gives the HOMO-LUMO gap in nanofragments of ordered niobates and titanates somewhat higher than direct or indirect experimental optical gap. Thus, one can speculate on the nature of disorder in different spatial scales: (i) there is a sizeable structural disorder in nanoscale regions produced by large on-site displacements of Pb atoms from average cubic positions; (ii) the correlations in occupation of B -sites by two types of B -cations play essential role in mesoscale regions, that is, the distribution of Mg and Nb atoms in the lattice is only partially random.

This work is supported by the Russian Foundation for Basic Research (Project no. 12-02-00879).

[1] I.-K. Jeong, T.W. Darling, J.K. Lee, Th. Proffen, R.H. Heffner, J.S. Park, K.S. Hong, W. Dmowski, T. Egami, Direct observation of the formation of polar nanoregions in $\text{Pb}(\text{Mg}_{1/3}\text{Nb}_{2/3})\text{O}_3$ using neutron pair distribution function analysis, *Phys. Rev. Lett.* **94**, 147602-147605, (2005).

[2] S.A. Prosandeev, E. Cockayne, B.P. Burton, S. Kamba, J. Peltzel, Yu. Yuzyuk, R.S. Katiyar, S.B. Vakhrushev, Lattice dynamics in $\text{PbMg}_{1/3}\text{Nb}_{2/3}\text{O}_3$, *Phys. Rev. B* **70**, 134110-134120, (2004).

Effect of metallization method on the dielectric properties of PZT ceramics

E.V. Barabanova¹, O.V. Malyshkina¹, S.I. Pugachev²

1- Tver State University, Tver, Russia

2- State Marine Technical University of St. Petersburg, Saint-Petersburg, Russia

email address: pechenkin_kat@mail.ru

Ceramics on the base of lead zirconate-titanate (PZT) is most widely distributed piezoelectric material. In the present work a study is made of the electrode application method and processing on the dielectric properties of the PZT ceramics. The choice was made of PZT samples supplied with three types of electrodes prepared by industrial metallization, microwave metallization, and with the aid of a special silver paste annealed under the same conditions as those of industrial metallization. The industrial technology of piezoceramic materials metallization is based on the recovery of noble metals (usually silver) from the oxides by the high temperature firing-on method.

The application of metal coatings by the microwave method (UHF-metallization) is a novel technological procedure implemented with the scheme proposed in [1].

We have shown that at room temperature the graphs of the dielectric characteristics dependence on frequency are practically the same for all samples: there exists a maximum in the frequency dependence of the dielectric loss $\varepsilon''(\nu)$ and the semicircle arc on the diagrams of complex permittivity $\varepsilon^*(\varepsilon')$. It was of interest to examine the temperature dependence of the dielectric loss tangent $\text{tg}\delta$. The behaviour of the dielectric characteristics was studied in the course of heating up to 320°C followed by cooling. All the samples under study are characterized by a smooth phase transition of the first kind with the Curie region of 270 to 300°C. In addition to the maximum on the $\text{tg}\delta$ temperature dependence corresponding to the phase transition, the samples prepared by UHF and industrial metallization contain one more maximum $\text{tg}\delta$ at 80°C (Fig. 1, b). This maximum is not observed during the first heating of the samples with silver paste electrodes. However similar peak appears at 60°C at repeated heating, while after the third heating it shifts toward the same value of 80°C (Fig. 1, a). It may be supposed that this is the way in which the paste is firing-on the ceramics analogously to industrial metallization

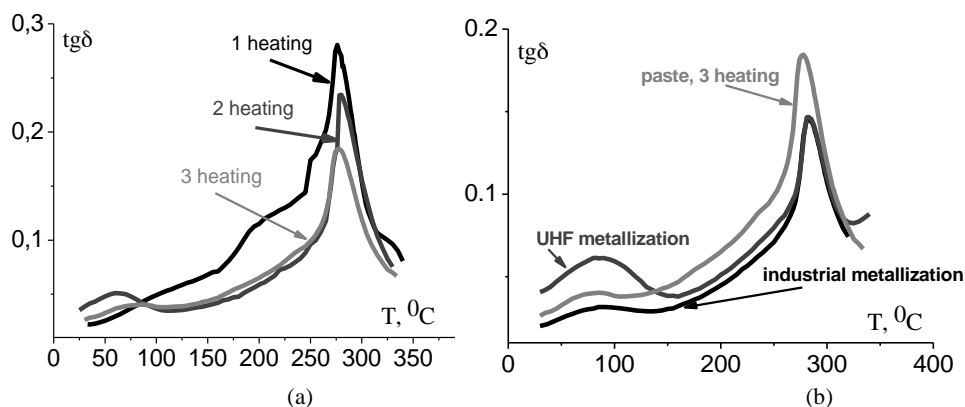


Figure 1 Dielectric tangent loss dependence on temperature for: (a) sample with silver paste annealed three times at 400°C; (b) samples with three types of electrodes prepared by UHF metallization, industrial metallization and with silver paste after third heating

but at lower temperatures. Then it may be assumed that the relaxation process observed at 80°C most likely corresponds to the dielectric properties of the near-electrode layer (boundary between material and electrode) rather than the properties of the material itself.

[1] RU Patent № 2256634 //Bershtein L.A. et al. Method of piezoceramic element metallization. 2004.

Conductivity and Dielectric Properties of Nd₅Mo₃O₁₆-Based Solid Solutions

E.P. Kharitonova, V.I. Voronkova

M.V. Lomonosov Moscow State University, Faculty of Physics, Leninskie gory, 119991, Moscow, Russia

voronk@polly.phys.msu.ru

Fluorite-like Nd₅Mo₃O₁₆ and Pr₅Mo₃O₁₆ compounds attracts attention as materials with mixed electron-oxygen conductivity [1, 2]. Depending on synthesis conditions and atmosphere oxygen content the formula of compounds can be written as Nd₅Mo₃O_{16+d} or Pr₅Mo₃O_{16+d} (0 ≤ d ≤ 0.5). Pr, Nd and Mo contents may also vary into compounds, whereby solid solutions with fluorite-like structure a formed in Nd₂O₃-MoO₃ system at 42.9 - 46.7% Nd₂O₃ [3]. According to [4] in the case of Pr₅Mo₃O₁₆ (d = 0) all oxygen positions in the structure are occupied, however extensive cavities were found in the structure. These cavities may be occupied by free interstitial oxygen. This oxygen may participate in the formation of the high conductivity of the compound. However, the vacancy mechanism of conductivity is also not excluded, as well as the possibility of increasing the oxygen conductivity, when heterovalent substitutions introduced into the Nd₅Mo₃O_{16+d} structure.

The aim of the present work is synthesis of Nd₅Mo₃O₁₆-based solid solutions in Nd₂O₃-MoO₃ system, pure and doped with Ca, Pb, Nb, Zr, and investigation of their dielectric and conductive properties.

Polycrystalline samples of Nd₆Mo₄O₂₁, Nd₅Mo₃O_{16.5}, Nd₁₄Mo₈O₄₅, PbNd₄Mo₃O_{16+d}, Nd_{5-x}Zr_xMo₃O_{16+d} (x = 0 - 0.1), Nd_{5-x}Ca_xMo₃O_{16+d} (x = 0 - 1), Nd₅Mo_{3-x}Nb_xO_{16+d} (x = 0 - 0.5) have been obtained by solid state synthesis in air. According to X-ray all of the samples belong to Nd₅Mo₃O₁₆ fluorite-like structure.

Electrophysical measurements shows that conductivity of xNd₂O₃+(1-x)MoO₃ (x = 0.429 - 0.467) slightly increases with increasing of Mo content, whereas doping of heterovalent Ca, Pb, Zr and Nb substitutions does not change the conductivity compared with pure Nd₅Mo₃O_{16+d} (Figure 1). These substitutions strongly affect on Nd₅Mo₃O_{16+d} dielectric properties, resulting to a significant change in the intensity, width and temperature of dielectric permittivity peak, which was observed near 550 - 600 °C in pure fluorite-like compounds (Figure 2).

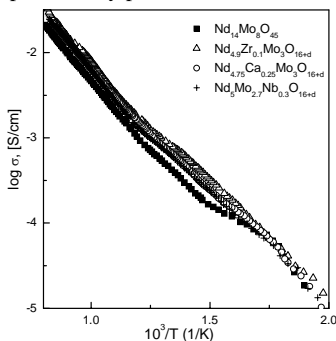


Figure 1. Conductivity temperature dependencies for fluorite-like samples (1 MHz).

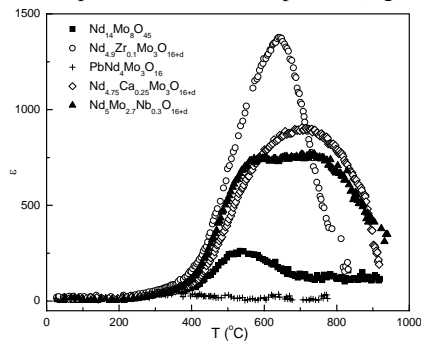


Figure 2. Dielectric permittivity temperature dependencies for fluorite-like samples (1 MHz).

Heterovalent substitution Nd³⁺ with Ca²⁺, Pb²⁺, Zr⁴⁺ and Mo⁶⁺ with Nb⁵⁺ should influence on the amount of oxygen vacancies in the structure of the compound. However, as mentioned earlier, such substitution did not affect the electrical conductivity. Thus, the high oxygen conductivity of Nd₅Mo₃O₁₆-based fluorite-like compounds presumably is not caused by the vacancy conduction mechanism. More likely, that oxygen conductivity may be connected with the presence of free movable oxygen in the interstices of the structure.

[1] M. Tsai, M. Greenblatt, W.H. McCarroll, Oxide ion conductivity in Ln₅Mo₃O_{16+x} (Ln = La, Pr, Nd, Sm, Gd, x ~ 0.5) with a fluorite-related structure, Chem. Mater., vol. 1, pp. 253-259, (1989).

[2] V.I. Voronkova, E.P. Kharitonova, D.A. Belov, M.V. Patrakeev, O.N. Leonidova, I.A. Leonidov. Fluorite-like compound with the Nd₅Mo₃O₁₆ type structure with mixed electronic-ionic conductivity. The 19th International Conference on Solid State Ionics, June 2-7, 2013. Kyoto, Japan. Program. pp. Mon-E-057.

[3] V.I. Voronkova, E.P. Kharitonova, D.A. Belov, Synthesis and electrical properties of a new fluorite-like anionic conductor in the Nd₂O₃-MoO₃ system (43–47 mol% Nd₂O₃), Solid State Ionics, vol. 225, pp. 654-657, (2012).

[4] M.J. Martinez-Lope, J.A. Alonso, D. Sheptyakov, V. Pomyakushin, Preparation and structural study from neutron diffraction data of Pr₅Mo₃O₁₆, J. Solid State Chem., vol. 183, pp. 2974-2978, (2010).

Growth and properties of KTiOPO_4 single crystals doped with barium and chromium

E.I. Orlova¹, I.A. Verin², N.I. Sorokina², V.I. Voronkova¹

1- M.V. Lomonosov Moscow State University, Faculty of Physics, Leninskie gory, 119991, Moscow, Russia

2- Shubnikov Institute of Crystallography, Russian Academy of Sciences, Leninsky pr. 59, 119333 Moscow, Russia

voronk@poly.phys.msu.ru

Potassium titanyl phosphate KTiOPO_4 (KTP) family is an attractive object of investigation due to its unusual property combination: ferroelectric, superionic and nonlinear optical properties. The objects of present research work were the growth of KTP crystals with different contents of chromium (KTP:Cr) and barium and chromium (KTP:Ba:Cr), the study of obtained crystals physical properties and atomic structure since there are some differences regarding the occurrence of chromium in the structure of KTP [1, 2].

Spontaneous flux crystallization was used for growth KTP:Cr single crystals with the addition of 0.05 and 1 mol.% of Cr_2O_3 to the flux. KTiOPO_4 crystals doped with different concentration of Ba (1, 2, 3 mol.%) and Cr (0.1 mol.%) were grown by flux method. Average size of obtained crystals is about 5-6 mm. In these crystals faces {201} and {011} are only well developed. Lattice parameters change lightly. KTP:Ba:Cr and KTP:Cr (0.05 mol.%) single crystals have light green color which indicates the presence of Cr^{3+} in the structure. KTP:Cr (1 mol.%) is reddish-brown suggesting the presence of chromium ions in the structure in the two valences of 3+ and 6+ [2].

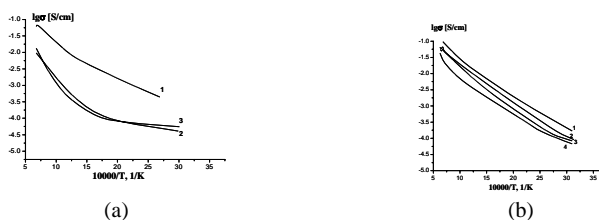


Figure 1. (a) Conductivity dependencies for (1) undoped KTP, (2) KTP:0.05mol\%Cr and (3) KTP:1mol\%Cr . (b) Conductivity dependencies for (1) undoped KTP, (2) $\text{KTP:1mol\%Ba:0.1mol\%Cr}$, (3) $\text{KTP:2mol\%Ba:0.1mol\%Cr}$ and (4) $\text{KTP:3mol\%Ba:0.1mol\%Cr}$.

Temperature dependences of ferroelectric permittivity and conductivity of obtained crystals KTP:Cr and KTP:Ba:Cr were measured from 20 to 950°C at the frequency of 1 MHz. Incorporation of chromium has little influence on ferroelectric phase transition temperature for the KTP:Cr crystals but significantly reduces the conductivity lowering it by almost two orders of magnitude (Figure 1). This can be explained by a decrease in the number of vacancies in the positions of potassium atoms due to compensating for differences between charges of trivalent chromium cations and tetravalent titanium cations [3, 4]. So it is an indirect confirmation of chromium occurrence in the position of the titanium atom in the KTP:Cr structure. For the KTP:Ba:Cr crystals the temperatures of ferroelectric phase transition drop with the increasing of barium concentration and fall on 40°C approximately for the sample with maximum content of barium. The conductivity of crystals doped with Ba and Cr decreases by about half an order of magnitude compared to pure KTP as shown in Figure 2.

The precise X-ray analysis of KTP:Cr(0.05mol\%) and KTP:Cr(1mol\%) allowed to determine the chemical formula of investigated samples: $\text{K}_{0.996}\text{Cr}_{0.005}\text{Ti}_{0.995}\text{OPO}_4$ and $\text{K}_{1.00}\text{Cr}_{0.02}\text{Ti}_{0.98}\text{OPO}_4$, respectively. X-ray studies confirmed that chromium atoms in these structures are located near Ti1 and Ti2 positions, more likely occupying the position in the octahedron Ti(2)O_6 with smaller volume. In the KTP:Cr crystals the titanium octahedra become less distorted as compared with pure KTP, that is consistent with the results of studies [2]. To make clear the scheme of barium and chromium occurrence in the KTiOPO_4 crystals precision investigation of their atomic structure will be carry out.

[1] C.V. Kannan, S. Ganesamoorthy, G. Bocelli, L. Righi, P. Ramasamy, Growth, structural and optical studies of chromium doped KTiOPO_4 single crystals, *J. of Cryst. Growth*, vol. 252, pp. 328-332, (2003).

[2] S. Norberg, V. Streltsov, G. Svensson, J. Albertsson, Dopant positions in strontium/chromium- and barium-doped KTP, determined with synchrotron X-radiation, *Acta Cryst.*, vol.56, pp. 980-987, (2000).

[3] P.A. Morris, A. Ferretti, J.D. Bierlein, G.M. Loiacono, Reduction of the ionic conductivity of flux grown KTiOPO_4 crystals, *J. Crystal Growth*, vol.109, pp. 367-375, (1991).

[4] T. Hörlin and R. Bolt, Influence of trivalent cation doping on the ionic conductivity of KTiOPO_4 , *Solid State Ionics*, vol.78, pp. 55-62, (1995).

Calorimetric study of ferroelectric $\text{BiInO}_3\text{-PbTiO}_3$ crystals

L. Xu, J. Xiao, B. F. Costa, J. A. Paixão

CEMDRX, Department of Physics, University of Coimbra, Rua Larga, 3004-516 Coimbra, Portugal

E-mail address: jxiao@ua.pt

Nowadays, both the automotive and aerospace industries have expressed the needs for actuation and sensing at higher temperatures, and specifically, the ferroelectrics high Curie temperature (above 500 °C) are also demanded. A solid state solution of $\text{BiInO}_3\text{-PbTiO}_3$ meets the high Curie temperature requirement. From the high temperature solution method using Pb_3O_4 and Bi_2O_3 as self-flux, we had grown the ferroelectric $x\text{BiInO}_3\text{-(1-x)PbTiO}_3$ crystals, with $x = 0.3, 0.4$ and 0.5 (shortly named as BIPT03, BIPT04 and BIPT05, respectively). Specific heat of different quality BIPT single crystals has been precisely measured with special attention to the temperature region between the ferroelectric phase transition temperature ranges (530-580 °C). It was assumed that excess specific heat in the paraelectric phase has a fluctuation nature and the experimental data were analyzed. From the curves of heat-flow vs temperature (DSC trace), the “thermal” T_c and the enthalpy changes can be obtained with the temperature of the onset peak in the heat flow associated with the disappearance of the ferroelectric order. The T_c of BIPT03, BIPT04 and BIPT05 is 555, 556 and 558°C, respectively. The T_c was found to elevate with the increase of PbTiO_3 composition.

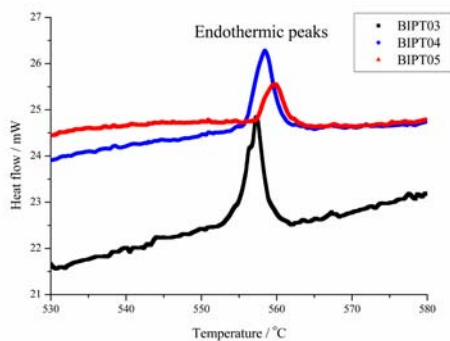


Figure The heat flow vs temperature (DSC trace) for BIPT

[1] R. E. Eiter, C. A. Randall, et al., *New High Temperature Morphotropic Phase Boundary Piezoelectrics Based on $\text{Bi}(\text{Me})\text{O}_3\text{-PbTiO}_3$ Ceramics*, Jpn. J. Appl. Phys., 40, 5999 (2001).

[2] R. Duan, R. F. Speyer, et al., *High Curie temperature perovskite $\text{BiInO}_3\text{-PbTiO}_3$ ceramics*, J. Mater. Res., 19, 2185 (2004).

Relaxor Strontium-Barium Niobate: A Lead-Free Anisotropic Electrocaloric Material

F. Le Goupil¹, J. Dec², A-K. Axelsson¹, L. J. Dunne^{1,3}, M. Valant⁴, G. Manos⁵, T. Lukasiewicz⁶,
A. Berenov¹, and N. McN Alford¹

1- Department of Materials, Imperial College London, London SW7 2AZ, UK

2- Institute of Materials Science, University of Silesia, 12 Bankowa Str., PL-40-007Katowice, Poland

3- Department of Engineering Systems, London South Bank University, London SE1 0AA, UK

4- Materials Research Laboratory, University of Nova Gorica, Nova Gorica, Slovenia

5- Department of Chemical Engineering, University College London, London WC1E 7JE, UK

6- Institute of Electronic Materials Technology, 133 Wolczynska Str., PL-01-919 Warsaw, Poland

Main author email address: jan.dec@us.edu.pl

Solid solutions of the strontium-barium niobate $\text{Sr}_x\text{Ba}_{1-x}\text{Nb}_2\text{O}_6$ where $0.25 < x < 0.8$ (SBN) are environmental friendly (lead free) polar materials of oxygen octahedral family. This type of materials is recognized as very prolific due to its five different cationic crystallographic sites. Consequently, physical characteristics of SBN are strongly correlated to composition and chemical bonding. As a result of the compositional flexibility, SBN is recognized to exhibit diverse properties. Correspondingly, its potential applications are based on very attractive pyroelectric, electromechanical, electro-optic, photorefractive, and nonlinear optical and dielectric properties.

Structurally strontium-barium niobate is distinguished by its open tungsten bronze structure, i.e. the compound contains five AB_2O_6 formula units per tetragonal unit cell in which six A sites are occupied by five divalent metal ions A. As a result the empty sites give rise to quenched electric random fields even in the stoichiometric compound. Consequently, by changing the ratio between strontium and barium components one may tune the system from ferroelectric ($x < 0.5$) to a generic relaxor ($x > 0.6$) behavior while maintaining the structure unchanged [1].

Results reported in our contribution represent the first direct ECE study of strongly anisotropic non-perovskite materials. It is shown that both the absolute values of ECE and the width of the temperature range over which they are observed strongly depend on the direction of applied electric field [2]. These results are confirmed both by direct experimental measurements on single crystals cut in different directions, and theoretical predictions based on statistical mechanics. Our direct ECE measurements have also evidenced that, contrary to the polar nano-regions found in known perovskite relaxors, the PNRs are highly anisotropic in tetragonal tungsten bronze SBN75. This anisotropy highlights another promising feature of these tungsten bronzes; A solid state cooling device utilizing a highly textured form of these materials would allow for an optimized use of the ECE response, by making the most of the largest ECE directional component instead of just averaging the ECE values of randomly oriented polycrystalline systems.

[1] A.M. Glass, Investigation of the Electric Property of $\text{Sr}_{1-x}\text{Ba}_x\text{Nb}_2\text{O}_6$ with Special Reference to Pyroelectric Detection, J. Appl. Phys., vol. 40, pp. 4699-4713, (1969).

[2] F. Le Goupil, A-K. Axelsson, L. J. Dunne, M. Valant, G. Manos, T. Lukasiewicz, J. Dec, A. Berenov, and N. McN Alford, Anisotropy of the Electrocaloric Effect in Lead-Free Relaxor Ferroelectrics, Advanced Energy Materials, (to be published).

Direct measurements of the electrocaloric effect in relaxor ceramics

Mehmet Sanlialp, Vladimir V. Shvartsman, and Doru C. Lupascu

*Institute for Material Science and Center for Nanointegration Duisburg-Essen (CeNIDE),
University of Duisburg-Essen, Universitätsstraße 15, 45141 Essen, Germany*

mehmet.sanlialp@uni-due.de

Demand for energy-efficient refrigeration technologies with a reduced environmental impact has stimulated interest to materials that exhibit the electrocaloric (EC) effect. The EC effect is a change of temperature or entropy of a dielectric material under an applied electric field at adiabatic or isothermal conditions, respectively [1]. In spite of intensive studies of EC materials during the last 5 years, reliable direct measurements of the EC effect still remain a challenge [2].

In this presentation we report on the development of an experimental setup based on a differential scanning calorimeter for EC measurements of bulk samples at quasi-isothermal conditions. The setup allows measurements in the temperature range 200-500 K at applied electric fields up to 70 kV/cm. The methodology of the EC measurements is discussed. We performed the EC measurements from the PMN-PT, PLZT and BZT-BCT, BNT-BT-KNN relaxor families.

The effects of temperature and electric field magnitude on the measured EC effect are studied. Furthermore we compare the results of direct EC measurements with indirect estimations of the EC effect based on the Maxwell relations to judge the compatibility of these two measurement methods.

In addition we show the design and functionality of another experimental setup based on a quasi-adiabatic calorimeter for EC measurements of bulk samples.

[1] J. F. Scott, Electrocaloric materials, *Annu. Rev. Mater. Res.*, 41, 229-240 (2011).

[2] M. Valant, *Prog. Mater. Sci.*, 57, 980-1009 (2012).

Close-circuit domain quadruplets in BaTiO₃ nanorods embedded in SrTiO₃ film

V. Stepkova¹, P. Marton^{1,2}, N. Setter³ and J. Hlinka¹

¹- Institute of Physics, Academy of Sciences of the Czech Republic, Na Slovance 2, 18221 Praha 8, Czech Republic

²- Institute of Mechatronics and Computer Engineering, Technical University of Liberec, Studentská 2, 46117 Liberec, Czech Republic

³- Swiss Federal Institute of Technology, Lausanne CH-1015, Switzerland

stepkova@fzu.cz

Nowadays, different kinds of ferroelectric nanostructures are attracting growing attention of scientific and application community. A significant progress in processing techniques makes realization of different kinds of ferroelectric nanostructures possible. Ferroelectric nanorods, nanowires, nanotubes, nanodots and exotic vortex domain states are becoming popular due to their great potential for future applications, including information storage. Here we report about our recent theoretical study of BaTiO₃ nanorods embedded in paraelectric SrTiO₃ matrix (see Fig. 1a). [1]

The composite structure is modelled in a framework of the Ginzburg-Landau-Devonshire model using phase-field approach [2]. As expected, the properties of BaTiO₃ nanorods are different from the bulk. Our observations have shown that nanorods of 10-80 nm diameter have a rhombohedral ferroelectric state, with local polarization close to the $\langle 111 \rangle$ directions, due to mechanical clamping by the SrTiO₃ matrix. Stable configurations obtained for the 10-80 nm diameter nanorods typically break up into 4 domains, separated by 2 perpendicular planar domain boundaries intersecting the axis of the rod (Fig. 1b). We have found three possible stable configurations: the up-up-down-down-type domain structure with 109- and 71-degree domain boundaries (Fig. 1c), the up-down-up-down-type domain structure with two 109-degree domain boundaries (Fig. 1d) and the domain structure with two 71-degree domain boundaries and uniform sense of the z-component of the polarization (Fig. 1e). All these domain structures are stable with respect to a small external electric fields. Interestingly, the axial polarization component of these structures can be switched without perturbing the vortex arrangement of in-plane polarization components. It was also shown that BaTiO₃ nanorods embedded in SrTiO₃ matrix maintain ferroelectricity up to 380 K (Fig. 2), which is about 10 K below the cubic-tetragonal phase transition of stress-free BaTiO₃ bulk state. Thus, the quadruplet states could be considered as the basic stable configuration for a broad range of diameters (about 10-80 nm) and broad range of temperatures. Moreover, the in-plane clockwise or anticlockwise component of the polarization can be reversed by inhomogeneous electric fields and possibly used for information storage.

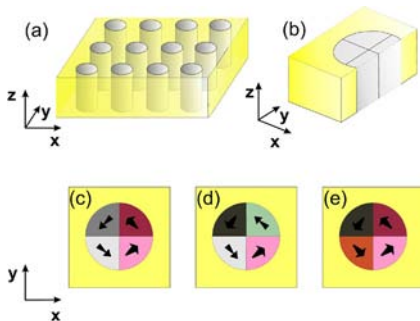


Figure 1 Scheme of the investigated heterostructure and its nanodomain states: (a) brush-like arrangement of the BaTiO₃ nanorods embedded epitaxially in the $\langle 100 \rangle$ oriented SrTiO₃ epitaxial film; (b) stable domain structure within the 40 nm nanorod, z-components of polarization arranged in a up-up-down-down manner; (c) another stable domain structure, with z-components of polarization arranged in a up-down-up-down manner.

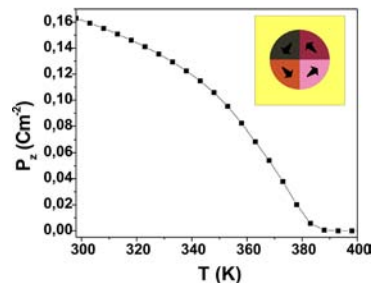


Figure 2 Temperature dependence of the average remnant polarization (in up-up-up-up state) within the 20 nm BaTiO₃ nanorod.

[1] V. Stepkova, P. Marton, N. Setter, J. Hlinka, "Close-circuit domain quadruplets in BaTiO₃ nanorods embedded in SrTiO₃ film", Phys. Rev. B 89, 060101(R), (2014).

[2] P. Marton, I. Rychetsky, J. Hlinka, "Domain walls of ferroelectric BaTiO₃ within the Ginzburg-Landau-Devonshire phenomenological model", Phys. Rev. B 81, 144125, (2010).

Rare-earth polar order and polarization due to multiferroic domain formation in YCrO_3

B.Kh. Khannanov¹, E.I. Golovenchits¹, and V.A. Sanina¹

1 - A.F. Ioffe Physical Technical Institute RAS, Saint Petersburg, Russia (Federation)

Boris.Khannanov@gmail.com

Multiferroics belong to the class of compounds in which magnetic and ferroelectric orderings coexist. Of particular interest are recently discovered multiferroics of type II where polar ordering is induced by a special magnetic ordering [1]. Magnetic and polar orders in type II multiferroics arise at similar temperatures and there is a giant magnetoelectric effect. Unfortunately, the temperatures at which such orderings emerge are typically rather low, i.e., 30 – 40 K.

Recently a polar order below the temperature of transition into the antiferromagnetic state with a weak ferromagnetism of the Cr subsystem (T_N) has been observed in the orthochromites RCrO_3 with magnetic rare-earth R ions [2]. This means that a new multiferroic of type II in which ferroelectricity emerges at the same temperature as magnetic ordering has been found. Temperatures T_N of orthochromites are rather high, i.e., 130 – 250 K. A critical role of weak ferromagnetism of the Cr subsystem and exchange interaction of magnetic R-Cr ions in the polar order was reported in [2]. This order was affected by the external magnetic field, which pointed to a rather strong magnetoelectric effect. The authors put forward the hypothesis that the polar order formation below T_N in the orthochromites with magnetic R ions was determined by two factors. They were the influence of the polarizing electric field that broke the central crystal symmetry and the effect of the exchange field of the ordered Cr subsystem on R ions that stabilized the polar state. No polarization was observed in the orthochromites with nonmagnetic R ions. Note that the investigation of polarization at $T > 200$ K in [2] was complicated by a growing leakage current in the polycrystalline samples studied.

Orthochromites have the symmetry of an orthorhombically distorted perovskite with a centrosymmetric sp.gr. $Pbmm$. The unit cell contains four formula units. The Cr^{3+} ions are in the planes $z=0$ and $z=c/2$ in nearly undistorted octahedra of oxygen ions. The axes of these octahedra, however, deviate from the z axis, along which they lie in the undistorted cubic phase. The R^{3+} ions are in the planes $z=c/4$ and $z=3c/4$. They occupy highly distorted polyhedra of eight oxygen ions. The symmetry of local positions of the R^{3+} ions is C_s , and hence the electric dipole moments of the RO_8 quasi-molecules are non-zero and lie in the (001) planes. The dipole moments of four quasi-molecules in the unit cell compensate each other, i.e., the hard antipolar or antiferroelectric states emerge in the rare-earth subsystem.

YCrO_3 is a model object for studying the nature of polar order in orthochromites and the influence of the magnetic and antiferroelectric subsystems on this order. Ions of Y^{3+} are nonmagnetic and only the subsystem of Cr^{3+} ions is magnetic (the Γ_4 (G_5F_2) (notation for Bertaut [3]) state at all temperatures below T_N). Nevertheless, the polarizations along both the c axis below $T_N \approx 135$ K and in the (001) plane at $T < T^* \approx 300$ K were observed in YCrO_3 in our experiments. As noted above, YCrO_3 , like all orthochromites with any R ions, has an antiferroelectric ordering in the (001) plane.

This paper is concerned with studies of polarization, dielectric permittivity, conductivity, dynamic magnetic susceptibility, and microwave magnetic dynamics of single crystals of YCrO_3 with nonmagnetic $\text{R} = \text{Y}$ ions are shown to exhibit polarization below $T^* \approx 300$ K with the orientation along the [110] direction and additional polarization P_c below T_N of the magnetic ordering of YCrO_3 .

The presence of impurity ions in the local R-ion positions with different electric dipole moments results in frustrations in the electro-dipole subsystem of the rare earth ions in YCrO_3 . Polar defects in YCrO_3 are likely to be lattice distortions near impurity Bi^{3+} and Pb^{2+} ions that substitute Y^{3+} ions during growth of single crystals if Bi_2O_3 or PbF_2 are used as solvents in the solution-melt, respectively. In this case, the soft antiferroelectric state for which the antiferroelectric phase transition can occur rather than the hard antipolar state arises in the YCrO_3 . In our opinion, just this state modified by the presence of two (or several) interacting electro-dipole subsystems of R-ions is responsible for the polarization observed at $T < 300$ K. Crystals of YCrO_3 grown by two different methods had qualitatively differing polar properties, magnetic properties being identical.

Near T_N , the polarization domains that exist at $T < T^*$ and the antiferromagnetic domains that arise below $T < T_N$ must match each other and form coupled polar-antiferromagnetic domains in orthochromites. In this case the polarization observed at $T < T_N$ can change in its magnitude and orientation.

The work was supported by the Government of RF (project N0.14.B25.31.0025).

1. T.Kimura, T. Goto, H. Shintani, K. Ishizaka, and Y. Tokura, Nature (London) **426**, 55 (2003).

2. B. Rajeswaran, D.I. Khomskii, A.K. Zvezdin, C.N.R. Rao, and A. Sundaresam, Phys.Rev. B **86**,214409 (2012).

3. E.F. Bertaut, in Magnetism III, edited by G.T. Rado and H. Suhl (Academic), N.Y., 1968, p. 149.

Domain Switching by Electron Beam Irradiation of Z+ Polar Surface in Mg-doped Lithium Niobate

D.S. Chezganov, M.M. Smirnov, D.O. Alikin, M.M. Neradovskiy,
D.V. Zorikhin, D.K. Kuznetsov, V.Ya. Shur

Ferroelectric Laboratory, Institute of Natural Science, Ural Federal University, , 51 Lenin Ave., 620000 Ekaterinburg, Russia

dmit.chezganov@gmail.com

The formation of the static domains with depth about 250 μm as a result of focused electron beam irradiation of Z⁺-polar surface was demonstrated in MgO-doped lithium niobate single crystals (MgOLN). The created domain patterns were visualized by high-resolution methods including piezoresponse force microscopy (PFM), atomic force microscopy (AFM), scanning electron microscopy (SEM) and confocal Raman microscopy (CRM). The main stages of the domain structure formation were revealed and explained in terms of original model. Periodically poled nonlinear-optical ferroelectric crystals are used for various photonic devices nowadays. The creation of the precise domain structure and decrease of its period stimulates the development of various domain switching methods. The irradiation of the crystal surface by focused electron beam is considered as one of the promising approaches. The method had been applied mostly for periodical poling by electron beam irradiation of Z⁻-polar surface of lithium niobate single crystals (LN) [1]. The formation of the shallow surface domains as a result of electron beam irradiation of Z⁺-polar surface of crystals of LN has been demonstrated recently [2]. We will discuss the formation of the bulk domain structure produced by focused electron beam irradiation of Z⁺-polar surface in MgOLN. Several microscopic methods have been used for domain investigation. Scanning electron microscope (Auriga Crossbeam, Carls Zeiss, Germany) attached with electron-beam lithography system (Elphy Multibeam, Raith, Germany) was used for electron beam irradiation. The static domain structures at the surface revealed by chemical etching were visualized by SEM, AFM and optical microscopy. PFM allowed to obtain the surface domain images without etching. CRM was used for reconstruction of the domain evolution by analysis of the domain images obtained at the different depth in the crystal bulk [3].

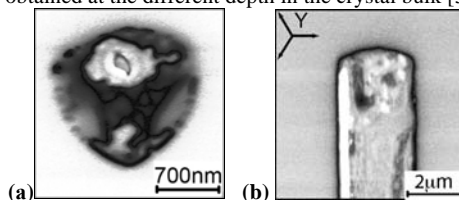


Figure 1 PFM images of domains appeared as a result of electron beam irradiation: (a) point exposure, (b) scanning along a line.

The formation of isolated domains in the bulk close to the irradiated surface was revealed after point exposure (Fig. 1a). Application of PFM and CRM allowed us to reveal the stable domains of hexagonal shape with transverse dimension up to 2 μm and a depth about 250 μm . The bulk comb domain shape was revealed after scanning along a line. The chains of isolated domains appeared near the surface for accelerating voltage 15 kV and a dose below 6 $\mu\text{C}/\text{cm}$. The solid domain lines have been visualized close to the irradiated surface for larger dose (Fig. 1b). The solid lines broke up into the isolated domain chains at a depth about 50-100 μm . The line width and domain depth increased with the dose. The instability of the domain wall shape and appearance of the domain fingers have been observed during scanning. The main stages of domain evolution were revealed. The observed effect had been attributed to polarization reversal under the action of the field produced as a result of electron beam irradiation taken into account the crucial role of the bulk screening of the depolarization field by injected electrons and conductivity of the charged domain walls. The observed effect can be used to form stable regular domain structures in MgOLN for nonlinear optical devices.

The equipment of the UCSU “Modern Nanotechnology”, Institute of Natural Sciences, UrFU has been used. The research was made possible in part by RFBR and the Government of Sverdlovsk region (Grant 13-02-96041-r-Ural-a), by RFBR (Grants 13-02-01391-a, 14-02-01160-a, 14-02-31255-mol_a, 14-02-31864-mol_a), by OPTEC LLC, by Ural Federal University development program with the financial support of young scientists.

[1] H.Ito, C.Takyu, H.Inaba, Fabrication of periodic domain grating in LiNbO₃ by electron beam writing for application of nonlinear optical processes, *Electronics Lett.*, Vol. 27(4), pp. 1221-1222, (1991).

[2] E.V. Emelin, A.I. Il'in, L.S. Kokhanchik, Recording of domains by an electron beam on the surface of +Z cuts of lithium niobate, *Physics of the Solid State*, Vol. 55(2), pp. 540-546, (2013).

[3] V.Ya. Shur, P.S. Zelenovsky, et.al., Investigation of the nanodomain structure formation by piezoelectric force microscopy and Raman confocal microscopy in LiNbO₃ and LiTaO₃ crystals, *J. Appl. Phys.*, Vol. 110, pp. 052013-1-6, (2011).

PLD Growth and Domain Patterns of Highly Tetragonal Epitaxial PZT (110) Thin Films

M. Mtebwa¹, L. Feigl¹, N. Setter¹

¹- Ceramic Laboratory, Swiss Federal Institute of Technology of Lausanne, CH-1015 Lausanne, Switzerland.

Email: mahamudu.mtebwa@epfl.ch

Extensive work have been reported on the PLD growth and properties of (100) oriented single crystalline epitaxial PZT thin films [1, 2]. On the other hand, reported (110) PZT thin films are mainly polycrystalline and of compositions close to MPB [3-5]. Furthermore, the commonly used processing techniques are MOCVD and sputtering. While the most direct way to get (110) PZT thin films is by using (110) oriented substrates such as SrTiO₃ (110), Si substrates have also been used whereby preferential (110) orientation is enhanced by using buffer layers such as Ru and PbTiO₃ [4, 6]. Epitaxial relaxed 1000 nm thick (110) Pb(Zr_{0.52}Ti_{0.48})O₃ thin films grown on 200 nm thick SrRuO₃ bottom electrode with SrTiO₃ (110) substrate by radio frequency (rf) sputtering were reported by Ouyang et al. [5]. On these films, 90° walls extending along [111] were observed. In addition, a low field longitudinal piezoelectric coefficient of about 200 pmV⁻¹ was measured. The high piezoelectric activity was explained assuming that 90° domain walls are mobile.

In this work we report the growth of high quality epitaxial, mono-crystalline Pb(Zr_{0.05}Ti_{0.95})O₃ thin films with step flow growth mode by PLD on SrTiO₃ (110) substrate. The substrates were etched with BHF and annealed in air for 1hr at 1000° C. For good quality film-electrode interface, conductive La_{0.8}Sr_{0.2}MnO₃ was used as the bottom electrode because unlike SrRuO₃ as it is not affected by double surface termination of SrTiO₃ (110) substrate. The reciprocal space map analysis shows that the films are under unsymmetrical in-plane strain along [001] and [1-10] orientations. As grown films are self-poled however domain patterns can be modified by systematic poling procedures with PFM tip. Details of the growth and the resulting domain patterns before and after poling will be reported.

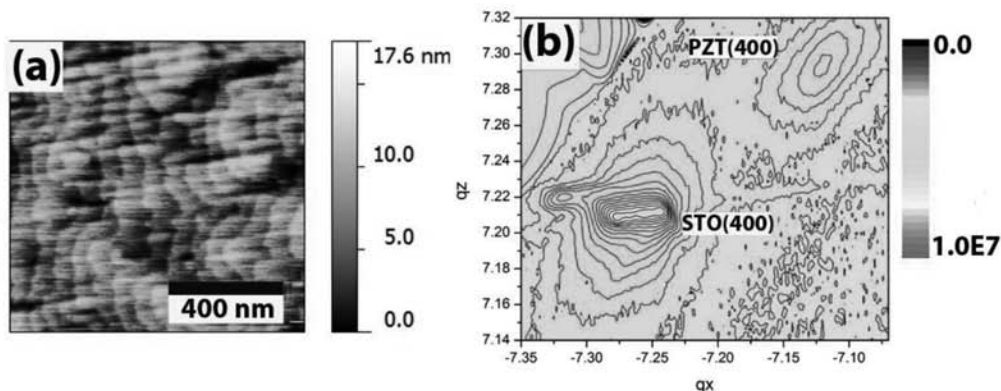


Figure 1 : A 80nm thick Pb (Zr_{0.05}Ti_{0.95}) O₃ thin film. (a) AFM image. (b) Reciprocal space map of in-plane (400) peak showing PZT film under compressive strain.

- [1] N. Izyumskaya, Y.-I. Alivov, S.-J. Cho et al., Processing, Structure, Properties, and Applications of PZT Thin Films, Critical Reviews in Solid State and Materials Sciences, vol. 32, pp.111-202, (2007).
- [2] C. S. Ganpule, V. Nagarajan, H. Li, et al., Role of 90° Domains in Lead Zirconate Titanate Thin Films, Applied Physics Letters, vol. 77, pp.292-294, (2000).
- [3] K. Saito, I. Yamaji, T. Akai, et al., Domain Structure and Residual-Strain Characterization of Epitaxial Pb(Zr,Ti_{1-x})O₃ Thin Films, IEEE, (2001).
- [4] Chun-Sheng Liang and Jenn-Ming Wu, Characterization of highly (110)- and (111)-oriented Pb(Zr,Ti)O₃ films on BaPbO₃ electrode using Ru conducting barrier, Applied Physics Letters, vol. 87, pp. 022906-1- 022906-3, (2000).
- [5] J. Ouyang, J. Slusker, I. Levin et al., Engineering of Self-Assembled Domain Architectures with Ultra-high Piezoelectric Response in Epitaxial Ferroelectric Films, Advanced Functional Materials, vol. 17, pp. 2094-2100, (2007).
- [6] D. Ambika, V. Kumar, K. Tomioka et al., Deposition of PZT thin films with {001}, {110}, and {111} crystallographic orientations and their transverse piezoelectric characteristics, Advanced Materials Letters, vol. 3, pp. 102-106, (2012).

Domain wall conduction in Ytterbium Manganite

M. P. Campbell¹, J. R. Whyte¹, A. Kumar¹, J. M. Gregg¹

¹- Centre for Nanostructured Media, School of Mathematics and Physics, Queen's University Belfast, Belfast BT7 1NN, United Kingdom

mcampbell69@qub.ac.uk

Hexagonal manganites have previously been shown to have interesting electrical properties at ferroelectric domain walls [1]. In ErMnO_3 [2] for example, domain walls are seen to have increased or decreased resistivity, compared to the bulk domains, depending on the local polarisation configuration at the boundary. Similar behaviour was predicted for other members of the series, such as YbMnO_3 studied here.

A combination of Piezorepsonse Force Microscopy (PFM) and conductive-Atomic Force Microscopy (c-AFM) was used to investigate YbMnO_3 and confirm the expected conductive behaviour. As shown in Figure 1(b), the inhomogeneous electrical properties of YbMnO_3 appear to be more pronounced than literature reports for ErMnO_3 [2]. From comparison of the c-AFM and PFM images, Figure 1, it is apparent that the conductivity of the domain wall is greatest where the polarisation vectors meet 'tail to tail' and varies as a function of the relative polarisation angle: mimicking the bulk when parallel and lowest in a 'head to head' configuration. This behaviour can be explained via the electrostatic potential within the domain wall and will be discussed further in the poster. The explicit relationship between domain configuration and conductivity suggests a direct route for manipulating the electrical properties making YbMnO_3 a promising material for domain wall engineering and devices.

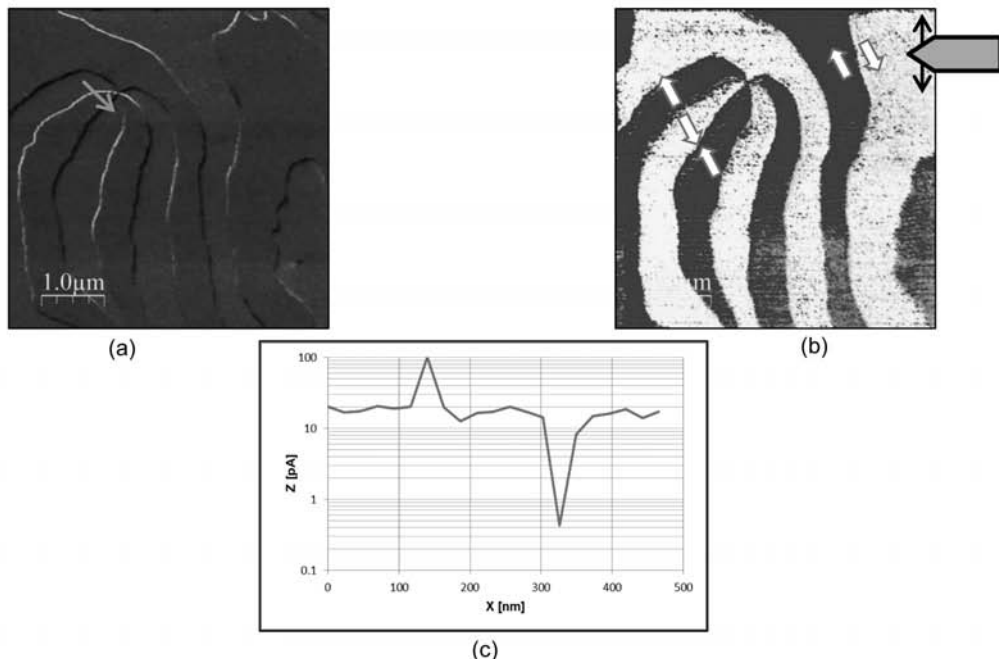


Figure 1. (a) A c-AFM scan of a six-fold domain wall vertex in YbMnO_3 , $5\mu\text{m}\times 5\mu\text{m}$. The domains are clearly visible with white and black walls showing high and low conductance relative to the grey bulk. (b) Lateral PFM phase map conveying the scan orientation, with arrows depicting the relative domain polarisations. (c) The line profile of the local conductivity along the diagonal arrow near the vertex in (a).

[1] T. Choi et al, Insulating interlocked ferroelectric and structural antiphase domains in multiferroic YMnO_3 , *Nature Materials*, 9, 253-258, (2010)

[2] D. Meier et al, Anisotropic conductance at improper ferroelectric domain walls, *Nature Materials*, 11, 284-288, (2012)

Study of planar domain structures in LiNbO₃ crystals using Raman spectroscopy and X-ray diffractometry

A. Irzhak, D. Irzhak, L. Kokhanchik

*Institute of Microelectronics Technology and High-Purity Materials RAS
142432, Russian Federation, Moscow region, Chernogolovka, Academician Ossipyan str., 6*

irzhak@iptm.ru

This work presents results of planar domain structures formed in LiNbO₃ crystal study. Domain structures were formed on the crystal surface layer using electron-beam irradiation in the SEM. Using this method planar domain structures were formed in +Z-cut [1] and Y-cut [2] of LiNbO₃ crystals. These structures were investigated using methods of Raman spectroscopy [3] and X-ray diffractometry [4].

Figure 1(a) presents dependence of the frequency shift of the depth of the crystal for the inverted and non-inverted regions of the crystal. Inverted region is characterized by a frequency shift near the surface down to 5 microns. This indicates the presence of the crystal lattice deformation in this area.

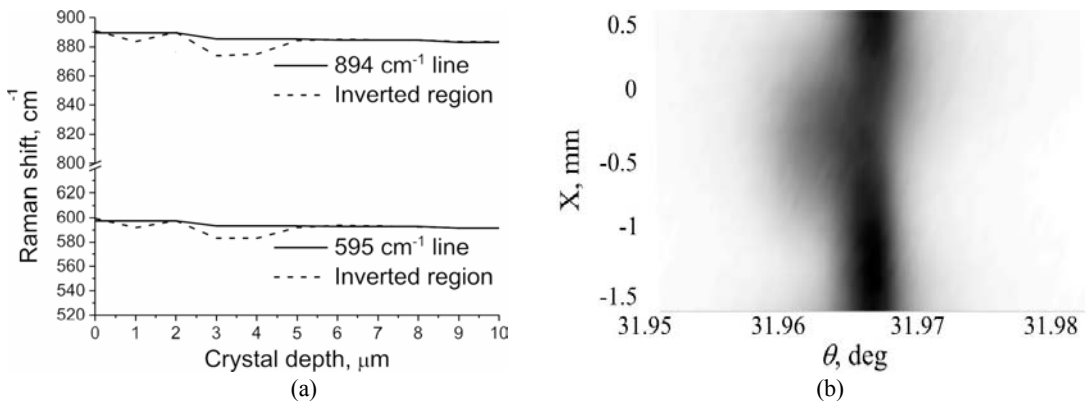


Figure 1 +Z-cut of LiNbO₃ crystal, U= 15 kV, I= 0,5 pA: (a) Frequency shift of the depth of the crystal for the inverted and non-inverted regions of the crystal; (b) Angle distribution of diffracted x-ray intensity crossing the inverted region.

X-ray data shown on Figure 1(b) also detects deformation in inverted region. High intensity of x-ray diffuse scattering corresponds to the high concentration of crystal lattice defects.

Combination of Raman spectroscopy and X-ray diffraction data has allowed to determine the thickness of the inverted layers formed at different accelerating voltages and electron beam irradiation doses.

- [1] Emelin, EV; Kokhanchik, LS; „Recording of domains by an electron beam on the surface of+ Z cuts of lithium niobate, Physics of the Solid State, vol. 55 , N 3 ,pp. 540-546, (2013)
- [2] Kokhanchik, LS; Punegov, DV; „The Possibility of Planar Periodic Domain Structures Engineering on the Y-Cut Surfaces of LiTaO₃ Crystals by E-Beam Point Writing, Ferroelectrics, vol. 373, N 1, pp. 69-76, (2008)
- [3] Hammoum, R.; Fontana, MD.; Bourson, P.; Shur, VY.; Characterization of PPLN-microstructures by means of Raman spectroscopy. Applied Physics A, vol. 91, N 1, pp. 65-67. (2008).
- [4] Kokhanchik, LS; Irzhak, DV; Antipov, VV, Characterization of periodic domain structures in lithium niobate crystals by scanning electron microscopy and X-ray diffraction analysis, Journal of Surface Investigation. X-ray, Synchrotron and Neutron Techniques, N 4, pp. 546-552, (2008)

X-ray diffraction and Raman spectroscopy studies in $\text{Na}_{1/2}\text{Bi}_{1/2}\text{TiO}_3\text{-SrTiO}_3\text{-PbTiO}_3$ solid solutions

M. Dunce, E. Birks, A. Kuzmin, R. Ignatans, A. Plaude, M. Antonova, A. Sternberg

Institute of Solid State Physics, University of Latvia, Kengaraga 8, LV-1063, Riga, Latvia

marija.dunce@cfi.lu.lv

Previously a transfer from relaxor to ferroelectric state, passing different stages of relaxor behaviour, was established in triple solid solutions $(1-x-y)\text{Na}_{1/2}\text{Bi}_{1/2}\text{TiO}_3\text{-}x\text{SrTiO}_3\text{-}y\text{PbTiO}_3$ (NBT-ST-PT $1-x-y/x/y$) by studying their dielectric properties [1]. In this study, NBT-ST-PT 40/60- y/y solid solutions were investigated by x-ray diffraction and Raman spectroscopy. Although compositions with low concentration of PT exhibit pure relaxor behaviour even without electric field-induced phase transition to ferroelectric state, some traces of tetragonal phase were observed in x-ray diffraction patterns. An amount of tetragonal phase and a degree of tetragonality upon temperature variation were determined for several compositions with different content of PT, using the Rietveld method [2]. We found that the tetragonal phase persists in a wide temperature range of relaxor state. An influence of local inhomogeneous lattice strains on the broadening of x-ray diffraction maxima and concentrations of tetragonal and cubic phases was studied. Strong first-order Raman scattering due to the tetragonal phase was observed for all studied compositions independently of PT content. The spectral features as functions of temperature and PT concentration are discussed for different types of lattice vibrations.

[1] E. Birks, M. Dunce, M. Antonova, and A. Sternberg, Phase Transitions in modified $\text{Na}_{1/2}\text{Bi}_{1/2}\text{TiO}_3\text{-SrTiO}_3$ Solid Solutions, *Phys. Status Solidi C*, vol. 6, pp. 2737-2739 (2009).

[2] A. C. Larson AC and R. B. Von Dreele, General Structure Analysis System (GSAS), Los Alamos National Laboratory Report, LAUR: pp. 86-748 (1994).

Solid state reaction of multifunctional strontium modified $\text{CaCu}_3\text{Ti}_4\text{O}_{12}$ powders

L.A Saska⁽¹⁾, A.A Felix⁽²⁾, A.Z. Simões⁽¹⁾, M.A Ramirez⁽¹⁾

1. Faculdade de Engenharia de Guaratinguetá, Universidade Estadual Paulista, UNESP, Guaratinguetá, SP, Brasil.
2. Instituto de Química, Universidade Estadual Paulista, UNESP, Araraquara, SP, Brasil.

The study of advanced ceramic materials is constantly a topic of mutual interest in science [1]. Few studies have been conducted analyzing the substitution of Ca^{2+} by the Sr^{2+} [2]. In this work, the calcium was substituted by strontium in amounts of 0%, 5%, 10%, 50%, 90% and 100% in the $\text{CaCu}_3\text{Ti}_4\text{O}_{12}$ (CCTO). The powders obtained by solid state reaction were characterized by means of thermal analysis such as TG (thermogravimetry), DTA (differential thermal analysis), dilatometry, X-ray diffraction (XRD) and scanning electron microscopy (SEM-EDS). A weight loss at around 6% can be attributed to carbonates decomposition and is evident at a temperature of 950° C. After calcination and milling processes, the particles presented approximately spherical shapes (see Figure 1a). High percentages (over 50%) of Ca^{2+} by Sr^{2+} substitution reveal necks between the particles (see Figure 1b).

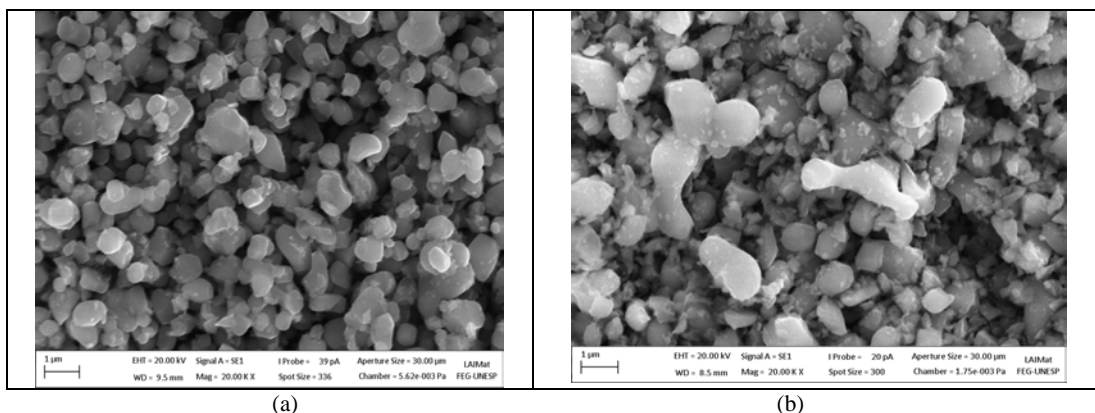


Figure 1. Scanning electron microscopy by: (a) sample with 0% substitution of Sr^{2+} in place of the Ca^{2+} (CCTO) and (b) sample with 90% substitution of Sr^{2+} in the place of the Ca^{2+} (CCTO 90% Sr).

Energy Dispersive Spectroscopy (EDS) analysis showed differences on stoichiometries similar to what expected theoretically (see Table 1) except of oxygen element where EDS technique is not accurate.

Table 1. Stoichiometric equation of the samples obtained from de results of the EDS technique.

Sample	Stoichiometric equation
CCTO	$\text{Ca}_1\text{Cu}_{3,15}\text{Ti}_{4,08}\text{O}_{19,24}$
CCTO 5% Sr	$\text{Ca}_{0,945}\text{Sr}_{0,055}\text{Cu}_{3,34}\text{Ti}_{4,23}\text{O}_{19,04}$
CCTO 10% Sr	$\text{Ca}_{0,874}\text{Sr}_{0,126}\text{Cu}_{3,18}\text{Ti}_{4,02}\text{O}_{25,92}$
CCTO 50% Sr	$\text{Ca}_{0,438}\text{Sr}_{0,562}\text{Cu}_{3,07}\text{Ti}_{3,67}\text{O}_{30}$
CCTO 90% Sr	$\text{Ca}_{0,105}\text{Sr}_{0,895}\text{Cu}_{2,88}\text{Ti}_{3,82}\text{O}_{17,80}$
SCTO	$\text{Sr}_1\text{Cu}_{2,55}\text{Ti}_{3,42}\text{O}_{21,43}$

[1] Chung, S.Y.; Kim, I.D.; Kang, S.J. Strong nonlinear current-voltage behaviour in perovskite-derivate calcium copper titanate. Nature Materials v. 3, p. 774-778 (2004).

[2] Schmid, T.; Sinclair D.C. Anomalous increase of dielectric permittivity in Sr-doped CCTO ceramics $\text{Ca}_{1-x}\text{Sr}_x\text{Cu}_3\text{Ti}_4\text{O}_{12}$ ($0 < x < 0.2$). Chemical of Materials Communications, 22, 6-8, 2010.

Properties and Deposition of TiNO_x Thin films using Reactive Magnetron Sputtering

H.H. Kim¹, D.C. Oh¹, and G.I. Jang²

1- Display Eng. School, Doowon Tech. University, Jurawi-Gil 159, Paju-Eu, Paju, Gyeonggi, Korea

2- Advanced Materials Eng., Chungbuk Nat'l University, Naesudong-Ro 52, Heungduk ku, Chungju, Chungbuk, Korea

hhkim@doowon.ac.kr

This study was done on electrical and optical characteristics of solar absorber using experimental equipment. TiNO_x thin films were prepared on aluminum substrates by reactive dc magnetron sputtering technique and annealed from 200 to 350°C in air for 2 hrs. The results of thermal stability showed that the solar selective thin films of TiNO_x were stable for use at temperature of 350 °C. The sputtering conditions were as follows; current density of 200~450 mA/cm², voltage of 150~350 V, T-S distance of 10 cm, sputtering time of 10~30 min, and gas ratio $\text{O}_2 : \text{N}_2$ of 1 : 1~5 : 1. The thickness of thin films was measured by alpha step profilometer and about 200 nm. The crystallinity and surface properties were estimated by X-ray diffractometer (XRD) and scanning electron microscopy (SEM). The exact composition and optical properties of TiNO_x thin films was measured by Auger electron spectroscopy and UV-Vis-NIR spectrophotometry. The roughness of thin films on atomic force microscopy (AFM) showed very smooth and was approximately 0.1~0.2 nm. Their grain size was also very small. Atomic force microscopy showed that thin film layers became very rough with increasing annealing temperatures and that their grain sizes became very large. The optical properties were a solar absorptance of 0.80 ~ 0.90 and a thermal emittance of 0.01 ~ 0.03.

- [1] K. Lee, Preparation and Characterization of Black Chrome Solar Selective Coatings, Journal of the Korean Physical Society, vol. 51, pp. 135-144, (2007).
- [2] K. Lee, Deposition of Cermet Solar Selective coatings for High Temperature Applications, Journal of the Korean Solar Energy Society, vol. 26, pp. 57-64 (2006)
- [3] T. Lee, D. Kim, H. Kim, W. Yeo, Application of Pulse Current Electrolysis to the Large scale of Copper and Aluminium Substrates for Solar Selective Coatings on Solar Collectors, Journal of the Korean Energy Eng., vol. 5, pp. 108-114(1996).
- [4] H. Lee, J. Kim, S. Lee, Y. Kang, S. Lee, M. Park, A Study of Reflectance Variations of Solar Concentrators, Journal of the Korean Solar Energy Society, vol. 30, pp. 107-114 (2010)

Electric field distribution on grain boundaries in LiNbO_3 thin films

D.A. Kiselev, R.N. Zhukov, A.S. Bykov, S.V. Ksenich, M.D. Malinkovich, Yu.N. Parkhomenko

National University of Science and Technology "MISIS", Leninskiy pr. 4, 119049 Moscow, Russian Federation

dm.kiselev@gmail.com

Thin films of Lithium Niobate (LiNbO_3) possess a number of advantages over bulk material including the possibilities of producing step index profiles, selectively introducing dopants, and the fabrication of multilayer structures. In addition there are certain applications where only thin films can be used as, for example, when a large refractive index difference between the film and the substrate is necessary. The prospect of producing high quality (oriented and possessing low optical loss) thin films of LiNbO_3 on silicon substrates is particularly attractive because the silicon provides a rigid and flat substrate ideal for large area processing of devices by lithographic techniques and it allows for the integration of lithium niobate electro-optic and silicon integrated circuit technology. The surface charges (electrons and holes) injected to the ferroelectric surface would influence the data storage density and further impact the bit readout, signal reliability and stability. It is an emerging task to quantitatively determine surface charges densities as well as their exact contributions to the physical properties.

The studied LiNbO_3 films were deposited by radio-frequencies magnetron sputtering of the single-crystalline target in $\text{Ar}/\text{O}_2=1$ atmosphere (0.6 Pa) on n-type Si (111) substrates ($\rho = 2 \Omega \cdot \text{cm}$). The subsequent thermal annealing of the obtained structures has been done in air at 700 °C for 2 hours. Atomic force microscopy measurements indicate that the surface roughness of the LiNbO_3 thin films was 8 nm, which meets the demands for practical waveguiding devices. The local electric field distribution on grain boundaries of polycrystalline LiNbO_3 thin film have been investigated by electrostatic force microscopy (EFM) using scanning probe laboratory NTEGRA-Prima (NT-MDT). From EFM images was seen that with increasing voltage the contrast of EFM signal at the grain boundary becomes gradually more intense signal compared to the grains. Also, we made measurement a nanoscale current as a function of bias voltage (I-V characteristic) for grain and grain boundary. Completely distinct conducting processes and resistive switching effects were observed in the grain boundary and volume grain. At lower voltages the electrical conduction is dominated by the grain boundary and is associated with the redistribution of oxygen vacancies in the grain boundary under external electric fields. From the point of view of applications, the results point to the possible application of the modulation of electrical conductivity in thin films of LiNbO_3 , which are also applicable to other ferroelectric materials and multiferroic.

Charge transport phenomena in PLZT thin films

A. Sigov, Yu. Podgorny, A. Vishnevskiy, and K. Vorotilov

Moscow State Technical University of Radioengineering, Electronics and Automation, Moscow, Russia

E-mail: sigov@mirea.ru

Doping by lanthanum is widely used to compensate hole conduction in PZT. In this report we have tried to establish main mechanisms of charge transport in sol-gel PZT films with different La concentrations for various regions of the electric field. $\text{Pb}_{1-x}\text{La}_x(\text{Zr}_{0.48}\text{Ti}_{0.52})_{1-x/4}\text{O}_3$ films with $x = 0, 0.02, 0.05, 0.08, \text{ and } 0.1$ are deposited by spin-on sol-gel techniques on platinum plated silicon substrates with intermediate pyrolysis of each layer at 400 °C and final annealing at 650 °C for 20 min. The final thickness of the PLZT films is about 240 nm. As expected, doping by La effects on polarization behavior of PZT films, the values of remanent polarization P_r and coercive field E_c decrease with the increase of La content (23 $\mu\text{C}/\text{cm}^2$, 52 kV/cm respectively for undoped film; 7 $\mu\text{C}/\text{cm}^2$, 25 kV/cm for the film with $x = 0.02$, and so on). Current-voltage dependencies are studied at the voltage ramp speed of 0.005 and 0.0025 V/s. It was found that the I - V dependencies of all PLZT films have two characteristic regions: low- and high-voltage. In the low-voltage region (up to 80 – 90 kV/cm) the influence of La concentration is negligible and has no definite relationship, see the Figure. The leakage current in this region is determined mainly by the high resistance of depletion region of the reverse-bias Schottky barrier at the electrode-ferroelectric interface, as a result the current is practically independent of La content. In the high-voltage region the Schottky barrier breakdown occurs above some threshold voltage and the current is mainly determined by the film bulk resistance. As a result, the dependence of the leakage current on La concentration becomes particularly pronounced in this region. At the 2% La content, the leakage current in this region reduces by about two orders in contrast to an undoped PZT film. Further increase of La content leads to an increase of leakage current as a result of change in conductivity mechanism from p - to n -type. The conductivity mechanism in this case is a combination of a limited interface injection and bulk limited drift-diffusion.

Strontium Titanate Thin Film Multilayer Structures for Switchable FBAR Applications

A. Kozyrev¹, A. Mikhailov¹, S. Ptashnik¹, N. Alford², P. Petrov²,

1 - Department of Physical Electronics and Technology Saint-Petersburg State Electrotechnical University, 5 Prof. Popova Street, Saint-Petersburg, Russia, 197376

2 - Department of Materials, London Imperial College, London SW7 2AZ, United Kingdom

Main author email address: mikhailov@umwlab.com

Development of film bulk acoustic resonators (FBAR) is one of the promising areas of modern microwave electronics. The operating frequency of these resonators is determined by the thickness and by the elastic characteristics of the material they are made of, which limits substantially the ability of their effective dynamic tuning. Therefore, development of FBARs with ability to electrically control their resonance frequency is an challenging problem, which could lead to a significant improvement of the modern filter devices and microwave systems.

A possible solution of this problem is to replace the piezoelectric materials traditionally used for FBAR fabrication, with ferroelectric materials in paraelectric phase. A good candidate is the strontium titanate (STO), which in the absence of an external electrical field exhibits only electrostrictive properties. However, an applied dc bias induces a piezoelectric effect. The intensity of the applied field determines the value of the piezoelectric coefficient.

It was shown in [1, 2], that by changing only the sign of the applied bias field to one of the layers in a resonator with two ferroelectric layers, it is possible to realize a switch of its operating frequency to a twice higher value. This effect was contributed to the selective excitation of the normal acoustic modes in this acoustic resonator. If the direction of the bias field in the both layers is the same, there are effectively excited the odd normal modes, and if the polarities of the bias fields applied to the both layers are opposite then only even normal modes are effectively excited. In structures with one piezoelectric layer, the excitation of even modes is impossible.

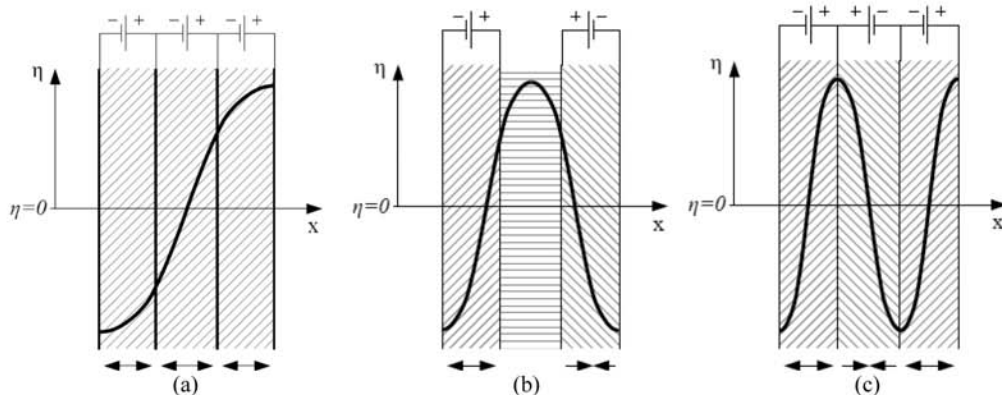


Figure 1. One dimensional schematic layout of the multilayer resonance structures with three ferroelectric films. The solid lines show the profiles of the mechanical displacement (η) standing waves for the first (a), second (b) and third (c) normal modes. Different angles of background shading correspond to the different signs of the DC polarity in the layers. On the top side of the graphs the polarity of the DC field applied to the individual active layers depicts. (It has to be emphasized that the sign of the DC field polarity is not important. It is only important its change that occurs at the active layers interface.

This work presents an FBAR architecture with improved tuning range. It is based on a multilayer structure with three ferroelectric layers (we will call them active layers) separated by conductive electrodes, where one could change not only the amplitude of the DC bias field applied to the layers but also its polarity, hence individually change the value and sign of the induced piezoelectric coefficients. In turn, piezoelectric coefficients distribution along the structure defines the excitation efficiency of each normal acoustic mode (fig.1).

- [1] T.R. Gururaja, A. Shurland, and J. Chen. Medical ultrasonic transducers with switchable frequency bands centered about f_0 and $2f_0$. Proceedings of 1997 IEEE Ultrasonic Symposium, pages 1660–1662, August 1997.
- [2] A.B. Kozyrev, A.K. Mikhaylov, S.V. Ptashnik et al. Electronically switchable bulk acoustic wave resonator based on paraelectric state ferroelectric films. Electronics Letters. – V. 47, No 24, pages 1326–1327, 2011.

Pulsed laser deposition and characterization of compressively-strained SrTiO₃ thin films

Š. Bagdzevičius^{1,2}, J. Banys¹, N. Setter²

¹ Faculty of Physic, Vilnius University, Sauletekis str. 9/3, LT-10222 Vilnius, Lithuania

² Ceramics Laboratory, Swiss Federal Institute of Technology (EPFL), CH-1015 Lausanne, Switzerland

Main author email address: sarunas.bagdzevicius@ff.vu.lt

The aim of this work was to investigate processing conditions and deposit epitaxially strained STO (SrTiO₃) thin films with smooth and well defined interfaces for further research. Influence of deposition temperature, laser fluence and repetition rate, ambient pressure on growth mode and film quality was studied. Heteroepitaxial STO thin films were deposited on LSAT (001 oriented) ((LaAlO₃)_{0.3}-(Sr₂AlTaO₆)_{0.7}) single crystal substrates with STO buffer layer (Fig. 1a) and LSMO (La_{0.8}Sr_{0.2}MnO₃) electrode by pulsed laser deposition with KrF excimer laser ($\lambda=248$ nm). STO and LSMO ceramics were used as the targets. Substrates were cleaned with acetone and isopropanol and annealed in argon flow at 1250°C at the same time controlling La vapour pressure at LSAT substrate surface [1] to get atomically flat surface. Best quality STO films were obtained at 780°C deposition temperature, with 2 Hz laser repetition rate and 40 mJ energy. The oxygen pressure was 0.1 mBar during deposition and was raised to 1 mBar during cool down. Both LSMO electrode and STO thin films showed good epitaxy (Fig. 1b) and crystallinity, XRD STO 002 reflex rocking curve FWHM was 0.039° (STO film thickness 100 nm, LSMO electrode thickness 17 nm, STO buffer layer thickness 10 nm). Obtained thin films were analysed by structural and local characterization techniques – XRD, temperature dependent AFM (Fig. 1 a, b)/PFM, TEM and RHEED.

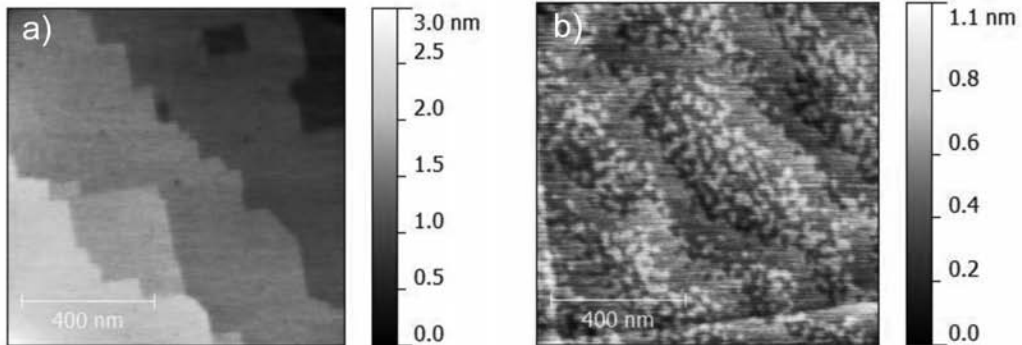


Figure 1. AFM images of a) STO buffer layer after annealing, b) SrTiO₃ heteroepitaxial thin film STO/LSMO/STO/LSAT (STO thickness - 100 nm, LSMO - 17 nm, STO buffer - 10 nm).

Acknowledgements

This work has been financed by the Lithuanian-Swiss cooperation programme "Research and development" joint research project "SLIFE", project code LSP-12 007.

References

[1] J. H. Ngai et al., Adv. Mater., 22, 2945 (2010).

Injected charge as a cause of slow dielectric relaxation in thin film Pt/BSTO/Cu structures

T. Samoylova, M. Gaidukov, A. Gagarin, A. Tumarkin, A. Kozyrev

Saint Petersburg Electrotechnical University "LETI", Prof. Popova Str., 5, Saint-Petersburg, Russia

mlpeltech@gmail.com

There is a problem of capacitance slow relaxation in ferroelectric tunable sandwich capacitors after control voltage switching-off (Fig.1 a) [1]. Reasons of such phenomenon are attributed in literature to space charge formation and its redistribution under drift and diffusion conditions [2,3]. In work presented sandwich capacitor structure based on BSTO thin film with different film-metal interface conditions (BST/Pt and BST/Cu) is investigated by microwave signal with short-circuit conditions by direct current on electrodes.

A top interfacial layer is formed in vacuum and therefore is depleted with oxygen but enriched with free electrons. As a result, contact close to "ohmic" is formed at a top BST/Cu interface. A bottom Pt/BST interface is formed in oxygen plasma and therefore appears to be enriched with excess oxygen, providing a high density of deep localized trap states in the band gap of BST film. The lack of a chemical interaction between Pt and BST results in the formation of a low permittivity layer ("dead" layer) between Pt electrode and BST film.

Model for electric field distribution with "dead-layer" included is suggested (Fig.1 b). The initial (just after voltage switching-off) distribution of a built-in electric field along the BST film thickness is derived from the solution of Poisson equation for the three-layered structure, composed of a dead layer (d_f), a space-charge layer (d_p) and a free of space-charge layer. Thermally released charge carriers, being to the left and to the right sides of a zero field plane (x_0), drift in the space-charge-induced electric field to opposite electrodes. Upon coming to Cu-electrode, carriers leave BST film. However, the presence of a dead layer keeps the carriers from entering to Pt-electrode. Calculated results for initial relative remnant capacitance $\Delta C_{r0}/C_0$ based on model suggested (Fig.1 c) are in good agreement with experimental data.

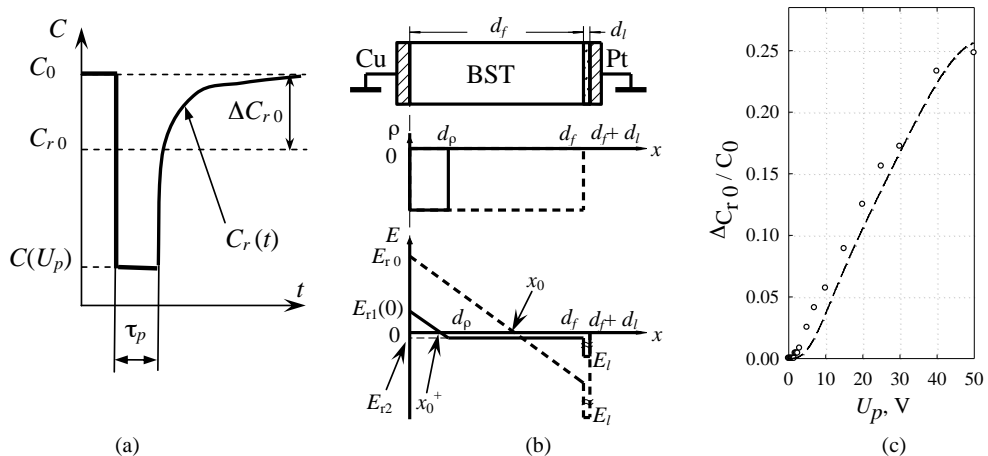


Figure 1 Schematic of a capacitance response to pulsed voltage. (a) Sketch of capacitor structure, space charge distribution (ρ) and electric field distribution (E). (b) Simulated remnant capacitance deficiency $\Delta C_{r0}/C_0$. (c)

For microwave applications of BSTO film-based structures it is important to minimize the remnant effects attended with their slow relaxation. One way to resolve this problem could be the use of three-layered dielectric, including two linear dielectric layers, meant for blocking the injection, in addition to BSTO layer.

The reported study was partially supported by RFBR, research project No. 13-02-12096 ofi_m.

[1] P. K. Petrov, N. M. Alford, A. Kozyrev et al., Effect of ultraviolet radiation on slow-relaxation processes in ferroelectric capacitance structures, *J. of App. Phys.*, 107, pp. 084102 (2010).

[2] A. K. Tagantsev, I. Stolichnov, E. L. Colla, and N. Setter, Polarization fatigue in ferroelectric films: Basic experimental findings, phenomenological scenarios, and microscopic features, *J. of App. Phys.*, 90, pp.1387-1402 (2001).

[3] V. V. Lemanov, B. M. Goltsman, V. K. Yarmarkin, and Y. A. Boikov, Slow Dielectric Relaxation in SRO/BSTO/SRO Ferroelectric Thin Film Capacitor Structures, *Ferroelectrics*, 286., pp. 251-259, (2003).

PZT films prepared by sol-gel with low lead content seeding layer

K.Vorotilov, D. Seregin, A.Sigov

Moscow State Technical University of Radioengineering, Electronics and Automation, Moscow, Russia

E-mail: sigov@mirea.ru

Ferroelectric PZT thin films remain playing a key role as an active media in integrated ferroelectric devices due to a rather low crystallization temperature typical to lead based perovskites. Main trends in microstructure transformation connected with the lead content are reported e.g. in [1]. The main nucleation mechanism for the films with low or middle lead content is direct nucleation of {111} perovskite (Pe) grains on {111} platinum. Volume nucleation proceeds with creation of small pyrochlore (Py) particles. Nucleation and growth rates of Pe grains are increased with the lead excess in the film. At a very high lead content in PZT films ($x=30 - 50$ mol. %) PbO crystals stimulates nucleation of {100} Pe grains due to a good lattice correlation. As a result of high growing rate and growing in {111} and {100} directions, the Pe grains become smaller and not all from them are growing through the whole thickness of the film.

In this work the two-step crystallization process is used. At the first step crystallization with a low nucleation rate is used for large Pe {111} grains formation. Further crystallization is carried out at the Pb excess conditions for prevention of Py formation. Thus samples with a combination of seed layers from solutions with 0 and 5 wt.% Pb excess and the main layers with 15 and 30 wt.% Pb excess are formed.

It is shown that the seed layer from solutions with the low Pb content leads to improvement of polarization properties of PZT films. For example if the seed layer is formed from the solution with 5% Pb excess, and other layers are deposited from solution with 30% Pb excess, then residual polarization is increased ($P_r=33.8 \mu\text{C}/\text{cm}^2$ with the seed layer and $P_r=26 \mu\text{C}/\text{cm}^2$ without it).

An effect of the seed layer becomes less pronounced if the seed layer is not preliminary crystallized.

[1] AS Sigov, KA Vorotilov, OM Zhigalina. *Ferroelectrics*. 433(1), 146-157 (2012).

Control of carrier injection into dielectric BST thin films

S. Hillmann, S. Li, K. Rachut, T.J.M. Bayer, A. Klein

Technische Universität Darmstadt, Institute of Materials Science, Jovanka-Bontschits Str. 2, 64287 Darmstadt, Germany

shillmann@surface.tu-darmstadt.de

Barium strontium titanate (BST) is a high permittivity oxide with a wide range of applications, e.g. as tunable dielectrics or non-volatile memories. Therefore electrical and dielectric properties are of major interest. Usually insulating behaviour is requested but for the investigation of charge transport properties high charge carrier injection is required to avoid injection limited charge transport. There are two possibilities: (i) choosing a contact material with negligible injection barriers at the interface, e.g. $\text{In}_2\text{O}_3:\text{Sn}$ as electrodes [1], and (ii) insertion of a low permittivity layer between dielectric and electrode (artificial dead layer) [2].

A common electrode material for BST is Platinum which forms a barrier height between 0.5eV and 1eV depending on the deposition conditions [3]. Thus, the current is limited by the injection barriers at the interface. In this contribution Al_2O_3 was inserted as artificial dead layer material. Compared with BST ($\epsilon_r \approx 350$) it has a low permittivity of $\epsilon_r \approx 7$. A large part of the applied voltage drops down therefore in the Al_2O_3 which shifts the Fermi level of Pt upwards (see right part of Fig.1). BST was deposited by rf-sputtering whereas atomic layer deposition was used for the deposition of Al_2O_3 . The layers were prepared directly back-to-back without leaving the UHV.

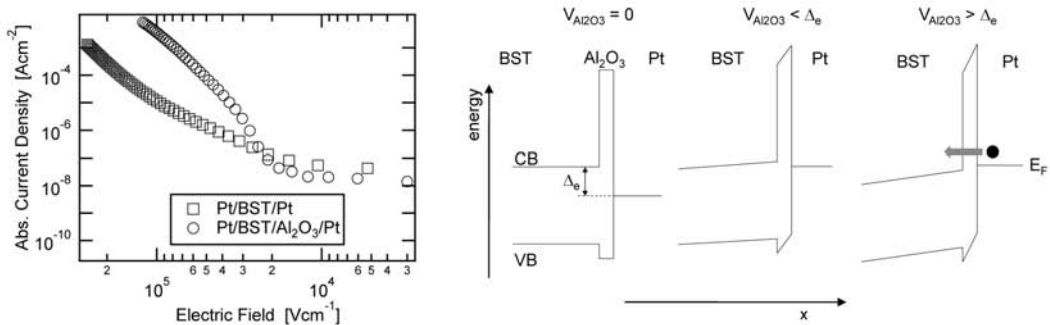


Figure 1: Double logarithmic presentation of J-V characteristics of a sample with (circles) and without (squares) Al_2O_3 layer (left). The current density with Al_2O_3 is higher than without Al_2O_3 . Energy band diagram for different voltages (right). The arrow in the right diagram indicates tunnelling through Al_2O_3 from Pt into the BST conduction band. $V_{\text{Al}_2\text{O}_3}$ and Δ_e denotes the potential drop in the Al_2O_3 layer and energy difference between the Fermi level of Pt and the BST conduction band, respectively.

It will be shown that the choice of substrate and BST target are crucial for the injecting properties of the sample. A rough Pt bottom electrode can cause a non-uniform BST surface and therefore local differences in the current voltage behaviour. Different BST target materials also lead to different current densities, which is assigned to different impurity concentrations. Furthermore the artificial dead layer thickness plays an important role. If the layer is too thin the voltage drop in the Al_2O_3 layer will not be large enough to shift the Fermi level over the conduction band of BST. If the layer is too thick, tunnelling will become unlikely and electric field will decrease. An investigation of different Al_2O_3 thicknesses will be shown. In situ X-ray photoelectron spectroscopy was used directly after deposition to get information about composition, layer thickness and Fermi level position.

[1] S. Li, C. Ghinea, T. Bayer, M. Motzko, R. Schafranek, A. Klein, Electrical properties of (Ba,Sr)TiO₃ thin films with Pt and ITO electrodes: dielectric and rectifying behaviour, *Journal of Physics: Condensed Matter*, 23, 334202, (2011).

[2] S. Li, A. Wachau, R. Schafranek, A. Klein, Y. Zheng, R. Jakoby, Energy level alignment and electrical properties of (Ba,Sr)TiO₃/Al₂O₃ interfaces for tunable capacitors, *Journal of Applied Physics*, 108, 014113, (2010).

[3] R. Schafranek, S. Payan, M. Maglione, A. Klein, Barrier height at (Ba,Sr)TiO₃/Pt interfaces studied by photoemission, *Physical Review B*, 77, 195310, (2008).

Dielectric response of $\text{Pb}(\text{Zr},\text{Ti})\text{O}_3$ thin films on platinized silicon substrate in THz-IR frequency range

G.A. Komandin¹, O.E. Porodinkov¹, I.E. Spector¹, A.A. Volkov¹, K.A. Vorotilov², D.S. Seregin²,
A.S. Sigov²

1 - Department of Submillimeter Spectroscopy, A.M. Prokhorov General Physics Institute, Moscow, Russia

2 - Moscow State Technical University of Radioengineering, Electronics and Automation, Moscow, Russia

E-mail: komandin@ran.gpi.ru

Heterostructures on the base of $\text{Pb}(\text{Zr},\text{Ti})\text{O}_3$ (PZT) crystalline solid solution are under intensive study as a component of integrated ferroelectric devices [1]. A detailed knowledge of the dielectric properties of the separate layers of heterostructures is necessary to create devices. However, the structure parameters of PZT deposited on a metal layer differ sufficiently from the bulk ones. In this work the layered $\text{Pb}(\text{Zr}_{0.48},\text{Ti}_{0.52})\text{O}_3/\text{Pt}/\text{TiO}_2/\text{SiO}_2/\text{Si}$ structures are optically studied to extract the specific dielectric response. PZT films are deposited by sol-gel techniques.

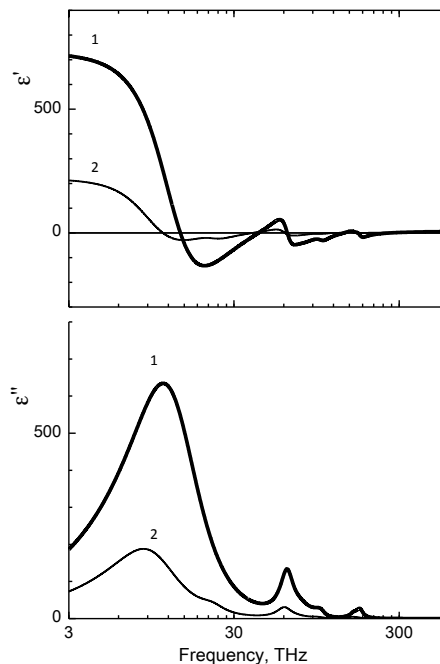


Figure 1. THz-IR dielectric spectra of the PZT films with thicknesses of 1160 (1) and 2180 nm (2)

The THz-IR transmission and reflection spectra (in the range of 5 – 5000 cm^{-1}) of the heterostructures are experimentally measured from the PZT-film side to calculate the spectra of real $\epsilon'(f)$ and imaginary $\epsilon''(f)$ parts of PZT film dielectric function. The dispersion analysis is performed and the spectral parameters are found. In addition, measurements of reflection spectra in the s and p polarizations at the angles of 6 and 30 degrees permit one to identify the longitudinal components of the lattice vibrations [2].

Calculated dielectric spectra of thin PZT films are presented in Fig. 1. A significant difference is observed between properties of the films of different thickness.

The work is supported by the Russian foundation for basic research, grant N 12-02-00203-a.

[1] J.F. Scott. Application of modern ferroelectrics. Science, vol. 315, pp. 954-959, (2007).

[2] E.A. Vinogradov, I.A. Dorofeev, Thermally stimulated electromagnetic fields of solids, Physics – Uspekhi, vol. 52, pp. 425-459, (2009).

Composition control of multicomponent ferroelectric films

A.V. Tumarkin, S.V. Razumov, A.G. Gagarin, M.M. Gaidukov, A.B. Kozyrev

Department of Physical Electronics and Technology, St. Petersburg Electrotechnical University

197376, 5 Prof. Popov str., St. Petersburg, Russia

avtumarkin@yandex.ru

Ferroelectric films have received much attention as promising materials for the creation of microwave tunable devices. The most extensively studied ferroelectric materials for the use in microwave devices are solid solutions of barium strontium titanate (BSTO) in the paraelectric state [1].

The microwave characteristics of ferroelectric devices strongly depend on the structure properties of the ferroelectric films. In this context, we have studied the effect of the deposition temperature on the structural characteristics of ion-plasma deposited BSTO films and their electrical properties.

The results of structural characterization of the BSTO film samples by XRD showed that films grown on sapphire in the temperature range 600-900°C contain blocks of (111), (110), and (100) orientations.

Fig. 1a shows the dependence of the average grain size in various phases on the film deposition temperature. It is clear that changes in the deposition temperature result in change of the BSTO film growth mechanism from layer-by-layer to pyramidal island. This can be explained by a change in the mechanism of mass transfer of sputtered atoms from the surface diffusion to the gas-phase transport with the increase of the deposition temperature [2]. These alterations are accompanied by a change in the crystal lattice orientation and by an increase in the grain size.

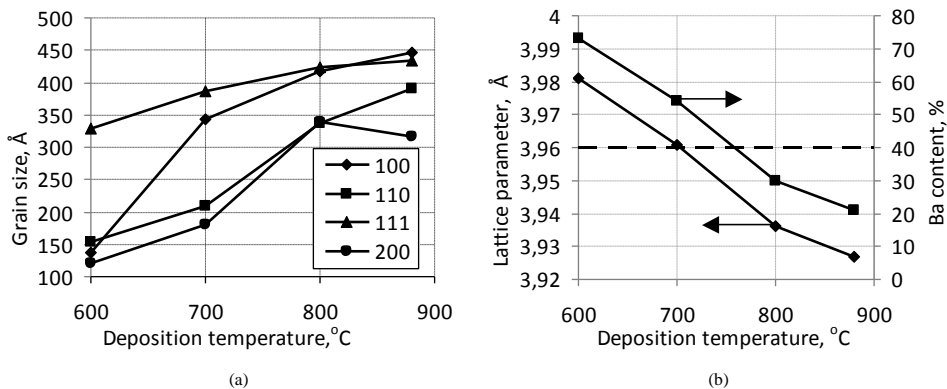


Fig.1 (a) - Dependence of the average grain size in various phases on the film deposition temperature. (b) - Lattice parameter and composition of the BSTO films vs. deposition temperature.

Fig. 1b shows the dependence of the lattice parameter on the film deposition temperature. There are two reasons for this change of the ferroelectric films' lattice parameter: the mechanical stresses in the film caused by the lattice mismatch and the difference in thermal expansion coefficients of the film and substrate; the change of the composition (Ba and Sr ratio) in the multicomponent film.

In polycrystalline films the mechanical stresses relax on the crystallite boundaries, leading to the absence of the integral stress in the sample [2]. Therefore, it can be concluded that the change in the cell parameter of polycrystalline BSTO film indicates changes in its composition (e.g. the ratio of barium and strontium).

At low deposition temperature an impurity polytitanates of barium and strontium, visible by X-ray diffraction analysis, form on the substrate together with BSTO grains and change the Ba and Sr content in the ferroelectric phase. With an increase of the deposition temperature only the pure BSTO grains occur, and lattice parameter of the BSTO film decreases (see Fig. 1b), approaching the value of the lattice of the target material (in our case 3,946 Å for $\text{Ba}_{0.4}\text{Sr}_{0.6}\text{TiO}_3$ at 760°C). At high temperatures the volatility of the barium increases and BSTO film becomes depleted of Ba with the corresponding decrease of the permittivity and tunability.

Under these technological conditions, the best properties are exhibited by the BSTO films deposited at a temperature of 760°C ($C_{\text{max}}/C_{\text{min}} = 5$; $\tan \delta < 0.02$ at 2 GHz), which has opened up new possibilities for the use of barium-strontium titanate in devices operating in the microwave range.

This work was partly supported by RFBR, research project No. 13-02-12096 ofi-m and by the Ministry of Science and Education of the Russian Federation.

- 1]. Tumarkin A.V., Tepina E.R., Nenashva E.A., Kartenko N.F., and Kozyrev A.B.: Microwave Properties of Film $\text{Ba}_x\text{Sr}_{1-x}\text{TiO}_3$ Ferroelectric Variconds with a Magnesium Containing Additive. *Tech. Phys.*, vol. 57 (6), pp. 787-791, 2012.
- 2]. Tumarkin A.V., Serenkov I.T., and Sakharov V.I.: Investigation of the Initial Stages in the Growth of Barium Strontium Titanate Ferroelectric Films by Medium Energy Ion Scattering. *Phys. of the Solid State*, vol. 52 (12), pp. 2561-2564, 2010.

Dynamic pyroelectric response of ferroelectric films on various substrates

A.V. Solnyshkin^{1,2}, A.A. Bogomolov¹, I.L. Kislova³, V.A. Belyakov¹

1- Tver State University, Sadovij per. 35, 170002 Tver, Russia

2- National Research University of Electronic Technology "MIET", Zelenograd, 124498 Moscow, Russia

3- Tver State Technical University, M. Koneva str. 12, 170023 Tver, Russia

E-mail address: a.solnyshkin@mail.ru

An interest in the study of thin ferroelectric films is attracted by their promising applications as functional elements of the modern microelectronics and sensor technology. The practical use of the films in sensor and detectors of electromagnetic radiation requires a detailed study of their behavior under various external influences. In particular, for pyroelectric detectors of thermal radiation and thermal imaging systems with the thin-filmed ferroelectric functional elements it is necessary to consider factors related to heat diffusion peculiarities in the multilayer structures, mechanical stress and strain caused by thermal expansion of the layers and others. In most cases the thin ferroelectric layers are rigidly connected with the substrates. Therefore the films are free to deformation in a direction perpendicular to their surface at the same time an extension or compression in the plane of the film can only occur with the substrate simultaneously. Consequently, the film is in a state of partial clamping. Usually, pyroelectric properties of the films on substrates are considered for the cases of homogeneous heating. Thus, the main aim of this work was to analyze the pyroelectric response detected in the ferroelectric film structures by the dynamic method, i.e. under the nonuniform heating of the ferroelectric layer and substrate.

Below, as an example, the ferroelectric thin film of lead zirconate titanate (PZT) on steel substrates is considered. Thicknesses of the ferroelectric layer and substrate were equal to 1.1 μm and 70 μm respectively. Aluminum circular electrodes with diameters of 2 mm and thickness of 0.1 μm were deposited on a free surface of the film. The pyroelectric parameters of the samples were determined by the dynamic method using a He-Ne laser ($\lambda = 6328 \text{ \AA}$, $P = 20 \text{ mW}$). Laser beam intensity was modulated by a mechanical chopper forming irradiation pulses of rectangular shape at a frequency of 20 Hz. For the analysis of observed pyroelectric response, calculations of temperature changes were performed for each layer of the Al/PZT/Steel structure. Defining the rate of temperature change, pyroelectric current was calculated for two cases: 1) the thermal strain of the substrate was not taken into account; 2) the thermal strain of the substrate was taken into account. The experimental and calculation results are presented in the Figure 1.

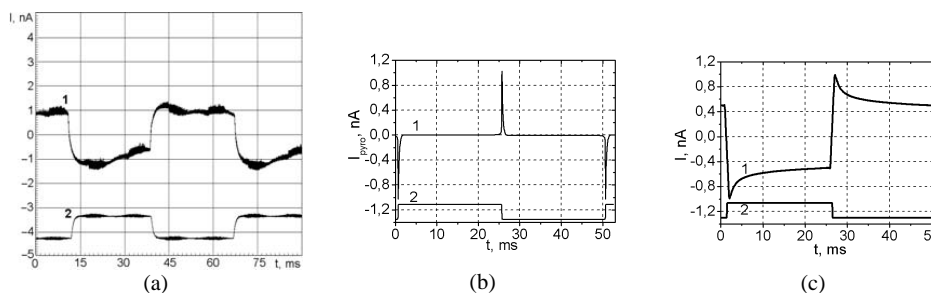


Figure 1 Dynamic pyroelectric response of Al/PZT/Steel structure (curve 1) and reference signal (curve 2) for the determination of the current direction and phase of the pyroelectric response. (a) Experimental data. (b) Calculation results excluding the thermal strain of the substrate. (c) Calculation results taking into account the thermal strain of the substrate.

The calculated pyroelectric response induced only by the heat diffusion (Figure 1 b) is significantly different from the response observed experimentally (Figure 1 a). If we take into account the thermal strain of the substrate which is mechanically connected with the ferroelectric film, the agreement between the experiment (Figure 1 a) and calculation (Figure 1 c) is observed. A significant difference between the thermal expansion coefficients of the dielectric film and the metal substrate leads to the additional strain of the ferroelectric layer causing the occurrence of the piezoelectric component of the observed response. The strict quantitative agreement requires varying the piezoelectric coefficients of ferroelectric layer and the thermal characteristics values of the elements used in the heterogeneous structure, such as the electrode, the ferroelectric film and the substrate. Also, the analysis of time dependences of the dynamic pyroelectric response allows to determine the thermal characteristics of the layers of ferroelectric filmed structures.

Measurement of Polarization Structure in Layered Piezoelectric Thin Films Using Scanning Nonlinear Dielectric Microscopy

H. Odagawa¹, T. Yanagitani², Y. Cho³

1- Kumamoto National College of Technology, 2659-2 Suya, Koshi, 861-1102, Japan

2- Nagoya Institute of Technology, Gokiso-cho, Showa-ku, Nagoya 466-8555, Japan

3- Tohoku University, 2-1-1 Katahira, Aoba-ku, Sendai 980-8577, Japan

odagawa@kumamoto-nct.ac.jp

Piezoelectric thin films such as ZnO and AlN are widely used in ultrasonic applications, especially in surface acoustic wave filters and sensors, bulk acoustic wave filters and high frequency ultrasonic transducers. It is known that polarization of those films becomes uniform in the film growth process naturally.

Recently, it is reported that polarization direction of ZnO and AlN thin film fabricated by sputtering method can be changed by growth condition, and polarization inverted structure can be obtained [1]. It will be very important results for high performance piezoelectric device applications. However, there are no useful nondestructive techniques to measure the layered polarization structure.

Scanning nonlinear dielectric microscopy (SNDM) is a purely electrical method for observing the polarization distribution without being influenced by the shielding effect with free charge [2, 3]. Generally, in order to achieve high special resolution, SNDM uses a very narrow probe. The depth in which the SNDM detects the polarity of a specimen largely depends on the radius of probe tip. Consequently, by changing the probe tip which has different radius, SNDM can detect the depth profile of polarization structure.

In this research, a method for obtaining a depth profile of polarization structure in a layered piezoelectric thin film is proposed. We will show the estimation method of the depth profile using a few probe tips having different tip radius by calculating the relation between the measurement depth and the tip radius. Also, we will show some measurement results in ZnO and AlN films which have layered polarization-inverted structure, and an estimation result using this method.

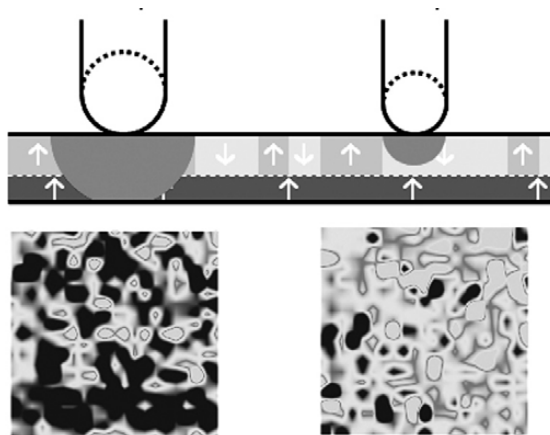


Figure 1 Measurement results of ZnO thin film using SNDM using different probe tip and schematic illustration of the relation between measured depth and tip radius.

[1] M.Suzuki, T.Yanagitani and H.Odagawa, 2012 IEEE Ultrasonics Symposium Proceedings, pp. 1922-1924 (2012).

[2] Y.Cho, A.Kirihara, and T.Saeki, Denshi Joho Tsushin Gakkai Ronbunshi 78-c-1, pp. 593-598 (1995) [in Japanese], Electronics and Communication in Japan, Part 2, 79, Scripta Technica, Inc. (1996).

[3] Y.Cho, A.Kirihara, and T.Saeki, Rev. Sci. Instrum. 67, pp. 2297-2303 (1996).

Low Frequency Relaxation of Barium-Strontium Niobate Ceramics Under Light Irradiation

K. Bormanis¹, A.I. Burkhanov², Luu Thi Nhan³, M. Antonova¹, and S.V. Mednikov³

¹ Institute of Solid State Physics, University of Latvia, Riga, LV-1063, Latvia

² Volgograd State Architectural and Engineering University, Volgograd, Russia

³ Volgograd State Technical University, Volgograd, Russia

E-mail: bormanis@cfi.lu.lv

A study of the low- and infra-low frequency relaxation in the $\text{Sr}_{0.75}\text{Ba}_{0.25}\text{Nb}_2\text{O}_6$ (SBN-75) ceramics under white irradiation is reported. Effective dielectric permittivity $\epsilon'_{\text{eff}}(E)$ and dielectric loss $\epsilon''_{\text{eff}}(E)$, $\tan\delta_{\text{eff}}$ are determined from measurements performed on a modified Sawyer-Tower circuit of polarisation loops at frequencies of 0.1, 1.0, and 10 Hz and different field intensities E . Anomalies on the $\epsilon'_{\text{eff}}(E)$ and $\epsilon''_{\text{eff}}(E)$ curves of SBN-75 (Fig. 1) are observed before and after illumination.

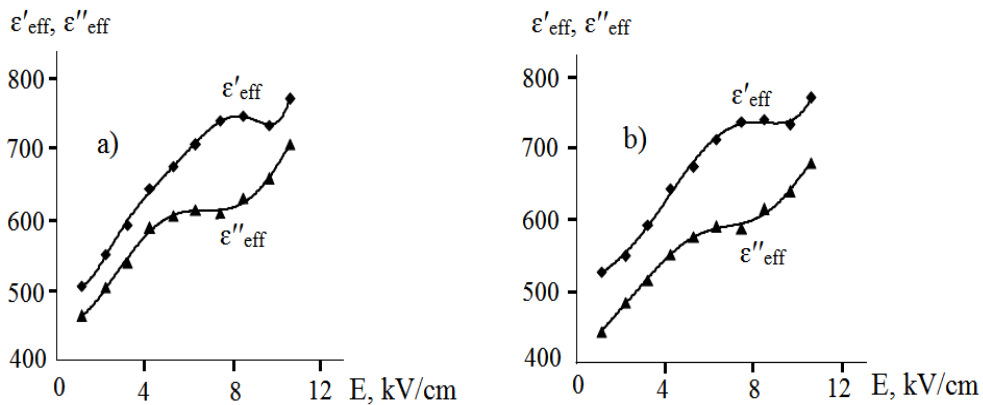


Fig. 1. Dependence on field intensity of $\epsilon'_{\text{eff}}(E)$ and $\epsilon''_{\text{eff}}(E)$ at frequency 0.1 Hz and $T=62^\circ\text{C}$: a – non-irradiated SBN-75 sample, b – irradiated SBN-75 sample.

Effective parameters $\tan\delta_{\text{eff}}(E)$, ϵ'_{eff} , and ϵ''_{eff} obtained from polarisation loops before and after irradiation at frequencies below 10 Hz, the interval representative of relaxation of polarisation in the relaxor phase of the SBN-75 ceramics, show that irradiation mainly causes some decrease of the values of $\tan\delta_{\text{eff}}$ and ϵ''_{eff} .

Most likely the anomalies are due to relaxation of the space charge. Irradiation is shown to reduce the contribution of space charge at temperatures (i.e., near T_m) corresponding to the range of the relaxor phase. The decrease of dielectric loss at irradiation of the SBN-75 ceramics points to rise of unbalanced carriers compensating the space charge in the material.

Resistance to Radiation of Lithium Niobate Crystals

M.N. Palatnikov¹, K. Bormanis², N.V. Sidorov¹, and O.V. Makarova¹

¹*Institute of Chemistry, Kola Science Centre RAS, Apatity, Murmansk Region, Russia*

²*Institute of Solid State Physics, University of Latvia, Latvia*

E-mail: bormanis@cfi.lu.lv

A series of lithium niobate crystals containing rare earth and alkaline elements – LiNbO₃; LiNbO₃:Y (0.46 % mass); LiNbO₃:Y,Mg (0.32, 0.24 % mass); LiNbO₃:Mg (0.27 % mass); LiNbO₃:Gd (0.004, 0.04, 0.26, 0.43 % mass) have been prepared along with ostensibly pure LiNbO₃ for the study of optical transmission before and after γ -irradiation. The features of optical transmission of the samples are determined with respect to the dosage of ionising radiation, the type and concentration of the admixture.

The change of the optical transmission by γ -irradiation of LiNbO₃ crystals containing admixtures is found to be substantially dependent on the type and concentration of the admixture while resistance to radiation compared with ostensibly pure LiNbO₃ crystal may be considerably higher or considerably lower. The strongest change of the optical transmission of the studied samples is observed in the case of Gd admixture (LiNbO₃:Gd, [Gd] = 0.004–0.04 % mass). In the same crystals a considerable shift of the edge of fundamental absorption to longer wavelengths is observed pointing to a remarkable amount of charged defects having emerged in the crystal structure.

The obtained data allow to propose using the change of optical transmission of the LiNbO₃:Gd ([Gd] = 0.004–0.04 % mass) crystals in γ -dosimeters for the ~1 – 160 Gy range. The radiation colouring saturates at high doses of γ -radiation presumably due to irradiative annealing of defects. For instance, the change of transmission of the LiNbO₃:Gd ([Gd] = 0.04 % mass) at ~160 Gy and $5 \cdot 10^4$ kGy is practically the same. Of the number of examined samples the most resistant to radiation are LiNbO₃:Gd (0.26 % mass), LiNbO₃:Gd (0.43 % mass), and LiNbO₃:Mg (0.27 % mass) crystals the optical transmission of which practically does not change (≤ 3 %) at doses $\sim 5 \cdot 10^4$ kGy of γ -irradiation.

The study has been supported by grant 12-03-00515-a of the RFFI and by grant HIII-1937.2012.3 of the President of Russian Federation.

Fabrication of regular microdomains patterns by the AFM method in helium-implanted optical waveguides on strontium-barium niobate crystals.

Yadviga Bodnarchuk, prof dr Tatyana Volk, dr Radmir Gainutdinov, Feng Chen, Hongliang Liu

Shubnikov Institute of Crystallography RAS

Email: deuten@mail.ru

For the first time microdomains and regular microdomain patterns were fabricated using AFM method in planar optical waveguides formed by helium-ion implantation on SBN-Nd crystals. In this method the local polarization reversal occurs under applying dc-voltages to an AFM tip contacting to the crystal surface. The domain formation in implanted crystals differs essentially from this process in unimplanted ones. In the unpoled (polydomain) implanted crystals the polarization values switched under equal voltages of opposite sign are nonequal. After poling in external fields E_{ext} , the polarization reversal may be achieved in the crystals poled by the negative field $-E_{ext}$ only. We relate this unipolarity of switching to the domain pinning by the buried damaged layer formed by He-irradiation. Using the raster lithography method specified 1D and 2D microdomain patterns were recorded. The recording and decay characteristics of these patterns are affected by pinning effects as well.

Heat capacity of nanocrystalline BaTiO₃ ferroelectric ceramics

S.N. Kallaev^{1,3}, Z.M. Omarov¹, K.G. Abdulvakhidov², S.A. Sadykov³

*1 -Daghestan Institute of Physics, Daghestan Scientific Centre of the Russian Academy of Sciences, ul. Yagarskogo 94, Makhachkala, 367003 Russia * e-mail: kallaev-s@rambler.ru^b*

2 - Southern Federal University, Bolshaya Sadovaya 105/42, Rostov-on-Don, 344006 Russia

3 - Daghestan State University, Gadjeva st. 43-a, Makhachkala, 367000 Russia

In this work, the heat capacity of the nanostructural BaTiO₃ ceramics is studied over a wide temperature range (150—600 K). The BaTiO₃ ceramics for the study was prepared by the solid-phase method. Before sintering, the synthesized charge was subjected to severe action in Bridgman anvils in combination with shear deformation (SAShD) [1]. The particle sizes were 50—1200 nm depending on the applied pressure. The samples were sintered in vacuum (10⁻³ mm Hg) at a temperature of 1000°C for 1 h.

On the temperature dependences of the heat capacity of the nanostructural samples of BaTiO₃ ceramics there are two peculiarities of the phase transitions: substantial smearing of the phase transition over a wide temperature range (as is the case in relaxors) and nonlinear decrease in the phase transition temperature with increasing the applied pressure.

From the temperature dependence of the heat capacity of BaTiO₃, the change in the phase transition entropy and the temperature dependence of the spontaneous polarization $P_S(T)$ can be found using the known thermodynamic relationships. The reference sample has $P_S \sim 24 \mu\text{C}/\text{cm}^2$, and P_S of the nanostructured samples is several times higher.

The physical causes of the diffuse phase transition observed experimentally can be as follows: high concentration of point defects, formation of dislocation skeleton, crystallite boundaries, and macroscopically nonuniform plastic deformation. The shift of the phase transition toward lower temperatures with increasing pressure can be due to the decrease in the crystallite sizes (size effect).

Thus, this study shows that the SAShD method makes it possible to produce nanostructured BaTiO₃ ceramics and to control its physical properties. In this case, the defect structure play main role in the formation of the physical properties of the ceramics.

[1] K. G. Abdulvakhidov, M. A. Vitchenko, I. V Mardasova, E. N. Oshaeva, and B. K. Abdulvakhidov, *Tech. Phys.* **52** (11), 1458 (2007).

NMR study of ^7Li spin-lattice relaxation in $\text{Li}_2\text{O}-7\text{GeO}_2$ compounds

A. Nesterov¹, O. Petrov², M. Trubitsyn¹, M. Vogel², M. Volnianskii¹

1- Oles Honchar Dnipropetrovsk National University, prosp. Gagarina 72, Dnipropetrovsk 49010, Ukraine

2- Institute of Solid State Physics, Technical University Darmstadt, Hochschulstr. 6,64289 Darmstadt, Germany

Nesterov.alexsey@gmail.com

Solid electrolytes, containing mobile Li ions, were intensively studied during last years. In particular, high ionic mobility in the compounds of the lithium germanate family $\text{Li}_2\text{O}-x\text{GeO}_2$ renders them promising candidates for new superionic conductors. One of the most popular substances of the family is lithium heptagermanate with $\text{Li}_2\text{O}-7\text{GeO}_2$ stoichiometry. Earlier it has been shown [1] that conductivity σ of $\text{Li}_2\text{Ge}_7\text{O}_{15}$ (LGO) single crystal is determined by interstitial Li ions, moving along the structural channels. Moreover, it is known that LGO can be prepared by heat treatment in glass, glass-ceramic and polycrystalline states [2]. In order to explore the role of long range order, electric properties of the states mentioned were studied in [3]. To study the mechanisms for lithium ion conduction in $\text{Li}_2\text{O}-7\text{GeO}_2$ compounds, we perform ^7Li NMR spin-lattice relaxation studies on crystalline, glassy, and glass-ceramic samples in the temperature interval 300-800 K.

LGO single crystals were grown from the melts by Chzochralskii method. LGO glass samples were quenched from 1500 K to room temperature. The procedure of heat treatment for LGO glass-ceramic and polycrystalline samples was reported in [3].

^7Li spin-lattice relaxation was measured in the magnetic field $B=8.45\text{T}$, corresponding to a resonance frequency of $\omega_L=2\pi\cdot 139.9\text{MHz}$, by using of the solid-echo detection method. The sequence $90_x-\Delta-64_y$ was applied to increase contributions from the lines of satellite transitions. The echo delay was set to $\Delta=20\mu\text{s}$.

The dependence of the spin-lattice relaxation time T_1 on inverse temperature is plotted in Fig. 1 for $\text{Li}_2\text{O}-7\text{GeO}_2$ samples in different phase states. It is obvious that ^7Li spin-lattice relaxation is slowest in LGO single crystal and becomes faster when long range order changes for structural disorder in polycrystalline and glass samples. Fastest spin-lattice relaxation is observed for the glass-ceramics.

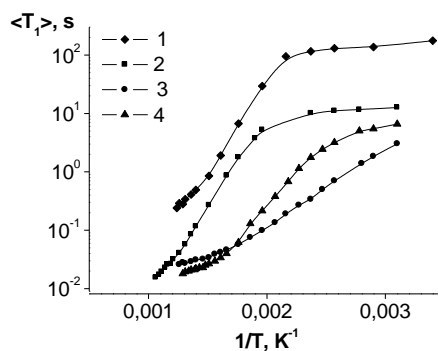


Figure 1 Dependence of T_1 on inverse temperature for LGO: 1 - single crystal, 2 - polycrystal, 3 - glass-ceramics, 4 - glass.

The data obtained by NMR are consistent with previous results of conductivity measurements reported in [3]. It can be concluded that the ^7Li spin-lattice relaxation time T_1 , measured by NMR, probes the mean lifetime of Li ions in quasi-equilibrium interstitial positions. Comparison of microscopic NMR results with macroscopic conductivity data, confirms that charge carrier transfer in LGO is provided by mobile Li ions.

[1] M. Volnianskii, S. Plyaka M Trubitsyn and Yahia A. Obaidat, Ion conduction and space-charge polarization processes in $\text{Li}_2\text{Ge}_7\text{O}_{15}$ crystals, Physics of the Solid State, vol. 54, pp.499-503, (2012)

[2] Marotta A., Pernice P. and Aronne A, The non-isothermal devitrification of lithium germanate glasses, J. Therm. Analysis, vol. 40, pp.181-188, (1993).

[3] M. Volnyanskii et al., Thermal and electrical properties of glass-ceramic based on lithium heptagermanate, Physics of the Solid State, vol. 54, p.889-891, (2012).

Suppression of slow capacitance relaxation phenomenon in $M/Ba_xSr_{1-x}TiO_3/M$ ceramic ferroelectric structures by annealing in oxygen atmosphere.

V.N. Osadchy¹, D.M. Kosmin¹, A.V. Tumarkin¹, A.G. Altynnikov¹, A.D. Kanareykin¹, I.V. Kotelnikov¹, R.A. Platonov¹, A.B. Kozyrev¹, E.A. Nenasheva²

¹Saint-Petersburg Electrotechnical University, 5 Professor Popov Street, St-Petersburg, 197376, Russia

²Girikond Research Institute, 10 Kurchatova Street, St. Petersburg 194223, Russia

Contact author: mlpeltech@gmail.com (Tumarkin A.)

Ferroelectrics (FE) and in particular $Ba_xSr_{1-x}TiO_3$ (BSTO) ceramic in paraelectric state are promising for use in microwave electronics. The nonlinearity in FE dielectric permittivity (ϵ) under applied electrical field enables the development of a variety of tunable devices [1-3]. The main parameter of such devices is their switching time under short control voltage pulses with duration between $(10^{-3}-1) \mu s$. However, when a unipolar pulse voltage is applied, the response of the FE ceramic based metal/FE/metal (M/FE/M) capacitor structures become ambiguous. This is because, besides the fast response process (soft mode response, <1 ns), there are slow relaxation processes, which cause up to 20% of the capacitance value to relax (i.e., return to initial state after the pulse duration) for a time $\tau \sim 10^3$ s.

In this work we report the properties of the M/FE/M multilayer structure based devices, where the annealing operation for FE ceramic was performed before the electrodes deposition and patterning. Unknown earlier effect of the annealing process to the FE capacitor structure the suppression of slow relaxation phenomena was observed. The absence of slow relaxation phenomenon for M/FE/M structures based on annealed ceramic illustrated in Fig.1. This effect, can be attributed to the decrease of oxygen vacancies concentration in the BSTO ceramic and to the increase of the granule sizes.

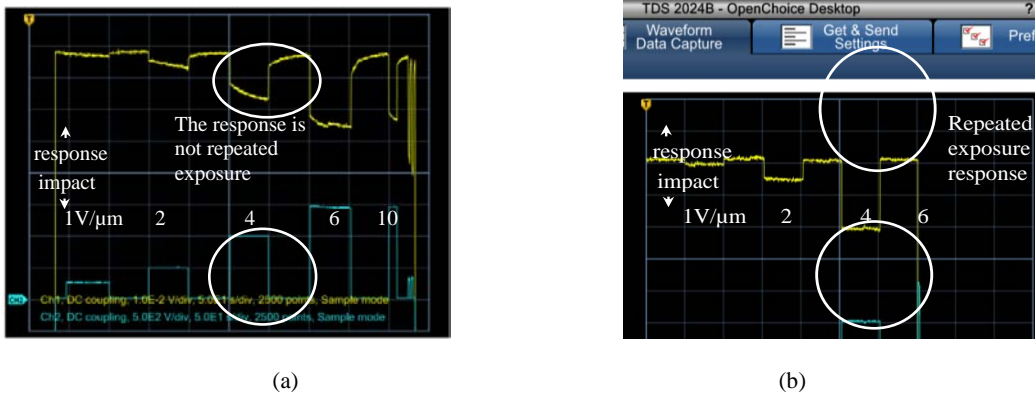


Figure 1. Time diagrams of the responses Me/FE/Me structures based on (a) not annealed and (b) annealed ceramic on the steps of the electric field.

[1] L. Sengupta, C. DuToit, S. Chen, A. B. Kozyrev, V. N. Osadchy, A. S. Pavlov, and D. M. Kosmin, Integr. Ferroelectr. 70, 61 (2005).

[2] A. Kanareykin et al. Proc. IPAC'13, p. 2486 (2013).

[3] H. Xu, N. K. Pervez, and R. A. York, Integr. Ferroelectr. 77, 27 (2005).

The dynamics of thermal processes in capacitance thermal-to-electric energy converter

R.A. Platonov, V.A. Volpyas, O.I. Soldatenkov, A.B. Kozyrev

Saint-Petersburg Electrotechnical University, 5 Professor Popov Street, St-Petersburg, 197376, Russia

r.a.platonov@gmail.com

The work is devoted to the development of a new class of the ferroelectric devices enabling the direct conversion of heat energy to the electrical one. The thermal-to-electrical energy converter can utilize man-made waste heat or waste heat from natural environments for electrical energy generation.

The conversion of thermal energy to electrical one by the use of variable capacitors is based on the following principle: if a capacitor of capacitance C_1 is charged up to a charge of Q , and the capacitance C_1 is then decreased down to C_2 by a variation of its temperature, thermal work is done and an additional electrical energy (ΔW) is produced according to the equation $\Delta W = 0.5Q^2(1/C_2 - 1/C_1)$. Variation in the capacitance C_1 by the temperature can be provided by the use of a dielectric material having temperature-dependent dielectric constant (for example, ferroelectric films). The average electric power produced by a capacitance thermal-to-electric power generator is determined by the following factors: the value of temperature-dependent capacitance, the capacitance ratio ($k = C_1/C_2$) under the temperature variation, the voltage applied to the capacitor and the frequency of temperature modulations.

In point of efficiency of the thermal-to-electric power generation, ferroelectric materials such as $(\text{Ba,Sr})\text{TiO}_3$ films demonstrate a number of advantages in comparison with other dielectrics [1]: high dielectric constant and strong temperature dependence of the dielectric constant at temperatures being close to the phase transition, i.e. a high value of capacitance ratio at temperature variation can be obtained. The frequency of the temperature modulations is determined by both the switching time of the heat modulator and the dielectric film thermal time constant. Therefore, apparatus and method for converting heat to electrical energy must provide: (i) high-speed modulation of the heat flow and (ii) rapid thermal response of the temperature-dependent capacitance to modulated heat flow. The capacitance thermal-to-electric power generators based on thin ferroelectric films for thermal-to-electric energy conversion and microelectromechanical systems (MEMS) providing the heat flow modulation up to 1 MHz [2] can satisfy these requirements.

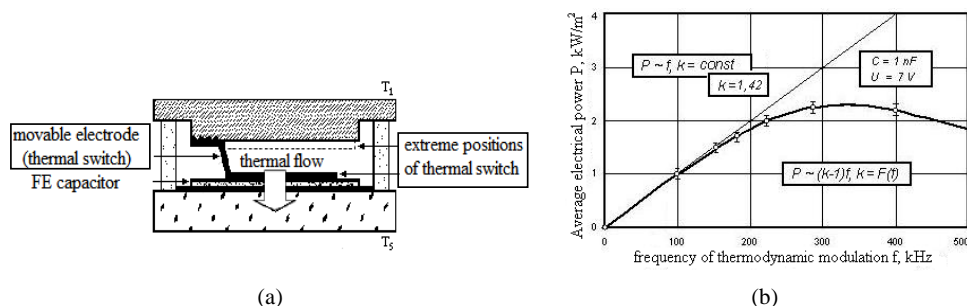


Figure 1. Schematic design of a thermal-to-electric energy converter (a) and average electric power produced by a capacitance thermal-to-electric power generator as a function of the frequency of temperature modulations (b).

The results of analysis of the dynamics of thermal processes in the structure consisting of a ferroelectric (FE) thin film capacitor incorporated in MEMS (Figure 1 (a)) are described in this work. A movable electrode of MEMS (controlled by electric voltage) operates as a heat switch enabling a cyclic heating and cooling of the ferroelectric capacitor. Integrating the capacitance converters in a system, an output electric power of $\sim 1 \text{ kW/m}^2$ can be obtained. The increase of the thermal cycle frequency is limited by the thermal inertia of the “FE capacitor/substrate” structure. For the studied thermal-to-electrical power converter, the average electric power has the maximal value of 2.3 kW/m^2 at $f \sim 340 \text{ kHz}$ and is decreased at higher frequencies (Figure 1 (b)) because of the decrease in temperature variation in the ferroelectric film.

[1] A. Kozyrev, A. Ivanov, T. Samoiloova, O. Soldatenkov, K. Astafiev, L. S. Sengupta, Nonlinear response and power handling capability of ferroelectric $\text{Ba}_x\text{Sr}_{1-x}\text{TiO}_3$ film capacitors and tunable microwave devices, Journal of Applied Physics, vol. 88, pp. 5334-5342, (2000).

[2] V. K. Varadan, K. J. Vinoy, K. A. Jose, RF MEMS and Their Applications (John Wiley and Sons Ltd.), (2003).

Actuator for precision positioning based on single crystalline lithium niobate

I.V. Kubasov¹, M.D. Malinkovich¹, A.S. Bykov¹, R.N. Zhukov¹, D.A. Kiselev¹, S.V. Ksenich¹

1- National University of Science and Technology "MISiS", 119049, 4, p. 339, Leninsky av., Moscow, Russia

kubasov.ilya@gmail.com

The ability of ferroelectrics to change their shape under the application of an external electric field is widely used for precise positioning. The most common materials for this purpose are different piezoceramics based on PZT, BT, ST or quartz. Despite their high electromechanical conversion coefficient devices made of ceramics have several disadvantages, such as low operation temperature, hysteresis, considerable non-linear temperature dependence of the piezoelectric modules and creep. Single crystalline materials don't have these negative properties but they are not used for precise actuating due to their low piezoelectric modules. One way to increase displacements is in using of a bimorph actuator design. This structure has higher electromechanical conversion coefficient and keeps all the advantages of a ferroelectric single crystal. In order to create such bimorph structures it is necessary to form domains with opposite orientations of the spontaneous polarization vector in a crystal plate.

Earlier, we suggested the method of producing a single crystalline bimorph by an annealing in a non-uniform electric field [1]. This particular way is difficult due to screening of the electric field in the crystal volume because of the high concentration of intrinsic carriers near T_c .

In this paper, we offer the way to form a bimorph structure based on a single crystalline lithium niobate plates (LiNbO_3 , LN). Bimorphs based on LN single crystal are stable in wide temperature range due to a number of material qualities: relatively high T_c value (about 1140 °C), the absence of a hysteresis and creep.

The bimorphs were formed in single crystal LN plates by using a non-uniform thermal field in the IR lamp heating system. We used the effect of domain switching under the influence of a temperature gradient around T_c . The domain wall in our bimorphs was located at a half of the depth of crystal plates. Cantilevered bending displacements of the 7 cm LN bimorph with the thickness of 1.5 mm were $\approx \pm 17 \mu\text{m}$ in the voltage within $\pm 300 \text{ V}$ (Figure 1). These structures were also tested by cyclic loading under the variable electric field. After more than 10 million working cycles the bimorphs don't change their electromechanical properties and shape of the voltage-deformation dependence. By using different electrodes' configurations it is possible to achieve other types of deformations, e.g. torsion.

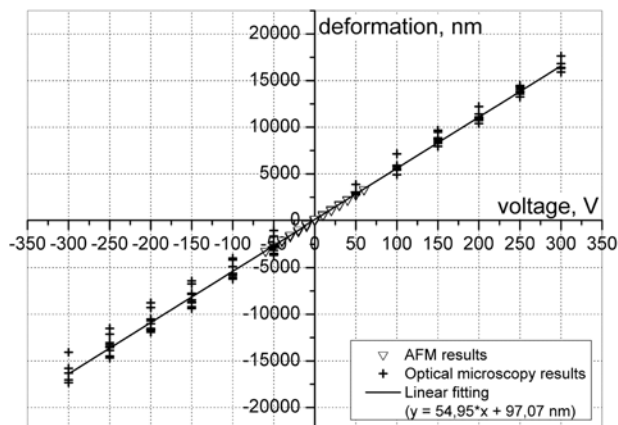


Figure 1 Bending cantilevered deformation of the single crystalline LN bimorph. Data were collected by using optical and atomic force microscopy

From the point of view of applications, single crystalline LN bimorph actuators can be used for precise positioning in probe microscope techniques, for an adjustment of laser resonators and as wave guides with exact variable geometrical characteristics.

[1] V.V. Antipov, A.S. Bykov, M.D. Malinkovich, Y.N. Parkhomenko, Formation of bidomain structure in lithium niobate single crystals by electrothermal method, *Ferroelectrics*, vol. 374, 1, pp. 65–72, (2008).

Light-induced absorption in $\text{Bi}_{12}\text{TiO}_{20}:\text{Al}$ crystal

V. Dyu¹, E. Khudyakova¹, S. Shandarov¹, M. Kisteneva¹, A. Akrestina¹, Yu. Kargin²

1- Tomsk State University of Control Systems and Radioelectronics, 40 Lenin Avenue, Tomsk 634050, Russia

2- Baikov Institute of Metallurgy and Material Sciences of the RAS, 49 Leninskii pr., Moscow 119991, Russia

valeriya.dyu@gmail.com

Light-induced redistribution of charge carriers on defect centers in the nominally pure bismuth titanium oxide ($\text{Bi}_{12}\text{TiO}_{20}$) crystals is accompanied by photochromic effect [1, 2] and causes an increase in the photorefractive sensitivity of one to IR radiation [3, 4]. We report here on the investigation of light-induced absorption in the Al-doped bismuth titanium oxide ($\text{Bi}_{12}\text{TiO}_{20}:\text{Al}$) crystal having the thickness of 6.6 mm along the [100] crystallographic direction.

It was established that that the transmittance of the crystals in the spectral range 490–900 nm is enhanced both upon exposure to IR ($\lambda_e=1064$ nm) and red ($\lambda_e=650$ and 660 nm) laser radiation. By contrast, the exposition by green laser light results in darkening of crystal for the same spectral region. The typical experimental spectral dependence for the changes in optical absorption $\Delta\alpha(\lambda)$ consequently exposition by light with the wavelength of 660 nm is shown by circles in the Figure 1 (a). The solid line in this Figure is the approximation taking into account 5 intracenter transitions [5] in addition to the impurity absorption caused by photoexcitation of electrons to the conduction band from deep donor centers [2].

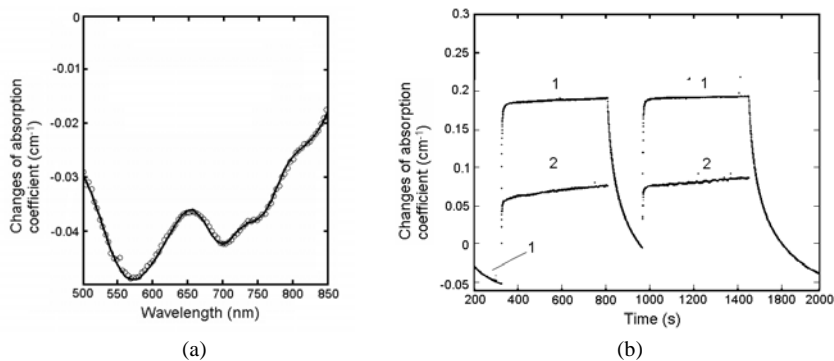


Figure 1 Spectral dependence of the changes of absorption coefficient after irradiation by light with the wavelength of 660 nm (a) and dynamics of the changes of absorption coefficient (b) for the wavelengths of 650 nm (1) and 532 nm (2) in $\text{Bi}_{12}\text{TiO}_{20}:\text{Al}$ crystal.

The typical experimental results for time evolution of changes in light absorption in $\text{Bi}_{12}\text{TiO}_{20}:\text{Al}$ crystal for wavelengths of 650 nm (dependence 1) and 532 nm (dependence 2) are shown in Figure 1 (b). In this experiment the red beam with the intensity of ~ 15 mW/cm² was used both as an exposing and a reading one uninterruptedly (from 0 to 1770 s). The green beam with the intensity of ~ 320 mW/cm² was turned on for time intervals from 320 to 800 s and from 965 to 1460 s only. It can be seen that turning on a green light at $t = 320$ and 965 s results in growth of light absorption both for red and green light. Subsequent to turning off a green beam at $t = 800$ and 1460 s we observed the bleaching of the crystal for red as well as for green light. It interesting to note that an oscillating behavior for changes in absorption for green light was observed sometimes (see the dependence 2 at time interval from ~ 1100 to 1400 s in Figure 1 (b)). The combination of the models introduced in Refs. 2 and 5 have been used to interpretation of observed phenomena.

This work is done in the framework of the Governmental order of Ministry of education and science of the Russian Federation on 2013 year (project № 7.2647.2011) and with the support of by the Russian Foundation for Basic Research (project Nos. 12-02-90038-Bel_a).

[1] O.V. Kobosev, S.M. Shandarov, A.A. Kamshilin, and V.V. Prokofiev, Light-induced absorption in a $\text{Bi}_{12}\text{TiO}_{20}$ crystal, J. Opt. : Pure Appl. Opt., vol. 1, pp. 442-447, (1999).

[2] A.L. Tolstik, A.Yu. Matusевич, M.G. Kisteneva, S.M. Shandarov, S.I. Itkin, A.E. Mandel', Yu.F. Kargin, Yu.N. Kul'chin, and R.V. Romashko, Spectral dependence of absorption photoinduced in a $\text{Bi}_{12}\text{TiO}_{20}$ crystal by 532-nm laser pulses, Quantum Electron., vol. 37, pp. 1027-1033 (2007).

[3] S.G. Odoulov, K.V. Shcherbin, and A.N. Shumeljuk, Photorefractive recording in BTO in the near infrared, J. Opt. Soc. Am. B, vol. 11, pp. 1780-1785 (1994).

[4] P.V. Dos Santos, J. Frejlich, and J.F. Carvalho, Direct near infrared photorefractive recording and pre-exposure controlled hole-electron competition with enhanced recording in undoped $\text{Bi}_{12}\text{TiO}_{20}$, Appl. Phys. B, vol. 81, pp. 651-655 (2005).

[5] M.G. Kisteneva, A.S. Akrestina, S.M. Shandarov, S.V. Smirnov, O.N. Bikeev, K.P. Lovetskii, and Yu. Kargin, Photo- and thermoinduced changes of the optical absorption in $\text{Bi}_{12}\text{SiO}_{20}$ crystals, J. Holography Speckle, vol. 5, pp. 280-285 (2009).

Piezoelectric Laser Scanning/Deflecting Manipulator for Organizing the Swarm of the Nanosatellites

S. Navickaitė¹, R. Bansevicius², V. Jūrėnas³, V. Bakanauskas⁴

1-4 Institute of Mechatronics, Kaunas University of Technology, Kęstučio g. 27, LT-44312 Kaunas, tel. +370 37 300909

sigita.navickaite@ktu.lt

Nanosatellites are small satellites used in space missions and applications such as earth observation with high resolution camera or transmitting high bandwidth data, space science, astronomy and verification of new technologies in orbit [1, 2]. Nanosatellites in generally are measured in dimensions of 10 cm x 10 cm x 10 cm and their mass is 1–10kg [3]. Seeking to reach the aims of the missions there are used special high tech equipment in nanosatellites. One of such equipment is piezoelectric-based manipulators that can be responsible for precision manipulation of such objects, such as cameras, lasers, mirrors, optical elements and other. A satellite swarm is an ensemble of mutually interacting spacecraft's performing a number of tasks in a coordinated manner [4].

In this paper authors focus on the problem of communication between the agents of the swarm. Novel design piezoelectric manipulator driven by piezoelectric actuator is presented. The main task for the manipulator is the precision positioning of the laser beam. The laser beam must be deflected and poisoned accurately from one nanosatellite to another.

Presented manipulator effectively controls the direction of a laser beam in the space. This device can steer a light beam around x axis for both continuous and step scanning modes by controlling voltage. The manipulator (Figure 1 (a)) consists of: mirror 1 for deflecting the laser beam, thin layer of polarised piezoelectric material with sectioned electrodes 2, kinematic pair sphere-cylinder 3, 4, made from permanent magnet, mirror motion limiting supports 5 and sections of electrodes 6, 7.

Connecting harmonic electrical signal to electrode 6, with frequency, corresponding resonant frequency of bending form of a system mirror 1 - piezoelectric thin layer 2, results in rotation of a mirror around x axis. Reverse of the motion is realized by connecting the same voltage to electrode 7.

Laser scanning/deflecting accuracy, thermal and dynamic characteristics of the manipulator were investigated experimentally.

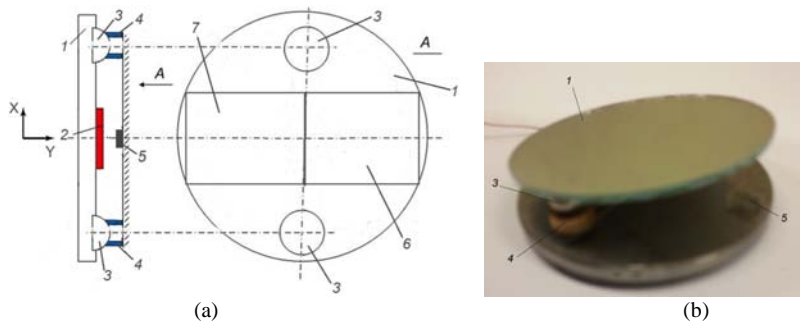


Figure 1. Piezoelectric laser scanning/deflecting manipulator. (a) Schematic view. (b) Investigated piezoelectric laser scanning/deflecting manipulator.

Acknowledgment

Postdoctoral fellowship is being funded by European Union Structural Funds project "Postdoctoral Fellowship Implementation in Lithuania" within the framework of the Measure for Enhancing Mobility of Scholars and Other Researchers and the Promotion of Student Research (VP1-3.1-ŠMM-01) of the Program of Human Resources Development Action Plan.

[1] R. Mahmood, K. Khurshid, A. Zafar, Q. ul Islam, ICUBE-1: First Step towards Developing an Experimental Pico-satellite at Institute of Space Technology, Journal of Space Technology, Vol 1, No. 1, pp. 5-10, (2011).

[2] R. WILKEA, Adaptive Communication System for Pico Satellites, Poster, Prague May12, pp. 1-5, (2011).

[3] G. Mantzouris, MICRO AND PICO SATELLITES IN MARITIME SECURITY OPERATIONS, Journal of Naval Science and Engineering, Vol.8, No.2, pp. 1-30, (2012).

[4] D. Izzo, L. Pettazzi, Autonomous and Distributed Motion Planning for Satellite Swarm, JOURNAL OF GUIDANCE, CONTROL, AND DYNAMICS, Vol. 30, No. 2, pp. 449-459, (2007).

Fabrication For Magnetic Nanoparticle System of $M_{0.9}Fe_{0.1}O$ (M=Ni, Cu) By Co-precipitation

J. Miao¹, J. Xiao¹, M. R. Silva¹, M. Kumaresavanji², J. P. Araújo², B. F. Costa¹, J. A. Paixão¹

1- CEMDRX, Department of Physics, University of Coimbra, Rua Larga, 3004-516 Coimbra, Portugal

2- IFIMUP and IN-Institute of Nanoscience and Nanotechnology, and Departamento de Física, Faculdade de Ciências, Universidade do Porto, Rua do Campo Alegre, 687, 4169-007 Porto, Portugal

E-mail address: xiao@pollux.fis.uc.pt

The exchange bias (EB) effect, which is due to exchange interactions across the interface between ferromagnetic (FM) or ferrimagnetic (FiM) and antiferromagnetic (AFM) regions, are one of the foreland fields of spintronics. This work focuses on the investigation of magnetic nanoparticles system with FiM/AFM structure (such as MFe_2O_4 /MO system, M=Ni, Cu), to realize the enhancement of EB effect and acquire the relationship between the microstructure and magnetic properties for satisfying the application requirements.

The $M_{0.9}Fe_{0.1}O$ (M=Ni, Cu) nanocomposite samples were synthesized by the sol-gel method. Phase composition analysis showed these nanocomposites were respectively composed of a ferrimagnetic MFe_2O_4 (M = Ni, Cu) and antiferromagnet MO (M = Ni, Cu) phases. The magnetic properties of the samples were investigated by measuring their magnetization as a function of temperature and magnetic field. These results indicated that the magnetic hysteresis loops of the samples sintered in air atmosphere at 550 °C for 3h exhibit a negative shift and an enhanced coercivity at low temperature, which is ascribed to strong exchange coupling between the FiM and AFM grains.

[1] J. Nogués and I.K. Schuller, exchange bias, *J. Magn. Magn. Mater.*, 192, pp. 203-232 (1999).

[2] J. Nogués, J. Sort, and V. Langlais, Exchange bias in nanostructures, *Phys. Rep.*, 422, pp. 65-117 (2005).

Enhanced Polarization Fluctuations in $\text{PbZr}_{0.72}\text{Sn}_{0.28}\text{O}_3$ Compared to PbZrO_3 Single Crystals Studied by Brillouin Light Scattering

Jae-Hyeon Ko¹, Min-Seok Jeong¹, Byoung Wan Lee¹, Krystian Roleder²,
 Annette Bussmann-Holder³, Andrzej Majchrowski⁴

¹ Department of Physics, Hallym University, 1 Hallymdaehakgil, Chuncheon, Gangwondo 200-702, Korea

² Institute of Physics, University of Silesia, ul. Uniwersytecka 4, PL-40-007 Katowice, Poland

³ Max-Planck-Institut für Festkörperforschung, Heisenbergstr. 1, D-70569 Stuttgart, Germany

⁴ Institute of Applied Physics, Military University of Technology, ul. Kaliskiego 2, PL-00-908 Warsaw, Poland

Main author email address: hwangko@hallym.ac.kr

There has recently been a lot of interest in the nature of phase transitions of antiferroelectric PbZrO_3 and its complex compounds [1-6]. In order to get more insights, the elastic anomalies of $\text{PbZr}_{0.72}\text{Sn}_{0.28}\text{O}_3$ single crystals were investigated by using Brillouin spectroscopy as a function of temperature. Figure 1 shows the temperature dependence of the Brillouin frequency shift (proportional to the sound velocity) and the full width at half maximum (FWHM, proportional to the acoustic attenuation coefficient) of the longitudinal acoustic (LA) mode propagating along the [100] direction of $\text{PbZr}_{0.72}\text{Sn}_{0.28}\text{O}_3$ single crystals along with those of PbZrO_3 . It is clear that the softening of the LA mode becomes more substantial by addition of Sn cations into the B-site of the perovskite structure. This is accompanied by much larger growth of the FWHM compared to PbZrO_3 . The degree of these elastic anomalies is more substantial compared to $\text{PbZr}_{0.78}\text{Sn}_{0.22}\text{O}_3$ [6]. These results clearly demonstrate that the polarization fluctuations in the paraelectric phase of PbZrO_3 are enhanced by increasing the Sn content. The appearance of the precursor polar regions is also corroborated by the observation of weak birefringence in the cubic phase. This enhancement is interpreted within the framework of the polarizability model and the resulting lattice instabilities [2].

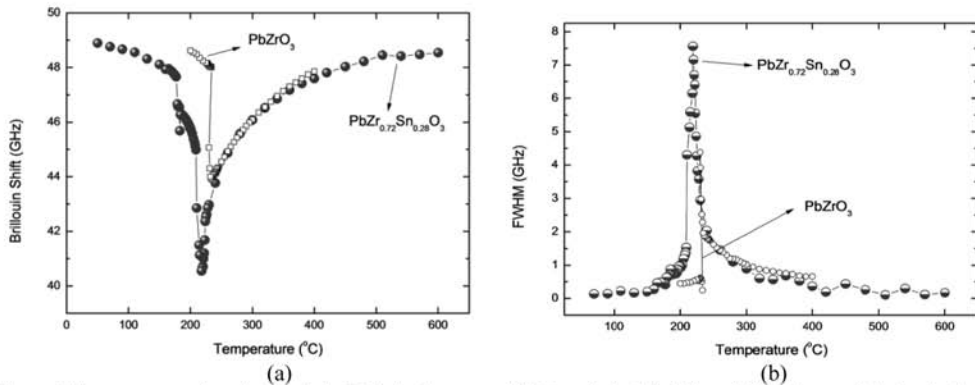


Figure 1 The temperature dependence of the Brillouin frequency shift (a), and the full width at half maximum of the longitudinal acoustic (LA) mode of the $\text{PbZr}_{0.72}\text{Sn}_{0.28}\text{O}_3$ single crystal (b), propagating along the [100] direction of the cubic coordinates. The same data of the pure PbZrO_3 , which were taken from Ref. [1], are shown for comparison.

***Acknowledgments:** This work was supported by the Defense Research Laboratory Program of the Defense Acquisition Program Administration and the Agency for Defense Development of Republic of Korea and by the Basic Science Research Program through the National Research Foundation of Korea (NRF) funded by the Ministry of Education, Science and Technology (2013R1A1A2006582).

- [1] J.-H. Ko, M. Górný, A. Majchrowski, K. Roleder, A. Bussmann-Holder, Mode softening, precursor phenomena, and intermediate phases in PbZrO_3 , *Phys. Rev. B*, vol. 87, p. 184110, (2013).
- [2] A. Bussmann-Holder, J.-H. Ko, A. Majchrowski, M. Górný, K. Roleder, Precursor dynamics, incipient ferroelectricity and huge anharmonicity in antiferroelectric lead zirconate PbZrO_3 , *J. Phys.: Condens. Matter*, vol. 2, p. 212202, (2013).
- [3] A. K. Tagantsev et al., The origin of antiferroelectricity in PbZrO_3 , *Nat. Commun.*, vol. 4, p. 2229 (2013).
- [4] J. Hlinka, T. Ostapchuk, E. Buixaderas, C. Kadlec, P. Kuzel, I. Gregora, J. Kroupa, M. Savinov, and J. Drahokoupil, Multiple soft-mode vibrations of lead zirconate, arXiv:1401.3730v1.
- [5] I. Jankowska-Sumara, K. Szot, A. Majchrowski, K. Roleder, Thermal hysteresis of local instabilities in paraelectric phase of $\text{PbZr}_{0.96}\text{Sn}_{0.04}\text{O}_3$ single crystals, *J. Appl. Phys.*, vol. 113, p. 187209 (2013).
- [6] M. Mączka, T. H. Kim, M. Ptak, I. Jankowska-Sumara, A. Majchrowski, S. Kojima, High-resolution Brillouin scattering studies of phase transitions and precursor phenomena in $\text{PbZr}_{0.78}\text{Sn}_{0.22}\text{O}_3$ single crystals, *J. Alloys Compd.*, vol. 587, pp. 273–277 (2014).

Spatial modulation instability in undoped Lithium niobate Fabry-Perot interferometer

A. S. Perin, V. M. Shandarov, V. G. Kruglov

Tomsk State University of Control Systems and Radioelectronics, Tomsk, Russia

perin.anton@gmail.com

Light field propagation in nonlinear medium is accompanied by modification of its spatiotemporal structure due to the self-action effects. The one of most attractive among them is spatial modulation instability of broad light beams extensively studied in last years [1]. The characteristics of the self-action effects may essentially vary if the propagation direction of light beam is changed within the anisotropic media or the medium is bounded. For example, formation of regularly ordered light patterns becomes possible in nonlinear optical cavities. Similar effects were observed in photorefractive crystals with both, self-focusing and self-defocusing nonlinear response [1, 2]. In this work, we study the features of spatial self-action of light fields in photorefractive Fabry-Perot interferometers based on undoped lithium niobate (LiNbO_3) plate.

The Fabry-Perot interferometer (FPI) on X-cut LiNbO_3 plate with optically polished opposite sides is used in experiments. The geometrical dimensions of the crystal are $1 \times 15 \times 10 \text{ mm}^3$ along X, Y, Z axes, respectively.

The idea of experiment is a study of spatial modulation instability characteristics on the incidence angle of a light beam onto the interferometer surface. The source of coherent radiation is a CW solid-state laser (Nd^{3+} :YAG, light wavelength $\lambda=532 \text{ nm}$, output power is near to 50 mW). The FPI sample is exposed to light beams with the almost homogeneous light field which is formed from the laser beam by collimators and a square shape diaphragm. The size of a diaphragm window is $3 \text{ mm} \times 3 \text{ mm}$. Polarization of light corresponds to the extraordinary wave in the crystal, and its intensity is 35 mW/cm^2 . To investigate the light patterns at the FPI output plane, a BS-FW-FX33 laser beam analyzer is used.

As the result of FPI exposure we observe formation of regular 1D patterns (Fig. 1 d, e, f) within the initially homogeneous images of the light fields (Fig. 1 a, b, c) at the output surface of FPI. These patterns correspond to the stationary modulation of the material refractive index within FPI due to the photorefractive effect. These

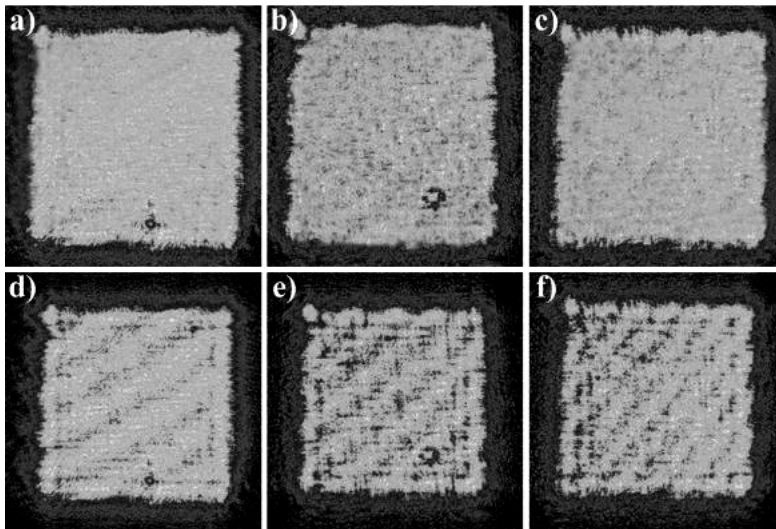


Figure 1 Images of light patterns at the output facet of X-cut FPI: (a), (d) – normal incidence, (b), (e) - incidence angle of 5 degrees from the normal, (c), (f) - incidence angle of 10 degrees from the normal.

patterns occurred in 60 minutes after the start of exposure. Images in Figure 1 d, e, f, demonstrate the variation of the pattern period on the angle of the input light beam incidence.

[1] Nan Zhu, Ru Guo, Simin Liu, Zhaohong Liu and Tao Song, "Spatial modulation instability in self-defocusing photorefractive crystal $\text{LiNbO}_3:\text{Fe}$ ", *J. Opt. A: Pure Appl. Opt.* 8, 149 (2006).

[2] H. Buljan, M. Soljacic, T. Carmon, and M. Segev, "Cavity pattern formation with incoherent light", *Phys. Rev. E* 68, 016616 (2003).

Topological defects of the optical anisotropy parameters as a tool for stress tensor field reconstructions in glasses

Yu. Vasylykiv, M. Smyk, I. Skab, R. Vlokh

Institute of Physical Optics, 23 Dragomanov Str., 79005 Lviv, Ukraine

vlokh@ifp.lviv.ua

We have shown that the residual mechanical stresses existing in initially isotropic glass media yield in appearance of polarisation singularities of the optical wave front. It has been experimentally revealed the topological defects of the optical anisotropy parameters (the phase difference and the angle of optical indicatrix rotation) in $\text{Li}_2\text{B}_4\text{O}_7$ and LiB_3O_5 glass samples, which originate from the spatial distribution of optical birefringence caused by residual mechanical stresses. We have found that the strength of topological defects of the optical indicatrix rotation angle is equal to $\pm 1/2$, and the light acquires no integrated phase difference when the ray propagates through the center of defect on the front and back surfaces of the sample. These singularities should lead to the appearance of optical vortices with the topological charge ± 1 . The annealing of the samples brings about annihilation of the polarisation singularities, homogenisation of spatial distribution of the phase retardation and practical zeroing of the retardation, thus suggesting vanishing of the residual stresses.

We have shown experimentally that close spatial domains around these topological defects represent nothing but the stressed-state regions where the principal axes of the optical indicatrix do not depend on the direction of light propagation, although the principal refractive indices and the principal components of the stress tensor depend on it. Following from these features, it has been found that these domains are the regions of the 3D stressed state. However in some particular cases these domains can appear to be the regions of the 2D stressed state. The simple criteria on determination whether we deal with 2D or 3D optical anisotropy parameters distribution on the basis of revealing of topological defects of optical indicatrix orientation were formulated. It has been experimentally shown that topological defects of optical indicatrix orientation can appear in few projections at 3D distribution of optical indicatrix parameters which appears at the bending of glass plate by the concentrated loading.

The $\text{Pb}_2\text{P}_2\text{Se}_6$ crystals – new efficient acoustooptic materials

O. Mys¹, A. Grabar², I. Martynyuk-Lototska¹, B. Zapeka¹, M. Kostyrko¹, R. Vlokh¹

1- Institute of Physical Optics, 23 Dragomanov Street, 79005 Lviv, Ukraine

2- Institute for Solid State Physics and Chemistry, Uzhgorod National University, 54 Voloshyn Street, 88000 Uzhgorod, Ukraine

vlokh@ifp.lviv.ua

We have experimentally determined the acoustic wave velocities for $\text{Pb}_2\text{P}_2\text{Se}_6$ crystals and on the basis of these results have calculated full matrices of elastic stiffness and compliances coefficients. For estimating of the acoustooptic figure of merit M_2 of $\text{Pb}_2\text{P}_2\text{Se}_6$ crystals we have determined the parameters of the slowest acoustic waves, the figure of merit for acoustooptic interaction with which is seem to be high. On the basis of analysis of anisotropy of acoustic wave velocities it has been found that the slowest QL acoustic wave propagates along crystallographic b axis and possesses the velocity (2664 ± 14) m/s. The M_2 for the interaction with this wave can be equal to $\sim 100 \times 10^{-15} \text{ s}^3/\text{kg}$. Within the QT waves propagated in crystallographic planes the minimal velocity of (1180 ± 150) m/s acquire the QT_1 wave which propagates in bc plane under the angle of 39 ± 1 deg or 140 deg in respect to c axis with the polarization vector belonging to the bc plane. The M_2 for the interaction with this wave can reach value $\sim 1150 \times 10^{-15} \text{ s}^3/\text{kg}$ that is comparable with the same value for TeO_2 crystals. Besides we have found that the principal slowest QT wave with the velocity ~ 740 m/s propagates in $c'b$ under the angle of 45 ± 1 deg in respect to c' axis, while the angle between c and c' axis is equal to 35 deg. The M_2 for the case of interaction with this wave can be as high as $\sim 4000 \times 10^{-15} \text{ s}^3/\text{kg}$ at the same effective elasto-optic coefficient. Thus one can refer the $\text{Pb}_2\text{P}_2\text{Se}_6$ crystals to the one of most efficient acoustooptic material for infrared spectral range. We also present the results for thermal expansion coefficients of $\text{Pb}_2\text{P}_2\text{Se}_6$ crystals determined in a wide temperature range both in the crystallographic system and in the coordinate system based on eigenvectors of thermal expansion tensor. The thermal expansion coefficients of $\text{Pb}_2\text{P}_2\text{Se}_6$ are almost independent of temperature, thus making the crystals very suitable for many applications, particularly acoustooptical.

Optical Modulation of Femtosecond Laser-Written 1D Photonic Lattice in Lithium Niobate

A. Kanshu¹, V. Kruglov¹, A. Perin¹, D. Petnev¹, V. Shandarov¹, F. Chen²

1- Tomsk State University of Control Systems and Radioelectronics, 40 Lenin prosp., 634050 Tomsk, Russia

2- School of Physics, Shandong University, Jinan 250100, People's Republic of China

ShandarovVM@svch.rk.tusur.ru

Multi-element periodic optical waveguide systems (photonic lattices, PL's) exhibit unique features in the linear and nonlinear diffraction of light beams. The nonlinear diffraction can lead to light localization within these structures in forms of discrete lattice solitons or discrete gap solitons [1, 2]. The one of approaches to form similar PL's is based on photorefractive properties of some electrooptic crystals [3, 4]. The main aim of this work is experimental demonstration of possible optical modulation of one-dimensional (1D) PL's based on stationary laser-written waveguide systems in photorefractive lithium niobate (LiNbO₃). We also investigate the linear and nonlinear discrete diffraction of light within these PL's.

The 1D PL's are formed in X- cut wafers of photorefractive LiNbO₃ of congruent composition by direct laser writing using a Ti:Sapphire femtosecond laser at $\lambda=800$ nm wavelength, 100 - 150 fs pulse length and a pulse energy up to 1 mJ. The intense light influence results in the refractive index decreasing of LiNbO₃ [5] that may form a channel optical waveguide between two crystal areas processed with the focused light beam. The spatial period of PL we study is 25 μm that results in very low coupling between adjacent waveguide channels. To vary this coupling, we use the optical modulation of the PL exploiting the photorefractive properties of the crystal wafer. For this purpose we use the amplitude masks illuminated with the laser radiation of $\lambda=532$ nm wavelength.

In experiments we study the intensity distributions at the output surface of PL in the cases before their optical modulation and after it for the same conditions of light excitation within the PL. These conditions include the

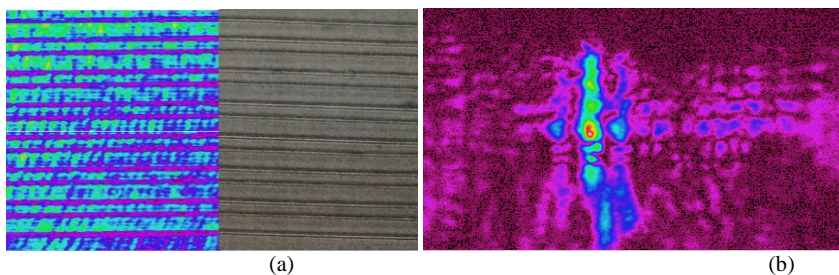


Figure 1 : a) Near field diffraction of light on femtosecond laser-written PL (left) and its optical microscopic image (right); b) Light pattern at the output surface of the optically modulated PL ($\lambda=633$ nm).

single-element excitation of light with wavelength of 633 nm (He-Ne laser) and optical powers from 1 to 5 μW for the linear regime and from 10 to 100 μW for the nonlinear regime. Fig. 1 a illustrate the topology of the PL observed using the near-field diffraction patterns and the optical microscopy. The light pattern at the output surface of the optically modulated PL (the exposure time is 60 minutes at light power 50 mW) obtained with single waveguide excitation is shown in Fig. 1 b.

In conclusion, we experimentally demonstrate and prove through the numerical modelling that the stationary PL's written in photorefractive LiNbO₃ by femtosecond laser radiation may be effectively modulated using low-power light sources of visible wavelength.

[1] D.N. Christodoulides, F. Lederer, and Y. Silberberg, Discretizing light behaviour in linear and nonlinear waveguide lattices, *Nature*, vol. 424, pp. 817-823, (2003).

[2] D. Neshev, E. Ostrovskaya, Yu. Kivshar, W. Krolikowski, Spatial solitons in optically induced gratings, *Opt. Lett.*, vol. 28, 710-712, (2003).

[3] Patrick Rose, Bernd Terhalle, Jörg Imbrock and Cornelia Denz, Optically induced photonic superlattices by holographic multiplexing, *J. Phys. D: Appl. Phys.*, vol. 41, pp. 224004-224007, (2008).

[4] W. Horn, S. Kroesen, J. Herrmann, J. Imbrock, and C. Denz, Electro-optical tunable waveguide Bragg gratings in lithium niobate induced by femtosecond laser writing, *Opt. Expr.*, vol. 20, pp. 26922-26928, (2012).

Oxygen-Ion Conductivity of Nanostructured R_2MO_5 ($R = Sm, Gd, Dy, Er, Y, Sc$; $M = Ti, Zr, Hf$)

L.P. Lyashenko¹, L.G. Shcherbakova², D.A. Belov²

1- Institute of Problems of Chemical Physics RAS, prospekt Semenova 1, Chernogolovka, 142432 Moscow region, Russia

2- Semenov Institute of Chemical Physics RAS, Kosygin St. 4, 119136 Moscow, Russia

lyash@icp.ac.ru

Recently it was found that single-crystalline and polycrystalline samples of R_2TiO_5 ($R = Sm, Gd, Dy, Er, Y$), $Sc_4Ti_3O_{12}$, and Gd_2MO_5 ($M = Zr, Hf$) contain nanodomains (10–600 nm in dimension) with different degree of order, coherent with the fluorite-like matrix. X-ray studies revealed that nanodomain - matrix lattice misfit accommodation layers give rise to dislocations. The formation of nanodomains coherent with the matrix fluorite-like phases under investigation can be explained in terms of their structure where high density of structural defects is responsible for the observed value of high internal stress.

The oxygen-ion conductivities and the activation energies of the compounds under investigation were determined in the temperature range 300–1000°C under air conditions using impedance spectroscopy. At 1000°C the conductivities and the activation energies of the investigated compounds were found to be in the range of 1.1×10^{-2} to 3.7×10^{-3} S/cm and between 1 - 2 eV, respectively. The highest value for the electrical conductivity was observed for the melt crystal $Sc_4Ti_3O_{12}$ possessing the lowest size of nanodomains. From the impedance spectra, we calculated the bulk capacitances of grains and grain boundaries for the investigated samples which were found to be $\sim 10^{-11}$ F (300 – 1000°C) and $10^{-7} - 10^{-5}$ F (300 – 1000°C), respectively.

To conclude, we have prepared and investigated the nanostructured fluorite-like R_2MO_5 materials with the improved oxygen-ion conductivity. It was shown that the investigated samples may reach much higher electrical conductivity, to be compared with conventional pyrochlore-like titanates $R_2Ti_2O_7$ ($R = Sm, Ho$) showing the electrical conductivity of $\sim 10^{-4}$ S/cm at 1000°C.

Piezoelectric Properties of La^{3+} doped PZT Ceramics across the antiferroelectric/ferroelectric phase boundary

I.V.Ciuchi^{1,2}, F. Craciun³, C. Galassi¹, L. Mitoseriu²

¹ISTEC-CNR, Via Granarolo, no.64, I - 48018, Faenza, Italy

² Faculty of Physics, Alexandru Ioan Cuza University, Iasi, 700506, Romania

³ISC-CNR, via Cassia 1216, I-00189, Rome, Italy

Contact author: ioana.ciuchi@istec.cnr.it (I. V. Ciuchi)

The piezoelectric properties of PLZT ceramics with 90/10 Zr/Ti ratio with La^{3+} (x) composition near rhombohedral-orthorhombic phase boundary with x=2, 2.5, 3, 3.1, 3.2, 3.3, 3.5, 3.8 and 4 at. % has been investigated. Piezoelectric material constants plotted as function of La concentration show strong discontinuities in slope with a transient region (from x=3 to x=3.3 La^{3+} at. %) from a maximum to a minimum values corresponding to transition from ferroelectric to antiferroelectric phase. The PLZT ceramics with La^{3+} at. 3 % content, located close to the transient region (near to ferroelectric region) show higher piezoelectric coupling factors (k_p , k_{31}), higher piezoelectric constants (d_{33} , d_{31}) and higher voltage coefficients (g_{31} , g_{33}). This study helps to clearly identify the location of boundary.

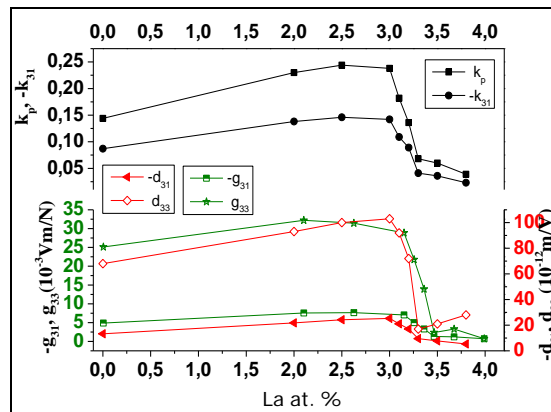


Fig. 1 Effect of La content (x) on piezoelectric coefficients of $\text{Pb}_{1-x}\text{La}_x(\text{Zr}_{0.90}\text{Ti}_{0.10})_{1-x/4}\text{V}_{x/4}\text{O}_3$ ceramics.

UNIAXIAL FERROELECTRIC IN EXTERNAL MAGNETIC FIELD

E.D.Yakushkin

Institute of Crystallography RAS, 119333, Moscow, Russia

yakushkin@ns.crys.ras.ru

It is well known the pinning-depinning effects of dislocations in diamagnetic crystals in an external magnetic field. That is the so called magneto-plasticity effect which is caused by spin-dependent processes. The ferroelectric domain walls moves in a potential relief like to dislocations movement and one may to expect the similar effects in polydomain ferroelectrics.

In this work the dielectric response of polydomain TGS single crystal was investigated at influence of an external magnetic field in real time. Such investigation was carried out for the first time.

It was revealed the essential change of a dielectric susceptibility and corresponding evolution of dielectric hysteresis loops in relatively weak (up to 1 tesla) magnetic field. The effect is obviously concerned with influence of a magnetic field on the domain walls pinning centers. In some way the effect is similar to the magneto-plasticity effect. It is also close related to aging phenomenon in polydomain ferroelectric single crystals, which is important for corresponding ferroelectric devices.

Optical and electro-optical properties of PZT crystal determined by Mueller matrix ellipsometry

Jakub Havlíček¹, Jaroslav Hamrle¹, Jaromír Pištora¹, Yoichiro Hashizume², Soichiro Okamura²

*1- VSB-Technical University of Ostrava, 17. listopadu 15, Ostrava, Czech Republic
2- Tokyo University of Science, 6-3-1 Nijuku Katsushika-ku, 125-8585 Tokyo, Japan*

jakub.havlicek@vsb.cz

We have investigated spectral dependence of optical and electro-optical (Pockels effect) properties PZT (Pb(Zr_{0.44}Ti_{0.56})O₃) film. The investigated structure was Au(10-20nm)/PZT(1um)/Pt(100nm)/Si, where Au electrode allows to apply voltage (60V per 1ms) in order to electrically polarize PZT crystal. The investigations were done using Mueller matrix ellipsometry [1,2], allowing to determine optical spectra in spectral range 0.8-6.2 eV. First, from Mueller matrix spectra we have determined spectra of permittivity elements of PZT film. Then, the spectra of Pockels effect (namely spectra of difference of diagonal permittivity elements, $r_{133}-r_{333}$) were determined by measuring difference of measured Mueller matrix spectra on applied electric field.

[1] H. Fujiwara, Spectroscopic Ellipsometry: Principles and Applications (Wiley) (2007).

[2] D.H. Goldstein, Mueller matrix dual-rotating retarder polarimeter, Applied Optics, 31, 6676-6683 (1992).

The temperature change in the piezoelectrocaloric element under the periodic electric field

A. Starkov¹, I. Starkov²

1- Institute of Refrigeration and Biotechnology, National Research University of Information Technologies, Mechanics and Optics, Kronverksky pr. 49, 197101 St. Petersburg, Russia

2- SIX Research Centre, Department of Radio Electronics, Brno University of Technology, Technická 12, 616 00 Brno, Czech Republic

ferroelectrics@ya.ru

New cooling technologies have fascinated scientific researchers for decades. Due to significant progress in material technology, huge magneto/electro/elasto/barocaloric effects have become available. These effects are changes in temperature and/or entropy of the body by the application or removal of external fields. Material having at least two caloric effects is called multicaloric. Interest in this group of substances is caused by the fact that the interaction of fields having different nature may result in a substantial increase in caloric effects [1]. As a consequence, multicalorics are extremely promising materials for solid-state cooling. However, at present the multitude of coupling of caloric and ferroic (i.e. nonlinear dependence of the polarization, magnetization, and elastic stresses on the external parameters) effects is not well defined.

According to the numerical calculations performed on the basis of the model presented in [2], multicaloric (magneto/electro/elasto) system of 30 layers provides cooling of 31 K. Unfortunately, the main drawbacks of the magnetocaloric structures are related to high costs and large sizes of magnetic field sources. The barocaloric effect has the same disadvantages that make it difficult to use them in spot cooling systems. Therefore, the electric field remains the only option for the generation of caloric effects in compact devices. For the realization of microcoolers, we propose the following scheme. The basic strategy relies on strengthening of the electrocaloric effect. For this purpose, an additional piezoelectric layer can be used as a solution. Furthermore, the cooling device consists of a set of thin elements which increases its heat capacity. Each element represents the bilayer system. The first layer is electrocaloric piezoelectric and the second one is conventional piezoelectric which properties do not depend on temperature. The electric field is applied to each layer in the system. The second layer of piezoelectric material is intended to create an elastic field which controls the electrocaloric effect in the first layer. In other words, the second layer acts as a thermal switch. The simulation results of steady temperature distribution in the two-layer system are shown in Figure 1. The presence of heat exchange with the environment is taken into account. Acting on the polarization of the first layer by the elastic field we can expect a small increase in caloric effect for each thermodynamic cycle. For a large number of cycles this increase can lead to a significant impact on temperature change. Thus, the findings of this study have important implications for solid-state cooler practical realization.

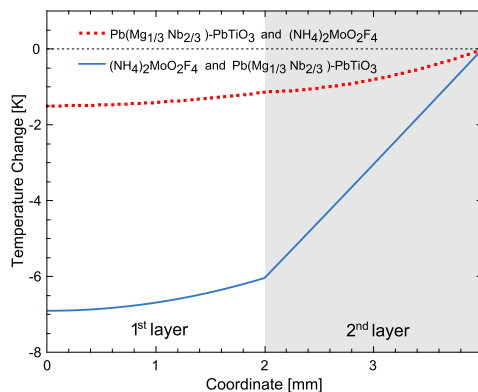


Figure 1 The temperature distribution calculated for a two-layered system. The maximum cooling temperature achieved is -6.85 degree.

[1] A. Starkov and I. Starkov, Solid-State Cooler: New Opportunities, *Ferroelectrics*, vol. 430 (1), pp. 108-114, (2012).

[2] I. Starkov and A. Starkov, On the thermodynamic foundation of solid state cooler based on multiferroic materials, *Int. J. Refrig.*, vol.37, pp. 249-256, (2014).

Nonlinear Optical Optical Limiting Effect of New Organotellurium Compounds Containing Azomethine and Azo Groups Under CW Laser Illumination

H. L. Saadon¹, Basil Ali¹, Adil A. Al-Fregi²

¹Laser Applications and Optical Materials Group, Department of Physics, College of Science, University of Basrah, Iraq

²Department of Chemistry, College of Science, University of Basrah, Iraq
Tel.: +9647817369647, E-mail: haithamsaadon@yahoo.com

Abstract

Two new organotellurium compounds containing azomethine and azo groups, [2-(2-hydroxynaphthylazo)phenyl][2-(2-methoxybenzylideneamino)-5-methylphenyl]tellurium dibromide (P1) and [2-(2-hydroxynaphthylazo)-5-nitrophenyl][2-(2-methoxy benzylideneamino)-5-methyl phenyl]tellurium dibromide (P2) were synthesized and doped in polyvinylprolidone (PVP) matrix. The nonlinear optical (NLO) properties of these compounds and doped polymer were studied using Z-scan technique at 532 nm. The Z-scan results reveal that the sample solutions and films exhibit self-defocusing nonlinearity. The P2/PVP solutions investigated here exhibit good optical power limiting.

Keywords:

Nonlinear optical properties, Z-scan, Optical limiting

First-order phase transformation in the new oxide ion conductors with pyrochlore structure containing B-site cations in different valence state

D.A. Belov^{1,2}, A.V. Shlyakhtina¹, K.S. Pigalskiy¹, A.N. Shchegolikhin³, I.V. Kolbanev¹, O.K. Karyagina³

¹*Semenov Institute of Chemical Physics, Russian Academy of Sciences, ul. Kosygina 4, Moscow, 119991 Russia*

²*Faculty of Chemistry, Moscow State University, Leninskie gory 1, Moscow, 119991 Russia*

³*Emanuel Institute of Biochemical Physics, Russian Academy of Sciences, ul. Kosygina 4, Moscow, 119991 Russia*

E-mail addresses: annash@chph.ras.ru; annashl@inbox.ru

We have studied the new compounds with fluorite-like (Ho_2RNbO_7 ($\text{R}=\text{Lu}, \text{Sc}$)) and pyrochlore-like ($\text{Sm}_2\text{ScTaO}_7$) structure as potential oxide ion conductors. In $\text{Sm}_2\text{ScTaO}_7$ pyrochlore we have observed the first-order phase transformation at $\sim 650\text{-}700^\circ\text{C}$ is related to rearrangement process in the oxygen sublattice of the pyrochlore structure containing B-site cations in different valence state and actually is absent in the defect fluorites. $\text{Sm}_2\text{ScTaO}_7$ pyrochlore undergoes a first-order structural phase transition at $\sim 650\text{-}700^\circ\text{C}$, as evidenced by a sharp change in conductivity and supported by TMA data and low frequency measurements of the dielectric permittivity and the loss tangent. The thermal expansion coefficient below and above the transition is $\sim 8 \times 10^{-6}$ and $\sim (13\text{-}16) \times 10^{-6} \text{ K}^{-1}$, respectively. The niobates Ho_2RNbO_7 ($\text{R}=\text{Lu}, \text{Sc}$) synthesized at 1600°C for the long time (up to 14 h) probably also start undergo a first order structural phase transition at $\sim 650\text{-}700^\circ\text{C}$, but effects characterizing that phase transition are expressed weakly. This phase transition associated with the re-arrangement process in the oxygen sublattice of the pyrochlore structure and is not typical for defect fluorites. The start of the pyrochlore structure formation in $\text{Ho}_2\text{LuNbO}_7$ niobate led to the small deviation from the Arrhenius behaviour near $650\text{-}700^\circ\text{C}$, the hysteresis of conductivity in the temperature range $350\text{-}750^\circ\text{C}$ and appearance of dielectric permittivity maximum at $650\text{-}700^\circ\text{C}$, which accompanied by a minimum in the temperature dependence of the loss tangent at very low frequencies. The conductivity, dielectric permittivity and loss tangent are more sensitive to the appearing of short-range pyrochlore order domains in $\text{Ho}_2\text{ScNbO}_7$ and $\text{Ho}_2\text{LuNbO}_7$ then X-ray technique.

Piezo Force Response of $\text{BiFeO}_3/\text{LaFeO}_3$ heterostructures

M. G. Ranieri¹, B. Z. Simões¹, M. A. Ramirez¹, A.Z. Simões¹

¹ Materials Science Department, Universidade Estadual Paulista- UNESP - Faculdade de Engenharia de Guaratinguetá, Zip-Code: 12516-410, Guaratinguetá-SP, Brazil.

Email address: alezipo@yahoo.com

BiFeO_3 (BFO) and LaFeO_3 (LFO) heterostructures were observed at room temperature at a temperature of 500°C for 2 hours on Pt/TiO₂/SiO₂/Si (100) substrates by the chemical solution deposition [1]. Dielectric permittivity and dielectric loss demonstrated only slight dispersion with frequency due the less two-dimensional stress or strain in the plane of the film. Room temperature magnetic coercive field indicates that the BFO/LFO and LFO/BFO present different magnetic behavior. Piezoelectric force microscopy (PFM) in out-of-plane (OP) and in-plane (IP) mode reflects domains with the polarization vector oriented toward the bottom electrode and grains with zero out-of-plane polarization.

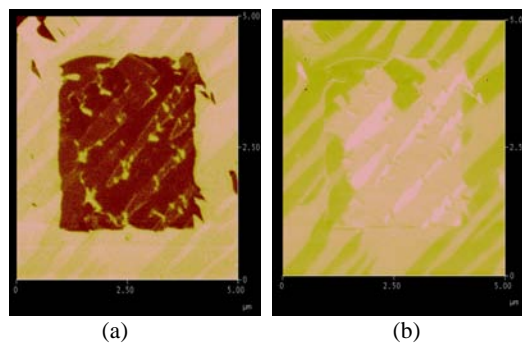


Figure 1. Out-of-plane (OP) and In-plane (IP) PFM images of BFO/LFO heterostructures deposited by the polymeric precursor method (a) (OP) and (b) (IP).

[1] L.V. Costa, R.C. Deus, C.R. Foschini, E. Longo, M. Cilense, A. Z. Simões, Experimental evidence of enhanced ferroelectricity in Ca doped BiFeO_3 Materials Chemistry and Physics, 144, 476-483 (2014).

Zn-Al₂O₃ metal-insulator layer on aluminium via combined electrochemical route

M. Starykevich, A.N. Salak, A.D. Lisenkov, M.L. Zheludkevich, M.G.S. Ferreira

Department of Materials and Ceramic Engineering/CICECO, University of Aveiro, 3810-193 Aveiro, Portugal

salak@ua.pt

Metal-insulator-metal and metal-insulator-semiconductor structures with aluminium oxide as dielectric layer are widely studied for application in nano-electronics. Al₂O₃ films have been used as high-ordered porous templates for formation of 2-D and 1-D nano-structured materials through their deposition into the pores [1]. The aluminium oxide templates with controlled morphology and thickness have been typically prepared using electrochemical methods, since the thickness of the film is proportional to the applied voltage [2]. However at the bottom of the pores an aluminium oxide barrier layer is formed that increases in thickness as the film grows. As this barrier layer is a good insulator the electrodeposition progress becomes difficult. Barrier-free or near-free membranes need to be used.

In this work, the Zn-Al₂O₃ metal-insulator plane structures were electrochemically formed to investigate the influence of the alumina barrier layer thickness on direct electrodeposition of zinc. The work was developed for homogeneous anodic films to be then transferred to the ordered porous templates. Alumina films with thicknesses in the range of 2 nm (native) to 58 nm (40 V) were formed by anodization of pure aluminium in a 0.1M ammonium pentaborate solution. Electrodeposition of zinc was performed in a nonaqueous solution, since application of water-free electrolyte removes the problems related to pH-sensitivity of both film and substrate. The eutectic solution used for deposition of zinc was prepared by adding 0.1M anhydrous zinc chloride to the mixture of choline chloride and ethylene glycol in the 1:2 molar ratio. This system was used due to its wide electrochemical window, low vapour pressure, low cost, non-toxicity, and air- and water stability. Electrodeposition processes in both AC and DC modes were studied.

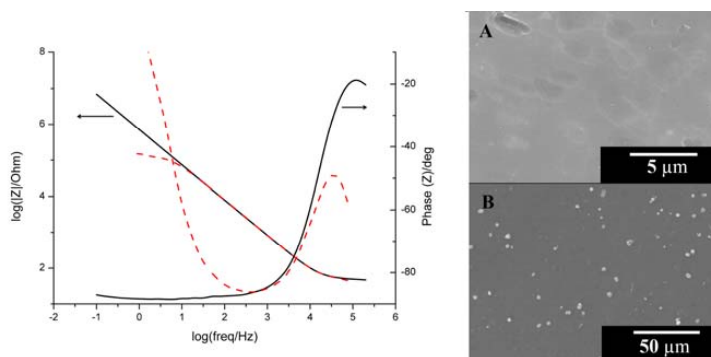


Figure 1. The impedance spectra of bulk alumina film (14 nm) in 0.1M ammonium pentaborate (solid line) and in choline chloride: ethylene glycol with 0.1M ZnCl₂ (dashed line) and SEM micrographs obtained after zinc deposition in DC mode on native (A) and at 1 kHz on 14 nm barrier layer.

Application of DC mode resulted in no deposition on the barrier layer (Fig. 1a). For the AC mode deposition, the optimum frequency range 10² to 10³ Hz was determined from the impedance spectrum (Fig. 1, dashed line). Within this frequency range, zinc was successfully deposited on all the alumina barrier layers at -1.6V±50 mV (Fig. 1b).

The financial supports of the European Commission and Portuguese Foundation for Science and Technology (FCT) in frames of the projects PIRSES-GA-2011-295273 – NANEL and PTDC/CTM-NAN/113570/2009, respectively, are gratefully acknowledged.

[1] A.M. Md Jani, D. Losic, N.H. Voelcker, Nanoporous anodic aluminium oxide: Advances in surface engineering and emerging applications, *Progress in Materials Science*, 58, 636-704 (2013).

[2] S. Tajima, M. G. Fontana, R.W. Staehle, Eds., in *Advances in Corrosion Science and Technology*, Plenum Press: New York, London, 1970.

Interface effect on the boundary of ferroelectric polymer and ceramic inclusion in nanocomposite PVDF/BPZT

M. V. Silibin¹, A. V. Solnyshkin¹, D. A. Kiselev^{1,2}, A. N. Morozovska³, E. A. Eliseev⁴,
S. A. Gavrilov¹, D. C. Lupascu⁵, V. V. Shvartsman⁵

1 National Research University of Electronic Technology "MIET", 124498 Moscow, Russia

2 National University of Science and Technology "MISIS", 119049 Moscow, Leninskiy pr. 4, Russia

3 Institute of Physics, National Academy of Science of Ukraine, 03028, Kyiv, Ukraine

4 Institute for Problems of Materials Science, National Academy of Science of Ukraine, 03142, Kyiv, Ukraine

5 University of Duisburg-Essen, Institute for Materials Science and Center for Nanointegration Duisburg-Essen (CENIDE), 45141 Essen, Germany

sil_m@mail.ru

Polar materials having piezoelectric, pyroelectric, and ferroelectric properties are widely used as functional elements of various devices in modern electronics, i.e. acoustic transducers, microelectromechanical systems (MEMS), memory elements, infrared sensors, thermal imagers, and others. Among such materials are ferroelectric single crystals, ceramics, as well as some polymers, such as polyvinylidene fluoride (PVDF) and copolymers based on it. Polymeric materials have a number of advantages in comparison with other substances, e.g. low density, the possibility of fabricating elements of any size and shape, mechanical elasticity, stability of electrophysical properties, simplicity and relatively low cost of production. At the same time, they are inferior to crystalline ferroelectrics in such parameters as the pyroelectric coefficient, piezoelectric modulus, elastic modulus, and spontaneous polarization. Therefore, attention of researchers has been attracted to objects simultaneously having properties of polymers and classical ferroelectrics. Such objects are composite films based on a polymeric matrix with addition of ferroelectrics, e. g. lead zirconate–titanate (PZT) ceramics, single crystals of the triglycine sulfate (TGS) group, and some relaxor ferroelectrics. Macroscopic behavior of composite films depends not only on the properties of the constituents, but also is strongly affected by the properties of the interface. The properties of the interface between the polymeric and ceramic/single crystalline components can be addressed using microscopic techniques. One of the most versatile and powerful techniques is piezoresponse force microscopy (PFM) developed for the investigation of ferroelectric materials at the nanoscale. Ferroelectric polymers, in particular, PVDF and its copolymers, offer an attractive combination of properties such as relatively high spontaneous polarization, piezoelectricity, chemically inert behavior, electrical strength and durability. These benefits together with benign processing demands explain the attention that polyvinylidene fluoride with trifluoroethylene P(VDF-TrFE) thin films receive, in particular, for nonvolatile memories and full-organic transistors. Also, recently, attention of researchers has more and more often been attracted to objects simultaneously having properties of polymers and classical ferroelectrics. Such objects are composition films based on polymeric materials with addition of ferroelectrics, i.e., PZT and barium lead zirconate titanate (BPZT) and single crystals of the TGS group.

In this work the local piezoelectric properties of ferroelectric composites consisting of P(VDF-TrFE) copolymer matrix with barium lead zirconate titanate ceramic inclusions were addressed both experimentally using piezoresponse force microscopy technique and theoretically applying the Landau-Ginzburg-Devonshire formalism. Copolymer samples were prepared by the solvent-cast method. Crystallization was performed for two to three hours at a temperature of 100 °C until complete evaporation of solvent. Film samples which thickness (d) varied from 10 to 20 μm were obtained. The fabricated films were not preliminary treated by stretching, high-temperature annealing, or applying a polarizing electric field. The same method was used to fabricate composite polymer films containing BPZT. The ferroelectric powder prepared preliminarily was added to the solution containing the dissolved copolymer. Composite samples with 10 – 50 % of volumetric fraction of the above crystalline ferroelectrics were obtained. A transient region with a width of approximately 40 nm has been found at the interface between the two constituents. It is shown that the piezoresponse in the vicinity of the interface is strongly affected by inhomogeneous stresses originating from an incompatibility of thermal expansion coefficients of PVDF and lead zirconate titanate.

Interfacial effects in Al/PVDF-TrFE/SiO₂/nSi heterostructures.

G.M. Vizdrik

*Laboratory of Crystal Optics, Institute of Crystallography, 119333, Moscow, Russia
gennadiy.w@googlemail.com*

Aluminum/PVDF-TrFE/silicon dioxide/n-silicon/aluminum heterostructure shows unusual behavior after treatment of the silicon wafer by chloroform and an iron stearate/ethanol mixture as compared with the devices without this treatment. The "negative capacitance" phenomenon arises in the region, where the heterostructure should be in "inversion" mode. It is suggested that this chemical treatment modifies Si/SiO₂ interface. This work also compares conductance of the heterostructures with and without the copolymer at frequency of 10 kHz. The conductance difference is explained from the chemical reactions point of view. This study is useful for better understanding of state retention in MFIS ferroelectric memory devices.

R. Tadros-Morgane, G. Vizdrik, B. Martin, and H. Kliem, Journal of Applied Physics 109, 014501 (2011).

Characterization of extruded ferroelectric film P(VDF-TrFE)

Xiaojing Zhu^{1,2}, Emiliano Bilotti^{1,3}, Xiangjian Meng², and Mike Reece^{1,3}

¹*School of Engineering and Material Science, Queen Mary University of London, London, E1 4NS, UK*

²*Shanghai Institute of Technical Physics(SITP), Chinese Academy of Sciences (CAS), Shanghai 200083, China*

³*Nanoforce Technology Limited, London, E1 4NS, UK*

Email: x.zhu@qmul.ac.uk

Ferroelectric copolymer poly(vinylidene fluoride and trifluoroethylene) [P(VDF-TrFE)] have been attracted much attention for its advantages of flexibility over ferroelectric ceramics. The ferroelectric performance of P(VDF-TrFE) derived from spin-coating, Langmuir-Blodgett and cast-stretching has been comprehensively investigated^[1]. However no ferroelectric performance of extruded P(VDF-TrFE) films has been reported yet. In this work, P(VDF-TrFE) films was extruded from melt and was hot pressed at different temperatures up to 120°C to obtain smooth and uniform films. Morphology results show that the P(VDF-TrFE) films have compact banded structures where the crystal grains stack closely together, suggesting the structure was not disturbed by the hot-pressing process. The film is highly crystallized in the ferroelectric low temperature (LT) phase and confirmed by the X-ray diffraction (XRD). The extruded film with a hot-pressed processing at 120°C achieved higher crystallinity than that without a hot-pressed process, as shown in Fig.1. The films show good ferroelectricity with a remnant polarization around 0.07C/m². Our research presents that the extruded-film technique is a simple way to prepare P(VDF-TrFE) thin films with a good performance.

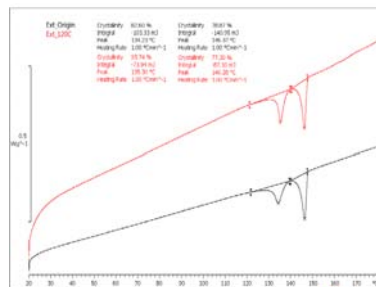


Figure 1 DSC results of extruded films (black) without hot-pressing and (red) hot-pressed at 120°C.

Reference

[1]R. V. Gaynutdinov, et al.*Polarization switching at the nanoscale in ferroelectric copolymer thin films*.Applied Physics Letters.**99**.14: 142904(2011)

Macro- and microscopic ferroelectric properties of P(VDF-TrFE) copolymer films

A.V. Solnyshkin^{1,2}, M. V. Silibin¹, A. N. Morozovska³, E. A. Eliseev⁴,
S. A. Gavrilov¹, V. V. Shvartsman⁵, D. C. Lupascu⁵

1- National Research University of Electronic Technology "MIET", Zelenograd, 124498 Moscow, Russia

2- Tver State University, Sadovij per. 35, 170002 Tver, Russia

3 Institute of Physics, National Academy of Science of Ukraine, 03028, Kyiv, Ukraine

4 Institute for Problems of Materials Science, National Academy of Science of Ukraine, 03142, Kyiv, Ukraine

5 University of Duisburg-Essen, Institute for Materials Science and Center for Nanointegration Duisburg-Essen, 45141 Essen, Germany

E-mail address: a.solnyshkin@mail.ru

Poly(vinylidene fluoride) (PVDF) and related copolymers, for instance poly(vinylidene fluoride-trifluoroethylene) (P(VDF-TrFE)), exhibit a variety of characteristic mechanical and electrical properties, such as piezoelectricity, pyroelectricity, etc. These properties are associated with cooperative orientation of molecular dipoles originated from their ferroelectric nature [1]. Crystallization from a melt produces the nonpolar α -phase consisting of trans-gauche-trans-gauche' ($TGT\bar{G}$) molecules packed in an antiparallel manner. Mechanical stretching transforms the α -phase into the polar β -phase which possesses a spontaneous polarization associated with parallel packing of all-trans ($TTTT$) molecules. This phase is responsible for ferroelectricity in PVDF. An addition of a fixed amount of trifluoroethylene (TrFE) or tetrafluoroethylene (TFE) to PVDF generates a random copolymer which favours crystallization from the melt directly to the ferroelectric β -phase. Various methods such as high temperature annealing, stretching and high electric field poling have been employed to introduce high degree of crystallinity (increasing the β -phase fraction) and perfect alignment of dipoles in polymer films.

In this work, a comparative study of the polarization switching properties of P(VDF-TrFE) copolymers on macro- and microscopic scales was investigated in the broad temperature range comprising the phase transition point and an analysis of their ferroelectric properties was carried out.

The samples of P(VDF-TrFE) (with $\approx 70\%$ of VDF) were prepared by the solvent-cast method. The films thickness varied from 15 to 25 μm . A part of the samples were polarized by the corona charge method. For studying the macroscopic switching processes, aluminum circular electrodes with diameters 8 – 12 mm were deposited on both surfaces. For macroscopic ferroelectric measurements the Sawyer-Tower method was used. The polarization switching in the unmetallized samples at the nanoscale level was studied by the piezoelectric force microscopy (PFM).

From the macroscopic measurements, it follows that applying the alternating electric fields up to 300 kV/cm does not lead to the reversal processes in the copolymer film samples. In this case, the polarization dependence on the applied field is linear like in linear dielectrics. Under the electric fields exceeded ~ 300 kV/cm, a formation of ferroelectric hysteresis loops was begun, thus the saturated hysteresis loops were observed in the fields above 400 kV/cm. According to hysteresis loop measurements the values of remanent polarization and coercive field were determined as ~ 3 $\mu\text{C}/\text{cm}$ and ~ 400 kV/cm. It was found that preliminary treatments (polarizing and annealing) of samples led to change the remanent polarization and coercive field of P(VDF-TrFE) copolymer. The microscopic ferroelectric measurements by PFM revealed partial polarization switching in local regions under a bias voltage in the range from -60 to $+60$ V.

Theoretical modelling of the P(VDF-TrFE) dynamic ferroelectric properties was performed with the special attention to the impact of the protonic transport on the polarization, dielectric susceptibility, losses and electric current hysteresis loops, as well as temperature hysteresis of the dielectric susceptibility and losses. In accordance with the theory, the peculiarities on the hysteresis loops (additional intersections, unusual loop shape, thickness behaviour of the coercive field and remnant polarization) and additional maxima on the temperature hysteresis possibly originate from the complex interplay between the relatively "sluggish" proton and "fast" phonon and electron sub-systems. Numerical simulations confirmed the absence of any unusual peculiarities in the dielectric P(VDF-TrFE) and their appearance in the case of proton-electron subsystem inclusion, when the Landau-Khalatnikov relaxation time is much smaller than the typical electron relaxation time and the latter is much smaller than the protonic time of P(VDF-TrFE). Thus we conclude that the situation in P(VDF-TrFE) becomes similar to the complex dynamics of polarization in other band gap semiconductor ferroelectrics with mixed-type conductivity and mobile charged defects [2].

[1] T. Furukawa, Ferroelectric properties of vinylidene fluoride copolymers, Phase Transition, vol. 18, pp. 143-211, (1989).

[2] A. N. Morozovska, E. A. Eliseev, P.S.Sankara Rama Krishnan, A. Tselev, E. Strelkov, A. Borisevich, O. V. Varenik, Nicola V. Morozovsky, Paul Munroe, S. V. Kalinin, Valanoor Nagarajan. Defect thermodynamics and kinetics in thin strained ferroelectric films: the interplay of possible mechanisms. (<http://arxiv.org/abs/1311.3116>)

The peculiarities of influence of copper and lanthanum dopants on ferroelectric and relaxor properties of PLZT ceramics: The investigations by dielectric and radiospectroscopy (EPR, NMR) methods

I. Bykov¹, Yu. Zagorodniy¹, L. Yurchenko¹, V. Trachevsky², V. Dimza³, L. Jastrabik⁴,
A. Dejneka⁴

1- Frantsevych Institute for Problems of Materials Science, National Academy of Sciences of Ukraine, Krzhyzhanovsky str. 3, 03142 Kiev, Ukraine

2- Technical Centre, National Academy of Sciences of Ukraine, 04070 Kiev, Ukraine

3- Institute of Solid State Physics, University of Latvia, 226063 Riga, Latvia

4- Institute of Physics ASCR, v. v. i., 182 21 Prague, Czech Republic

bykov@ipms.kiev.ua

Electron paramagnetic resonance (EPR), nuclear magnetic resonance (NMR) and dielectric spectroscopy investigations of PZT : n % La ($n = 1, 2, 3, 4, 5, 6, 11$) relaxor ferroelectrics and PLZT 8/65/35 doped by copper oxide from 0.005 to 3 wt.% was performed at room temperature. Behaviour of the complex dielectric permittivity $\epsilon^* = \epsilon' - i\epsilon''$ and polarization in relaxor electro-optical PLZT 8/65/35 ceramics modified by admixture of Cu is studied within the 20 – 400 °C range of temperatures at frequencies from 130 Hz to 106 Hz. The observed EPR spectra were shown to be the superposition of Cu^{2+} being in axial and cubic symmetry field. The axial symmetry spectrum is determined by Cu^{2+} substituted for Ti^{4+} with excess charge compensation by La^{3+} in the nearest neighbour; meanwhile cubic symmetry centers are those with the compensation in distant spheres. The ^{207}Pb NMR spectra of studied compounds show that increase of copper concentration from 0.005 to 3 wt.% leads to a visible increase in the intensity of the spectrum in a low field region. NMR spectrum presents the superposition of the Pb ions occupying sites with different symmetry of local environment and covalence of the chemical bond Pb-O, with less symmetry and more covalent chemical bond leading to a greater paramagnetic contribution from the given Pb ion. Thus, increasing of the copper content is accompanied by a change in the nature of the chemical bond Pb-O and leads to deformations of the structure, which has a significant impact on the ferroelectric and relaxor properties of PLZT. Increasing of lanthanum concentration up to 5 % is accompanied by a monotonic shift of the ^{207}Pb NMR spectrum to the strong field region. Further increase of lanthanum content causes a change of the line shape along with the shift, which means that the lanthanum begins to substitute for lead atoms having less covalent component of chemical bond. This is supported by the dielectric spectroscopy investigations where it was found that increase of Cu content shifts the maxima of $\epsilon'(T)$ and $\epsilon''(T)$ curves to a higher temperatures, increases the residual polarization, polarization of saturation and leads to increase of the coercive field.



Useful information

TELEPHONE NUMBERS

ECAPD 2014 Secretariat	+370 611 62286
Police Ambulance Fire	112
Taxi	1450

USEFUL LINKS

Conference website	www.ecapd2014.ff.vu.lt
Bus information	www.vilniustransport.lt
Railway information	www.litrail.lt
Airport information	www.vilnius-airport.lt

OPENING HOURS

Post Office	8:00 – 18:00 (08:00 a.m. – 06:00 p.m.)
Banks	8:30 – 18:00 (08:30 a.m. – 06:00 p.m.)
Shops	10:00 – 20:00 (10:00 a.m. – 08:00 p.m.)



VILNIUS UNIVERSITY
www.vu.lt



Vilnius, Lithuania
2014